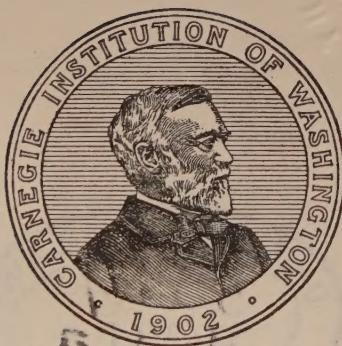# INTERFEROMETER EXPERIMENTS IN ACOUSTICS AND GRAVITATION

PART II

By CARL BARUS, Ph. D., LL. D.

Hazard Professor of Physics and Dean of the Graduate Department in Brown University

PREFACE.

The present report is in the main a development of the acoustic investigations with the pin-hole begun in the preceding communication (Carnegie Inst. Wash. Pub. No. 310, 1921). To this has been added an account of the progress of experiments on the value of constant of gravitation found with a vacuum apparatus—work which is feasible during a part of the summer months only. As the source of sound is necessarily of an arbitrary character, it has not seemed worth while to reduce the data to actual acoustic pressures, either positive or negative. Accordingly, the fringe deflections (s) of the mercury **U**-gage read by a vertical interferometer, as these are proportional to the pressures, are given throughout. Furthermore, a report of the large accumulation of numerical data obtained would have been awkward. Therefore, the graphs only have been given and are believed to suffice.

The introductory paper shows that the pin-hole probe responds effectively to nodes in organ-pipes, that it ignores the antinodes, and that an overtone may produce the fringe deflections even when the fundamental is excited. In the case of the usual air-blown diapason pipes, the presence of the air current naturally interferes with the acoustic experiment and the fringes are apt to be thrown out of the field. If, however, the pin-hole is surrounded by a minute bag of porous material like thin filter-paper (one or more ply), a consistent registry of nodes again appears, but constructed now on a base of increasing pressures, positive or negative. Even goldbeaters' parchment is sufficiently porous to function.

With a device so sensitive to nodal regions in vibrating pipes thus at hand, the construction of a pin-hole resonator suggests itself. Contrivances both of the open-pipe and closed-pipe types were tried out at length; but the latter, with but a single mouth and responding to a closed organ-pipe of the same pitch, is to be preferred in the interest of simplicity. Great difficulty was encountered in the construction of the pin-hole. Unless this is adapted to the resonator, no acoustic pressures whatever are evoked. It was eventually found that both the size and the slope of the walls of the pin-hole are critical; that a salient pin-hole generates acoustic pressure, a reëntrant pin-hole acoustic dilatation, and there is neutral behavior between the two. With a properly designed pin-hole, pressures whether positive or negative will be about equal; it follows, therefore, that by coupling them with the corresponding shanks of the mercury **U**-tube, an advantage in sensitiveness is secured. It does not seem feasible, however, to push the sensitiveness of the pin-hole indefinitely farther. The response is such that, below a certain threshold value of amplitude of sound-wave, the acoustic pressures evoked at the pin-hole drop off sheer. The pin-hole resonator is deaf to an organ-pipe sounding beyond a

iii

radius of 6 meters. I have described these occurrences by an exponential expression, which fits pretty well.

It is arguable that if a single pin-hole evokes a certain acoustic pressure, two pin-holes properly adjusted in series would enhance that pressure and the project of relaying pin-holes would seem quite feasible. All experiments with this end in view remained persistently negative. With so many pin-holes in series that the excursion of the mercury in the **U**-tube was absolutely dead-beat, owing to the increasing air resistance introduced, the acoustic response was no better than for a single pin-hole.

The experiments have a direct bearing on the behavior of sensitive flames. If an adjusted pin-hole burner becomes turbulent by slight increase of pressure within, a sound-wave passing the burner will supply this pressure acoustically. Finally, the experiments with branched tubes and one or two (salient and reversed) pin-holes, begun at the end of the present paper, present many points of interest both on account of the low values of pitch which such structures harbor and of the eventual bearing of the data obtained on the sensitiveness of telephones.

Within its restricted field (radius 6 meters), the pin-hole resonator serves admirably for the acoustic survey of the interior of a room in which an organ-pipe is sounding. If the phenomena were visible, the room would probably have the stratified appearance of a vacuum-tube stimulated by electric discharge. For a given position of the pipe, nodal regions alternate with anti-nodal regions, quite irregular in distribution but none the less fixed in position.

I have cut through this acoustic topography in all directions from the position of the pipe, with the expectation of arriving at some general facts as to distribution; but except for the case of reflection from surface close at hand, I have not made much headway. It is thus very difficult to state the results otherwise than by the graphs in the text. These show a difference in the character of a survey between walls contrasted with one toward an open door; but (*a priori*) one would not be able to predict the occurrence of either type.

In the succeeding paper an account is given of the repetition, under very satisfactory instrument conditions, of certain experiments made long ago. These treat the effect (if any) of an electric current on rays of light, passing in parallel with the current through the same long channel, both in case of an exhausted tube and of an electrolytic trough. Such an effect was hardly to be expected and none was found. In the sequel some useful improvements are added to the self-adjusting interferometer, an apparatus not only of very general usefulness but almost indispensable when separate interferometer adjustments are frequently to be renewed.

The work on gravitation, which is an endeavor to ascertain to what degree the constant may be found in a self-contained apparatus under ordinary laboratory conditions, contains two groups of measurements. The first, made in a moderate vacuum of a few millimeters and with a relatively thick quartz fiber, gave a value trustworthy within a small percentage. Encouraged by this result, I installed a much thinner fiber, giving excursions 5 to 10 times larger,

the needle swinging in vacua approaching 0.001 mm. The mean elongations of the needle at night seem to be trustworthy, but the long period of the needle could not be found with anything like adequate accuracy. So dependent is this period on the thermal environment that early morning and afternoon observations may vary from 600 to 800 seconds, the individual data themselves being quite accurate. A storm passing over the laboratory dropped the period from 750 to 626 seconds, after which it rose again to 712 seconds. Of course it would be possible to determine the modulus of the fiber by a separate small body, but this would be at variance with the plan of the experiments, while the taking apart of a rigorously sealed apparatus containing a loaded quartz fiber is always a very delicate operation. The experiments will be resumed this summer under the highest attainable exhaustions, as the experiments show this to be indispensable.

CARL BARUS.

BROWN UNIVERSITY,
   Providence, Rhode Island.

CONTENTS.

Chapter IV.—*Gravitational Experiments.*

CHAPTER I.

EXPERIMENTS WITH THE PIN-HOLE PROBE.

1. Partly closed pipes.—In the apparatus described in the last report the metal foil carrying the pin-hole was cemented normally to one end of a glass quill-tube (fig. 1, inset) about 30 cm. long, the other end communicating with the closed mercury shank of the U-tube by a short piece of rubber tubing. Changes of mercury level resulting from pressure at the pin-hole were read off by a vertical interferometer (fig. 3, inset). The length of rubber tubing used for connection at *e* here seemed to make little difference, unless this length was considerable. Deflections were reduced about one-half by lengths of tubular connector of about 1 meter between the pin-hole and the mercury surface. With quill-tube connections the decrease was often less; thus, to insert a few data for guidance:

| Length of connector........ | 25 | 65 | 100 cm. |
| Deflection, *s* .... | 95 | 80 | 60 fringes |

and the decrease would probably be still smaller if a uniform, clear-bore tube were used, instead of pieces joined together. In general, however, periodic relations occur, as investigated in §§ 5 to 7, 34, *et seq.*

The sound intensities used in the following paragraphs are merely incidental. It will therefore suffice to give the fringe deflections, *s*, in the interferometer telescope (fig. 3) in arbitrary scale-parts (collimator micrometer in .01 cm.). As a rule the fringe breadth was somewhat less than 2 scale-parts, though 3 and even 4 scale-parts per fringe were occasionally used. Taking the former estimate, the pressures Δh in centimeters of mercury $(U - U')$ to be obtained from Δs scale-parts (*s* being the reading) follow the equation

$$2\Delta h = \lambda(\Delta s/2) \quad \text{or} \quad \Delta h = (\lambda/4)\Delta s = 1.5 \times 10^{-5}\Delta s \text{ cm.} = 1.5 \times 10^{-4}\Delta s \text{ mm.}$$

Pressures may thus be estimated as between 10^{-4} and 2×10^{-4} millimeter of mercury per scale-part, Δs. It was frequently convenient to shift the zero-point either to the right or left of the scale reading from $s = 0$ to 100.

Using a quill tube 25 cm. long with the pin-hole at the end, the effect of partially stopping the tube was next ascertained. This could be done neatly with different lengths of the common furry tobacco-pipe cleaner. The original experiments with Helmholtz resonators excited by the telephone were very curious. Thus the g'' resonator showed strong harmonics ($s = 90$ scale-parts) at d'' and g'' (the former embracing the neck connector, the latter belonging to the resonator alone) with the clear probe. Inserting the furry wire, the deflections were eventually quite as large, but of very slow growth. Indeed, the harmonic g'', which was weak for the clear probe, was much enhanced by the stopped probe. Similar results were found with an f'' resonator, the

harmonics being d'' very strong and f'' weak for the clear probe. With the furred wire pushed in, even as far as 10 to 20 cm., both harmonics were gradually enhanced in the lapse of time, the f'' particularly, which was so faint as scarcely to be recorded in case of the clear tube. Finally, the c'' resonator with a strong harmonic at a' and a weak one at c'' retained its characteristics with the stopped pipe. Similarly, slow-growing deflections were obtained in the former report in case of slight leakage at the telephone plate or elsewhere in the closed sound chamber.

On repeating these experiments some months after with a closed c'' pipe 30 cm. long, I was unable to reproduce the former results. Furred wires 5, 10, 20 cm. long now acted nearly instantaneously, reducing the deflection to one-half or less, sometimes even to one-tenth. The deflection does not, however, diminish with the length of tube, partially stopped, if time is allowed in extreme cases (20 cm.). Longer wires were not always more harmful than shorter wires, though I obtained no definite evidence of periodicity here after many trials. Sound-waves are probably wiped out, like the waves of the sea entering a marshy shore. (Cf. § 5 et seq.)

2. Overtones in long, closed tubes.—These were of brass, about 2.5 cm. in diameter, closed at one end with the telephone (fig. 1) by which they were actuated. Lengths of 60 and 30 cm. were tried. It was not usually difficult to record with the pin-hole probe the overtones to which the pipe responded on blowing. In some of the harmonics, the pressure increments passed to pressure decrements on commutating the telephone current; but this was not the case with all the harmonics. One might conclude hastily that the commutator notes originated in the telephone, yet this is not the case as a rule. I failed to find any general result from the large number of tests made.

The closed pipe (30 cm. long with harmonics at c' g'' e''' $\flat b'''$ when blown) responded to c' e''' $\flat b'''$ strongly; but the g'', for some reason, could not be evoked intensely, being in all the trials only just audible. A number of experiments were made with this pipe (fig. 1, inset, T telephone, P pipe, ss probe), particularly with reference to the location of the nodes in depth below the mouth. The long, rigid system PT was couched on a light 4-wheeled carriage, and rolled to and fro on the table over the stationary probe ss, to the outside of which a narrow centimeter scale had been attached. The natural overtone g'', though not obtained on blowing, came out very strongly (fig. 1) when the pipe was excited with the telephone (1,000 ohms resistance). The nodes are quite sharp, lying at 10 cm. of depth and at the bottom. The antinode lies somewhat above 20 cm. of depth and is equally sharp. The pressure does not here fall off to zero. Probably higher overtones are in presence. No effect was produced by commutation of the telephone current. Accentuated loudness of g'' was evident to the ear.

Nothing was obtained on raising the pitch; but as the limit of the electric siren was a'', the other overtones, e''' $\flat b'''$, were unavailable.

On lowering the pitch there was no response until g' was reached. This it will be noticed is not an overtone of the closed pipe, nor would it be of the open pipe. Nevertheless, the survey in depth (fig. 2) brought out the node and antinode of the octave g'' very pronouncedly, though the telephonic resistance had to be decreased one-half (500 ohms) to obtain equivalent deflections. The pitch g', therefore, while leaving no impression of its own, evokes the natural overtone g'' of the pipe, the node being somewhat broader and the antinode sharper. Here also commutation was ineffective.

The pitch was now lowered as far as possible on the electric siren, reaching c', d', e' when a response was again registered as shown is figure 3. Unfortunately, the pitch was fluctuating and not easily controlled or identified in this low region, and the three notes seemed to be about equally effective. The curve a shows the fundamental, when brought out under 500 ohms, very weak and unsteady. It was, again, very apt to be accompanied by the overtone
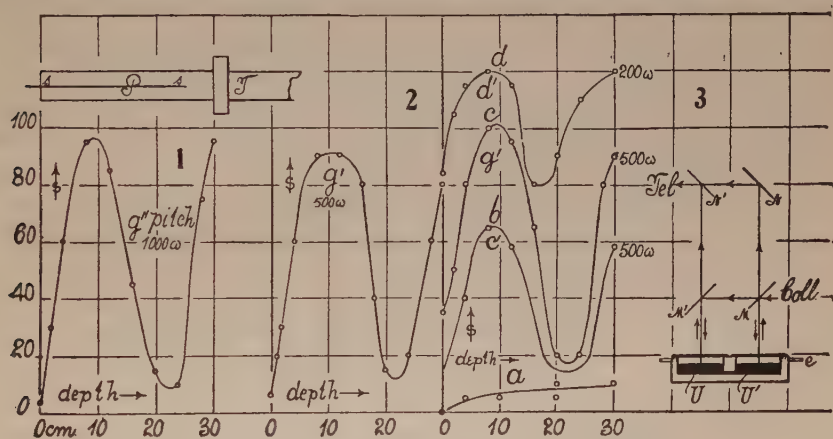
g'' (audibly, though intermittent), as appears from the graph b, figure 3. To be assured that there was nothing wrong with the pin-hole probe, the pitch was then raised to g', whereupon the g'' overtone (curve c, fig. 3) came out even more strikingly than heretofore.

Finally (fig. 3, d), the pipe was removed from direct attachment (cement) to the telephone, one end of it stopped with a perforated rubber cork, and this joined at the perforation with a short rubber tube to the mouth-piece of the telephone. The pitch was thereby raised to d'. Setting the telephone for d', the overtone near a'' nevertheless was the only one identifiable. The pressure distribution in depth, moreover, has somewhat varied compared with the cases above for similar conditions, as may be seen by inspecting the graphs b and d. It follows, therefore, that the only note which the tube will steadily maintain is g'' and that this may be evoked by the lower harmonics, either g', c', or even c, as well as by g''.

Further experiments were made with the endeavor to clear up certain anomalous results with Helmholtz resonators. These were joined with a short end of rubber tubing at their necks with the mouth-piece of the telephone

into which a corresponding adjutage had been screwed. In the survey in pitch
(fig. 4, p) the c'' appears as but a secondary maximum, the large maximum
being near a'. No other maxima occur. A survey in depth below the mouth
of the resonator is also shown in the same figure, both for the a' and c''. The
latter attains a maximum pressure at about 2 cm. within the mouth, and then
falls off to the nearly constant values, as far as the bottom or neck. The a'
increases well into the neck. It is natural, therefore, to take a' as the note of
the telephone and resonator together, while c'' is the pitch of the resonator
alone. To test this further, a g'' Helmholtz resonator was examined, as in
figure 5, curve p. The note near a' is still present, though it has naturally been
somewhat raised in pitch; but the proper pitch g'', which is now remote, comes
out strongly. There is still a question relative to the resonance in the U-tube.
Making the telephone and the U-tube a closed region with an external pin-hole
(as explained in the last report), the curves a, b of figure 6 were obtained with
different resistances (500, 1,000 ohms) in the telephone circuit. In curve c
the telephone current is commutated. As a result some of the minima are
changed to dilatations without modifying the general contours as a whole.
On comparing the curves of figure 6 with those of figures 4 and 5, it is
hardly probable that the note at a' in the latter is due to the note near a' of
the former. Otherwise there should be evidence of the occurrence of the
very loud $\sharp c''$ and some of the g'' of
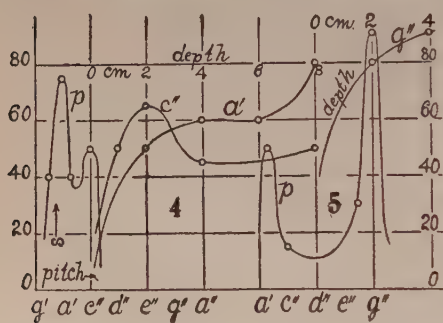
figure 6 in both the curves of figures 4 and 5.

To contrast with the 30-cm. closed pipe, the smaller one, 14 cm. to the
telephone plate and 2.5 cm. in diameter, was inserted. This, when blown,
gave a sharp c'', a shrill a''' overtone and others not available. Tested with the
pin-hole probe for harmonics, the curve p, figure 7, was obtained at 1,000 ohms
in the telephone circuit, showing besides the $\sharp c''$ maximum, a marked a' and a'',
both of which are abnormal. The note $\sharp c''$ was now examined for distribution
of pressure in depth (curves $\sharp c''$, fig. 7) and the results found are such as
would be expected for a fundamental. The graphs for 1,000 and 2,000 ohms
in circuit are alike in character. The a'' was then examined for pressure dis-
tribution in depth, and though it was a little difficult to maintain this high pitch
steadily, the graph of figure 7 (a'') came out clearly in all trials. The loudness
is somewhat reduced, 1,000 ohms being in circuit, so that the fundamental $\sharp c''$
at 2,000 ohms has about the same intensity as the fundamental in the a'' curve.
If, therefore, we subtract the ordinates of the former ($\sharp c''$, 2,000 ohms) from
the latter (a'', 1,000 ohms), we would get a graph suggesting a node or maxi-
mum pressure in the middle of the closed pipe. In other words, the closed
pipe $\sharp c''$ would here seem to be endeavoring to vibrate like an open pipe with
an antinode at the mouth and at the vibrating telephone-plate. There would

have to be but little accommodation, as an open a'' pipe is also about 14 cm. long. Another explanation, such as is given in the next paragraph, is perhaps not more exacting; but neither accounts for the rise of acoustic pressure from mouth to closed end.

In the same way as at a'', the a' was now examined in depth with 500 ohms in circuit, the graph after many repetitions showing the character of a' curve in figure 7. This is doubly inflected, thus strongly implying the occurrence of the overtone near a''' superimposed on the fundamental. It was noticed that the tone-color changed perceptibly with slightly different speeds of the motor-break. Hence the overtones are probably intermittently present; i. e., only on sharp tuning. This might account for the absence of a minimum in the a'' curve (fig. 7), even if not vouched for by evidence. The a'' being shrill, pressures are often marked even at the mouth of the pipe.
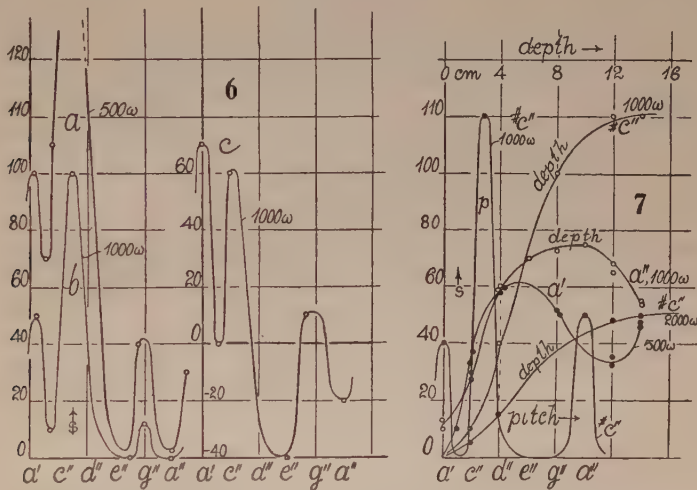
If we assume that both the a' and a'' are accentuated because they evoke the natural overtone a''' of the pipe, it must not be overlooked that this occurs in a medium of continually increasing acoustic pressure or density from the mouth of the pipe inward to the telephone-plate.

3. Pressures in wind-blown diapason pipes. Porous envelopes.—When the pipes are blown by a bellows apparatus, the air current passing through the pipe seriously interferes with the acoustic registry. Thus, in an ordinary rectangular c'' pipe, the fringes are thrown out of the field of view for any position of the pin-hole within the pipe. Inclosing the pin-hole with a test-tube 10 cm. long and 1 cm. in diameter had no reducing effect, even when the neck was constricted so as just to admit the quill tube. A piece of pure rubber tubing closed at the outer end and loosely fitting the quill tube gave a small deflection at the middle of the organ-pipe, but not at the ends. This suggested the method of procedure; for it has been shown in the earlier work

that acoustic pressures leak (so to speak) through a porous septum and may thus be measured.

The plan, therefore, was to surround the quill tube S (fig. 8) carrying the pin-hole O with a narrow cylindrical bag EE of filter-paper, the open end of the bag being fixed to S, at aa, with cement. Pressure involving air transmission would have to pass through the pores of the paper, all other modes of ingress being sealed off. If air transmission is not essential, the flexible walls of EE are operative at once. The seal at aa, as well as at the outer end of the envelope, must be perfect; otherwise the pressures resulting from air currents are registered and the fringes leave the field throughout. Thus a bag EE merely pushed over the quill tube is unavailable. If the organ-pipe (f'') is blown intensely, a relatively large pressure will be indicated as soon as the pin-hole O enters within the plane of the mouth of the pipe. These pressures rapidly fall off to about one-fifth when the pin-hole is 1 cm. off on the outside
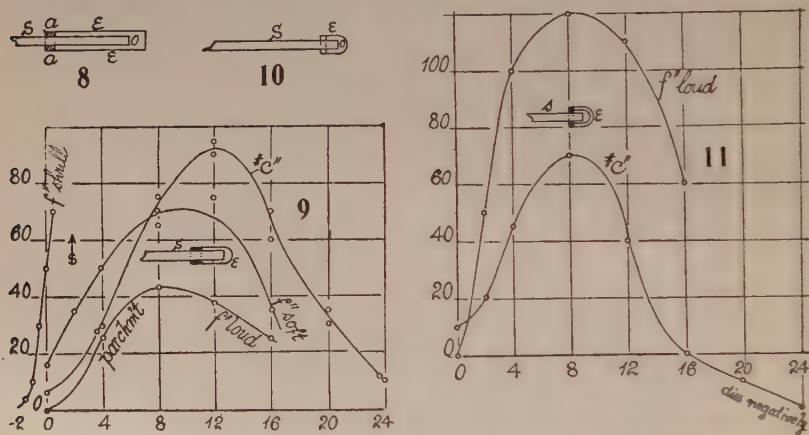
of the mouth, and then gradually vanish at from 1.5 to 2 cm. beyond the mouth. The graph is shown in figure 9 over the negative abscissas.

The high graph in figure 9 summarizes the results obtained with a diapason pipe 24 cm. long from open end to embouchure and giving a sharp c''. The pipe was blown with a specially adapted Fletcher bellows, and though it was a little difficult to control the intensity, the node near the middle comes out satisfactorily. An f'' pipe, 18 cm. long, similarly blown, was much too shrill for the manometer, the fringes leaving the field, and the endeavor to reduce the intensity to manageable limits is less successful and trustworthy. Nevertheless, the character of the graph f'' is fairly well indicated. Results of the same kind were obtained with a small bag of filter-paper, E, figure 10. This was compressed, when wet, around the end of a glass rod and allowed to dry thoroughly. It was then attached to the probe S with cement and thin wire. The graphs, being essentially like figure 9, need not be given. As before, a very weak f'' note was needed to keep the fringes in the field. When the filter-paper E, figure 10, was moistened, all action ceased, to be restored, however, when the paper was again dry.

The short bag (fig. 10) easily admits of being doubled or quadrupled to reduce the sensitiveness and keep the fringes of the strong f'' in the field. Figure 11 shows the graph obtained with the envelope (inset) of two-ply filter-paper. We here definitely encounter the result which will frequently occur in the sequel, that in case of the now shrill f'' the graph is erected on a succession of increasing acoustic pressures from mouth to embouchure of the organ-pipe. The $\sharp c''$ curve, on the contrary, is erected on a succession of decreasing pressures, which dip, when the probe is near the embouchure, into marked acoustic dilatations. Nevertheless the node or maximum pressure in the f'' pipe is still in the middle. The node in the c'' pipe has been displaced apparently from 12 cm. to 8 cm. below the mouth. This is very unusual and to be ascribed to the superimposed dilatation; but the curve is otherwise smooth.

The next experiments were made by surrounding the pin-hole with a four-ply envelope of thin filter-paper (fig. 12, inset). These graphs accentuate the results of the preceding figure. The strongly blown f'' pipe, with a node in the middle, has its pressures not only built up on a base or succession of increasing pressures, but this succession actually begins with well-marked dilatations at the mouth of the pipe. The acoustic compression is zero 2 cm. within the pipe, and not again. The c'' pipe now has its node in the middle, while the compressions are zero at the mouth and at about 16 cm. within (agreeing with the preceding case). Thereafter, however, the march into dilatations becomes much more precipitous. Pressure decrements are nearly constant from 20 cm. within to the embouchure at 24 cm. It is interesting to note that at 16 cm. within, the absence of compression when the pipe is sounding passes into dilatations as the sound dies down, returning to zero when the sound ceases.

The absence of pressure increments when the bag is moistened with water has already been indicated. Similarly, if the pin-hole is surrounded by a tight cylindrical case of the thinnest mica (0.03 mm. thick), the U-tube does not react, however intensely the f'' note is sounded. With an impervious bag of very thin flexible goldbeater's skin, some response was obtained, as shown in the lower curve of figure 9. These deflections for an intense f'' were of slow growth to a maximum, as if the bag were slightly porous, or sufficiently flexible and soft to contract. One may note that this reduced curve is much like the upper curve (two-ply filter-paper) in figure 11 and erected on a base of increasing pressures. With the bags removed, the deflections were in all cases enormous, throwing the fringes far out of field.

4. Continued. Long probe tube and varied pin-holes.—Another method of reducing the effect of strength of the f'' pipe consists in elongating the quill tube of the probe as far as the less effective lengths of § 5, or of providing it with pin-holes of diameters either short of or beyond the optimum. The quill tube used was 40 cm. long, not counting the (wider) rubber connectors at the U-tube. The foil carrying the pin-hole was preferably shaped like a percus-

sion cap and cemented to the end of the quill tube, which it fitted snugly. It was then punctured with the end of the finest cambric needle. This gives a very robust apparatus not liable to spring leaks accidentally.

The graph obtained with the strongly blown f'' pipe is shown in figure 13. It is all but normal, with a node near the middle. The only suggestions of the air-current effect were obtained at the observations after 16 to 18 cm. in depth. These, as the pipe-note dies down, run as much as $s = -20$ into negative fields. In the full-sounding pipe these dilatations are overpowered by the acoustic vibrations.

Very different from this is the graph for the c'' pipe, the note of which was naturally very much weaker. Here the acoustic effect does not supervene and the graph obtained is almost identical with the corresponding graph in
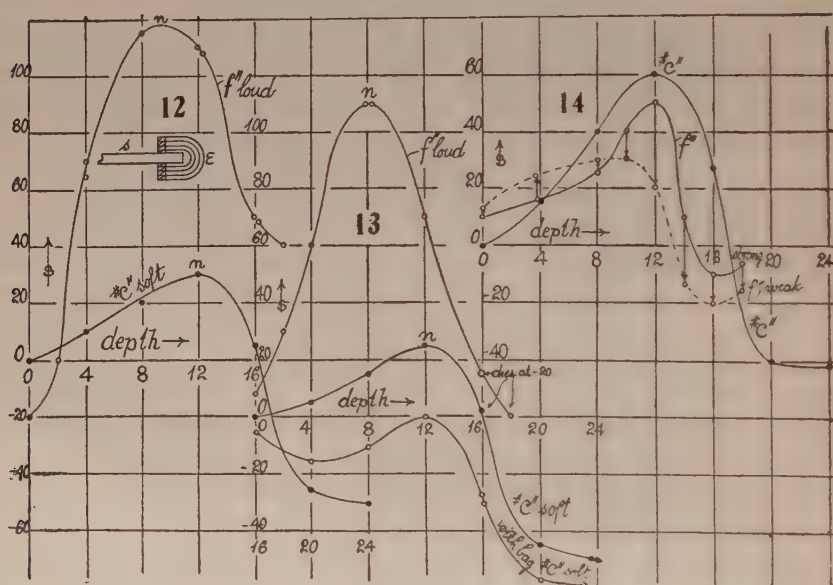
figure 12. Like this, the deflection at 16 cm. of depth dies off to $s = -20$. It was therefore thought well to provide the long probe with a (one-ply) filter-paper sheath, as in figure 8. The resulting graph (the lowest in fig. 13) now lies wholly in the region of dilatations, with only the node reaching up as far as $s = 0$. Nevertheless, this is correctly placed, on a succession of increasing dilatations from mouth to embouchure.

Figure 14 (upper curve) is the graph obtained with a probe about 24 cm. long, but carrying a very fine pin-hole. The c'' pipe here exhibits the general character of figure 13, except that the node is much more accentuated and the internal $s = 0$ at about 18 cm. of depth. This also falls off to $s = -20$ as the sound dies away. At 20 to 24 cm. of depth, s even approaches -50, in case of the full-blown pipe. The strong f'' necessarily threw the fringes out of the field of view, showing even $s = 70$ scale-parts at the mouth of the tube, $s = 20$ at 2 cm. outside, etc., as in figure 9.

It is, however, quite possible to bring the shrill f'' down to negative displacements, and this may be done by selecting a very fine pin-hole probe. The graph obtained is the lower curve in figure 14, beginning with a compression at the mouth of the pipe. The pressure distribution is peculiar, with a sharp, displaced node at 12 cm. of depth, from which the curve descends almost sheer to negative values. The record is at least a duplicate; for the shrill note in dying out increases the pressures for depths smaller than the middle, roughly speaking, and decreases them for depths beyond this. The arrows point out the trend of the weak-note curve. This seems to retain the node in its middle place, so that the shrill note is much modified by the overtones present.

5. Pin-hole probes in series.—If the pressures on the two sides of the pin-hole are different, one may argue that a series of probes should relay each other; for the inner pressure of any pin-hole would become the outer pressure of the antecedent pin-hole, in succession. A set of pin-holes was therefore prepared, consisting, as suggested in figure 15, of quill tubes s', each 4 cm. long, provided at one end with the cap-shaped piece of copper foil, cemented in place and punctured. These were joined by short ends of rubber tube, the pin-hole ends pointing in the same direction. A similar set of quill tubes, each 4 cm. long, was also at hand, without obstruction (*i. e.*, clear bore), to be joined end to end for comparison with the pin-holes series $s's''$. The telephone-blown pipe T, sounding $\sharp c''$ (fig. 1), was used as a source of sound, the outer pin-hole being about 4 cm. within the mouth. The fringes were enlarged (3 scale-parts). The pipe s communicating with the **U**-gage (U, fig. 15) was about 6 cm. long.

The results obtained are shown in figure 16, where little circles indicate the fringe deflections for the clear-bore tubelets in succession (the end tube being necessarily a pin-hole), and black discs the deflections for the pin-hole series. There is practically no difference so far as intensification or increased deflection is concerned, the pin-holes, if anything, acting as a slight obstruction in the tube. Hence one must conclude (so far as I see) that the pressures on the two sides of the intermediate pin-hole are the same, there being no discernible relay effect.

What the curve, figure 16, brings out very strikingly, however, is the periodic distribution of pressure, at least in the initial parts of the tube ss'', figure 15, connecting the end pin-hole s'' with the gage U. The first node or maximum is here probably within the tube s, so that the distance in tube-length between the first two apparent maxima is only 23 cm. The distance between the next two maxima is 27 cm., and between the minima 29 cm., which is probably an approach to the half wave-length of the pitch near $\sharp c''$. In the former report I investigated the effect of enlarging the free air space of the shank U of the gage. The results, beginning with a mere shell-like space, eventually enlarged to a volume somewhat short of a cubic decimeter, were, however, so complicated in their relations that but little interpretable information was obtained. This is not so with the behavior of the pipe ss'', and it appears

2

that if successive λ/2 are added to the length, but little change of the deflection or sensitivity is to be expected. The minima, though relatively weak, do not here fall off as far as zero.

To further test this result I put pin-holes at two successive nodal points or maxima. The results were:

```
Pin-hole at end only........................deflection 100
Pin-hole at second and third node.............deflections, 100, 90, 110, etc.
```

for different pin-holes inserted at the second node. In like manner, pin-holes at the first and second node (remainder of the tube removed) gave the same deflection, nearly, as a single pin-hole at the end of the tube. Examined individually at the first node, about the same deflection was obtained from each pin-hole. With the pin-holes at the end of tubes each λ/2 in length and placed successively end to end, no reduction of deflection showed itself even beyond a meter.

In further experiments it appeared that the periodic effect gradually dies away and is only marked at the beginning. Thus glass quill tubes 150 cm. and 300 cm. in length with a pin-hole at the end did not further reduce the sensitivity.

The endeavor to corroborate the results for the $\sharp c''$ pipe with an e'' pipe was not so direct. The latter, telephone-blown, developed both an e'' (maximum deflection +60, minimum 10 scale-parts) and a $\flat e''$ (minimum deflection −20 scale-parts). It was difficult to follow the periodicity with this interference beyond 25 cm. of length, though much time was given to the work. At the end of a quill tube 150 cm. long the pin-hole probe showed undiminished deflection for both notes. The same was the case with a quill tube 300 cm. long. It is probable that long tubes more easily accommodate different wave-lengths.

The outcome of this work has thus been, in general, that with a quill-tube connection between **U**-gage and pin-hole of more than 1 or 2 wave-lengths in length the pressures become nearly uniform. It seemed worth while, therefore, to reëxamine the long (30-cm.), closed c' pipe (i. e., wind-blown) of figures 1, 2, etc., with the advantages specified, of a quill-tube connector 300 cm. long. The telephone-blown pipe gave a fundamental $\flat b$, with a preference for the anomalous overtone f'. The curves obtained are given in figure 17, a being found for the position I and b for the position II of the commutator of the telephone current. In case of the curve c, a new pin-hole probe with quill tube 30 cm. long was added to the 300-cm. connecting quill pipe. When the pitch of the telephone reached f', the note called out was the first overtone f'' of the closed $\flat b$ pipe. The case presented is thus much like figures 1 and 2. But while the above graphs (for short connecting-tubes) showed no effect of reversal of the telephone current, the present curves are thereby completely reversed. Similarly, the curve c for the 330 cm. connector differs merely in pin-hole sensitivity. This result is so surprising that in figure 18 the case of a short connecting-pipe (35 cm.) has been repeated, the open circles corresponding to position II and the black disks to position I

of the switch of the telephone current. The curves (here both of low sensitivity) are practically identical. Thus the telephone is here capable of placing either a condensation or a dilatation at the nodes of the first overtone of the closed organ-pipe; but it can do this only if the length of the quill connecting-tube between **U**-gage and pin-hole is one or more wave-lengths (here λ=90 cm.) and not if it is but a fraction of a wave-length (short tube 35 cm.). In the latter case marked pressures only are found at the nodes and the dilatation at the antinodes is slight or wanting. The reason for the potency of the telephone is not hard to surmise; but the coöperation of the connecting-tube in the result is difficult to account for.

Figure 19 is another graph obtained a little later for a length of connecting-pipe of 180 cm. between **U**-gage and pin-hole. It practically tells the same story as figure 17, with the exception of a more marked tendency of the deflections to become positive, or compressions.
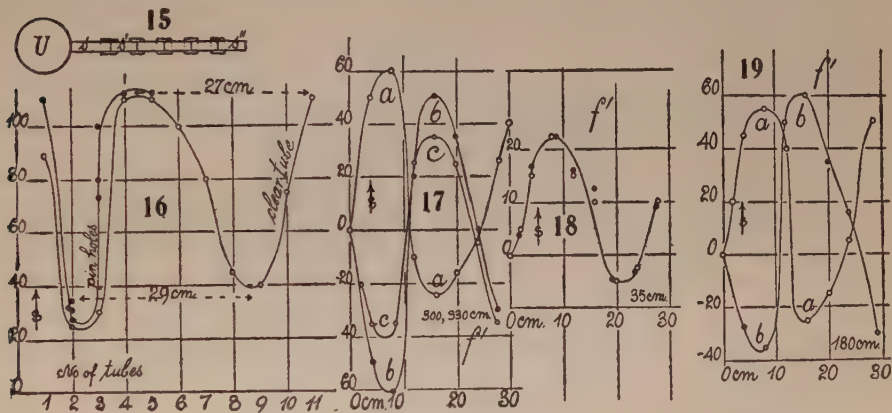
Finally, figure 20, the fundamental ♭♭ was now easily produced with the same quill-tube length, 180 cm. The graph was not subject to commutation, all deflections being compressions increasing from the mouth inward as far as the telephone plate. The note being relatively weak, the limiting deflection did not exceed 30 or 40 scale-parts, and irregularities in figure 20 are due to the difficulty of motor control at this low frequency.

As this experiment with pin-holes in series is of considerable importance in its bearing on the pin-hole probe, the experiments were also carried out for a closed region, as shown in figure 21. Here U is one shank of the **U**-gage, with its quill-tube connection, qq, leading to the telephone T. The connector qq carries a lateral branch made up of a succession of pin-holes $p'p'' \ldots p$, about 4 cm. apart, held together by short ends of gum-rubber tubing. The region offered two convenient harmonics, d'' (compression) and $\sharp d''$ (dilatation), very close together, which were tested. The results at d'' were:

Number of pin-holes								
....	1	2	3	4	5	6	7	8
Deflection		20	35	25	27	25	30	30 scale-parts

the last pin-hole being at the end of a tube 24 cm. long. The minimum at
♯d'' was much stronger, showing:

Number of pin-holes....	1	2	3	4	5	6	7	8	
Deflection	—100	—110	—105	—110	—95	—95	—95	—90	scale-parts

The pin-holes are naturally not quite equally efficient; apart from this the
effect produced by 8 pin-holes in series is not very different from that of a
single pin-hole, in spite of the very large resistance which must thus be
introduced into $p'p$. Here it was interesting to notice that whereas with
1 pin-hole there is some vibration of the mercury columns of the gage, and
with them of the fringes, the motion in the case of 5 or more pin-holes is abso-
lutely dead-beat. With 8 pin-holes the full deflection is reached gradually and
the return to zero equally so. A series of lateral pin-holes thus offers a
means of damping without much loss of sensitivity, which may be advanta-
geous; but the main result of the tests is the non-harmonic character of the
action of a series of pin-holes in a lateral branch, the sound-waves proper
taking the path $TqqU$, figure 21. Furthermore, the impossibility of amplifying
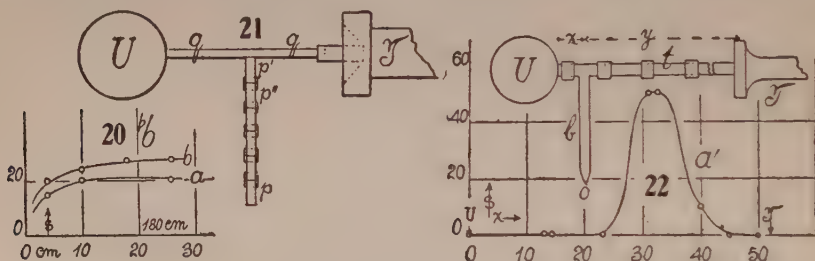
either the compression or the dilatation characteristic of a single pin-hole by
a series of pin-holes is substantiated.

6. **Evanescence of (weak) vibration in closed (tubular) regions.**—The
preceding methods of determining the character of the vibration in the tubes
connecting the **U**-gage with the course of sound did not lead to results as
thoroughly consistent throughout as would be desirable. I therefore, at a
later date, returned to the original investigation of the case of a closed quill
tube t, between the telephonic sound generator T and the gage U, figure 22
(inset). The pin-hole o, attached to a lateral branch-tube b, could be moved
from point to point of t, by aid of the short rubber connectors on the sectional
lengths in t. These admitted of their replacement in turn by the branch-tube b.
Thus the vibratory state throughout the whole length $(t=x+y)$ of t was
determinable from the acoustic pressure observed at U for a given x or y
location of pin-hole.

In the first experiments, t was 52 cm. long. The rather insensitive tele-
phone, actuated by the electric siren, was kept at the pitch a', while the probe
passed from end to end of t. The results are given in the curve figure 22, and
show a marked node at $x=32$ cm. from the **U**-tube or $y=20$ cm. from the

telephone plate. Between the position of this crest (a') along t and the **U**-gage ($x=32$ cm.) no acoustic pressure on vibration could be detected at any pitch; but between the node and the telephone plate ($y=20$ cm.) a succession of nodes of increasing pitch was determinable, as, for instance, a g'' maximum near 11 or 12 cm. from the plate. This made it seem probable that the air vibration evoked by the telephone plate is here largely confined in the quill tube, within the first quarter wave-length (for a', $\lambda=76$ cm.) from the plate; and that beyond this, toward the **U**-gage, there is no vibration, but only an air-content relatively at rest. In other words, that within the quill tube the vibratory air motion received from the telephone is soon damped out. If this surmise should prove correct, it would throw much light on the acoustic behavior of the connector tubes t, as well as the phenomena as a whole. The answer to this question depends on the telephone used and will be treated in this and the following paragraphs.

To investigate the question fully, it is manifestly necessary to search for all the harmonics obtainable for a given position of the pin-hole branch b along the tube t. Results of this kind are given in figure 23, t length 52 cm., at positions $y=44$, 39, 29, 20, 13, 8 cm., respectively, from the telephone plate. In the first case of the lower group ($y=29$) the deflections are all very small, but a few fringes in value and largely negative. Vibration within the tube has nearly ceased. The possible low $\sharp c'$ maximum ($\lambda/4=30$ cm.), which it would have been interesting to search for, was beyond the range of the electric siren. Its occurrence is improbable. In a later trial, weak response was obtained, not at $\sharp c'$, however, but at the a below it.

At $y=20$ cm. the very marked maximum near a', already referred to, is in presence. As the pitch rises, the vibration dies out here very slowly, the acoustic pressure eventually dipping even into negative values. The curve would probably have risen again at a'', and a detailed investigation would have brought out more secondary sinuosities.

The next curve with the pin-hole probe about $y=13$ cm. from the plate is totally different from the preceding, and probably also contains more secondary serrations than the graph reproduces. Its chief maximum near f'' ($\lambda/4=12$ cm.) is again near a quarter wave-length from the plate. Nevertheless the former a' maximum has not vanished, though it is now nearer g'.

The group of curves in the upper part of figure 23, referring to larger and shorter distances y from the telephone plate, is in the main corroborative. At $y=39$, 44 cm., there is practically no vibration demonstrable at any pitch, excepting the small negative acoustic pressures near e''.

The curve for $y=8$ cm. from the telephone plate, where the chief crest should lie near c''' ($\lambda/4=8$ cm., out of range), shows accentuation of the secondary crests near $\sharp d''$ and $\sharp a'$. This is to be expected from the nearness of the probe to the plate and the irregularity of tube connection there. The c''' maximum, found later, was not strong.

Elongating the quill tube t from 52 cm. to 76 cm. by the insertion of a new section, the group of curves in figure 24 was investigated. These recall the

preceding set for the same y, so that the additional elongation has had little influence. Vibration is absent practically at $y=63$, 40 cm. from the telephone plate, and the weaker maxima begin to appear at about $y=23$ cm.; but the presumptive $\lambda/4=23$ cm. crest, which should be near f', does not appear. In its place the secondary crests are near a', e'', a''. The curves for the pin-hole at $y=20$ and $y=13$ cm. from the telephone plate closely resemble the preceding cases (fig. 23) for like distances y and similar remarks apply.

The connector quill tube t was now further elongated from $x+y=76$ to 103 cm., and the curves of figure 25 thus obtained. As usual, there was practically no displacement above a few fringes (usually negative) at $y=36$, 65 cm., etc., from the telephone plate. The excitation is low even at $y=30$ cm. What is quite unexpected, however, is the total change of the type of curve for $y=20$ cm. The former dominant a' crest has been degraded and two new maxima near f' and f'' appear wholly out of keeping with the earlier $\lambda/4$ hypothesis. The curve has merely retained its broad response to all ranges of
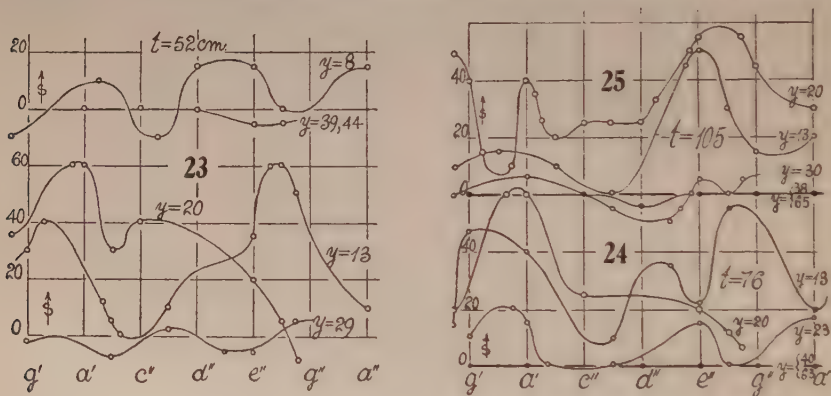
pitch between f' and a''. The curve for $y=13$ cm. is also modified. Its single high crest is still at $\lambda/4=13$ or c'', but this occurrence must now be considered incidental.

Thus the conditions of vibration within the quill tubes near the telephone are very complicated; but from the above observations as a whole one may be inclined to conclude that the dominant excitation is present only for a distance of about a quarter wave-length from the plate. If the pin-hole probe is inserted within this interval, the U-gage, with a proper selection of pitch, registers corresponding high acoustic pressures. Beyond this distance from the telephone plate, the vibrations in the quill tube are rapidly damped out and the pin-hole probe at these points produces almost no registry of pressure. It follows, therefore, that almost any length of connector tube t (fig. 22) is permissible (a convenience which will be much used below) provided the source of sound is of the kind here treated.

These data also afford a possible clue for the interpretation of results obtained in the preceding report on the air volume of the shank of the U-tube at which the acoustic pressures are measured. This volume could be increased

from a mere crevice of about 50 c. c. to nearly 400 c. c. (the largest available) without essentially modifying the registry of the U-tube. Under the impression that the volume in question partakes of the vibration, such a result seems surprising. If the region of vibration is confined to the other end of the connector tube t, the volume conditions at the U-gage may thus be of secondary consequence.

7. The same continued. Stronger excitation.—The preceding results were obtained with a telephone of rather poor response, which needed relatively strong currents to excite it (about 200 ohms in circuit). It seemed necessary to test the case with a more sensitive instrument, requiring at least 1,000 ohms in the same circuit to keep the fringes within the field. A closer approach to the U-gage, $i.$ $e.$, a shorter quill-tube length $t = x + y$ (fig. 22, inset), where y is the distance of the pin-hole probe from the telephone plate, also suggested itself as an essential supplementary test.

Results with this more active telephone, even when operating under 1,100 ohmic circuit resistance, are recorded in figure 26, where the distance $x = 13$ from pin-hole to U-gage is constant. The lower curves (t small), in comparison with those of the preceding paragraph, not only give evidence of high intensity but are relatively simple. Both point to a crest near a' and another near the octave a''. The distances of

the pin-hole probe from the telephone plate, $y = 13$ and 20 cm., respectively, recalling the former e'' and g' maxima, are here ineffective. The quarter wave-length of $\sharp d''$, corresponding to $y = 13$, and the half wave-length of $\flat a''$ for $y = 20$ have no bearing on these results and offer no suggestion. The graphs merely report that both a' and a'' evoke a strong node within 20 cm. of the telephone plate.

The upper curves of figure 26 refer to long quill-tube connectors ($t = 122$, 147 cm.), while the pin-hole remains at the same distance $x = 13$ from the U-gage. Not only has the intensity decreased throughout, but the curves are more complicated. The a' crest is particularly weakened and for $t = 122$ it has been split into an a' and c'' maximum, while for $t = 147$ it is being obliterated. The a'' crest is broadened but retains its location. Thus at points of t far away from the telephonic source, the vibration again tends to be gradually damped out.

In the development of these results two methods were followed; in the first the distance $y = 20$ cm. of probe and telephone plate was kept constant and t successively elongated from $t = 33$ to 100 cm. The graphs so obtained
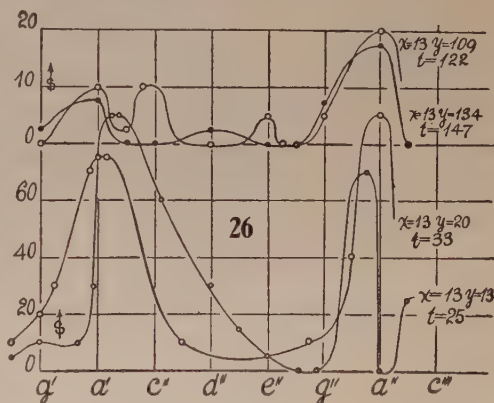
are given in order in figures 27, 28, 29. These, while evidencing much differ-
ence in detail, in their main features are not unlike. In all, the tendency to place
a crest near a'' persists, though at $t=58$ it is broadened. To a less extent the
maximum near a' is the rule; at $t=58$ this is divided between ♭a' and c'' and at $t=100$ between ♭a' and b', so that minima intervene for a'. The low pitch crests are, moreover, of much smaller intensity than the a'' crests and at $t=147$ the former seem to be vanishing. The latter fall off somewhat ($s=90$ to 60) as the tube-length t increases from 33 to 100 cm.; but these relations may be and probably are periodic, as is evident from the high value at $t=73$, and particularly at $t=147$.
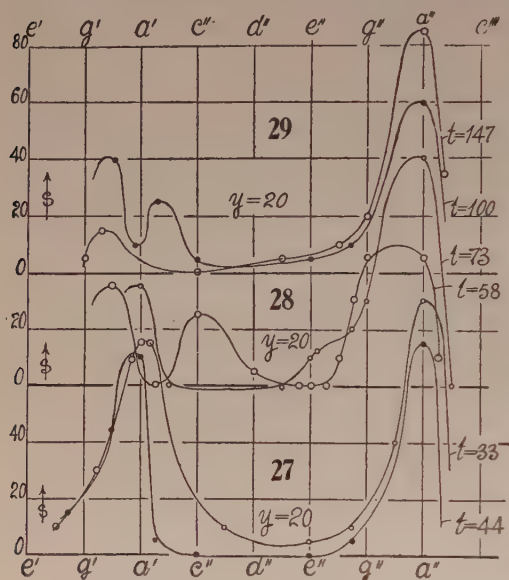
One may infer in general that the high-pitch crests with the pin-hole at a given distance y
from the telephone plate are not greatly modified by the length x of the
remainder of the tube t, while the low-pitch crests tend to vanish (as in fig. 26)
when the quill-tube length t increases.

The second method consisted in keeping $t=100$ constant and increasing the
probe-telephone distance y, successively. The graphs thus obtained are given
in figures 30, 31. These, as would be expected, are far less consistent than the
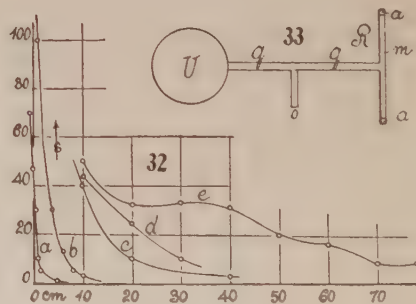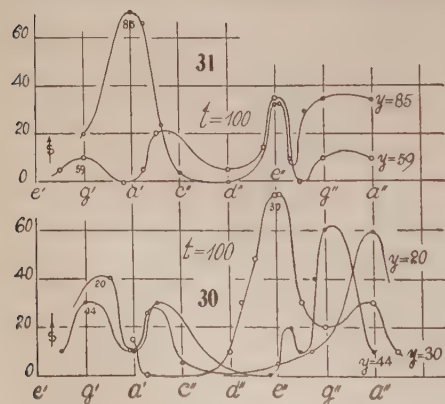
preceding set, and it is hardly practicable to adequately describe them. In
fact, one here explores the type of vibration at all positions y, through the
whole range of pitch variation. The upper crests shift from e'' to a'' and the
lower from g' to b', and there are a variety of small maxima, some of which
it was thought best to ignore.

In one respect, however, the present graphs are decisive: they completely negative the preceding results of the absence of appreciable vibration in the tube t in the part between somewhat over $\lambda/4$ from the telephone plate and the end of the U-gage. There is now no evidence of a rapid damping-out of vibrations beyond any distance from the plate within the range observed. In other words, if vibration is present at any point of the tube, then the insertion of the pin-hole probe there produces acoustic pressure, provided the point in question is the seat of a node. Thus, in figure 31, the pin-hole at $y=85$ from the telephone plate indicates a very remarkable node of pitch a', only $x=15$ cm. from the U-gage. The whole content of t throughout its 100 cm. of length is intensely vibrating; for it is not credible that the pin-hole can do more than evoke acoustic pressure, without modifying the preëxisting node appreciably.

One feature of these graphs is perhaps intelligible, even if it does not work out quantitatively in any simple way. The small values of y, figure 30 (*i. e.*, nearness to the plate), are accompanied by the location of the dominant crests in high pitch, whereas the large values of y, figure 31, evoke a high crest (if present) in low values of pitch. In figure 30, $y=20$ would imply a half wave-length of $\flat a''$, and $y=44$ a whole wave-length of $\flat g''$; if these were allowed to pass, the crest at e'', for $y=30$, should be a half wave-length of $\sharp c''$, which is quite out of accord. In figure 31 the crest at a' for $y=85$ comes no nearer than a whole wave-length of g'. Finally, it is hard to understand why, at $y=59$, the complete survey from e' to a'' strikes no dominant node or crest.

8. Excitation outside the organ-pipe. Reflectors. Capsule.—The response of the pin-hole probe falls off sheer beyond the mouth of the pipe, as shown in curve a, figure 9. The endeavor to increase this by the use of reflectors has been but slightly successful. In figure 32, several cases are given. The effect (curve b) of surrounding the pin-hole with a thistle tube (mouth 3 cm. in diameter) vanishes somewhat beyond 10 cm. from the pipe. A glass bell-jar 10 cm. in diameter surrounding the pin-hole (focused) collects (curve c) the sound-rays sufficiently to produce fringe deflections within about 50 cm. between jar and pipe. A pasteboard hemisphere, however, even though 15 cm. in diameter, was scarcely superior as an amplifier to the thistle tube.

Another method of endeavoring to amplify the fringe record of the sound-wave outside of the organ-pipe is given in figure 33. Here R is the usual capsule device of the phonograph, consisting of a metal disk R with an annular ridge aa, less than a millimeter high. To this the very thin mica disk m is carefully cemented at its edges. The center of the disk R is perforated and communicates with the U-gage U by the quill tube qq, provided with a lateral branch carrying the pin-hole o. We here return to the closed region vented at o. Disk m, of thin mica, paper, and other materials, was tried out at length, but with no greater success than the moderate results obtained with concave mirrors. Well within 1 cm. of distance between the mouth-end of the organ-

pipe and the disk m, deflections up to 60 cm. were obtainable; beyond 1 cm. the effect rapidly vanished, particularly with telephone-blown pipes. At a distance of a few millimeters the harmonics could be picked out here without entering the organ-pipe. A variety of other arrangements was tried; for instance, the pin-hole was placed in qq, close to m. The results were about the same. Possibly a shank of small volume (shell-like space) at the U-tube would contribute to increased sensitivity.

9. Continued. Resonator.—Differing from the preceding results, a spherical resonator (f''), surrounding the pin-hole, gave, even with a short quill-tube connector, a record (fig. 32, curve d) more marked than the bell-jar and an evanescence with distance far more gradual.

This device, being thus the most efficient amplifier for sound-waves coming from a distance, deserves careful scrutiny, and further experiments were made with it, using the f'' pipe and bellows and a Helmholtz resonator. The quill tube between the U-gage and pin-hole was elongated to about 300 cm. and the mouth of the resonator placed toward the organ-pipe. To avoid complications from wind currents, this was directed at right angles to the axis of the resonator prolonged, or (with equal efficiency here) longitudinally away from it. Thus no air current blew towards the resonator. The results obtained are summarized in the graph e, figure 32. The curve is more or less sinuous, probably owing, as I originally supposed, to different positions of the pin-hole tube in the mouth (which modifies pitch), to reflection from objects on the table, and to other similar details; but deflection of about 5 scale-parts was obtained even at a meter. Purity of pitch seemed to be more important than loudness of note. Thus, on surrounding the resonator, except on the front side, symmetrically by a bell-jar, 6 inches in diameter, no action at all was perceptible, in spite of the reflection from the inside of the jar. No doubt there is here an interference between the bell-jar pitch and the resonator pitch; or two wave-trains (one deformed by the reflection) cross the resonator in opposite directions and obviate any cumulative effect. It was thought that sinuosities in the graph e could similarly be referred to the interaction of direct and reflected wave-trains. Curiously enough, the f'' resonator responds slightly to a c'' pitch, indicating a common overtone in c^{iv}.

The experiments were repeated with a c'' pipe and a c'' resonator, and this gave substantially the same results, although the c'' note was much less intense than the f'' note. The following is an example of the data obtained:

Distance from pipe to resonator......	10	20	30	40	50	60	70 cm.
Deflection in scale-parts............	35	33	30	25	25	25	20

The organ-pipe blew across or away from the axis of the resonator. By careful adjustment of the pin-hole position in the resonator, deflections were brought up to 40 scale-parts at a distance of 30 cm. The resonator in the axis of a bell-jar reflector again refused to operate. In the present tests the f'' resonator did not respond.

More pronounced results were obtained with an open cylindrical resonator, 21 cm. long and 3 cm. in diameter, blowing f'' nearly. The pin-hole was in the center, the connector 300 cm. long. The presence of some cause producing sinuosities in the graphs was here very obvious in certain positions. Moreover, the largest deflection appeared while the f'' note was dying down, with slight lowering of pitch. Thus at 20 cm. the deflection of 45 scale-parts for the strong note increased to 60 scale-parts for the weak and flatted note, showing the relative importance of pitch. With this resonator it was easy to obtain deflection of 5 scale-parts and over, even at a distance of 2 meters.

Finally, experiments were tried with two pin-hole probes on a T-branch at the end of the 300 cm. connector quill tube. One pin-hole was surrounded with the c'' and the opposite pin-hole with the f'' spherical resonator. With a response to the c'' pipe alone of about 13 scale-parts, the f'' pipe alone gave 18 cm. This is less than half the above intensities for the same distance (20 cm.). Nevertheless, each pipe, separately, is definitely effective in presence of the other. When both pipes sounded together, the response was but 10 scale-parts, less than either alone, though there is some question with regard to the relative intensities of the blown notes when combined. The experiment shows, however, that the overtones in different parts of a region may be successively or simultaneouly evoked and recorded and has a bearing on the complicated curves in the earlier report.

CHAPTER II.

ACOUSTIC TOPOGRAPHY IN A ROOM.

10. Introductory.—A plan of the room is given in figure 34, where W, W' denote the unbroken walls, I the interferometer and **U**-gage, L the electric lantern, A other apparatus. The coördinates along which the surveys are to be made are x, y, z; y being between walls, x toward the open door, and z above the table T. For more refined work, I, L, A, etc., should have been removed to another room; but for my present purposes this is unnecessary.

The pin-hole probe described in Chapter I has there been found useful for the location of nodes in pipes and other vessels, both telephone and wind blown. These experiments indicated the exceptional sensitivity of the probe
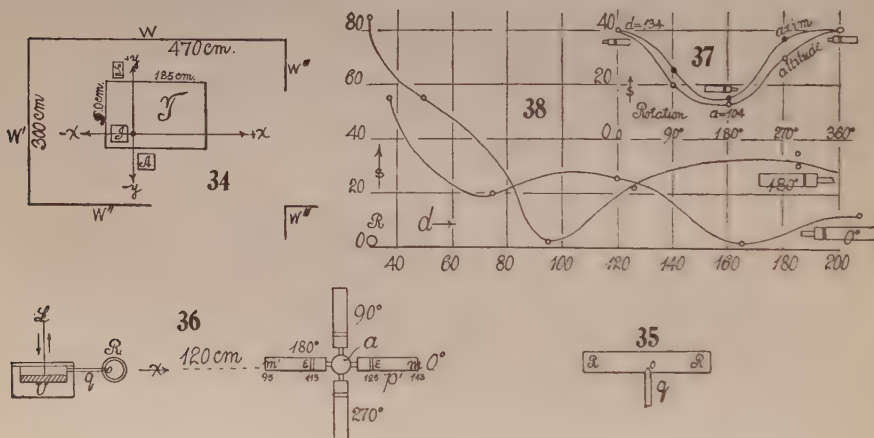
to nodes. It is relatively quite unresponsive to ventral segments or to wave-trains. The pressure variations in question are converted into static pressures through the intervention of the pin-hole and measured at a mercury **U**-gage, read by displacement interferometry. As the pipes to be employed were to be of all kinds and intensities, the fringe displacements will again be reported, as measured on an arbitrary scale, s (0.01 cm. collimator-plate micrometer). The width of a fringe was, however, on the average about 2 scale-parts ($s=2$). Thus the corresponding pressure increments p are readily found from $p=0.00015\ s$ millimeters of mercury. The apparatus can be made more sensitive by enlarging these small fringes; but these would then usually be thrown out of the field of the telescope and the screw micrometer become necessary to restore them, which is irksome, particularly with fringe **U**-gages.

The pin-hole probe at the end of an eighth-inch pure-rubber tube of any length (2 to 3 meters or more), at the other end of which is the **U**-gage, is at once available for introduction anywhere. It fails, however, to give an

appreciable acoustic record except in the inside sounding-pipes. The plan of associating the pin-hole probe with a resonator, of either the open or closed type, thus suggests itself, and a convenient form of the open pin-hole resonator is shown in fig. 35.

11. Pipe axis varying in altitude and azimuth.—The work with resonators was at first very confusing because of the lack of consistency in the results obtained on different days. Thus the old cylindrical resonator A, at long distances, sometimes gave no fringe displacement above 1 or 2 scale-parts; at other times 15 scale-parts at 130 cm. and 10 scale-parts at 200 cm. were the rule, or even more than this (15 scale-parts at 200 cm.). Three open cylindrical f'' resonators of different diameters were therefore provided and tuned on the interferometer by comparison with the f'' pipe at 50 cm. The initial results were:

	Length.	Diameter.	Deflection (scale-parts).
	cm.	cm.	
A	21.4	3.1	$s=23$
B	21.7	4	$s=13$
C	23	2.1	$s= 2$

This tuning by elongation must be carefully done to at least 1 mm. in length; otherwise the response dwindles rapidly in distance. The adjustment must be made, moreover, not by blowing the resonator, but by the interferometer test for resonance at a small distance (50 cm.). The final result was that C overtook A in sensitivity, whereas B showed little improvement. In the tests at $d=200$ cm. between f'' pipe and resonator, the axis of the latter was placed across the line of junction for greater symmetry. The position of the pin-hole was in the middle of the resonator. With distance, $d=200$ cm.

A, $s=15$ scale-parts B, $s=10$ scale-parts C, $s=20$ scale-parts

These results for s did not greatly diminish, even at $d=300$ cm., so much depending on the pitch of the f'' organ-pipe, whether awakened by a forced or by a dying air current. In the latter case, with the gradual depression of pitch, however small, the deflections usually fall off in steps, showing definite response to intermediate harmonics. It made little difference here, moreover, whether the quill-tube connection of pin-hole probe and **U**-gage was long (300 cm.) or short (20 cm.), so that the short connector was used for convenience, a quill-tube elbow putting the pin-hole into the middle of the resonator. Hourglass-shaped resonators (open double cone with pin-hole at the gorge), from which I expected increased sensitivity, were failures throughout; but as the resonator of small diameter (C), after tuning, was more efficient than either A or B of larger diameter, C was preferred for the following experiments. It (RR, fig. 35) was later provided with a central lateral tubulure, securing the pin-hole probe qo, without leakage.

I had frequently noticed, when the organ-pipe at a distance (200 cm.) gave a marked fringe deflection, that practically no response was obtained on moving the organ-pipe to a new position only 1 or 2 feet away on the same radius and with no change in the orientation of the pipe. The resonator was therefore now in a region which, on a much larger scale, would be called a sound shadow, though this term is here inapt and misleading. I shall call them null regions. The room (fig. 34) in which the experiments were made was an alcove about 5 meters high. The effect produced at the resonator would thus have to be an aggregate of the multiple reflections reaching it from all directions.

An early method of exhibiting the distributions in question consisted in the rotation of the f'' organ-pipe, on a long radius, through its axis in a plane either normal and symmetrical to the axis of the resonator or in a plane through the axis. The installation is shown in elevation in figure 36, where U is the closed shank of the **U**-tube, R the open cylindrical resonator seen end on, o the pin-hole on the quill tube, q, p the organ-pipe in its first position (90°, 180°, 270° following), a the axle and wind-supply device. The distance Ra was 120 cm., Rm' 95 cm., RE' 113 cm., RE 125 cm., Rm 143 cm. The pipe is from 17 to 18 cm. long from mouth m to embouchure E. Thus the mouth is nearly half a meter nearer R in the position 180° than in the position 0°, and yet the effect on the resonator is here much stronger for the altitude 0° than for the nearer altitude 180°, as indicated by the graph, figure 37, where little circles indicate the results for rotation in a vertical plane (fig. 36) and black disks the rotation in a horizontal plane. The mean distances in centimeters of pipe and R are marked d.

Owing to the change of pitch with the loudness of the organ-pipe, it is difficult to get a smooth curve; but the marked effect at R of the azimuth or altitude of the pipe is none the less evident. I was at first inclined to look for interferences between the wave-trains issuing at the mouth and at the embouchure of the pipe, 17.5 cm. apart. The wave-length of the f'' pipe is about 48 cm., however, and a change of path difference from the 0° to the 180° orientation, for instance, effective at the ends of the resonator, seems unlikely. These path differences are practically identical.

12. Continued. Pipe acting from different distances.—Further information as to the active and null regions in the room may be obtained by changing the distance between the fixed resonator R and organ-pipe, for a definite orientation of the latter in altitude. To do this, I attached a long board to the table, with the distance for R marked upon it, and then successively slid the pipe, held in a standard about 30 cm. above the board on the average, from position to position. These distances trend ($+x$ direction) toward the open side of the room. Beginning with the 0° (pipe-mouth away from R) for the pipe-axis and using a note of mean loudness, the curve 0° given in figure 38 was obtained. The curve is markedly sinuous and there is a null region at R when the pipe is about 160 cm. away from it. Rotation of the pipe on its own axis, except when very near R, did not in general make any difference.

In contrast with this, the survey for the pipe altitude 180° (mouth towards the resonator R) is a totally different curve. Here R is in a null region when the pipe is at a distance of about 100 cm., and the sinuosities are differently placed. Maxima and minima in the 0° and 180° graphs are almost inversions of each other. There are greater fringe deflections at the beginning, as the pipe is much nearer the resonator. Rotating the pipe on its axis here, the wind from the embouchure may produce complications. Similarly, figure 39 gives the graphs for pipe altitudes of 90° (mouth up) and 270° (mouth down). The curves are again markedly different from each other and from the curves of figure 38. In the 270° curve the pipe-mouth is relatively much nearer to the resonator than in the case of the 90° curve for the same mean distance, and hence the former shows much greater fringe deflections here.
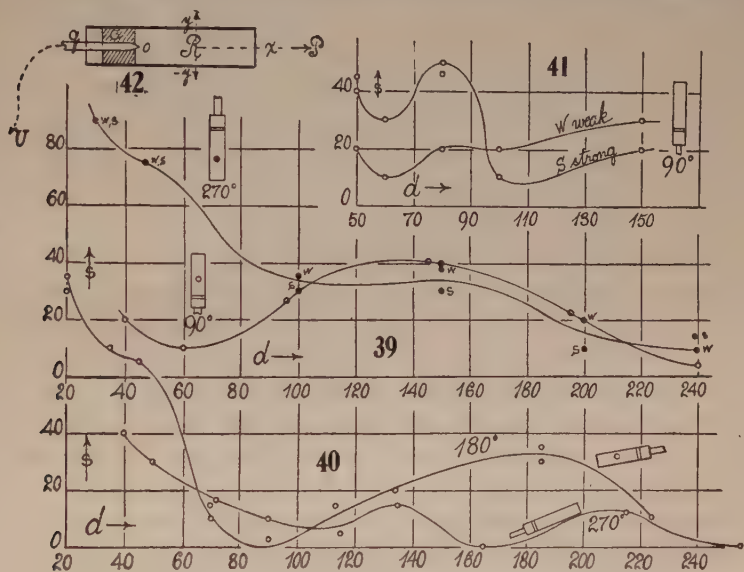
In fact, at the mean distance of 15 cm. the fringes are thrown out of the field of view. There are no null regions at R, except when the 90° orientation is too far removed for discrimination (240 cm.); but it is curious that the fringe deflection is greater at 160 cm. than at 60 cm. In case of the 270° orientation, I tested both a weak, but full, and a strong forced pipe note, the data being distinguished in the figure by W and S. There is here relatively little difference, possibly because the mouth of the pipe is near the table, but one may notice that W and S are reversed beyond 200 cm. In the other orientations, however, the difference is often of great moment.

Accordingly, in figure 40 I repeated the experiments with slightly different altitudes (pipe-axis prolonged passing through R), for intermediate points d and for longer distances. In case of the orientation 180° the graph is practically the same as before; but for 0° and within 150 cm., a soft note being aimed at, it is quite different. The reason for this (as the sequel will show)

is to be referred chiefly to an insufficient appreciation, in this preliminary work, of the importance of small lateral differences of location for the same radial distance. In addition to this is the uncontrollable annoyance of slight but effective changes of organ-pipe pitch. There are now two null points, the old one at 160 cm. and a new one at about 250 cm.

The effect of soft (W) and loud (S) notes was specially studied in the 90° orientation (fig. 41). The W graph is of the same nature as the preceding curve (fig. 39). The S graph, however, differs from it materially, and here again there is an inversion between $d=90$ cm. and 100 cm. from R.

The relations met with in these cases are thus complicated by the overtones of the pipe and inadequate sharpness of the resonator. Overtones are usually evoked by an impulsive blast at the beginning. If the identical intensity of air current is gradually reached, no overtone is awakened. This phenomena was frequently noticed in the course of these experiments, a large fringe deflection persisting after an abrupt increase of the intensity of blowing, whereas a gradual growth to the same intensity produced but little deflection. Again, the change of pitch accompanying diminished intensity of blowing is immediately felt by the resonator, which often responds more strongly to the weaker note. In spite of all these misgivings, there is no doubt that the curves reproduce, though as yet crudely, because the steps in distance are too long throughout, actual conditions in the room, which itself endeavors to vibrate, possibly like a large organ-pipe, under the excitation of the small pipe within. Overtones are awakened in every special case with distinct relations to the room, depending on the position of the exciting pipe. Such distributions would necessarily be fluctuating, or very mobile in position, with small differences at the pipe, resembling the behavior of the stratified column of a cathode tube. In fact, the organ-pipe itself holds a compressed bundle of stream-lines within, as it were, very much like an electric coil grasps its magnetic lines of force. They escape at once, as seen in the graph a on the left of figure 9, diverging rapidly into space as soon as this confinement is relaxed. Such analogies must be used cautiously, however, since the sensitiveness of the pin-hole probe depends essentially on the proximity of nodes. It will not register a simple wave-train in free air.

13. The closed pin-hole resonator.—In the preceding paragraph the outstanding trouble encountered was ascribed to the organ-pipe, *i. e.*, to the continuity of notes lying very close together, but to only one of which the resonator responds effectively. A further difficulty is referable to two ends of the open cylindrical resonator (fig. 35), with a pin-hole in the middle within; for these ends, being 22 cm. apart, are liable to lie in regions differing acoustically. The advantage of the tube is the ease with which it may be accurately tuned by mere elongation, and hence its sensitiveness. The Helmholtz resonator, probably for this reason, was found much less responsive.

Hence the closed pin-hole resonator qR, figure 42, consisting of the cylindrical tube (1.9 cm. diam., effectively 22 cm. long) R, closed by the snugly fitting cork c, which carries the pin-hole probe qo, is preferable. The pin-hole o is at the base of the tube R, the quill tube q being connected by a length of gum-rubber tubing (2 meters) with the **U**-gage. This resonator has but one mouth and thus tests acoustically a single point, as it were, of the region, while the tuning may be effected with nicety by moving the cork c within R, or by elongation at the mouth of R.

The endeavor to increase the sensitivity of the closed resonator, by placing other resonators judiciously near it, met with no marked success. If the distance between the organ-pipe and the closed resonator is partly bridged by an open resonator, the deflection may sometimes be increased 20 or 30 per cent, but this would be anticipated. In all other azimuths the open resonator is liable to reduce the deflection even as much as 50 per cent. Indeed, at a distance of 10 cm. between the nearer mouths of the resonators, the reducing effect was still appreciable. Under other circumstances, difficult to state, a similar small increase of sensitivity may occur; but the expectation of relaying the closed pin-hole resonator by a sequence of auxiliary resonators adjusted with regard to it met with failures only.

I may here also advert to the difficulty of constructing a sensitive pin-hole resonator, either of the closed or open cylindrical type, simple as the device appears. Most of them give no deflection whatever, even when tested with a variety of pin-holes and when carefully tuned. There seems to be some relation between the pin-hole probe and the resonator very difficult to ascertain. Long and patient trials with all manner of devices netted me but one closed and one open resonator adequately sensitive; and these were obtained by mere accidental combinations of pin-holes and a variety of tuned cylinders. The endeavor to replace the pin-hole by a porous diaphragm (filter-paper) was in vain. The paper must be pricked and then not more than once. Elsewhere I have mentioned the disturbing effect of small objects on the table near the resonator. Even the clamps and standards should be as distant as possible. Finally, a given initially good resonator (metal foil) in the lapse of time often seems to lose its virtue. A reduction of sensitivity to one-fourth or one-fifth of the original value was met with. The whole subject will be systematically treated below, §§ 34, 35.

In a series of experiments made somewhat later, I met with better success by using conical glass tubes. Carefully grinding off the end, one eventually arrives at an optimum, the hole being somewhat larger than used in the experiments heretofore. It was further brought out that for pressures the pin-hole must be salient, _i. e._, at the point of the tube. The same size of hole (or two or more holes) at a blunt or reëntrant end of a tube gives scarcely any deflection whatever. If the pin-hole is carried backward from the bottom of the closed resonator by a capillary tube the deflection grows rapidly less with the length of the tube.

3

14. Transvere (y) acoustic survey.—The preceding survey, made in the direction RP, figures 34, 42, toward the open end of the room, by moving the organ-pipe, may be referred to as longitudinal in the x direction. The present survey, made by moving the resonator R, figure 42, parallel to itself, is thus transverse (y direction), and it may be further desirable to test the distributions along a vertical (z) through R, all for a fixed position of the organ-pipe. This plan of attack, by moving the sensitive small resonator on a long rubber tube (2 meters long, $\frac{1}{8}$-inch bore), is in many respects preferable, so that it may be additionally necessary to repeat the longitudinal survey by moving R for a fixed pipe and to rotate the axis of R relatively to the coördinates chosen. The work involving so many permutations is inevitably confusing, and small insets showing the position of pipe and resonator relative to each other will be found attached to each curve. The rotation for altitudes is that of figure 36, 0° referring to a trend toward the open end of the room. In all the present cases the pipe was at $x=0$, $y=0$, and at $z=40$ cm. above the table, as this was sufficiently remote to prevent direct air-current effects, even at $x=0$ and $y=0$. Negatives x and y were practically inaccessible because of apparatus,
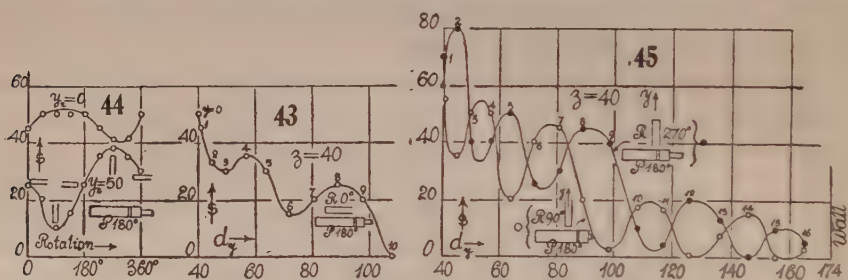
and negative z is below the table. Guided by the above experience, it is necessary to make the observation in successive small steps of $\Delta y=10$ cm. Accordingly, the resonator was successively displaced from $y=0$ to $y=170$ cm. in decimeters. In the graphs it was found convenient to introduce the oblique distance $d=\sqrt{y^2+40^2}$ between *centers* of organ-pipe and resonator; but the coördinate value (y) is given in small numerals in *decimeters,* on the graphs, at each point. In all these cases the pipe is oriented at 180° in altitude, *i. e.,* the mouth pointing from the door of the room. The wall is at $y=174$ cm. from the pipe.

In the first series, figure 43, the exploring resonator is in azimuth 0°. The graph is sinuous, neatly outlined, and consistent. The horizontal wave-lengths from maxima are $\Delta y=40-0$; $80-40$; $2(100-80)$ cm., or about 40 cm.; from minima, $\Delta y=65-30$; $100-65$, or 35 cm. The pipe λ is, however, 48 cm.; and although the two former are less than the latter (pipe 40 cm. high), they bear no immediate relation to it. For it is difficult to account for the approximate constancy of the λ found, unless there is stationary wave-production by virtue of reflection from the $+y$ wall. In such a case the organ-pipe at $y=0$, $z=40$ cm. and its image at $y=350$ cm. and $z=40$ cm. behind the wall coöperate, sending out wave-lengths of 48 cm. and nodes about 24 cm. apart in

the track of the resonator, and it will presently be argued that nodes probably coincide with the crests or maxima of the graphs. It seems advisable, however, to postpone this discussion until a larger number of relevant data have been gathered. A contribution which immediately presents itself is given by the rotation of the resonator in azimuth, at a fixed position along y. The results obtained in this way for rotations in steps of $45°$ are shown in figure 44, the upper curve referring to the mean position of R at $y=0$ and the lower to the position $y=50$ cm. The two graphs are opposite in phase, though the curve for $y=0$ is not as striking as would be anticipated from the nearness of R to P. At $y=50$ cm., however, the azimuth $90°$ corresponds to a pronounced minimum and the azimuth $270°$ to an equally pronounced maximum. Consequently, in making a further survey in y, these two azimuths, when the centers of P and R are coördinates, should be chosen for contrasts.

The two series of results (pipe in azimuth $180°$ at $y=0$ and resonator in azimuth $90°$ and $270°$, respectively, with its center at y) are given in figure 45. The curves are pronouncedly harmonic from $y=0$ to the wall, and they are almost exact inversions of each other, crests in the one taking the place of troughs in the other throughout. Moreover, the crests seem to lie in successive levels: an initial high one ($y=10$ to 20 cm.); an intermediate lower one ($y=30-80$ cm.); a still lower one (100 to 140 cm.) beyond, etc. It is not feasible to go much beyond 160 cm., for with the wall at 174 cm. the resonator pitch is beginning to be modified. A curious result is the highly developed initial maximum and minimum, the position being not at the nearer $y=0$, but beyond, at $y=20$ cm. The horizontal wave-lengths Δy to be obtained roughly from these curves are successively:

R-azimuth, $90°$:
    Crests......... $\Delta y = 35$, 31, 38, 31, cm.
    Troughs...... 31, 41, 30, 35, cm.   Mean $\Delta y = 34$ cm.
R-azimuth, $270°$:
    Crests......... $\Delta y = 30$, 33, 37, 34, cm.
    Troughs...... 35, 29, 41, 35, cm.   Mean $\Delta y = 35.5$ cm.

The precipitous descent of the graphs between $y=70$ and 90 in one case and $y=90$ to 100 in the other makes less impression than would have been anticipated, and the mean wave-length here, $\lambda = 35$ cm., does not differ from the preceding case of $\lambda = 37$ cm. by more than the observations of a single curve. The graphs, figure 45, were obtained independently, one after the other.

If, instead of the y coördinate, the distance d_y between the centers of resonator and pipe be taken, the data are as follows:

		Maxima					Minima			
Resonator, $90°$...	40	53	77	112	140	170	45	65	99	126	157 cm.
$\Delta d =$		13	24	35	28	30	20	34	27	31	cm.
Resonator, $270°$.. ..	45	64	93	126	156		..	53	75	114	146 cm.
$\Delta d =$		19	29	23	30			23	38	32	cm.

The first Δd is always small as compared with the remainder. Excluding it temporarily, the means are 29 and 26 for maxima and 30 and 33 for minima. There is no effect discernible, attributable to the position of the mouth, which

is in excess of y at 90° and the reverse for 270°. The mean interval is about 30 cm., which is nearer the semiwave length $\lambda/2=24$ than the preceding case; but it is still much too large, even if the uncertainty of measuring relatively to the bulky pipe be considered. However, it contains a suggestion that the d's may be more closely associated with the interpretation than the y's, seeing that one is here virtually dividing the table into half-period elements.

Now, in the line PP', 40 cm. above the table from pipe to pipe image, the nodes should follow each other at a distance of $\lambda/2=24$ cm. apart; but as the distribution above and below is hyperbolic, the nodes at the level of the table must be farther apart. Unfortunately, the equation is cumbersome; for if r is the radius vector from the source to a node at the table (40 cm. down) and $r'=r+n\lambda/2$, the corresponding radius vector from the image to the same node, and if $z=40$ cm., $\lambda=48$ cm., $\sqrt{(r+n\lambda/2)^2-z^2}+\sqrt{r^2-z^2}=350$, the distance from source to image. Knowing r' and r for two consecutive values, $n+1$ and n, the distance apart of corresponding nodes is found by projecting the two values of r or r' on the line PP'. Without attempting to carry this out here, it is easily seen that the increased distance so obtained is inadequate; $i.$ $e.$, not as large as the 35 cm. and over found in the experiments, in place of $\lambda/2=24$ cm. estimated to increase to 27 cm. or 29 cm. One should expect 7 or 8 nodes in place of the 5 or 6 recognized. It seems unlikely that a frequency of a near order can be contributed by the room itself, and the reflected waves, returning from 2 meters, would seem to be too weak to compete effectively with the outgoing wave-trains. Furthermore there is another wall (fig. 34) in the direction of negative y (at $y=-130$) and one at $-x=190$ cm.; and although instruments lie in the paths here, they only introduce further complication. However, the apparent result that the room, stimulated between walls by the strong pipe-note f'', responds with a stationary wave-train approximately in the pitch of bb' is of course out of the question.

There remains the reflection from the table, so that the pipe and its image 40 cm. below the table make the plane of the latter a region of reinforcement, or, with regard to the loss of $\lambda/2$ at the surface, a locus of nodes, though the term node would be strictly applicable only for the case of normal incidence near the line-pipe image. The next nodal locus is hyperbolic and therefore higher than 25 cm. above the table, out of reach of the resonator, which lies on it. Thus it is finally necessary to compound the phase reversed direct ray here in question with the corresponding phase reversed reflections from the walls, to get the disturbance at any point of the table. This succeeds experimentally, as I will point out presently, for walls close at hand (within a meter or two); but for walls as distant as those of the room, the reflection-wall effect is too small to account for variations as marked as those of figure 45. It is possible that a wide high wall, like W, may act obliquely by diffraction; but to speak on this subject, further inquiry will be needed. As a general fact, however, it is noticeable that a survey in y, between walls, produces a much more marked harmonic distribution of acoustic pressure along that axis than a similar survey along x toward the open door.

The striking opposition of phase which figure 45 presents for an inversion of the resonator on its middle point as an axis is perhaps more easily intelligible. As the length of the resonator is approximately $\lambda/4$, the rotation of 180° about its center will pass the mouth from a node to a loop of the stationary wave-train, or between corresponding 90° phase differences. Now, the pin-hole probe is sensitive to nodes (compressions) only and scarcely responds to wave-trains (or to the similar harmonic motion at the loops). The pin-hole resonator, however, might be thought to have the opposed quality, being stimulated by wave-trains (or loops) and probably to be insensitive to nodal phenomena or compressions. But (§ 16) this inference is not correct. We must therefore anticipate nodes at the maxima of the graph and loops at the minima, when the pin-hole resonator is used. In the same way null regions otherwise obtained are probably of the nature of ventral segments. The pin-hole alone, being far less sensitive, will usually give no record, except near the nodes within pipes. It follows from this that if half of the length of the resonator be added to the y coördinate of one of the graphs of figure 45, and half the same length be deducted from the other, i. e., if the mouth of the closed resonator be taken to define the y coördinate, the two curves of figure 45 will be found to coincide at their mean position in y. Hence, if the resonator is rotated in azimuth on a vertical axis passing *through its mouth,* the data obtained should be independent of azimuth. The experiments which follow will bear this out.

15. Further longitudinal (x) surveys.—For further elucidation (figs. 46, 47), I carried out four surveys along the positive x-axis, by moving the resonator along the table, in steps of 10 cm. The f'' pipe at $x=0$ was, as before, 40 cm. above the table and kept in azimuth of 180°. The curves refer to the azimuths 0°, 90°, 180°, 270°, and to the x-coördinate of the axis through the middle point of the resonator. The conditions are here very different from the preceding case, as x points toward the open door and there is no continuous wall near at hand. So far as the curves go (within a meter), only the azimuths 0° and 180° give promise of periodicity, and this is slight. The horizontal wave-lengths, so far as discernible, do not exceed 30 cm. Thus the region of positive x is less favorable to stationary wave phenomena.

The attempt was made to complete the subject by a survey in the direction of negative x (fig. 48); for this also is shut off by a wall at $x=-180$ cm. The pipe standing as above ($z=40$ cm.), the resonator ($z=0$) was oriented at 0°. Unfortunately, the interferometer apparatus (see fig. 34) was located on the line between 0 and 50 cm., so that the pipe-note was diffracted around and the resonator moved one side of it. The graph, figure 48, shows a mere dwindling of intensity here; but it is interesting to observe that as the wall is approached there is increased indication of periodicity. A mean horizontal wave-length of about 35 cm. may be made out. The inset in figure 48 gives the usual effect of rotating the pin-hole resonator at $x=-110$ or $d=117$ cm. for a somewhat different mounting.

Figures 49, 50, 51 are results obtained by moving the *pipe* ($z=40$ cm.) in the direction of positive x, for different azimuths of the pipe and resonator fixed at the origin. The steps in the two former are too large, and the curves merely indicate totally different distributions. This was remedied in figure 51 for different azimuths of the resonator ($z=0$). The graphs, nevertheless, are still largely decay curves. The case of R 90° and P 180° shows a null region at the origin, when the pipe is at $d=80$ cm. or $x=70$ cm., and the promise of
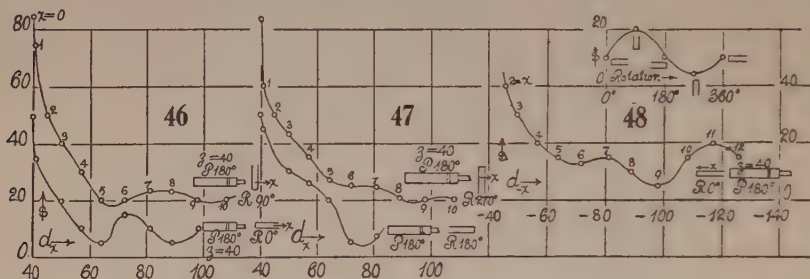
periodicity beyond. The orientations of figure 52 with the pipe ($z=40$ cm.) at 270° moving in x and the resonator ($z=0$) at the origin, at 90° and 270° in azimuth, seemed to be better adapted for a detailed survey. The case for R 90° is now a compound harmonic, which seems to dip into stationary wave-trains at a and b. The other curve is quite similar in general character, only less pronounced. Horizontal wave-lengths exceeding 35 cm. may be detected at the double inflections. I had hoped from the two positions of the resonator to get something akin to the open-pipe resonator charts (above, fig. 39, P 270°), but the latter is insufficiently detailed.
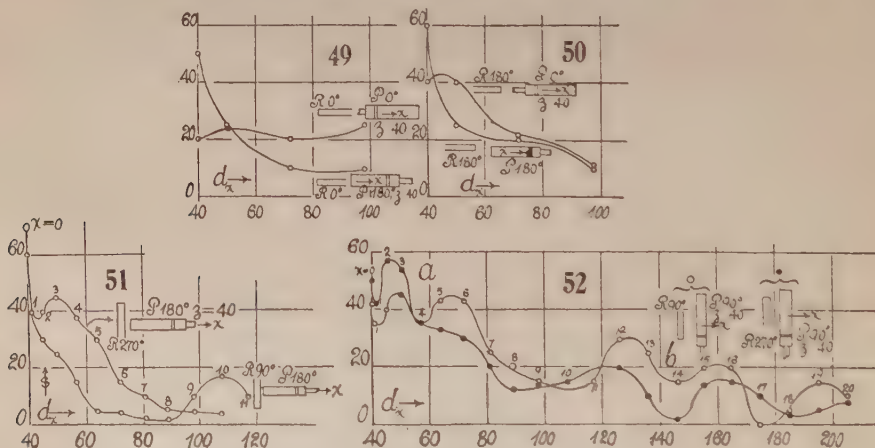
To contrast with the above data for the closed resonator, I also made a survey with the open resonator, both in the 0° . . . 180° and the 90° . . . 270° positions. The graphs obtained (here omitted) were largely sinuous decay curves with few marked features, the former case (0° . . . 180°) being particularly even. This is what would have been expected, since the open resonator may be regarded as comprising two closed resonators, with a common

nodal plane in the middle. Figure 45 would therefore lead us to anticipate partial neutralizations at least at remote positions in y, since the mouths of the resonator are $\lambda/2$ apart.

16. Survey in the vertical direction (z).—This was carried out by allow-ing the resonator to rest horizontally on the table, in a direction normal to the f'' pipe, the latter being raised successively in steps of 10 cm., keeping it in the same azimuth of 0°.

With the resonator at the origin and the f'' pipe at $x=30$ cm., figure 53, the curves are smooth and low, showing little detail, for the two positions of the resonator tested. It is noteworthy, however, that maxima appear at $z=40$ cm. above the table rather than at the smaller z values.

The resonator was now also brought to $x=130$ cm. vertically below the pipe (figs. 54, 55). The first graph (fig. 54) shows very definitely that after $z=30$ cm. there is unmistakable periodicity, with a wave-length of not much larger than 20 cm. Here is therefore a new result, referable, no doubt, to the stationary waves produced by reflection upward from the table. For this reason it seemed desirable to repeat the work with a new installation admitting of larger displacements in z. The graphs (fig. 55) for two positions of the resonator are essentially identical and nearly so with figure 54. The z distance between crests and troughs, however, now varies between 24 and 25 cm., and thus corresponds very closely to the semiwave-length, 24 cm., of the f'' pipe. In all cases the pipe must be raised some distance (40 cm.) before the periodic distributions begin.

The behavior here in evidence is very much like Melde's experiment, though it is now made with a string of air (as it were) between the actuating organ-pipe as one attachment and the table as the other. The only adjustment pos-sible is thus the length of the string. Since the resonator lies on the table, certainly to be regarded as a nodal surface, we look for the maximum of wave-production when the direct and return wave-trains coincide in phase at the mouth of the pipe. This will take place at intervals of $\lambda/2$, or $\Delta z=24$ cm. apart, conformably with the graphs. It would seem, however, that the maxima (in view of the loss of $\lambda/2$ at the table) should lie at $z=5\lambda/4$, $7\lambda/4$, etc., whereas in the graphs they lie at $2\lambda/2$, $3\lambda/2$, etc. The latter put a node at the mouth of the f'' pipe. This result is very important.

The x position of the vertical line of pipe and resonator is also effective. At $x=0$, for instance, the deflections were nearly uniform between $z=30$ and $z=115$ cm., varying but from 10 to 15 scale-parts, with a maximum near $z=60$ cm. For this reason a survey in z at different positions, $x=50$ and $x=80$ cm. (fig. 56), did not lead to additional results, the periodic curve being uncertain beyond $z=70$ cm.

Similarly,[*] with the pipe kept at the table ($z=0$) and the resonator raised vertically above it, the sinuous decay curves obtained (fig. 57) were without

---

[*] There is something about the pin-hole resonator which causes it to function with different sensitivity on different days, without any other interference whatever. The reason for this I have not been fully able to detect. It may be associated with the difficulty of constructing the resonator, to which I have already referred, but the contact breaker of the electric siren is more liable to be at fault.

novelty, except so far as they furnish strong corroborative evidence bearing on figures 54 and 55.

As the table is certainly a nodal surface, we here encounter the unexpected result of special sensitiveness to nodes on the part of the mouth of the pin-hole resonator. The opposition of phases instanced in figure 45 for a reversal of this resonator would have suggested the contrary opinion. The case is carefully tested in figure 58, where the pipe in azimuth 0° is $z=90$ cm. above the table, and the resonator vertically below the pipe is raised from the table at $z=0$. The evidence given by the curve is very satisfactory, the wave-lengths of the graph being 24 to 25 cm., or semiwave-lengths of the f'' pipe. There is complete absence of deflection at 10 to 12 cm. above the table, i. e., at $\lambda/4$ for the pipe, so that the ventral segment is inactive. As the pipe at $z=90$ cm.
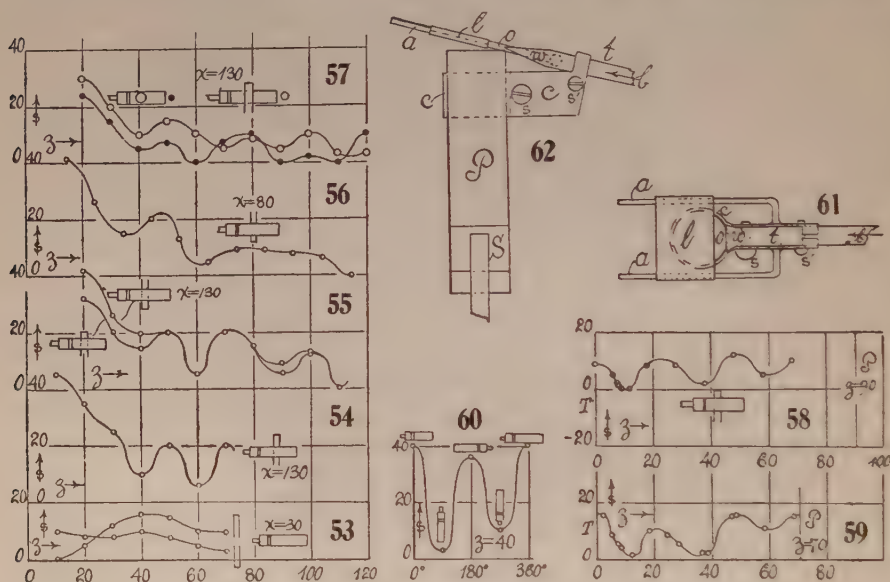
is approached by the resonator, the deflections naturally increase, but they do so very slowly. Obviously the present disposition with a raised pipe and with the resonator between pipe and table is the best of the methods tried for the z survey. Because of the important evidence obtained, I repeated it for an f'' pipe at $z=70$ cm. (nearly $3\lambda/2$). The results in figure 59 are of the same kind as to wave-length, inactivity for a resonator 12 cm. ($\lambda/4$) above the table, the marked effectiveness (maximum) of the distant node at the table ($z=0$) and a maximum near the pipe ($z=68$ cm.). Troughs and crests lie at positions which are multiples of $z=12$ cm. ($\lambda/4$).

The above results for normal reflection may be summarized as follows: Both the organ-pipe and the pin-hole resonator are stimulated in proportion as their mouths lie in a nodal region or surface; they remain relatively uninfluenced by a ventral segment. Consequently, an even number of half wave-

lengths lie between pipe and resonator when the response is a maximum. Although the mouths of the respective pipes are necessarily ventral segments, the anomalous features of these results disappear when it is remembered that the stimulating nodes are alternately dense and rare.

Conformably with the above, one might infer that in case of oblique reflections also, the highest crests will appear when the reflected note is returned in phase to the pipe; but this does not seem to be the case.

It remains to rotate the pipe in altitude (vertical x plane) on an axis passing through the node, $z=40$ cm., above the table on which the resonator lies (in azimuth 270°), below the pipe and normal to it. The graph is given in figure 60 and shows maxima for the horizontal positions and minima for the vertical positions of the pipe. Seeing that the mouth of the pipe is much nearer the resonator when the pipe points down, this result is striking.

17. Closed organ-pipe as a source.—This has the advantage of a single mouth, like the closed resonator. The endeavor to blow such a pipe with a telephone, as heretofore, was unsatisfactory. The note is much too fluctuating in pitch and, being richer in harmonics, is ill suited to the closed resonator. On rotating either pipe or resonator, the deflection depends on the distance between their mouths: at 10 cm. the deflection was but 22 scale-parts; at 3 cm. this increased to about 35 scale-parts, so that the pipe pointing downward gives the largest results, whereas if it points upward the deflection is scarcely 5 scale-parts.

In view of these complications, a loud, closed organ-pipe, to be blown by the bellows, was provided, constructed in plan and elevation as in figures 61, 62, where P is a thin brass pipe about 1 inch in diameter and 6 inches long, closed below with an oiled stopper S, for tuning. It is blown by the pipe-blower bwl, described in the last report (Carnegie Inst. Wash. Pub. No. 310, §§ 45, 46), where t is a ⅜-inch thin copper pipe, pinched down to a fine wedge at w. The current of wind b from a bellows produces at w a thin lamina of air, which strikes the sharp metallic lamina l, adjustable on the slide a. The embouchure O is thus adjustable. By setting $twla$ at an agle of 20° to 30°, an exceptionally loud note is producible, because of the large aperture of escape; but as the pitch decreases rapidly with the angle, the blower must be rigidly fastened. This is done by the collar cc of strip metal, tightened by the screw s. The bent ends of the strip grip the tube t as shown and are appressed by the screw s', the edge of the wedge w reposing on the edge of the pipe. The loud pure tones are easily tuned.

The deflections obtained with the new pipe were relatively large, for rotations of the pipe at a mean distance of $z=20$ cm. apart threw the fringes completely out of the field of view, except for the azimuth 270° of the resonator, when the pipe-mouth was down (minimum distance between mouths, 10 cm.). This available azimuth of the resonator was therefore retained and the pipe vertically over the resonator rotated in altitude (in the vertical x-plane), with

the results shown in figure 63. These data (maximum for mouth down and minimum for mouth up) seem to be largely referable to the distance between mouths of pipe and resonator. Figure 64 gives the results for rotating the resonator in azimuth with the pipe horizontal. Here, also, distance is the main feature; but the data suggest the suitable adjustment for an extended probing along the y coördinate (fig. 34), measuring distances between centers of resonator and pipe.

The first survey in y, figure 65, was made by keeping the pipe horizontal (in altitude 180°) at a mean distance of $z=20$ cm. above the table on which the resonator lay. The two graphs obtained within about $\Delta y=160$ cm. (the wall being at 174 cm.) refer to the azimuths 90° and 270° of the resonator, as in figure 45. Figure 65, however, is laid off in terms of y. If figure 45 be also drawn in terms of y, the figures, as a whole, are not dissimilar. There is much less detail in figure 65, which may perhaps be attributed to a louder pipe and a less sensitive resonator. We observe the same initial high plateau terminat-

ing beyond $z=20$ cm., an intermediate plateau still quite high extending beyond $y=70$ cm. (in figure 45 beyond 80 cm.), and a final lower plateau. Figure 65 is somewhat shifted throughout compared with figure 45 and presents no approximately definite wave-length in the compound graphs, which nevertheless tend to be inversions of each other. The mean elevation, $z=20$ cm., of the pipe in figure 65 is too small, being but half that in figure 45, so that larger z values must be tried when other pipe-altitude angles will also be available.
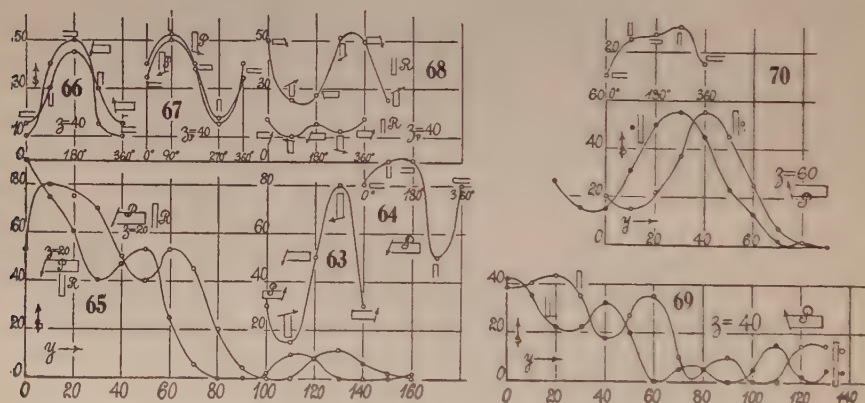
18. The same continued. Pipe at z=40, 60 cm., etc.—In the preceding experiments the rays of sound strike the table at large angles of incidence; in the main almost at glancing angles. It is, therefore, desirable to raise the pipe successively, keeping it in the same orientation as before (horizontal, azimuth 180°) and retaining the two positions (azimuth 90° and 180°) normal to the pipe of the resonator on the table. Distances are still measured between centers.

The effect of rotating the resonator is given in figure 66 for the horizontal pipe at $z=40$ cm., in one case blowing up, in the other down. There is very

little difference (the down blow would naturally be a little stronger from reflection and greater nearness), so that the rotation of the pipe on its own axis through the mouth is not of consequence. It is noticeable, however, that maximum deflections occur when the resonator is in 180° of azimuth, $i. e.$, parallel to the pipe and in the same sense, with a minimum for the opposite case. In the preceding paragraph this orientation threw the fringes out of the field, so that the 90° and 270° cases are here also retained for comparison.

Figure 67 shows the results of rotation of the resonator for a vertical pipe (mean $z=40$ cm.) with the mouth downward. Here the maxima and minima occur at a resonator azimuth of 90° and 180°, respectively. Rotating the pipe in its own axis is of no consequence, as the two curves indicate. They furthermore suggest 90° and 180° azimuths as advantageous for the z survey.

Tests were also made by rotating the pipe (mean $z=40$) in a vertical plane through x, for different azimuths of the resonator, below it on the table. Figure 68 is an example of results, complicated in this case by the different distances between mouths during rotation. The maxima and minima in the upper curve lie between the quadrants, and there are large variations which contrast strongly with the small differences in the lower curve with reversed resonator.

The results of the survey with the pipe horizontal (azimuth 180°) in height $z=40$ cm. and the resonators normal to it are given in figure 69. It appears at once that the increase of height has given greater detail to the curve than was the case in figure 65 for $z=20$ cm. Moreover, the curve as a whole has shrunk in the y direction. For instance, the sheer descent now begins at 40 cm. and 60 cm., respectively, whereas in figure 65 it began at 50 and 70 cm. In figure 69, moreover, there is a definite development of maxima and minima in the same vertical. The mean wave-lengths may be estimated in one curve as 36 cm. and in the other as 35 cm., and they therefore agree closely with the case of figure 45 for the same altitude.

If the curve for R at 90° be displaced to the right 15 to 20 cm. it will nearly coincide with the curve for R at 270°, so far as its dominant features are concerned. The depth or length of the resonator does not much exceed 11 cm., but the length of the tube with stopper was 14 cm. Thus (fig. 69) in the large maximum at $y=40$, the mouth of the resonator lies at $40+7=47$ cm.; in case of the next one, at 56 cm., the mouth lies at $56-7=49$ cm., which is as near coincidence as the location of maxima permits. The same result follows for all the other cases. It seems probable, therefore, conformably with the inference above (fig. 45), if the *mouth* of the resonator be used for the specification of the coördinates x, y, z and not the middle of the pipe, that but a single graph will appear, irrespective of the azimuth of the resonator.

Figure 70 gives the results of the survey in y, with the pipe oriented as before, but $z=60$ cm. above the table. The graphs obtained are unexpectedly simple, containing but a single pronounced maximum and minimum each, and all excitation terminates beyond $y=90$ cm. The reason for this may possibly, but not probably, be referable to the temperature of the room, which

was exceptionally cold. Hence the radiators near the wall at $y=174$ cm. would interfere with the homogeneity of the air, rendering it in a measure acoustically opaque, in accordance with the effect exhaustively discussed by Tyndall. As the edge of the table is at $y=93$ cm., it might be argued that the fine shades of acoustic intensity would be wiped out by diffuse reflection from the air beyond this.

The two curves obtained independently and consecutively are nearly but not quite alike, so that they may be brought nearly but not quite into coincidence by advancing one curve in the direction y and moving the other rearward half the length of the resonator tube, i. e., what is the same thing, taking the mean abscissa for a given ordinate.

The final survey in the direction y with $z=80$ cm. for the pipe in the same orientation is given in figure 71. Here the *mouth* of the resonator and not its middle point was placed at the divisions of y, so that the curves are in fact practically coincident, as already surmised. There is also an absence of detail, but the distinguishing feature of the curve for $z=80$ cm. is the advance of the maximum to $y=60$ cm.

The deductions (figs. 72, 73) from the above results will preferably be left for discussion later.

19. The y-z location of the chief maxima. Resonator on table in y; pipe above origin in z.—We may now proceed to get the angle of incidence of the acoustic ray from pipe to resonator when the response is an initial maximum or a minimum. Figure 71 gives both y and z at once, whereas in figures 70 and 69 the mean abscissas are to be taken; figure 65 is unavailable, because of the closeness of P and R; the maximum would here require a negative y. The data are (including fig. 45):

Maxima $z=80$ cm.	$y=60$ cm.	Minima $z=80$ cm.	$y=30$ cm.
60	35	60	5
40	10		
(Fig. 45) 40	10		

These results are constructed in figure 72 and the graphs are astonishingly linear, considering the difficulty of measurement. The slope of the locus is thus in round numbers:

$$\tan a = \frac{\Delta y}{\Delta z} = 1.25 \text{ or } a = 51.3°$$

The minimum line is parallel to this. Hence, if an acoustic ray strikes the table conformably with the equation $y/(z-32)=1.25$ or $y=1.25z-40$, the resonator response is unique among the maxima. With the pipe in this position a parallel line 24 cm. above it is the $y-z$ locus of the first minima. It is noteworthy that the vertical distance apart here happens to be $\lambda/2=24$ cm.; but the case for the pipe above the resonator at the origin ($y=0$) comes out $z_0=32$ cm. or $2\lambda/3$, to which it is difficult to assign a meaning.

The tangent of the angle of incidence from P to R at this maximum would, however, be variable, being $y/z = 1.25 - 40/z$, depending upon the elevation of the pipe. It is not impossible that what is interpreted as a linear locus may really be hyperbolic; but figure 65 clearly indicates that the high maximum (pipe-level, $z = 0$), here probably distorted by the wind current at the origin, tends actually to lie in negative y, conformably with the suggestion of figure 72.

Finally, if we construct the unique maxima of fringe displacement s_m in terms of the elevation z_p of the organ-pipe, a graph (fig. 73) of distinctly harmonic character results. In other words, the figures 65, 69, 70, 71 are as a whole alternately high and low, so that s_m vanishes harmonically with the
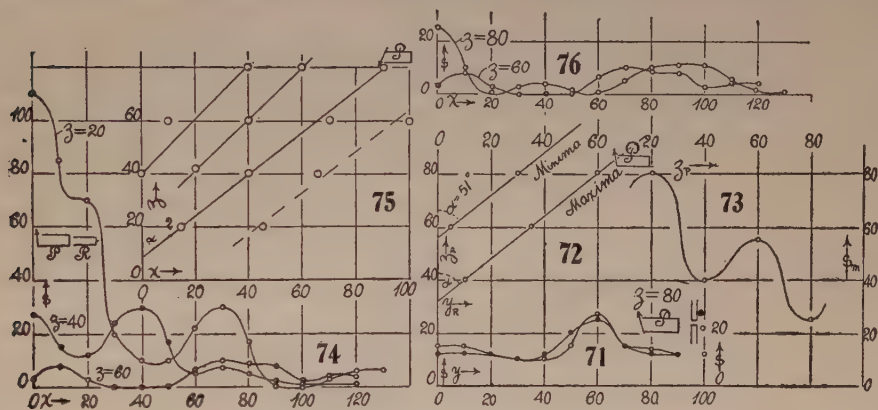
elevation of the pipe. This, when 60 cm. above the table, is more effective as a whole than when 40 cm. above. Similar harmonic relations will presently reappear in the horizontal displacement of the pipe.

20. Closed pipe. Survey in x. Pipe P and resonator R parallel.—
This march was along the cleared table as far as $x = 130$ cm. and toward the open door (fig. 34). The pipe was kept horizontal in azimuth $180°$ at a distance z above the table, while the resonator lay on it at x, also in azimuth $180°$, the mouths pointing in the same direction. Under these conditions the sound was diffracted around the pipe, which is thus an obstruction, and smaller deflections might be expected. They are given in figure 74, the mouth of the resonator being at the x coördinate. The curves show little detail and are low, probably for the reason given; but one easily distinguishes the successive minima and maxima about as follows:

Min. I.	— cm.	Max. I.		Min. II.	
20 cm.		$z = 20$ cm.	$x = 10$ cm. ?	$z = 20$	$x = 45$
40	20	40	40	40	65?
60	40	60	75	60	100
80	60	80	90	80	40

An anterior maximum develops in $z = 40$, $x = 0$?, and $z = 60$ cm., $x = 10$. The inset (fig. 75) shows the x-z location of minima and maxima, some of them uncertain. The z-x line of first maxima has a different intercept, but is again at about the same slope as heretofore, indicating an angle to z (since $\frac{\Delta x}{\Delta z} = \frac{60}{47} = 1.28 = \tan a$) of $a = 52°$. The equation with its new constant is

in round numbers $x=1.28z-11.5$, so that the variable slope of the angle of incidence is $x/z=1.28-11.5/z$. The maximum for the pipe above the resonator at the origin ($x=0$) would occur at $z_0=9.0$ cm., or $3\lambda/16$, which again has no meaning and does not agree with the preceding y survey. For the upper two loci (fig. 76) the slope is similar. The maxima for some reason flatten out when x is large and the first maximum for $z=20$ is not available. This accounts for the discrepancies. The wave-lengths of the flat curves are very long. On the whole the corroboration is fairly good, in view of the nature of the evidence. It is interesting to notice that at the origin the deflection s passes through a minimum near $z=60$ cm. and a maximum near $z=80$ cm. (*cf.* § 25).

The second survey in x was made with the pipe horizontal and in azimuth 90°, so as to be normal to the resonator in azimuth 0° on the table. The conditions here are then the same as in the preceding paragraph, and there is no diffraction around the body of the pipe. Curiously enough, however,
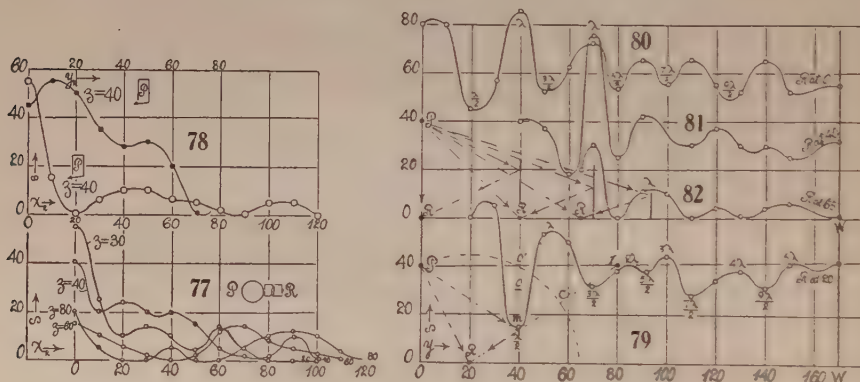
figure 77, which contains the graphs for the present case, is an exhibit of wave-curves much flatter than the preceding figure, and it is now difficult to recognize the successive maxima and minima, although the usual transfer of maxima into larger x values as z increases is obvious. With the obliteration of the minimum there is often a coalescence of maxima. Some influence lurks in these phenomena which has not been ascertained and which may reside in the pin-hole resonator functioning differently in different environments, or under different excitations. If the prominent maxima

$$
\begin{array}{cc}
z=80 \text{ cm.} & x=90 \text{ cm.} \\
60 & 70 \\
40 & 40?
\end{array}
$$

go together, the slope of the x-y locus of corresponding maxima will be about the same as in figure 72; but the $z=40$ maximum is vague because of the obliteration of the minimum at $x=30$, $z=40$ cm. The behavior at $x=0$ for different heights z is similar to the preceding, passing through a minimum near $z=60$.

Under these circumstances, a vertical position of the pipe above the origin with the mouth downward is worth testing. I have made only one survey for $z=40$ cm., figure 78, because of the flatness of curves and their marked dependence on fractions of pitch. The curve in figure 78, however, agrees substantially with figure 74 as to maxima and minima; for the minimum at $x=20$ cm. and the maximum at 40 cm. come out pretty well, so that the deductions already made would again apply. In the same figure and for the sake of contrast, I include a survey made in y, which will be found to agree substantially with the mean curve of figure 69, for the same $z=40$ cm. Thus:

Figure 69: Max., $y=$ 10, 50, etc.   Figure 78: Max., $y=$ 10, 50, etc.
        Min.   34, 68, etc.   Min.   37, 70, etc.

Hence it again appears that the survey in x toward the open door is materially different in character of results from the survey in y towards and between vertical walls. Thinking that the front part of the electric lantern of the interferometer (fig. 34) might possibly reflect or diffract, though to one side of y, I tried the difference between the front face (1 foot by 6 inches) closed and removed both for $x=50$ and $x=70$ of the resonator. There was no difference. With the same end in view, a large parabolic mirror was placed at $y=70$ cm. The results were a marked dissipation (mirror not focused) of sound; thus

Mirror in place: $s=40$ cm.; pointing downward $s=32$.
Mirror removed: $s=47$.

indicating a large negative effect varying with the direction of the axis of the mirror. A board 4 feet by 1 foot, vertically across $x=70$ cm., gave similarly:

Board in place: $s=33$ cm.
Board removed: $s=47$ cm.

also a dissipation (resonator at $y=20$ cm.) with the mouth toward the origin. This, however, suggested a more ample survey with reflectors as given in the next paragraph; for such results also can not but be periodic.

21. Vertical reflectors.—These experiments made in the y direction with the pipe vertical, mouth downward, at $z=40$ cm. came out with unexpected definiteness at once. They will therefore aid in disentangling the mysterious behavior of the resonator in the above paragraphs. This was placed on the table horizontally with the mouth toward the pipe (azimuth 270°). The vertical board 4 feet by 1 foot was then moved successively from $y=20$ cm. (about at the mouth of R) nearly to the wall at $y=174$ cm. The results are given in figure 79. The chief maxima are near $y=50$, 100, 150 cm., which suggests the wave-length of the f'' pipe $\lambda=48$ cm., here operating by oblique reflection. Between the maxima λ and 3λ, there is a subsidiary maximum which one might erroneously attribute to overtones, inasmuch as it is associated with weakly or strongly blown pipe-notes. Thus at 80 the largest deflection is obtained from the dying note, at 90 from a forced note; but the 2λ maximum is real. Distances between 150 cm. and the wall at 174 cm. were not available. A remarkable feature of the curve is the strong initial trough

at $y=40$ cm. If the board is placed more or less obliquely to y, the minimum tends to vanish, as shown at o' and o.

In the disposition given, two sound rays reach the resonator, one reflected from the board and the other direct, or with immediate reflection from the table. When the board is near the mouth of the resonator, these rays are reduced to one and the result is an accentuated maximum. As the board distance in y increases, the path difference steadily increases, with a simultaneous weakening of the reflected ray; nevertheless, figure 79 proves conclusively that it is not ineffective, as one might suppose.

In contrast with the preceding, the present graph, figure 80, for the same pipe position but with the resonator on the table at $y=0$ cm. (in azimuth 180°), is more regular. The curve lies in higher s. There is less repetition of sections; but nevertheless the same number of six maxima occurs, i. e., each maximum in figure 79 is reproduced and often accentuated in figure 80. The former minimum of $y=40$ has become a minimum somewhat below 20 cm.

The next survey in y was made with the pipe again at $z=40$ cm. and with the resonator on the table (in azimuth 180°) at $y=40$ cm. The graph (fig. 81) shows the same number of maxima as heretofore, with the sixth soon to vanish. The feature of the curve is the enormously developed second maximum, in contrast with the first or the others.

We are no doubt trenching on the case of favorable incidence, heretofore developed. The response was always stronger to the weak notes and they were used throughout, the difference being often over 10 scale-parts.

Finally, figure 82 gives the corresponding acoustic distribution with the pipe left in its former position, but with the resonator on the table at $y=65$ cm. in azimuth 180°. The first maximum is now relatively high, while the former huge second maximum has flattened and the fifth and sixth maxima have vanished behind the wall, W. Weak notes were essential, as the strong notes gave relatively little deflection, as before. As a whole, the present work has been strikingly successful and affords clear-cut evidence in the following treatment; but it fails as yet to shed definite light on the anomalously high second or other maxima.

These maximum ordinates (s_m) for path-differences $\lambda=0$, λ, 2λ, 3λ are constructed for the corresponding resonator position y_R in figure 83a. As compared with the diminishing initial maximum, the strongly harmonic distribution for the λ maximum, together with its decreasing amplitude, is well brought out. Like λ_0, 2λ is but slightly harmonic, while the odd 3λ is again markedly so. Distances between crests and troughs are here about 40 cm., though it would be necessary for their identification to insert intermediate resonator positions, say steps not exceeding 10 cm. In figures 79 to 82, in
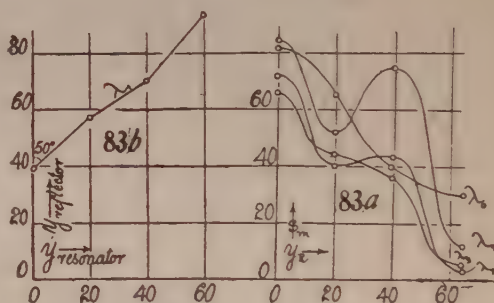
which the reflector only moves, the distance between crests oscillates between $\Delta y_R = 20$ to 30 cm., the mean values being 28, 29, 25, 27 in successive figures. This indicates a mean inclination of nodal planes to the table of $\sin a = (\lambda/2)\Delta y_R = (48/2)\times27=9$; or $a=63°$, if the nodal surfaces trail after the reflectors at the same speed.

Figure 83b supplies the relations of the resonator and reflector positions along y for the λ maximum. This is probably a straight line at an angle of about 50° to the vertical, as $\Delta y_{res.}/\Delta y_{refl.}=1.2$ nearly. The displacements of board and resonator are, in this view, proportional quantities ($y_{refl.}=1.2y_{res.}+40$), not very different in size.

22. Discussion of the preceding reflections.—In the graphs 79 to 82 there are three influences at work on the resonator. In the first place, the direct ray from the pipe is equivalent to a reflection from the table, a locus of reinforcement. A half wave-length has been lost. Then there are the two reflections, also with loss of $\lambda/2$, from the board normal to y and the wall at $y=-130$ cm. This may here be neglected, because it is always kept relatively very distant in the plan of the experiments. We thus have to compound the ray from the image of the source with the direct ray. The computation would be very cumbersome; but the construction in the graph itself is not so and is adequately correct. In figure 79, if we take the prominent minima, a circle is to be drawn with a center at R and a radius RP. Taking the first minimum at $y=40$ cm., the image is I at $z=40$, $y=80$. Hence $IC=27$ cm. is the path difference from the minimum at 40 cm., which is placed a little too high. In this way the following data were measured:

Minima: $y=40$ cm., $\lambda/2= 27$ cm. $y=110$ cm., $7\lambda/2=179$ cm.
            70      $3\lambda/2= 82$ $9\lambda/2=220$
            93      $5\lambda/2=126$
Maxima: $y=53$ cm., $1\lambda= 50$ cm. $y=130$ cm., $4\lambda=198$ cm.
            83      $2\lambda=105$ 155 $5\lambda=248$
          103      $3\lambda = 148$ · 25 $0\lambda= 4$

These results are convincing, being quite as accurate as the location of maxima and minima will permit. The minima of figure 80 treated by the same method give:

Minima: $y=25$ cm., $\lambda/2= 24$ cm. $y=103$ cm., $7\lambda/2=170$ cm.
          50      $3\lambda/2= 68$ 126 $9\lambda/2=215$
          80      $5\lambda/2 = 125$ etc.

with similar data for the maxima. Among these it will be desirable to locate the high second maxima in the successive curves. They occur as follows:

	Pipe at $x=y=0$ and	Resonator at $x=z=0$ and	Reflector normal to y, for maximum at	λ	s_0	s_1
Fig. 79	$z=40$ cm.	$y=20$ cm.	$y=53$ cm.	50 cm.	67	55
Fig. 80	40	0	40	50	83	85
Fig. 81	40	40	70	50	40	75
Fig. 82	40	65	93	51	30	12

As the resonator is successively displaced along y, the second (s_1) and first (s_0) maxima are alternately in excess—harmonic conditions which are common throughout these experiments (as already indicated), but for which no adequate quantitative relations have been found.

23. Reflection from boards of different areas.—These were placed normal to x, keeping the pipe, $z=40$ cm., $x=y=0$, and the resonator at the origin below it, as in the case of figure 80. Figure 84 shows the pressures at the origin when a large board, 150 cm. high, 50 cm. broad, is moving along positive x. Comparing this with figure 80 (board over 80 by 45 cm.²), it is seen that in addition to the initial maximum ($0 \times \lambda$) the odd maxima (λ, 3λ, 5λ), have retained their strength and position, whereas the even maxima (2λ, 4λ) are ill defined or displaced. A feature of the curve is the marked development of the second minimum ($3\lambda/2$). Owing to the position of the collimator, this
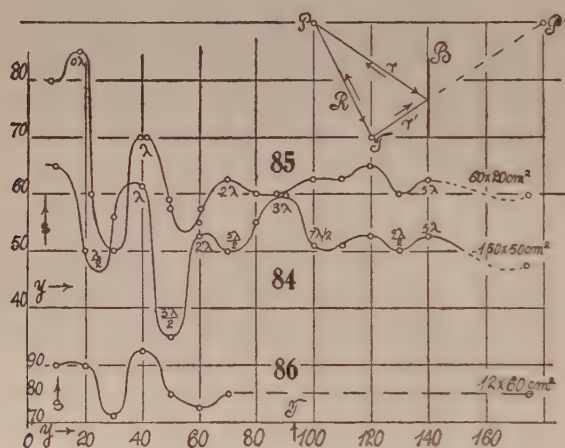
board could not be moved in the $-y$ direction as far as needed for complete symmetry. Its weight, moreover, dislocated the fringes, so that the curve, figure 85, for the next and much smaller board (60 cm. high, 20 cm. broad) is much higher owing to the enlargement of fringes incidentally resulting; but the reduction may be made from the data for the extreme points ($y=174$ cm.) and the factor would be $55/80=0.7$, nearly. It is remarkable that this relatively narrow board produces such conspicuous alternations, at least near the origin. The maxima, however, have for some reason been shifted toward greater y. The third and fourth maxima now lack definition, but the zero'th, first, second, and fifth are firm.

Carrying the reduction in area still further, I finally selected a narrow board, 60 cm. high and 12 cm. wide, obtaining the graph figure 86 with it for the same fringes. Here the first maximum and minimum still obtrude, but the second minimum is flattening out. As a whole, these results are rather what one would expect, inasmuch as the broader boards, containing more half-period elements, retain their effectiveness as reflectors at a greater distance

from the origin. I have not been able to get much information as to the cause of the wide differences in the value of the maxima and minima. The shift of the graph, figure 84, into smaller wave-lengths is intelligible, since the large board, with its stronger reflections, forces the resonator to respond to the slightly smaller wave-lengths of the intensely sounding pipe.

Conformably with the results obtained in figures 54 to 57 for normal reflection, one might argue that in oblique reflection also the maxima of fringe deflections would be obtained when the direct ray R (fig. 85 inset) and the rays r, r' reflected from the board B meet at the pipe P again, as a node, after rising from the table at T. If this is the case, two equations must be satisfied; for the case of nodes at the table:

$$(1) \qquad r + r' - R = m\lambda/2$$

m being a whole number. For the occurrence of nodes at the pipe mouth on return:

$$(2) \qquad r + r' + R = n\lambda$$

n also being a whole number. Thus

$$(3) \qquad R = \frac{2n - m}{4}\lambda$$

$$\begin{array}{lll} \text{If } m = 0, & R = \lambda/2, & 2\lambda/2, \quad \text{etc.} \\ \phantom{\text{If }} m = 1, & R = \lambda/4, & 3\lambda/4, \quad \text{etc.} \\ \phantom{\text{If }} m = 2, & R = -, & \lambda/2, \quad 2\lambda/2, \text{ etc.} \end{array}$$

Thus the stimulation should recur alternately for values of R made up of even and odd multiples of $\lambda/4$.

24. Reflectors displaced in $-y$.—Owing to the difficulty of managing the heavy reflectors on the table, a modification was devised (fig. 89, inset) of having the reflectors (r, r', sheet tin-plate 70 cm. high and 50 broad) hanging from a length of gas-pipe gg, stretched between the walls. T is the table on which the resonator R lies at the origin, P being the pipe 40 cm. above it. The apparent inactivity of the wall, W'' at $y = -130$ cm., had been confusing and a survey in this direction seemed desirable. The survey in the direction of positive y with the reflector r removed gave the graph figure 87, like the preceding, but much clearer. Keeping r' at $y = 40$, the reflector r was now moved in steps from $y = -130$ to 10 cm. and the graph figure 88 worked out. The curve is almost flat and not until the edge of the table at $y = -27$ cm. is passed does it ascend. Hence the $-y$ axis is here ineffective. This rather startling result, however, merely indicates that the effect of the reflector r' at close range predominates, until reflector r is also equally close. When the two, r and r', coöperate, r is within a half wave-length in y, the paths being eventually 90 cm. and 45 cm. and the path-difference about 1 wave-length. To further interpret this curious result, I removed all the apparatus at A, figure 34, and then made another similar survey in $-y$, which now gave the very striking graph figure 89. Within the available distances, this is quite like figure 87

for $+y$ points. It seems, therefore, as if in the direction $-y$ the sound-waves were formerly broken by diffuse reflection from smaller and irregular objects, but this is not true. The new graph merely witnesses the absence of the reflector r', r acting alone.

Great care had to be taken to keep the sheets r, r' vertical; otherwise any deflection from o to the limit was obtainable at the maxima. The survey in $-y$ was at best troublesome, inasmuch as the accumulation of apparatus interfered with observation. An accident at $-y=50$ changed the size of the fringes, and the higher values of figure 89 within $y=-50$ are attributable to this cause. In figure 87, excepting the initial crest, even multiples of λ correspond to low crests, odd multiples to high crests.
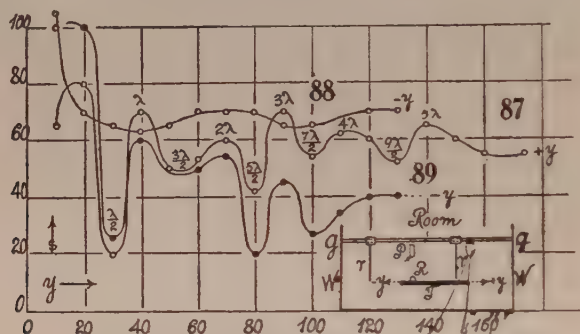
25. Organ-pipe displaced along y.—The question arose as to whether the removal of apparatus had materially modified the data of figure 69 above, with the pipe similarly placed ($x=y=0$, $z=40$ cm.). The new survey is given in figure 90. If the mean positions in figure 69 be taken, there is no practical difference in the y location of crests and troughs as compared with the present curve, except in case of the first maximum; but this is difficult to place in figure 69, as one of the curves terminates early at zero. The new curve has been carried beyond zero into negative y and here develops another maximum, thereafter falling off at the edge of the table, at T. There is also an apparent termination at the further table-edge T'. The size of maxima in observations made at long intervals of time apart would depend on incidental conditions (size of fringes, etc.). Then there is ever present the inevitable difficulty with slight changes of pitch in the strongly blown, as compared with the moderately blown pipe. My endeavor has been throughout to get the largest deflection, so that sometimes strong, at other times moderate, notes were used, whichever happened to fit the conditions.

With this satisfactory corroboration of the old results, it seemed further advisable to carry out a survey with pipe displaced successively in the y direction at constant z, corresponding to the z displacements at constant y above. The new results are summarized in the graphs, figures 90 to 94.

As above in the z displacement, so here the graph for $y=0$, $z=40$ (fig. 90) is most sharply featured, while the other graphs tend to show but one or two

marked maxima. Furthermore, if we regard the graphs as a whole, their maximum heights in s and other ordinates are alternately large and small. The pipe positions $y=0$, 40, 80 are thus more favorable to intense nodal phenomena than the positions $y=20$ and 60.

In several cases I carried the resonator beyond the edges T and T' of the table. Though the fringe deflections fall off at T, there is no break of discontinuity at least at T'. Sound rays, in such a case, meet freely in the air, although there is no reflection from the table. This may be interpreted as an absence of phase reversal in all the rays, which would leave the resultant unchanged. Though I have no extensive evidence on this question, it may nevertheless be suspected that the table is not perhaps as necessary for the development of these nodal phenomena as I have hitherto supposed.
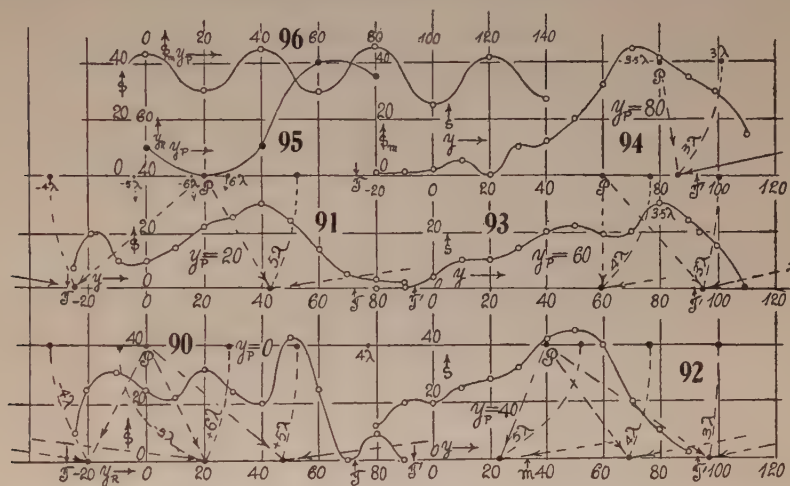
In the graphs, figures 91 to 94, it is difficult to identify the maxima corresponding to figure 90. If we plot the y positions of the pipe y_P and resonator y_R for the chief maxima, the result, figure 95, represents a complicated harmonic and is indefinite as to the maximum to be taken at $y_P=0$.

Figure 90 has another feature which deserves attention, inasmuch as the maxima (pipe at $x=y=0$, $z=40$) lie at $z=x=0$ and

$$y=-10, +20, +50, +80 \text{ cm.}$$

all at almost exactly $y=30$ cm. apart. This makes the oblique distance from pipe mouth to resonator mouth $\sqrt{y^2+40^2}$ or

$$d_y=41 \text{ and } 45, 64, 89 \text{ cm.}$$

numbers which have no obvious relation to the wave-length $\lambda=48$ cm., such as the preceding paragraph indicated. In figure 92 the pipe ($y=40$) is nearest the middle ($y=33$ at m) of the table; yet the graph is nevertheless characteristically non-symmetric. If the high maxima in figures 93 and 94 be regarded as produced by reflection from the wall (the hyperbolas of the nodal loci have been sketched in), the path-differences would be 95 and 90, respec-

tively, which might be interpretable as 2λ; but this is improbable, as it would not explain the remaining features of the curves, where the path-differences run too high in wave-lengths.

An important feature of figures 90 to 94 is the alternation of large and small amplitudes s, already adverted to, as the pipe at $z=40$ takes its successive positions $y=0$, 20, 40, 60, 80, in the xz plane. This distribution of maxima s_m of fringe deflection is shown in figure 96 and is strikingly harmonic with nearly constant amplitude. Possibly it would have been more nearly so if displacements of $\Delta y=\lambda/2=24$ cm. had been chosen. The pipe continually approaches the maximum in the graphs and overtakes it eventually (fig. 94). Figure 95, for a shifted pipe, is in contrast with figure 73, with its rapidly decreasing amplitude conformably with the elevation of the pipe.
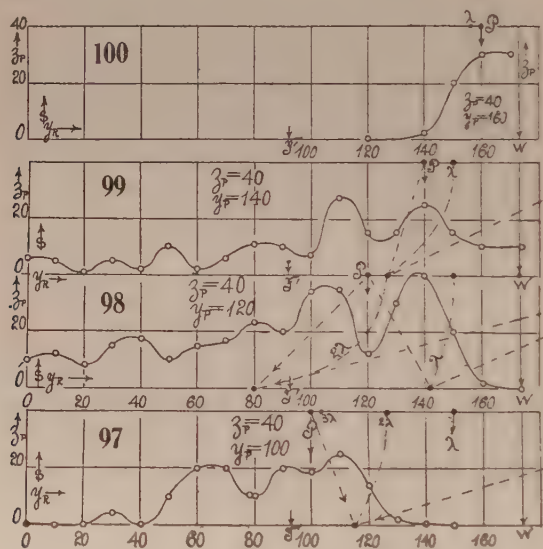
26. **The same continued.**—Some time after the conclusion of the above work, the graph, figure 97, was investigated with the pipe at $z_P=40$ cm. and $y_P=100$, therefore, quite off the edge of the table at T'. The curve again resembles figure 93, having two large maxima, one either side of P, though the accentuated maximum at $y_R=110$ may be influenced by reflection from the lamp-case. Like figure 93, the curve is low, as its maximum value s_m in figure 96 ($y_P=100$) indicates, so that it also falls in step with the alternations recorded by that curve. Figure 97 shows no appreciable influence to be ascribed to the edge of the table at T'.

This is particularly true of the next curve, figure 98, with the pipe at $y=120$ and $z=40$ cm., in which relatively large deflections, s, again abound, extending throughout the breadth y of the table. There has not, however (as in fig. 94), been an apparent coalescence of maxima; for in figure 98 the two crests are

separated by an equally marked trough lying under the pipe. Besides the intense nodal regions occurring quite beyond the edge T' of the table, the marked nodal intensity on the table was found to extend beyond the other edge. The curve at $y_R = 140$ cm. contributes a further crest, s_m, to figure 96.

Figure 99, with the pipe at $z = 40$, $y = 140$ cm., is again of a low order of intensity throughout, the highest crest, s_m at $y_R = 110$, contributing a trough in figure 96. Otherwise, however, in spite of the displaced pipe, it is not unlike the preceding curve (98), so that a crest now lies under the pipe.

The last curve, figure 100, for which the pipe lies at $z = 40$, $y = 160$ (*i. e.*, a little over $\lambda/4$ from the wall), seems to be a mere decay curve, instancing the direct effect of wave-trains from the pipe on the resonator. It ceases at about $y = 140$ cm., 20 cm. in horizontal displacement from the pipe, and there is no appreciable nodal intensity on the table. The semiwave-length from the wall W (λ path-differences inserted, in succession, in all the graphs) here lies beyond the pipe, so that the wall is the only nodal region attributable to reflection.

In figure 97 the path-difference λ of direct and reflected rays is ineffective, while 2λ only roughly approaches the maximum at $y = 110$; 3λ would strike the table beyond the origin. In figure 98 the λ path-difference is fairly coincident with the maximum at $y = 140$, but the 2λ path-difference misses the large maximum at $y = 106$. In figure 100 the λ path-difference actually coincides with a trough. Hence the relations of reflected wave-fronts are again vague and untrustworthy.

If in relation to figure 96 we measure multiples of $\lambda/4 = 12$ cm. from the wall at $y = 174$ cm., and compare them with the successive pipe positions, the relations are as follows:

$(\lambda/4)$ ×.	1	2	3	4	5	6	7	8	9	10	11	12	13	14	15 from wall
Dist. from origin.	162	150	138	126	114	102	90	78	66	54	42	30	18	6	—6 cm.
Pipe at..	160	..	140	..	..	100	..	80	..	..	40	..	20	..	.. cm.
Result ..	..	..	Min.	..	..	Min.	..	Max.	..	..	Max.	..	Min.	..	..

In the third row the pipe positions which correspond most closely to the $\lambda/4$ divisions are given, with the observed result in the last row. Thus there is a minimum for $6\lambda/4$ as well as for $3\lambda/4$, a maximum for $11\lambda/4$ as well as for $8\lambda/4$; so that an odd or an even number of quarter wave-lengths of pipe-distance from the wall does not seem to enter appreciably into an interpretation of the distribution of crests in figure 96, even though this has been the case in other experiments.

The conditions under diffraction from the wall W may be stated as follows, since the wave-length $\lambda = 48$ cm. is relatively long: Let r be the mean radius of the largest Huyghens zone for which the wall affords available space and let there be n half-period elements within it, when the pipe is at a distance b from the wall. We may then write

(1) $$r = \sqrt{nb\lambda + (n\lambda/2)^2}$$

from which

$$b = (r^2 - n^2(\lambda/2)^2)/n\lambda$$

Where the integer n passes from an even to an odd number, a curve like figure 96 should change from crest to trough, the number of half-period elements being even and odd, respectively. But the feature of the curve, so far as traced, is an almost equal distance, of about $\Delta b = 20$ cm., between crest and trough, whereas in equation (3) Δb increases rapidly as n decreases. The comparison is, however, not without interest, as when $b = 0$ (in the wall), $r = n(\lambda/2.)$ We may therefore assume a case in which $r = 200$ cm.; $\lambda = 50$ cm. (for simplicity), and $n = 8$, for $b = 0$. The data are then:

$n =$	8	7	6	5	4	3	2	1	
$b =$	0	27	58	97	150	229	375	787	cm.
$\Delta b =$		27	31	39	52	79	146	412	cm.
$-db/dn =$	25	29	35	45	...	...	...	...	cm.

Within the limits investigated ($y = 0$ to 174 cm.), Δb increases from 27 cm. to over 52 cm., so that both the Δb is too large ($\Delta y = 20$, crest to trough) and the increase is too rapid as compared with figure 96. If r, the limit of available wall-space in which the half-period areas lie, is taken twice as large ($r = 400$ cm.), the Δb within the available $\Delta y = 175$ of investigation would naturally be more constant, viz,

$n =$	16	15	14	13	12	11	10	
$\Delta b =$		26	27	31	33	36	42	45 cm.
$-db/dn =$	25	27	129	32	34	39	45	cm.

but they would, on the average, be much too large. Still, this method of viewing the phenomena, though inadequate, is better than what has preceded. seeing that there would be three or four other walls to be treated similarly. The nature of the approximation follows from

$$-\frac{db}{dn} = \frac{b}{n} + \frac{r}{n_0}$$

where $r/n_0 = \lambda/2$, a constant. Here b/n, as seen in the above data, is rapidly increasing and effective, even though $r/n_0 = 25$ is large and db/dn can not be less than $r/n_0 = \lambda/2$.

For comparison with the data for the f'' pipe. a survey was made with an open c'' pipe (diapason) and a corresponding c'' pin-hole resonator, of the closed type. The pipe was placed above the origin on the table. in $z = 40$ cm., as usual. The note seemed relatively loud, so that larger deflections were obtained than with the other pipe; but the pitch was too fluctuating for accurate work and it was difficult to fix a steady maximum deflection. Resonance, in other words, implies sharp tuning.

The character of the survey in the y direction (the wave-length being about 63 cm.), compared with figure 90 for the f'' pipe, presented nothing very striking. The chief maximum was under the pipe. It was interesting to note that the same conical pin-hole functioned equally well for both pipes, so far as could be discerned.

27. Nodal regions in free air.—The result obtained in the last paragraph, of marked nodal activity beyond the edge of the table, though not surprising

in itself, nevertheless made it necessary to elucidate these occurrences more systematically. One is quite apt to regard the reflection from the table as an important part of the phenomena. In some instances it must be so. Incidentally the present contribution will adduce new evidence bearing on the nature of the maxima and minima observed, and the computation of wave-lengths therefrom.

The first survey in $-y$ is given in figure 101, where the wall W'' of the room (fig. 34) is at $y=-130$ cm. The edge of the table is at $y=-27$ cm., so that the stretch $W''T$ is in free air. The pipe P is placed at $y=-20$ ($z=40$, $x=0$) vertically, very near the edge T. The resonator lies in $x=0$, in the plane of the table (prolonged if necessary) and at y. One observes four maxima, distinguished as $-\lambda$, -2λ, -3λ, -4λ, and this corresponds to the number of nodes or hyperbolæ which can occur between W'' and P. These hyperbolæ are again roughly sketched in, the conjugate focus (not shown) being 130 cm. behind the wall W''. It will be seen that the maxima now coincide with the hyperbolæ in turn, the first nodal surface ($\Delta y = 0 \times \lambda$) being at the wall W''. The figure also shows the direct and reflected rays for each case, meeting at the level of the resonator in the plane of the table prolonged. The figure thus discriminates between the fourth maximum (-4λ) and the first three maxima, $-\lambda$, -2λ, -3λ. In case of the latter the rays meet in the same phase but come from opposed directions, so that there is a break of $\lambda/2$ at the node. In this event nodal condensation and rarefaction are possible in free air from the opposition of vectors. The opposition is a maximum in the level of the pipe P; it is practically effective, however, as the experiments show, at levels much above and below it. At the maximum -4λ, the direct vector R and the reflected vector r are not in opposition relative to a vertical plane, though they would be so for a plane bisecting the angle ROr symmetrically. I suspect, therefore, that here the rays S reflected from the table provoke the node, so that here the table should be necessary.

The nodes increase in intensity from the wall W'' to the pipe P. This is not evident; for if the direct rays regularly increase, the reflected rays at the same time greatly decrease, and the intensity of interference depends essentially on the weaker ray, between P and W''. For like reasons one is apt to ignore the wall effect at long distances, believing that, for path-differences of 3λ (150 cm.) and over, no appreciable result could be expected, even where the required amount of path-difference was demonstrable. Beyond the distance $W''P$, however, R and r coöperate, and the case of a large maximum here is more easily intelligible.

Corresponding work with the pipe at $y=-40$, $z=40$ is given in figure 102. Here the first maximum ($-\lambda$) comes out clearly, the second (-2λ), though flattened, is correctly placed, but the third (-3λ) is apparently shifted toward the left. This may be due to the presence of the observer at the interferometer and the reflection resulting. Minima, in other words, have been obliterated.

The final graph, figure 103, with the pipe at $y=-60$, $z=40$, has additional characteristics from the nearness (70 cm.) of the pipe to the wall W''. The first and second maxima are correctly placed and much enhanced. The third is now impossible; but the marked height of the curve, nevertheless, persists in this region ($y=-20$ to -40). One would hesitate to ascribe it to reflection from the body of the observer. Similarly, the three curves (101, 102, 103) have a fixed maximum at $y=0$, which, though directly possible in figure 101, would not be so in figures 102, 103. There may be reflection from the vertical interferometer (near $y=0$) for these pipe positions. The alternation of the intensity of deflections or acoustic pressures is again evidenced by figures 101 and 102. Together with the preceding graphs, the case stands thus:

Relatively large acoustic pressure throughout: Pipe at $y=80$, 40, 0, -40 cm.
Relatively small acoustic pressure throughout: Pipe at $y=60$, 20, -20 cm.

The pipe at $y=-60$ cm. does not conform to this rule, possibly from the secondary disturbances mentioned. Finally, one may note the frequent occurrence of $\Delta y=30$ cm. between well-developed maxima or minima.
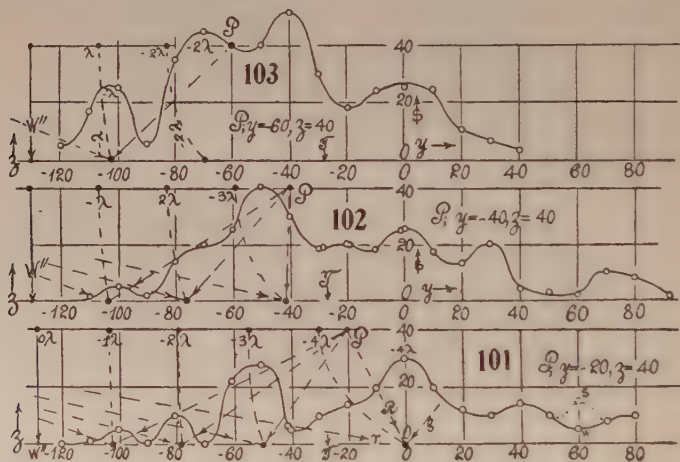
In the light of these solutions, we might hope to unravel the results of the preceding paragraph, with a view to the further identification of the maxima. This does not succeed nearly as well as was confidently expected. Turning to figure 90, the first two crests on the left (hyperbolæ sketched in) may be attributed to the corresponding wall W'', and their value would then be -4λ, -5λ (199 for 192 cm., and 238 for 240 cm.). In figure 91, the -4λ maximum lies at 198 instead of 192 cm. and the -5λ maximum is obscure. Thus even the -4λ values are bad. Possibly this may be associated with their position near the edge of the table. Moreover, the rays are opposed in direction and the observer is too near. Finally, the fit of sharp or flat notes, sometimes so distinguishable, may be a source of error in judging as to positions of maxima. There is no way at present of combating this.

In figure 90 the -5λ and $+6\lambda$ maxima happen to be nearly coincident; but the effect is not remarkable as compared with the following single $+5\lambda$

maximum. Promising as it seems that a coincidence something like this is an explanation of the occurrence of exceptionally high crests, no evidence was obtained, beyond the rough fit of -6λ and $+5\lambda$, in figure 91, showing nothing for -5λ and $+6\lambda$, moreover.

Turning to the right wall W, graph figure 90 has a maximum for a path-difference of $5\lambda(y=47)$, which agrees very well with experiment; but the maximum at $y=80$ would correspond to about 3.5λ and must have thus some other origin. In figure 91 the chief maximum belongs to the path-difference $5\lambda(y=43)$ and also fits well. Other crests are here uncertain. In the graphs, 92, 93, 94, however, the relation of the graph to the reflecting wall W is quite obscure. The hyperbolæ inserted show that these crests lie respectively at about 4.5λ, 3.5λ, 3.5λ (scant) of path-difference. As there is nothing to account for the anomalous half wave-length, some other cause for these crests must be sought. This suggests a consideration of the W' wall, normal to W and W''; or the wall W, which is very high compared with W'', and may contain an unfavorable number of half-period elements, the first zone having a radius of 70 to 90 cm. It is difficult to draw quantitative inferences here.

As to the W' wall, at a distance of 190 cm. from the $x-y$ plane of survey, as well as to the reflections across corners, these are relatively so distant that their effective participation is hardly probable.

In figure 90 the well-developed consecutive crests and troughs lie about $\Delta y=30$ cm. apart in the five cases available. There is another in figure 93. If one regards the effective impinging rays to be the axes of stationary waves produced by the totality of reflections within the room, the distance apart Δy of the crests in the graphs would conform to

$$\Delta y=\lambda/2 \sin a$$

where a is the angle of incidence on the table. Thus

$$\sin a=\lambda/2\Delta y=48/60=0.8, \text{ or } a=53°, \text{ nearly.}$$

But in figure 90 this angle would have to be constant throughout the whole survey of 120 cm. and it is difficult to understand where such parallel rays may come from. The incidence of the direct ray varies from $a=0°$ to $a=66°$, throughout the whole of which $\Delta y=30$ cm. In fact, the presence of this datum here and elsewhere is quite noteworthy.

To return again to the evidence given at the beginning of the paragraph, one may note that it implies the occurrence of nodal regions, floating, as it were, in free air, with a fixed position for each fixed position of the sounding organ-pipe. This heterogeneous air structure, which one might call flocculent, particularly characterizes the closed part of the room within the wall $WW'W''$, the ceiling, and the floor. To sustain itself, a nodal region would have to vibrate in all directions in reciprocation with the surrounding nodal regions. Thus the architecture is essentially on a large scale, so that occasional appearance of parallel regions intersected by the table, as in figure 90 and elsewhere, becomes more plausible. Nevertheless, the way of attacking these conditions quantitatively, or of accounting, for instance, for the repeated occurrence of

the angle $a=51°$ to $53°$, is more remote than the frequency of systematic results would lead one to expect.

28. Vertical-pressure variations at the crests and troughs.—The changes which the maxima and minima undergo along a vertical above the level of the table is investigated in figure 104. Here the graph, figure 94, with the pipe at $y=80$, $z=40$, was consulted and the resonator moved up vertically from the table, at $y=80$ and $y=20$ cm. respectively. The two graphs, figure 104, are laid off on the y position of the resonator, deflections s increasing upward, while the y coördinate of resonator and pipe increases downward. By plotting y, z, and s in this way, the pipe and resonator positions, as well as the deflections s, are all indicated. Turning first to the original maximum at the table, the deflections are seen to decrease to a minimum at $z=10$ cm. instead of $\lambda/4=12$, and then to increase to an enormous maximum at $z=30$ cm. instead of $\lambda/2=24$, the first nodal plane above the table. There is thus a tendency for the nodal plane at the table to reproduce itself at $\lambda/2$ above, which degenerates into $y=30$ cm. so far as the curve is correctly drawn. It might be supposed that the interference here is the wind from the pipe at $z=40$ in the same vertical; but the curve is too continuous throughout to supply any such evidence and the pipe blows away from the resonator. The second minimum, moreover, lies even above $5\lambda/4$, and the curves beyond the maximum largely indicate the rapidly decreasing intensity s with z.

The original minimum (fig. 104 at $y=20$ cm.) is at first too flat for the detection of characteristics. It then rises to a pronounced maximum at $z=40$ cm. above the table. Being at a long distance (60 cm.) from the pipe, there is here no draft interference. The wave-length path-difference, which lies at about $z=45$ cm., is not reached, and all intermediate and subsequent fluctuations are absent from the smooth curve observed. It does not, therefore, conform to any simple plan of node distribution upward from the table.

The graph, figure 105, is constructed in the same way and obtained by consulting figure 92, in which there is a maximum at $y=50$ cm. and a minimum at $y=90$ for the resonator reposing on the table, the pipe being at $y=40$, $z=40$. The maximum (fig. 105), with the resonator in the vertical at $y=50$, brings out the characteristics of the preceding figure. The minimum at $z=10$ is again too low, the maximum at $z=35$ is too high relatively to $\lambda/2$, and beyond this the curve merely falls off. The crests in figure 104, both when R is at $y=20$ and when at $y=70$, tend to approach the P level ($z=40$), quite so at $y=20$. The same is true in figure 105, even more nearly in both curves for R at $y=50$ and R at $y=90$.

With regard to the former minimum development (R at $y=90$), one may notice that in figure 105 it begins with a significant value, $s=18$, probably because of some alteration of adjustment from the preceding experiment. The minimum is not reached until $z=24$, which is a semiwave-length. Nevertheless, the maximum is again located at $z=40$ and near the pipe-level. The

construction and hyperbola show that the curve, when R is at $y=90$, trends as if there were a node on the table here, which is repeated when the path-difference is λ.

As in figures 104 and 105 the distance between crests and troughs is an increasing quantity upward, we may perhaps regard the distance between the first two or nearer crests to correspond roughly with the succession of nodal surfaces at the table. If the latter make an angle a with the table, this would be expressed by $\Delta z = \lambda/2 \cos a$, $\Delta z/\Delta y = \tan a$. Thus if $\Delta z = 30$ to 35, $\cos a = \lambda/2\Delta z = 24/33 = 0.72$ or $a = 44°$, which is not in good agreement with the larger angle found above ($51°$) in the work along y. The increase of distance between crests as the resonator approaches the pipe is referable to the direct influence of the loud pipe-notes without the intervention of nodes.
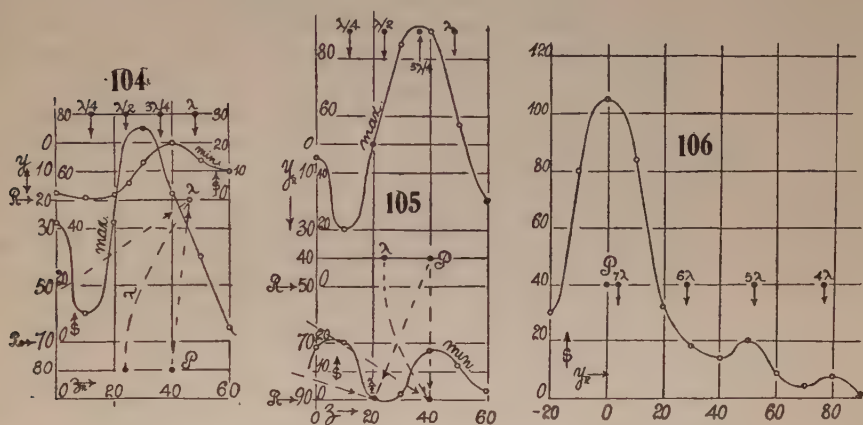
29. Survey in y in the pipe-level.—The graphs of the preceding paragraph seemed to indicate that intense pressure might be expected in the z level through the mouth of the pipe P. This was therefore placed $z=40$ cm. above the origin and the resonator carried in y at the same level in the yz plane. The results are given in figure 106, in which an enormous maximum is observable when the resonator passes the pipe at $y=0$. This, of course, is to be expected. The other maxima are meager by comparison and they agree roughly with path-differences of 4λ, 5λ, reckoned from the wall W on the right at $y=174$ cm. They are quite obliterated by the proximity of the pipe (6λ, 7λ), which here blows in the y direction from $y=0$. The curve, however, is continuous and probably not much influenced by the draft from the pipe-blower, for the resonator axis was normal to the current of air and its immediate effect would have been a pressure decrement.

30. Inferences.—The above work as a whole has shown that when the reflecting plate is relatively near to the pipe and resonator, the position of maxima and minima may be predicted as a case of ordinary interference and the wave-length computed satisfactorily. The distribution of intensity among

the crests and troughs, nevertheless, remains harmonic and has not been foreseen.

If the reflecting surfaces are relatively remote, the positions of crests and troughs can not, as a rule, be found by the same method satisfactorily. In certain instances there seemed to be an approximate fit; but as a whole the attempt was unsuccessful and the distribution of nodal intensities equally puzzling. It appeared, however, that when the organ-pipe, definitely placed, is sounded, the occurrence of nodal surfaces of a fixed position in free air is demonstrable everywhere. Distributions between walls are consistent and differ from distributions between wall and door. It is not improbable, moreover, that such surfaces are regularly grouped, since they are fashioned on a large scale of architecture, and may for reasonable distances be approximately parallel. If, then, they are intersected obliquely, for instance by the plane of the table, and if a is the mean angle between the latter and the nodal surface, the distance between crests on the table should be $\Delta y = \lambda/(2 \sin a)$. Hence this intercept, Δy, may have any value, depending upon the general shape of the room. If the prevailing value, $\Delta y = 30$ cm., be taken, $\sin a = 24/30$ or $a = 53°$ roughly. This angle between surfaces is also the angle of incidence of the rays, and has been encountered more or less closely in other paragraphs (§§ 19, 20, 21, 27). The distribution of intensities would then also depend on the fixed pipe position in relation to the given walls of the room, regarded as reflectors. Such an explanation is plausible and flexible, no doubt; but it has the great disadvantage that none of the results can be reproduced by computation; and the conviction that some other explanation may be found is not removed. This is particularly so, because the pin-hole resonator is practically unresponsive, except within ranges from the pipe which are small as compared with the dimensions of the room as a whole.

The pin-hole resonator is peculiarly stimulated by a node at its mouth. If this is in a compressional phase it enters the $(\lambda/4)$ tube of the resonator and returns with change of phase to meet the ensuing rarefaction at the mouth. The mechanism to do this with wave-trains seems to function less perfectly. The organ-pipe itself, as was found, is similarly stimulated to increased activity. The evidence of harmonic distributions of acoustic pressure obtained by the pin-hole resonator is sufficient in itself to prove that direct wave-trains are relatively without importance, except very near the pipe, for these would show the same intensities everywhere, with the exceptions of the regular diminutions with distance. Hence it is not surprising that expectations as to a predominating effect attributable to moving wave-trains is usually not realized.

The structure of the acoustic model of nodal regions determinable in the ways discussed in the above paragraph is nearly always quite unsymmetrical to the organ-pipe. Hence the reason for this structure is largely to be sought outside of the pipe, the latter merely giving it the possibility of exhibition. The pipe position in a given room, moreover, determines the particular distribution of nodal regions among the infinite number available.

31. Surveys (in x and y) in the plane of the wall.—These have an advantage over the surveys across the table, because there need be no interferences (apparatus, etc.) between the pipe and the wall and no appreciable nearby reflections. Hence one should expect mere decay curves (i. e., a diminution of acoustic pressure or nodal density with distance) from the normal let fall from the pipe to the wall outward, on all sides. Unsymmetric distributions are referable to causes outside of the pipe. The wall in $+y$ was inconvenient for this purpose, because of its distance from the observer and the heaters near it (hot wall). Hence the wall at $y=-130$ cm., with the pipe *behind* the observer, and 40 cm. above the plane of table (prolonged) in the xz plane, was chosen.

Figure 107 shows the distribution of acoustic pressure (deflection s) for the pipe P at $y=-60$, $P-W=70$ cm. from the wall W, along the vertical ($x=y=0\pm z$) in the wall, i. e., through the pipe normal. The figure also gives the y-z position of the pipe and the pipe normal N. It is seen that the dis-

tribution of acoustic pressure is distinctly periodic, that the foot of the normal is in a trough, and that the pressure distribution here happens to be symmetric with regard to it, so far as the locations of maxima and minima are concerned. The nodal intensity, however, is greater for the lower points than for points above the pipe normal. The possibility that with the pipe-mouth down, sound travels with less obstruction downward than up is soon to be negatived. The peculiar feature of symmetry of the rays r and r' (fig. 107) is such that they make an angle of incidence with the pipe normal of $39°$ at a glancing angle of $51°$ at the maxima.
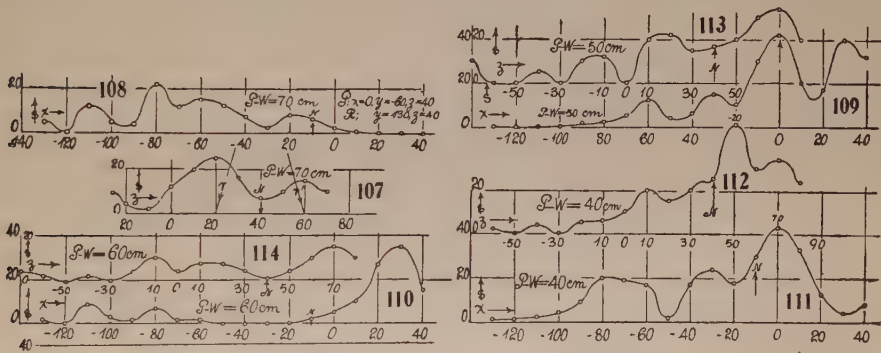
The next survey was made with the same pipe position ($y=-60$, $P-W=70$ cm.), but along the $\pm x$ direction through $z=40$ cm., the pipe-level. The anticipations were (as usual) quite disappointed, for the new graph (fig. 108) shows but doubtful variations until the wall (located at $-x=190$ cm.) is approached; at least, the marked deflections begin in the march toward the corner of the room. This might also lead one to suspect that the high maximum in figure 107 preceding may be similarly associated with deflection from the floor ($z=-100$ cm.). Neither of these surmises, however, is given any warrant in the following work.

Moving the pipe, at the same level, to $y=-80$ $(P-W=50$ cm. from the wall), the resonator mouth (also in this level and in the wall) displaced successively in x, gave evidence of the nodal distributions shown in the curve 109. The contrast with figure 108 is astonishing; for whereas the latter varies as it approaches the corner of the room, figure 109 is nearly without displacement near that corner, but now shows very large deflections near the *free end* of the wall $(x=42)$. (*Cf.* fig. 34.)

These unexpectedly complicated distributions of nodal intensity in the plane of the wall, under environmental conditions apparently so simple, made it necessary to pursue other intermediate x surveys, with the pipe kept in the same level and orientation throughout $(z=40$ cm., blowing away from wall), but with the pipe-distances $P-W=60$ cm. and 40 cm., respectively, from the wall at $y=-130$ cm. In other words, the pipe is displaced along the same fixed pipe normal to the wall. Figure 110, which is intermediate between figures 108 and 109, shows the maxima at $y=-130$ cm., and $y=-80$ cm. of the former, dwindling, to be deleted in the latter. Again the absence of nodal intensity between $x=0$ and 40 cm. for the pipe-distance $P-W=70$ cm. is replaced by a high crest when $P-W=60$ cm. and by two high crests when the pipe-distance is 50 cm. The remainder of the curves exhibit like harmonic changes less easily described. For each particular pipe-distance, *caet. par.*, there is a particular harmonic distribution of nodal density along x in the wall in the 40-cm. level above the table. These distributions are totally unlike, but pass continuously into each other, nevertheless. The same is further illustrated by the last of the x surveys, figure 111, with the pipe-distance from the wall $P-W=40$ cm. The nodal density has now again moved from the free end of the wall toward the corner of the room, though the high maximum at $x=0$ is retained.

It seems difficult to make out a relation for the maxima, such as was surmised in § 19, for instance; for the evidence which here abounds points to stationary locations for maxima and minima, as if the change were in intensity. Thus, at the coördinates x, z, the schedule would read

$z=$	40	50	60	70 cm.
$x=$ 30 cm.,	min.	max.	max. (1)	—
0	max.	max. (1)	—	—
— 20	min.	min.	—	max.
— 30	max. (1)	max.	—	min.
— 50	min.	min.	—	—
— 60	max.	max.	—	max.
— 80	max.	±	max.	max.
— 110	±	±	max.	max.

The distance apart of consecutive maxima or minima for the same graph or z is usually 30 cm. For $z=50$ cm. this is the case with all of them and the total number of such cases is 9, apart from doubtful cases. In relation to the above surmise of a shift of maxima with pipe-distance, the cases marked 1 in the schedule would be the only ones available, where $\Delta x/\Delta z=2$ or an angle of incidence of $63.5°$; but there is no warrant here for such combinations.

In the endeavor to throw further light on the complicated subject, I carried out the three surveys along the vertical z, in the x-z plane, the pipe being

placed in its former positions, correspondingly. These additional results are given in the graphs (figs. 112, 113, 114) for pipe-distances $P-W=40$, 50, 60 cm., and they are correlative with figure 107. The pipe normal here should foot at $x=y=0$, $z=40$ cm. These experiments in z were made some time after those above in x and before I appreciated the fact that small differences in the lateral (x) location of the pipe would produce an effect on the graphs, very much enhanced. Consequently, the ordinate marked N in the x and z graphs may be regarded as here belonging to the pipe normal. This, however, is of little consequence, for the promise of symmetry around the pipe normal ($x=0$, $z=40$) has already been dissipated by the x-graphs. The z-graphs are even more unsymmetric and independent, and inferences of the kind drawn for the x-graphs are less trustworthy. None of the graphs recall the curves obtained on lifting the pipe above the table (figs. 69, 70, 71), although the experiments are essentially similar and any given survey always reproduces the same graph. Thus it seems to follow again that the cause of the distributions recorded by the graphs must be looked for in the entirety of the environment surrounding the organ-pipe, for the particular stimulation received from the latter.

32. **Cylindrical survey.**—The unexpectedly non-symmetric results obtained in the last paragraph along the east wall W'' (fig. 34) induced me to try a similar group of experiments relative to the center (nearly) of the table. The resonator was therefore carried in a circle of radius r_R, around the plumbline let fall from the mouth of the pipe. The measurements were then repeated for successive levels of the pipe ($z_P=40$ cm. and $50=\lambda$ cm., nearly) and of the resonator ($z_R=0$, $12=\lambda/4$, $24=\lambda/2$ cm.). The relation of the different locations is suggested by the inset of figure 115, which is a reduced plan of the room, with the pipe in the vertical above P on the table. The directions $+y$ (west) and $-x$ (south) are thus toward walls, whereas $+x$ (north) and $-y$ (east) are largely toward open spaces from the table.

In the first exploration the mouth of the pipe P was $z_P=40$ cm. above the table. Carrying the mouth of the resonator on the table with its axis kept parallel to x, around the successive circles of radius $r_R=0$, 10, 20, 30, 40, 50 cm., gave the intensity distributions, s, contained in the graphs (fig. 115 and 116). These are again very definite and interrelated, but quite unsymmetrical to the pipe vertical. The oscillations in eastern and northern R displacements from the center (i. e., to open locations) are meager, while the s oscillations for southern and western directions, trending toward closed parts of the room, are very marked. As r increases from 0 to 10, 20, 30, the maximum nodal intensity lies toward the south; beyond this ($r=40$, 50 cm.) it moves to the west. All the maxima of intensity are larger than the intensity on the table, under the pipe ($r=0$) even at $r=50$ cm. (meaning a pipe-resonator distance of 64 cm.), the s value is a little in excess of $s=23$ for the normal case.

Another view of the results is given by the graph (fig. 117), which collects all the points on the line S-N along x, and on the line W-E along y. The

5

features of the latter are somewhat vague, but the S-N line presents very conspicuous crests and troughs. These are from 40 to 45 cm. apart, and situated on either side of, but without other appreciable reference to, the pipe vertical P in their contours. The inference would again be that we must look to other causes for their occurrence.

The mouth of the pipe was now raised in the same vertical to $z_P = 50$ cm. above the table, or a little over a wave-length (48 cm.). The data so obtained are constructed in the same way as before, in figures 118, 119 for the rotation of the resonator, and figure 120 for its corresponding $\pm x$ and $\pm y$ displacement. The central intensity ($r=0$) has increased, because of the λ-elevation, reproducing the results of figures 55 to 57. The curves as a whole are simpler in outline; the unique maximum is again transferred from S to W as r increases, this time a little sooner, in fact, $i.\ e.$, before r reaches 30 cm. For large values of r, intermediate azimuths would have been desirable; but as the phenomena are adequately given by the linear surveys of figure 120, the extra labor was thought superfluous. The W-E line has now much more detail and

would assist in interpreting the corresponding line in figure 117. By contrast the S-N lines in both figures (117, 120) are very much alike, the maxima and minima in the latter case having been shifted into the north or positive x for the elevated pipe. This also recalls the earlier result (figs. 72 to 74). The distances apart of crests and troughs is here somewhat more difficult to define; but it is still much above 40 cm. and the pipe vertical is ignored as before.

For the fixed position of the pipe it was now desirable to raise the plane of the resonator and the graphs (figs. 121, 122, and 123) contain the nodal intensities for an elevation $z_R = 12$ cm. (a quarter wave-length) above the table. This is the level of an antinode at the pipe normal and the curves are therefore low throughout, conformably with the evidence in earlier figures (58 and 59) for normal positions. Nevertheless, as we depart from the pipe normal or center, to circumferences of radii 10, 20, 30 cm., the unique maxima in the south become prominent and beyond $r=30$ cm. they again shift to the west.

In figure 123, the S-N line has the same characteristics as in figures 117, 120 with its two marked crests. Somewhat less certainly the resemblance in W-E lines may be detected. As in all the N-S lines the central trough lies for some reason to the right of the pipe normal. The maxima are far apart apparently.

The resonator was finally transferred to a level $\lambda/2 = 24$ cm. above the table and moved around the pipe axis, its mouth lying on successive circumferences of radii r, with the results given in figure 124. The maxima of all the curves are curiously flattened; but there is still a gradual transfer of the chief crest from S to W, as r increases. Probably intermediate observations would have modified the curves as drawn. Since $\lambda/2$ determines a nodal plane normally below the pipe, the intensities are all relatively large, but they fall off as a whole so rapidly with r that there is no intersection and all curves may be given in a single diagram.

The graphs showing the intensity s along the S-N and W-E directions in figure 125 now exhibit a total change of form. The two crests have seemingly all but coalesced near the pipe normal. Owing to an accident which somewhat dislocated the fringes, the indentation in the middle of the S-N curve and the bulge toward the right in the other may need modification; but this is of little consequence here, since the plane at a level of $z = 24$ above the table contains a single marked crest only.
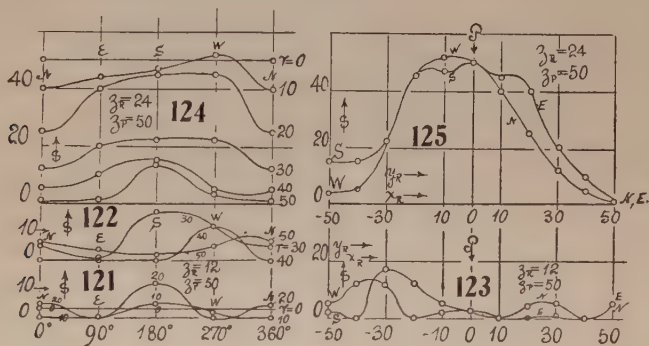
It is of further interest to bring the values of intensity together when the resonator moves up from the table on the same vertical. The values of s along x_R, at the different altitudes, z_R, are from south to north,

$x_R =$		-50	-40	-30	-20	-10	± 0	10	20	30	40	50 cm.
$z_R = 0$ cm.	$s =$	20	5	25	40	40	30	20	15	15	2	1 s. p.
$= 12$ cm.	$s =$	2	0	17	12	5	3	0	4	5	0	5 s. p.
$= 24$ cm.	$s =$	15	15	22	45	47	50	40	25	12	5	1 s. p.

As constructed in figure 126, with s laid off horizontally to the right z_R vertically and with the origin of *each* tripoint s-curve at the x position of the vertical to which it belongs, these vertical distributions of nodal intensity strike the eye. The intensities s on the table for the same x positions (fig. 120) are also sketched in. Under the pipe at $z_P = 50$ cm., the nodal surface at the table rapidly decreases in s intensity to the antinode at $z_R = \lambda/4$; s then rapidly increases again to the more pronounced nodal surface at $z_R = \lambda/2$, nearer the pipe. Toward the south, however, the distinction between node and antinode is not regularly sustained; at $x = -20$ cm. the antinode has gained in strength and at $x = -30$ cm. the strength of nodes and antinodes does not differ much. Beyond this ($x = -40$, -50), however, nodes and antinodes are again

sharply contrasted. Toward the north from the pipe normal ($x=0$) these differences die out more gradually, until at $x=50$ cm. the intensities are, for some further reason, reversed.

What is very surprising, however, is the observation that throughout the whole of the extent of a linear meter ($x=\pm50$) symmetrically to the pipe normal the nodal and antinodal planes at $z_R=0$, $\lambda/4$, $\lambda/2$ remain parallel to the table, so far as can be seen. The only distinction within this stretch is the distribution of nodal intensity as exhibited in the continuous curves sketched in, or separately in figures 117, 120, 123, 125. It would, therefore, here seem to be a mistake to associate wave-length with crests and troughs in these diagrams, however plausibly such inferences may obtrude. It is very much more probable that in the south some extraneous s distribution has been super-posed which has already been encountered in the vertical survey for the y-z plane in figures 104, 105.
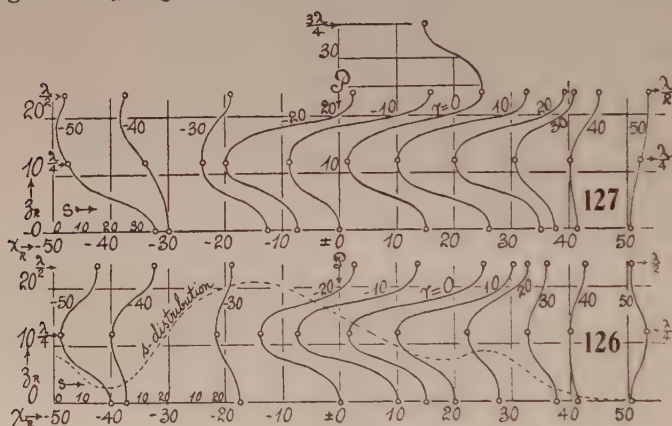
The west-east distributions ($\pm y$), though not so sharp in their features in figures 120, 123, and 125, show an equally pronounced character, when treated in the same way relative to vertical variations, in figure 127. At $r=0$ the second antinodal region is indicated. The tabulated values of the nodal intensity, s, for the W-E points along the successive verticals at y_R are ($\lambda=48$ cm.) :

$y_R=$		-50	-40	-30	-20	-10	± 0	10	20	30	40	50 cm.
$z_R=$ 0 cm.	$s=$	35	20	35	25	20	30	32	30	15	2	7 s. p.
$=$ 12 cm.	$s=$	5	12	12	0	2	3	0	0	1	0	4 s. p.
$=$ 24 cm.	$s=$	4	5	22	45	52	50	45	40	20	10	1 s. p.

Each of the triplet graphs is to be referred to an origin at the x_R marked on the curve, and the (horizontal) s intervals are 20 scale-parts. Since the edges of the table are at $y=\pm60$ cm. (nearly), the nodal plane does not extend quite so far ; but it does not follow that these edges have much influence on the results, since the same kind of graphs appear in figure 126, where the edges of the table are nearly 50 cm. farther. The degredation of the nodal plane occurs first at $y=50$ cm. in the east as it did in the north. In the west it is still strong at $y=-40$, and now promises to run through another cycle of

intensity, as it did in the previous case. The antinode, very nearly $s=0$ throughout the east, begins to lose identity between $y=-20$ and -30, to be followed by oscillations. Finally, the first nodal plane above the table degenerates here more obviously than before, between $y=-30$ and -40.

The records in figures 126 and 127 contain an almost complete example of a free nodal region sustaining itself $z_R=24$ cm. above the table, and figure 125 gives the acoustic pressures within it. These are largest near the pipe, though not quite symmetric, and it is possible that the direct ray may here influence the resonator. In general, however, i. e., at greater distances, the direct ray is relatively ineffective, and it is to the occurrence of nodal regions alone that the resonator then responds, even when the direct ray would seem to have the advantage of nearness.

33. Axial rotation of pipe. Second antinode.—As the pipe wind blows in a particular direction, it was of some importance to ascertain again whether this wind direction had any influence. The pipe was therefore rotated around its own axis in succession, producing winds blowing north, east, south, and west. In each case the fringe deflection s was 20 scale-parts, the resonator being at $r=3$ cm. (south) on the table and the pipe at $z_P=50$ cm. above the origin, as before. Thus there is no wind effect.

A further test consisted in lifting the resonator to $z_R=36$ cm. above the origin on the table. This is the second antinodal level ($3\lambda/4$), now very near the pipe at $z_P=50$ cm. The deflection obtained was about $s=30$ and is indicated in figure 127 on the $r=0$ curve. Thus, in spite of the proximity of the pipe (12 cm.), the second minimum is still distinctly present, though its intensity is naturally in excess of the $s=3$ of the first minimum. The next maximum would no doubt be enormous, as in figure 106, so that we here encounter the direct effect of wave-trains.

34. Improvements of the pin-hole resonator. Solid viscosity in mercury U-tubes.—Experiments with this end in view were made at great length, but at first little definite progress was achieved.

The plan immediately suggesting itself was the trial of an adjustable needle-valve pin-hole. The apparatus is shown in figure 128, where tt is a $\frac{1}{4}$-inch brass tube with a conical point c, carrying the pin-hole at its end o. The tube tt is closed by a long nut m, in which a waxed screw s, terminated by the needle n, is movable. The pin-hole o could thus be completely closed or opened in any degree by advancing or withdrawing the screw s. The lateral tubulure r communicates with the interferometer U-gage. The adjustable pin-hole was inserted into the tuned resonator R, as usual. After many trials with this promising apparatus, no fringe deflection whatever was observed until the needle n had been completely withdrawn; and the simple pin-hole so obtained, being too large, functioned badly. The adjustable fixture completely failed. Tests made by inserting the conical glass pin-hole, as above, worked as well as before.

In fact, the best available pin-holes for the resonator were made from glass quill tubes drawn to a blunt cone. Occasionally this was broken off at just

the right size of hole. Usually, however, it was necessary to enlarge it by grinding, or to close the conical end by gentle fusion and regrinding when cold. In any case it is a long and tedious process, as there is no adequate guidance. Thick-walled glass tubes, of the same size externally, produced no deflection. Brass resonator tubes about 2 cm. in diameter gave the best response to f'' pipes.

To throw further light on this intricate subject, it seemed advisable to operate with pin-holes in soft sealing-wax, as these could be more easily shaped. In this way new information was obtained. A thin sheet of wax was spread on thin paper closing the end of the quill tube t, figure 129. When the wax was punctured by a needle from the inside of the tube t, producing a conical hole as exaggerated in figure 130, the fringe deflections were positive and reached a maximum with the right size of hole. But when the thin wax sheet was punctured from the outside (suggested in fig. 131), the deflection obtained was to the same degree negative. In other words, in passing from the salient pin-hole 130 to the reëntrant pin-hole 131, acoustic pressures pass to acoustic dilatations; or the pressure excess is on the reëntrant or concave side of the conical pin-hole. It follows, therefore, that a cylindrical pin-hole must be inactive, if used with a resonator, and it is possible that the interminable record of failures experienced in the present work with metal foil is attributable to this cause.

The remarkable efficiency of glass quill-tube probes, with the pin-hole at a conical end, ground off, thus finds its explanation; for these are in conformity with figure 130.

To further verify the new results, holes were bored with a fluted conical reamer in small disks of brass, and these were then soldered to the ends of quarter-inch brass tubes, as shown in figures 132 and 133. The cones ended in pin-holes, drilled from within and without, respectively, by fine needles. No. 132 gave positive deflections of about 10 scale-parts, No. 133 negative deflections of about 5 scale-parts but very definite. It was found that on enlarging No. 133 from *within* with a needle, the deflections became positive; but on further enlarging the pin-hole, now from without, they became negative again. This proves, conformably with the earlier evidence, that only a very small depth of pin-hole (probably of the thickness of a piece of paper) is effective and the remainder of the cone is without importance.

Experiments with the wax pellets at the end of quill tubes (fig. 129) were now resumed, and figure 134 shows the results obtained on puncturing a number of them side by side successively from without. The (negative) maximum here passes with two holes. In figure 135 similar results are given, obtained on puncturing successively from within the quill tube, in this case with a small as well as with a larger cambric needle. The maxima obtained in all these experiments with wax are relatively small, the glass pin-hole resonator reaching deflections of 35 scale-parts under like circumstances of position, *i. e.*, it showed 3 times greater sensitiveness. The double resonator (open tube, two mouths, pin-hole central) was usually in excess of this, but the two mouths are confusing.

Fine slits cut in wax behaved similarly to the pin-holes above mentioned, producing pressure for a salient wedge, and the reverse. The endeavor to produce the same effects with rigid slits, however, led to no results.

A pin-hole made with two pairs of knife-edges (slits) at right angles to each other, leaving a square hole between, always behaved negatively, probably because a slit underlay the hole. Its negative sensitiveness, however, was ordinary (10 scale-parts). It is quite possible that the wedge angle (figs. 130, 131) plays a part quite as important as the size of the hole, though I have been unable to get definite evidence on this question. Frequently, however, holes successively reamed with a needle will show no further increase of sensitiveness when the use of a 10° or 20° wedge-shaped-point reamer will at once double the deflection.
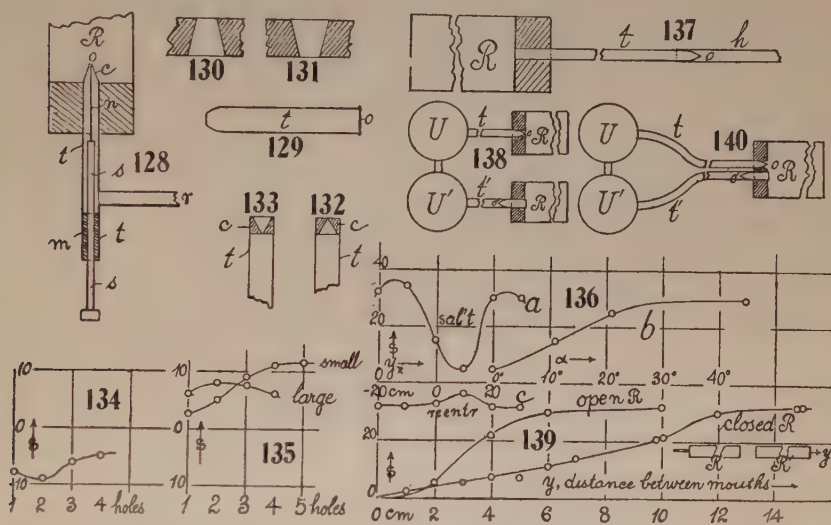
The case of figure 136a (salient pin-hole), when tested with a reëntrant pin-hole (fig. 133) resonator, supplied the results shown in figure 136c. The maxima and minima are throughout negative. It was supposed that if maxima were negative, minima might be positive; but this is not the case. Both salient and reëntrant pin-holes function in the same way, with an inversion of sign, but without change of sign for the same pin-hole. I have not, as a rule, been able to get more than 10 scale-parts for a reëntrant pin-hole, when a salient one gave over 30 scale-parts. The latter was usually found more sensitive.

In the preceding report (Carnegie Inst. Wash. Pub. 310, 1921, § 25) the transition of acoustic pressures into dilatations on the reversal of the conical pin-hole has already been treated in connection with the closed region. Testing this again, a glass cone giving a deflection of 40 scale-parts for pitch a', if salient, changed this to -25 scale-parts of pitch a' when reëntrant. In pitch c'' the deflection increased (negatively) to -50 scale-parts, the salient cone showing no deflection in pitch c''. I was not prepared, however, to find

copper foil, punctured from the outside with a fine needle, behaving similarly; but I obtained with the same adjustment −40 scale-parts of pitch a', while the reversed foil gave +40 scale-parts in pitch $\flat a'$.

The important question is thus adduced as to whether the pin-hole resonator with a reversed cone (fig. 137) will also produce a reversal of fringe deflections. The f'' resonator, with f'' closed organ-pipe, was therefore tested. the pin-hole cone being joined to the U-gage by a short end (20 cm.) h of rubber tubing. On trial an affirmative answer was obtained at once. Thus

Resonator.	Cone salient.	Cone reëntrant.
A............	Deflection 60 s. p.	Deflection —20 s. p.
B............	Deflection 40 s. p.	Deflection —25 s. p.
C............	Deflection 35 s. p.	Deflection —25 s. p.

The negative deflections were here numerically smaller than the positive deflections, a rule which does not hold generally, however. It was further to be expected that the negative deflection would decrease with the length of connector-tube t from the bottom of the resonator R to the reëntrant pin-hole o (fig. 137), the pipe h beyond being the rubber connection to the U-gage. This was also the case, though I obtained no decided harmonic relations; for example (resonator C, t connector varied, only):

Length of t......	5	10	21	46	100	150 cm.
Deflection	— 37	— 30	— 28	— 30	— 12	— 5

Thus the negative pin-hole resonator runs down in sensitiveness much more rapidly if treated in this way (pin-hole remote) than if the pin-hole is fixed in the bottom of the resonator and the connector-tube h of any length communicates with the U-gage. That at 50 or 100 cm. of removal from the resonator there should be such large deflections left is the surprising feature of these tests.

A final attempt to construct conical pin-hole probes was made by catching a small drop of wax at the end of a conical tube and then reaming out the wax with jeweler's broaches. It proved to be an easier method than grinding pin-holes to size, but the success was not remarkable.

In conclusion, a peculiar behavior of the U-tube, after long use, may be referred to here, and that is an exhibition of what is apparently solid viscosity. Thus, when the current of the telephone circuit is closed, the deflection appears instantaneously; but in the lapse of minutes, if the current is kept closed, the deflection gradually increases to a limit (depending on the time elapsed and on the amount of deflection), which may be 10 per cent larger than original deflection. If the current is now broken, the deflection vanishes instantly, leaving the residue of the 10 per cent in question (usually about 5 fringes) to vanish in turn gradually in the lapse of minutes. After this the zero is quite regained. We have thus a case not only of viscosity under stress, but of residual viscosity after stress ceases. Supposing there might be some electrostatic excita-

tion, I ionized the surrounding air with radium, but no effect was produced. The phenomenon can only be associated with the surface tension at the (glass-covered) free surface of the U-tube. I have not been able, thus far, to make these surfaces move quite in parallel under change of pressure. Hence capillary tensions enter in a slight extent to modify the deflections. These tensions are quite permanent in a given adjustment, as is evidenced by the permanence of the zero, even after rather rough handling. But if the gage is shaken by concussion, a new zero appears, to be permanent in its turn. It is thus in connection with the tension of the surface film of mercury (possibly enhanced by the age of the gage) that the phenomenon of solid viscosity functions. If it were also to appear in the case of rigorously pure and fresh mercury, it would have considerable theoretical interest, as the liquid surface here displays (i. e., under interferometer observations) the specific properties of a solid. From a practical point of view, U-gage deflections must obviously be read off at once, so that the zero may be regained throughout.

35. Positive and negative pin-hole resonators coöperating. Paired or twinned resonators.—It was shown in the earlier report (l. c., fig. 33) that if the two shanks of the U-tube are provided with reëntrant and salient conical pin-holes, respectively, no fringe deflection is obtained when the pin-holes lie within the same closed region (T-branch with the telephone at the third end). This was again tested with the same results, the reason being, as it was thought, that pressure and dilatation are balanced in the T-branch and the U-gage remains inactive. (See § 37.)

It is obvious, however, that the positive (pin-hole cone o salient) and negative (pin-hole cone o' reëntrant) pin-hole resonators, R and R', figure 138, must add their respective pressure effects at the gage UU', if they are provided with independent connector-tubes t and t'. The plate-glass covers of the cisterns UU' were therefore both sealed and put in communication with two resonators (B and C) of about equal strength. The results were: B alone $s = +60$; C alone $s = -55$; together $s = 110$, the fringes passing beyond the scale limits. A large number of similar experiments all indicated that the separate deflections may be added, at least roughly. The sensitiveness may thus be nearly doubled. It is probable, moreover, that two such resonators will interfere less with each other than two positive or two negative resonators (i. e., two identical resonators, generally), if placed a short distance apart (cf., inset, fig. 139). The data found for the two resonators B and C, when approaching each other coaxially, mouth confronting mouth, were:

Distance between mouths...	10	6	5	4	3	2	1	0.5 cm.
Fringe deflections ....$s = 110$	90	85	80	70	60	35	10	

The deflection thus falls off slowly and does not quite vanish, even with a mere crevice between the mouths. If the two resonators are parallel, side by side and mouth near mouth, the conditions are even much better. Thus about $s = 100$ was obtained for this contiguous position, indicating much reduced interference. Hence if RR', figure 138, are placed side by side, and

the connector tubes t, t' are of pure rubber, elongated if necessary, the twin apparatus is available for exploration.

With short connectors tt' in the interest of greater sensitiveness (the loss of deflection was here about 20 per cent per meter of t), I made a number of tests to find the maximum distance for which the twin resonator (fig. 138) would respond. The exploration proceeded in the x direction into the adjoining room and the pipe (resonators at origin) was at each stage moved about in a plane normal to x, to find the conditions of best response. The results are necessarily irregular, the only object being to find the limit. An example may be given:

$x=$	100	150	200	250	300	350	400	450	500	600 cm.
$s=$	90	100	25	33	25	10	15	4	10	1 scale parts

Thus the twinned resonators are able to hear to a distance of 6 meters, the deflection being then about a fringe. No doubt in an unbroken empty room the distance would be larger; but it is none the less suggested that the response of the pin-hole ceases abruptly, beyond a certain threshold limit of intensity.

Although a single resonator with a branched tube is ineffective for reasons already stated, the suggestion of using the bottom of the resonator R, figure 140, as a branch point for the connector tubes tt' to the gage UU' seems highly promising. One and the same resonator here functions in both (positive o and negative o') capacities. The apparatus, in fact, succeeded at once, without, as it seemed, much sacrifice of sensitivity. Figure 141a shows the fringe deflections obtained along y, for the case of short connector tubes tt' (30 cm. long), with the pipe at $x=50$, $y=40$, $z=50$, near the center of the table. In curve b the same result is extended with long connector-tubes (130 cm.). In curve c, finally, the results refer to a more distant pipe at $x=100$ cm., $y=40$, $z=50$. The curves fall off quite abruptly at the two edges of the table $y=-27$ and $+93$ cm. The extreme importance of tuning was noteworthy throughout, mild notes frequently giving large deflections, sometimes out of field, whereas strong notes of the same pitch to the ear dropped the fringes back to zero. A variety of experiments was made with this twin resonator, with results like the above, which need not therefore be reported.

36. Sound filtration. Resonator absorption.

—Tyndall's familiar experiments with sensitive flames relatively to the transmission of sound by paper and cloth may in a measure be repeated, though merely for orientation. Subjects of this kind have been so thoroughly investigated by Professor F. R. Watson * and his collaborators at the Engineering Experiment Station of the University of Illinois, in a specially designed acoustic laboratory, that it would be idle to attempt to add to their results with the resonator in its present stage. For this reason a suitable acoustic box was dispensed with and the cloth (like a handkerchief) was laid flat on the table, covering the resonator. There is one difficulty here, inasmuch as any interference at the mouth may change the pitch and a low result be obtained for this reason. The cloth must therefore lie

---

* Sound Proof Partitions, by F. R. Watson, Univ. of Ill., Bull. 127, 1922.

loosely, with the edges weighted down in the case of paper, etc. A few data may be given as examples:

Full deflection ....$s = 30$	Thin (¼-inch) loose cotton batting.... 11
Loose cotton plug in mouth of resonator o	Coarse muslin (flat)................... 9
Loose cotton plug all but withdrawn.. 10	Canton flannel 0-1
Handkerchief, flat 12	Filter-paper (flat).................... 10
Handkerchief, loose 15	Towel paper (flat).................... 5
Handkerchief, puckered 22	Foolscap (flat) 5

Thus, canton flannel is all but impervious to the ear of the resonator, under the conditions.

The marked disturbance produced by one resonator placed within a distance of $\lambda/4$ of another has often been referred to above. The actual effect may best be rated by placing the resonators coaxially with their mouths (one mouth in case of the double or open resonator) towards each other. In figure 139,
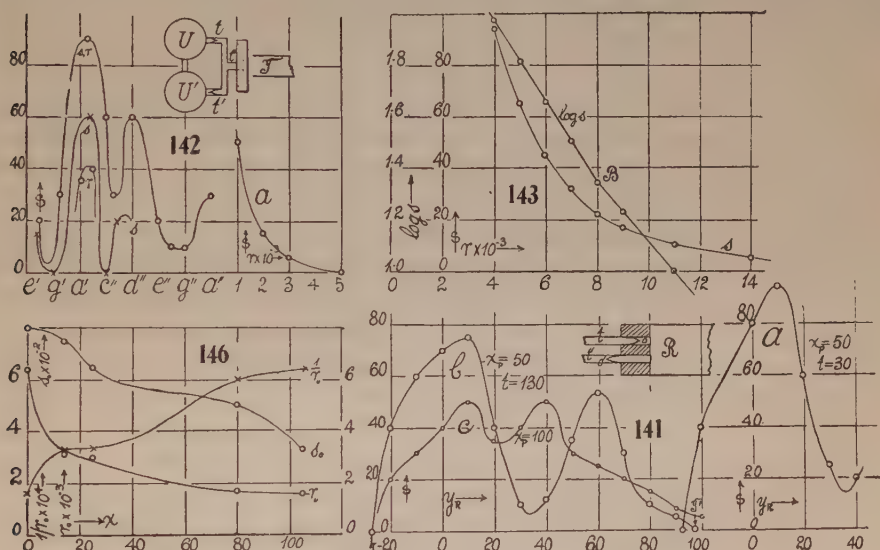
with the pipe at $z = 40$ cm. above the origin and the mouth of the pin-hole resonator (R in inset) at $x = 0$, $z = 0$, $y = 20$ (i. e., on the table), the mouth of the second resonator R' was moved from $y = 20$ (coincidence) to larger y values, both resonators being coaxial in y. The normal deflection in the absence of the second resonator was $s = 32$. In case of two closed resonators, the mutual interference did not cease until a distance between mouths of over 12 cm. ($\lambda/4$) had been exceeded. Moreover, the evanescence of the effect seemed to be accelerated between $y = 10$ cm. and 12 cm. The open resonator behaves very differently, its interference ceasing appreciably at a distance of 6 cm. between mouths. The far, or third, mouth here dips into other nodal distributions, which render it less effective. It is not necessary that the resonators be adjusted coaxially to obtain similar results. Bags of muslin or filter-paper, tight or loose, tied about the mouth of the resonator, usually cut off all deflection. Sometimes for an intermediate size of bag a small deflection is

observed. Similarly, a pin-hole resonator coaxially within another resonator
or a conical flare is at no advantage. The mouth of the pin-hole resonator
sunk within a cylindrical tube is always inactive, unless the mouth of the
resonator is flush with the open end of the tube or projects beyond it.

Figure 136 gives an example (curve b) of the reduced reflection observed
when the plane reflector (12 inches broad, 18 inches high) is rotated from
the original incidence, $a=0°$. With the plane at normal incidence, $a=0°$,
at $y=30$ and the pipe at $z=40$ cm. above the origin, the curve a shows the
corresponding distribution of nodal intensity found by the resonator moving
in y. Thus the minimum is at $y_R=10$ cm. Leaving the resonator in this
position, the board was now rotated on its vertical edge, successively, as far
as $45°$. The minimum gradually vanishes into the free deflection, $s=30$; but
the plane is still effective as a reflector or diffractor, until the angle of rotation
exceeds $30°$. Much depends on the lateral size of the reflector; but I did not
pursue the subject further.

37. The twinned pin-holes in branched tubes.—Thus far, all endeavors
to obtain registry at the U-gage, by providing the pipes t and t', figure 140,
with salient and reëntrant pin-hole probes within, respectively, and then join-
ing t, t' to a single pipe leading to the source of sound, proved failures. I made
a final attempt by attaching the salient and reëntrant conical probes immediately
at the U-gage (see inset, fig. 142) and then joining the two to a telephone by a
short T-branch. This method succeeded surprisingly well, the success being
referable either to the short connection (*i. e.*, to relatively great intensity of
sound together with a length favorable to the harmonics) or to a more suitable
selection of the aperture of the pin-hole cones.

I may premise that reversed probes, attached to the respective shanks of the
U-gage and open to the air, did not respond to organ-pipe or other notes.
Placed just within an adjutage of the telephone mouth-piece, both gave a strong
positive registry, *i. e.*, without distinction in sign, because of the reversal. In
fact, the reëntrant probe happened to be the more active. With the branched
tube described (inset), the response was even more marked. The success of
the experiment being thus assured, I carried it through the range in pitch
given in figure 142, where the inset indicates the connections. The fringe
displacement at the gage was now so ample that 5,000 ohms had to be placed
in the telephone circuit of the electric siren to keep the fringes within the field.
Stopping up the branch t' and opening U' to the air, or the corresponding
operation for t', gave the two lower curves (s, r) on the same diagram. Both
of these are positive, since the pin-hole probes are reversed. Apart from
some shift of pitch, these individual effects are nearly summed in the resultant
curve. Tests with both probes, either salient or reëntrant, gave obscure
differential results.

A rubber tube over a meter in length was now inserted at t'' (inset) between
the telephone and the gage apparatus (T-branch). With the resistance of
5,000 ohms in circuit, no response whatever was obtainable; but on reducing

the resistance of the telephone circuit successively to 1,000 ohms, the fringe deflections rapidly increased, as shown by the curve a, figure 142, for the same maximum note at a pitch near a′ here throughout. The falling off of the intensity s with the current is quite abrupt, so that a former inference that the pin-hole probe ceases to operate practically when a certain threshold value of intensity has been reached seems to be corroborated. A shorter tube insertion of about 30 cm. at t″ similarly decreased s to about 15 scale-parts. Thus, when the telephone in figure 142 (inset) was replaced by an f″ resonator, it was not influenced by the f″ organ-pipe, as is the case very strikingly in the adjustments figures 138 and 140.

If the curve a, figure 142, be expressed by the equation $s_0 = se^{r/r_0}$ presently to be discussed, where s_0 and r_0 are constants and s is the fringe deflection when the impedance of the telephonic circuit is r, the results are, $s_0 = 155$; $r_0 = 2,000$ ohms:

$$
\begin{array}{ccccc}
s\ (\text{observed}) = & 50 & 15 & 5 & 1 & \text{s. p.} \\
s\ (\text{observed}) = & 49.1 & 15.5 & 4.9 & 0.5 & \text{s. p.} \\
r = & 1,000 & 2,000 & 3,000 & 5,000 & \text{ohms}
\end{array}
$$

the agreement being quite as close as the observations warrant. Here s_0 is the deflection for the zero of impedance ($r=0$) and r_0 the resistance to reduce s_0 to $1/e$ of its original value. The relatively small value of r_0 which occurs here is noteworthy. Without entering into the details of the subject, some tests were also made of the effect of lengthening the quill tubes t and t′, between the pin-hole probe and the U-gage (fig. 142). The results showed not merely a shift of pitch for the high crest, but the indications of definite relation of length of tubes and maximmu sensitiveness. Thus the following data were obtained (4,000 ohms in circuit):

Length of tubes added	0	10	13	16	25	100 cm.
Fringe deflection, s	85	70	100	105	70	65

The optimum appears when each of the quill tubes t, t′ is about 16 cm. long and there is a minimum within this length. The usual harmonic conditions must therefore here also be satisfied; however, the reduction for long tubes (meter) is not as marked as when tubes are inserted between pin-holes and telephone.

38. Exponential relations of acoustic pressure to the amplitude of sound-waves.

—The strikingly close fit of the equation $s_0 = se^{r/r_0}$ proposed for the curve a, figure 142, deserves fuller consideration. Accordingly, a series of experiments was made with the short connection device (fig. 142, inset), by inserting large resistances successively in the telephone circuit and measuring the height of the unique crest near the pitch a′. The results are reproduced in figure 143, in which both the data for s and log s are plotted, in terms of the large resistance r in circuit. The curve for log s is again definitely linear, but with a break B at 8,000 ohms, owing no doubt to some incidental dislocation within the apparatus. It is thus advisable to compute the results in two series, 4,000 to 8,000 ohms and 8,000 to 18,000 ohms, separately. The former is more

accurate, since the fringe deflections are so much larger. The computations gave, $s_0 = 399$; $r_0 = 6,380$ ohms:

$r \times 10^{-8}$	4	5	6	7	8 ohms
s observed	95	65	45	32	22
s computed	94.0	65.5	45.6	31.8	22.1

true to about half a fringe. It will be seen that if the curve had been treated as an hyperbola, the inductive or other additional resistance would have to be negative. In the second case $s_0 = 190.5$, $r_0 = 8,620$ ohms:

$r \times 10^{-8}$	8	9	11	14	18 ohms
s observed	22	17	10	5	1
s computed	22.4	17.0	10.1	4.5	1.6

The constants are different here, owing to the break at B, into the cause of which it is not necessary to enter; but the present constant r_0, which is the resistance needed to reduce the original deflection s_0 or the equivalent acoustic pressure by $1/e$, departs so much from the preceding value for long tube-connections (fig. 142, a) that further elucidation will be needed. A preliminary remark on the equation used may be here in place. It was inferred in the preceding report (Carnegie Inst. Wash. Pub. No. 310, 1921, § 17) that for a given telephone carrying the large external resistance r, the equation $rs =$ const. fitted the curves within a range of low frequency adequately, when an unbranched quill tube connected the telephone with the U-gage then used. In the present experiments with branched tubes this hyperbolic equation (verified only for low frequencies, $n < 100$) no longer suffices, even if the form $s(r + r_0) =$ const. were substituted, for r_0 would have to be negative. The new observations were made for different lengths (x) of tubing t'', inserted between pin-hole probes and telephone. These lengths x were additions to the 19 cm. (about) at the branch tube and 8 cm. at the telephone mouth-piece, which remain fixed, the latter being wider than the quill tubes. The results are given for s and r in figure 144 and for log s and r in figure 145. The data and constants of the equation $s_0 = se^{r/r_0}$ are recorded in table 1.

As a whole the agreement is as good as the observations warrant, when the fringes do not leave the field or more than a few fringes are in question; nevertheless, more trustworthy constants could have been obtained by judicious inspection of figure 145 than are here deduced by the computations. The trend constant is constructed in figure 146, the abscissas now denoting the added length x in centimeters, while the ordinates are s_0, r_0 and $1/r_0$. The constants s_0 make up a sinuous line, which, however, definitely decreases as the tube-length x is longer; i. e., the initial fringe deflection or acoustic pressure is largest when very little tube-length x is inserted between pin-holes and telephone. Wave-motion is gradually damped out. Similarly, r_0 decreases when the tube-length x increases, the curve again being somewhat sinuous. In other words, the resistance r_0 to be inserted to reduce s_0 by $1/e$ is much greater for short tubes, as figure 146 as a whole indicates. If we examine the curve $1/r_0$ in terms of x, it would seem that further removal of length of about 20 cm. (i. e., the fixed length of T-tube, etc.) should reduce $1/r_0$ to zero

and s to s_0. A number of tests were therefore made, using perforated corks, short glass T-branches, etc., to reduce x. In all of these, however (see examples a, b, fig. 144), s_0 and r_0 decreased again; or $1/r_0$ increased. The relations for short tubes are therefore as usual harmonic. In one case of the short glass T-tube, for instance (curve a), the deflection s was increased from $s=25$ to $s=42$ (curve b) at 5,000 ohms by inserting an additional 15 cm. of tubing to the telephone. Thus it is improbable that the ranges of sensitiveness contained in figures 144 and 145 can be materially increased by locating the pin-holes closer to the telephone plate.

It is, finally, necessary to consider the case of the unbranched tube, for which $rs=\text{const.}$ was temporarily accepted in the earlier report. The data

TABLE I.—Values $s_0 = se^{r/r_0}$ for branched tubes.

Pitch	x	$r \times 10^{-8}$	Observed s	Computed s	$\log s_0$ / s_0	r_0 / $(1/r_0) \times 10^4$
	cm.	ohms				ohms
f'	14	1500	>120	12.5	2.579	
		2000	88	86.5	379	3115
		3000	42	41.3		3.21
		4000	20	19.7		
ba'	25	1000	>130	150	2.508	3000
		1500	110	102	322	3.33
		2000	70	69		
		3000	32	32		
		4000	15	15		
		5000	7	7		
g'		7000	1	1.5		
ba'	80	700	93	95	2.399	1653
		1000	60	62	251	6.05
		2000	15	15		
		3000	4	4		
ba'	105	500	80	78	2.214	1563
		1000	? 28	37	164	6.40
		2000	7	9		
		3000	2	2		
		4000	< 1	.5		
b'	0	....	....	....	2.601	6380
					399	1.57

newly investigated are given in figure 147, the adjustment being shown in the inset. The graphs a and a' contain s and $\log s$ in terms of r respectively for a salient pin-hole probe; b and b' give the corresponding values for a reëntrant probe, which happens to be somewhat less sensitive. Again, the logarithmic graphs are linear, with a break at B. In case of the salient probe, two sets of constants must therefore be computed, and they are given in table 2.

The agreement throughout is good, the error of the computation seldom exceeding a fringe in s, quite on a par with the measurements. The preliminary low-frequency equation $rs=\text{const.}$ must therefore be abandoned. The constant s_0 shows that a definite initial deflection can not be exceeded for any intensity of sound-wave obtainable from the given source. Moreover, because of the diminutions in s in rapid geometric progression, it is not possible to reach very great sensitiveness with the pin-hole probe. The

result explains absence of registry in case of the pin-hole resonator, when the sounding organ-pipe is a few meters distant, *i. e.*, the rapid decline of the deflections with distance. (§ 35.) Hence, since the amplitude a at the reso-

TABLE 2.—Values of $s_0 = se^{r/r_0}$ for short unbranched tubes respectively salient (g') and reëntrant (a').

Pitch		x	$r \times 10^{-8}$	Obs. s	Computed s	$\log s_0$ s_0	$1/r_0 \times 10^4$ r_a
			ohms				ohms
g'	short		3.57	98	98	} 2.564	1.60
			4.07	83	82	} 366	6250
			5.07	58	57		
			6.07	38	39		
			7.07	30	30.3	} 2.365	1.25
			8.07	23	22.7	} 232	8000
			9.07	17	17.0		
			10.02	13	13.0		
a'	short		1.12	>130	131		
			2.12	70	68.4	} 2.435	2.83
			3.12	35	35.6	} 272	3530
			4.12	18	18.6		
			5.12	10	9.7		
			6.12	7	5.1		
			7.12	4	2.6		

nator decreases linearly with the distance x of the pipe, the equation here takes the form $s = s_0 e^{x/x_0}$. Thus a deflection of 146 fringes at close range, falling to 54 fringes at 1 meter, would decrease further to 20 fringes at 2 meters,
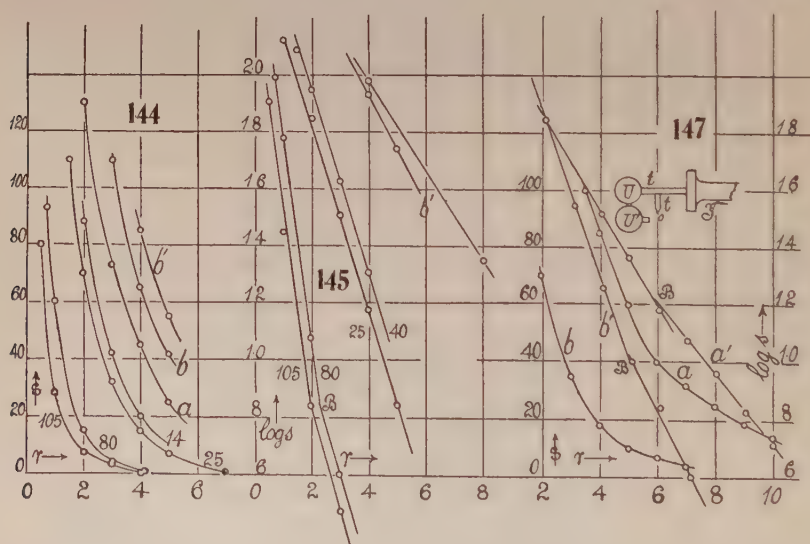
7.3 at 3 meters, 2.7 at 4 meters, etc., which is about the order of values obtained in the long-range experiments of § 35. Briefly, therefore, the exponential law seems to belong to the acoustic pressures evoked by the pin-hole probe. We may write $ir = i_0 r_0$ for the effective current i in the telephone, and

regard the amplitude a of the telephone-plate and of the sound-wave produced by it proportional quantities within the limits of observation, so that $i/a = i_0/a_0 = $ const. If, finally, s is replaced by the corresponding acoustic pressure p, the equation takes the form $p_0 = pe^{a_0/a}$, where a refers to the sound-wave in the quill-tube connectors.

If finally s_0 is constructed as a function of r_0, both increase together, rather roughly, as far as the break B in the logarithmic graphs, beyond which point s_0 decreases. With this grouping of data, the results of the former report (l. c.) are not in harmony. Thus, series 9, figure 18, as there obtained, would require $r_0 = 6,850$ and $s_0 = 78$ to be reproduced by the exponential equation. The old results were obtained by a metal-foil pin-hole, and either this or some other instrumental factor puts them in a different class from the newer results.

It was shown in the preceding report that a reversal of the telephone current (i. e., exchange of the leads of the telephone) may reverse all the harmonics, changing pressures into dilatations, or crests into troughs. In other cases, only certain harmonics were thus reversed. In the present experiments with branched quill tubes (fig. 142, inset), reversals at the chief crest ($\flat b'$) did not occur; but the intensity was about 10 to 20 per cent greater for one position of the switch than for the other. In such a case, moreover, one of the crests was very steep ($\flat b'$); the other a flat or double maximum (a' to $\flat b'$).

Different common telephones, tested at random (unipolar, bipolar), showed but little difference (within 20 per cent of fringe deflection), the s-displacement depending largely upon secondary details, such as the tight clutch of the plate of the telephone, the efficiency of the break at the primary, frequency increments, etc. Moreover, a given telephone, tested from day to day, in the lapse of time behaves with marked variability, deflections changing irregularly from 40 to 60 scale-parts. This question, though pursued for some time, was not brought to an issue; but it is probable that temperature expansions of the telephone-case change the stress of the telephone-plate and that the motor break varies.

In using the branch-tube (fig. 142, inset), the relative lengths of the parts tU and $t'U'$, tT and $t'T$ are of importance, supposing the branches to be short. When the latter pair was equal, the results were strongest when $t'U'$ exceeded tU by about 4 cm. Thus the deflection for equal branch-lengths was $s = 43$ cm. The 4 cm. excess in question changed this to 63 cm. In fact the effect of a single extra centimeter of length is here quite appreciable, even though $\lambda > 60$ cm.

39. Sensitiveness of telephones. Radio-telephones.—It has just been stated that the common telephones tested evidenced about the same sensitivity; but this was by no means the case with the high-resistance telephones used in wireless telegraphy, as would be surmised. One of these, adjusted as in figure 147 (inset) threw the fringes out of scale. It was necessary to reduce the primary voltage of the small inductor one-half (from 2 to 1 storage-cell)

6

and insert 10,000 ohms in the secondary, to obtain fringe displacements of reasonable size at the crests.

The use of both together (T, T', fig. 148, inset) thus produced the most sensitive apparatus so far examined. In the figure, U and U' are the two shanks of the U-tube, connected by quill tubes t and t' with the paired telephones T, T'. It is necessary to join t and t', which contain the salient (p) and the reëntrant (p') pin-hole cones, by the cross-tube a, so that the whole adjustment is H-shaped.

With this apparatus (inductor energized by one or two storage-cells) the deflections were:

Position of switch.	r	2 cells.	Pitch.	1 cell.	Pitch.
I	43,000 ohms	$s = 105$	bb'	s 27	b'
II	43,000 ohms	95		23	

The binaural telephone is thus of a higher order of sensitiveness than the above single telephones. The apparatus, moreover, gives four times as much deflection with two cells as compared with one cell and the switching of the telephone current slightly changes the deflections.

Surveys made between d' and c''' showed the main crest to be near c'' at 13,000 ohms, near b' at 23,000 ohms, and near a' at 33,000 ohms resistance in the telephone circuit. The smaller crests, all very sharp and abrupt near e'' and a'', behaved similarly. This may be an indication of self-induction in the resistance coils.

The lower crest (b') was particularly studied with regard to its conformity with the equation $\log s_0/s = r/r_0$, one cell actuating the small inductor. The results were as follows:

Switch I:
$$r \times 10^{-3} = \quad 14 \qquad 23 \qquad 33 \qquad 43 \quad \text{ohms} \quad s_0 = 152 \qquad\qquad \log s_0 = 2.182$$
$$\text{Observed } s = \quad 83 \qquad 51 \qquad 33 \qquad 20 \qquad\qquad r_0 = 49,500 \text{ ohms}; \ 10^5/r_0 = 2.02$$
$$\text{Computed } s = \ 79.2 \qquad 52.1 \qquad 32.7 \qquad 20.6$$
Switch II:
$$r \times 10^{-3} = \quad 14 \qquad 23 \qquad 33 \qquad 43 \quad \text{ohms} \quad s_0 = 203 \qquad\qquad \log s_0 = 2.307$$
$$\text{Observed } s = 105 \qquad 65 \qquad 41 \qquad 25 \qquad\qquad r_0 = 47,400 \text{ ohms}; \ 10^5/r_0 = 2.11$$
$$\text{Computed } s = 103 \qquad 66.4 \qquad 40.8 \qquad 25.1$$

These data are also given in figure 148, on the left.

It was purposed to carry out the same measurements with two cells in the primary circuit, but the available resistance (except for the data already given) proved inadequate. In place of this, a weaker telephone was installed in the same H-branch (fig. 148, inset) and the work completed both with one and with two cells, with the following results:

1 cell:
$$r \times 10^{-3} = \quad 3.3 \qquad 5.3 \qquad 7.3 \qquad 9.3 \text{ ohms} \quad s_0 = 39.6 \qquad\qquad \log s_0 = 1.598$$
$$\text{Observed } s = 22 \qquad 17 \qquad 15 \qquad 11 \qquad\qquad r_0 = 22,470 \text{ ohms}; \ 10^5/r_0 = 4.45$$
$$\text{Computed } s = 21.4 \qquad 17.5 \qquad 14.2 \qquad 11.6$$
2 cells:
$$r \times 10^{-3} = \quad 3.3 \qquad 5.3 \qquad 7.3 \qquad 9.3 \text{ ohms} \quad s_0 = 112.5 \qquad\qquad \log s_0 = 2.051$$
$$\text{Observed } s = 75 \qquad 66 \qquad 56 \qquad 52 \qquad\qquad r_0 = 34,480 \text{ ohms}; \ 10^5/r_0 = 2.90$$
$$\text{Computed } s = 75.3 \qquad 65.9 \qquad 57.7 \qquad 50.5$$

These data are also given in figure 148, on the right. They are less smooth than usual, owing partly to the low fringe deflections s and partly to difficulties with the contact breaker; but they fully suffice for the present comparisons. The numerical value of the slope of the lines log s increases with the sensitivity. The relation of constants s_0 and r_0 is probably incidental and due to secondary causes not fully appreciated thus far.

To obtain a suitable datum for sensitivity in general, it will be necessary to collect for comparison the successive constants s_0 and r_0 obtained. For since $\log s = \log s_0 - r/r_0$, it follows that the deflections of $s=1$ scale-part will occur when the resistance $r' = r_0 \log s_0$ is inserted into the telephone circuit. The data are as follows:

$r_0 \times 10^{-3}$	log s_0	$r' \times 10^{-4}$	Apparatus.
ohms		ohms	
2.0	2.761	0.55 ⎫	
6.38	2.601	1.67 ⎬	Fig. 142, inset.
8.62	2.279	1.96 ⎭	
3.11	2.579	0.80 ⎫	
3.00	2.508	0.75 ⎪	
1.65	2.399	0.40 ⎬	Fig. 142, inset.
1.56	2.214	0.34 ⎭	
6.25	2.564	1.60 ⎫	
8.00	2.365	1.90 ⎬	Fig. 147, inset.
3.53	2.435	0.86 ⎭	
49.5	2.182	10.8 ⎫	
47.4	2.307	11.0 ⎬	Fig. 148, 1 cell.
22.5	1.60	3.60	Fig. 148, 1 cell.
34.5	2.05	7.07	Fig. 148, 2 cells.

Since the constant r_0 is the resistance to increase the deflection s to the value s_0 (usually an excessive value, the full meaning of which on its bearing on the telephone apparatus as a whole is not easily interpreted), r_0 is of no immediate use. The quantity $r' = r_0 \log s_0$, which is the resistance to reduce the deflection to 1 scale-part or fringe, is thus a direct criterion of the sensitiveness of the telephone in a given mounting. Hence it appears that the binaural telephones, used together, are over ten times as sensitive as were the common telephones in the branch mounting used. If a definite degree is to be assigned, all telephones should of course be used singly and in the branch design of figure 142 (inset) or figure 147 (inset) for instance. These measurements were made, but are here omitted.

The data given for r' in the last binaural case shows that r' for 1 cell ($r'=3.6$) is just about half the value for 2 cells ($r'=7.1$) in the primary circuit, as it should be. Meanwhile the deflections s (fig. 148, right) are progressively from 3.2 to 4 times larger at the same resistances ($r=3,300$ to 9,300 ohms), since $\log s'/s = 0.453 + 10^{-5} \times 1.55r$. In this way a rather puzzling observation is adequately cleared up, with a corroborative bearing on the exponential equation accepted.

An interesting observation with the **H**-branch is the rapid change of pitch with the small differences in the lengths of quill tubes Up, pT, $U'p'$, $p'T'$ and a (fig. 148). Another is the occurrence of very high crests at low notes like c' ($\lambda=127$ cm.), d' ($\lambda=113$ cm.), etc., as well as at c'', etc. This is curious, as the parts Up, etc., were not, as a rule, larger than 10 cm. It is difficult to conjecture how such long waves are accommodated in the slender tubes. The cross-piece a is by no means indifferent. The following data are an example:

Cross-piece length	pitch c'';	$s=80$
4 cm.;		
8 cm.	b'	75
38 cm.	f	30
45 cm.	d'	20

If the first (c'') and last (d') of these data be compared, the frequency ratio is somewhat less than an octave. The induced voltage should therefore be somewhat less than 2, whereas the s ratio is 4. The case therefore resembles
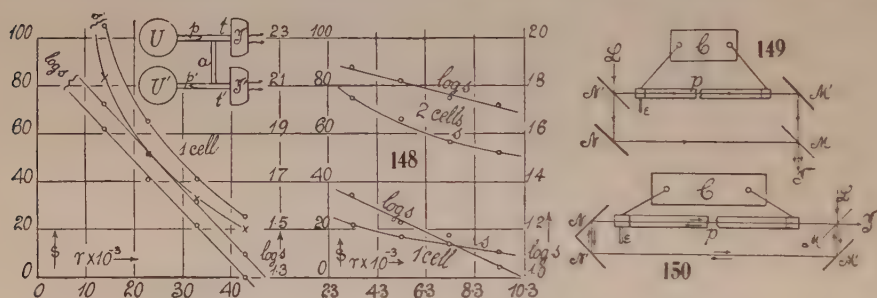
the introduction of 1 and 2 cells into the primary, just discussed. In fact, if e, n, i, r, s denote secondary electromotive force, frequency, effective current, resistance, and fringe displacement, respectively, and if the frequency in pitch be regarded as in direct relation to the break-circuit speed, there are four equations available, viz,

$$e=e_0n \qquad e=ir \qquad i=i_0s \qquad s_0=se^{r/r_0}$$

From these it follows that

$$n=\frac{i_0 r_0}{e_0} \log (s_0/s)^a$$

or, for any two frequencies and displacements, n and n', s and s'

$$\log s_0 = \log s + ns \frac{\Delta \log s}{\Delta(n/s)} = \text{const.}$$

If the first and fifth ($n=522$, 294), second and fourth ($n=489$, 348), of the above data be combined, $\log s_0$ somes out 2.38 and 2.39, respectively, which is the order of values tabulated above. The whole subject of branched tubes is well worthy of detailed investigation; but there is no room for further results here.

CHAPTER III.

VELOCITY OF LIGHT PASSING THROUGH PARALLEL CATHODE RAYS.

40. First method.—Many years ago I made the experiment of passing one component ray of the interferometer through a long exhausted tube, through which a current was passed, with the object of seeing whether any effect on the beam of light could be detected. The experiment has since been performed elsewhere, I believe, though I have misplaced the reference, with the same negative result which I obtained. Nevertheless, in view of the additional experience and facilities which I now possess, it seemed worth while to try it again.

In the first experiment (fig. 149), if L is a beam of white light from a collimator, $MM'\ NN'$ the mirrors of the interferometer, N and M half-silvers of equal thickness, and T the position of the telescope, the tube is placed at p. The ends are provided with metallic caps at the two ends and closed with glass plates. At one end is the exhaust-pipe E leading to a powerful air-pump. The induction coil C supplies the current.

The tube was 90 cm. long and about 5 cm. in diameter. Large fringes were installed. The exhaustion was carried to within 3×10^{-3} mm. Many experiments which need not be detailed here were tried, but not the slightest effect due to making and breaking the current could be detected at any pressure. A displacement of 0.1 fringe would certainly have been noticed.

41. Second method.—In the above experiment it is difficult to keep the fringes quiet while the heavy air-pumps are running. Moreover, it is obviously a more searching test if two rays are passed through the pipe p in opposite directions. Accordingly, in the new installation, figure 150 (notation the same as in fig. 149), the self-adjusting interformeter was utilized, M being the only half-silver. Fringes of any size are obtainable by rotating M' on a horizontal axis, if the vertical axis is available for coincidence of slit-images. Very large and superb fringes nearly free from quiver were therefore available and the tests were made at some length.

Again, however, not the slightest effect could be observed on making and breaking the current of the induction coil C, at any exhaustion. This was carried as far as about 4×10^{-4} mm.

The results of this very beautiful experiment are thus quite negative. Naturally, this is what one would have expected as the relative velocity of light c', in a medium of index of refraction μ, is $c' = c/\mu \pm v(1 - 1/\mu^2)$. Unless v is very large, $c' = c$ if $\mu = 1$. To indicate the extent of the evidence given by the experiment, let c be the velocity of light and $2v$ the effect on c produced

by the twofold current in the tube. Then $2vL/c$, if L is the length of the tube, is the corresponding path-difference, so that

$$2Lv/c = \lambda$$

per fringe. Thus

$$\frac{v}{c} = \frac{5 \times 10^{-5}}{2 \times 90} = 3 \times 10^{-7}, \text{ nearly}$$

Now, as one-thirtieth fringe displacement would certainly have been detected, v/c must be smaller than 10^{-8}.

42. Collinear trains of light-waves and an electric current.—The third experiment tried out by the present apparatus bears upon the possible effect of an electric current on light-waves traveling in the same line. True, the electrolytic results of Kohrausch on the motion of the ions show but very
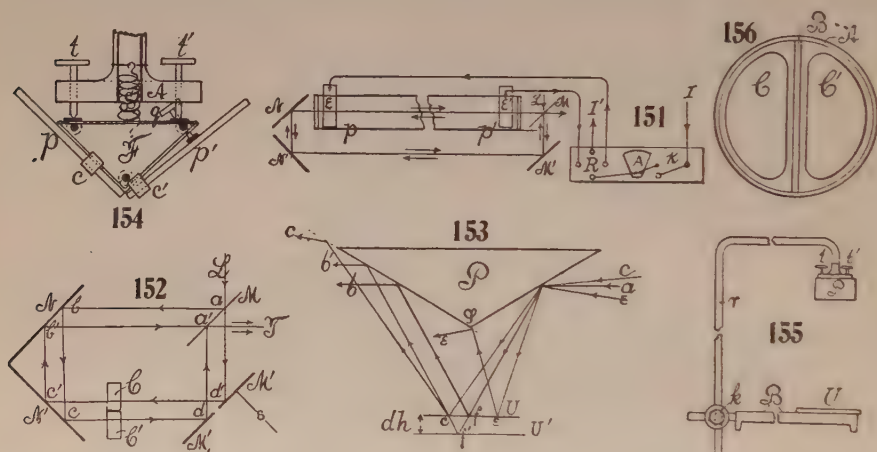
small velocities. But these velocities are aggregates. It is conceivable that, differentially, electronic motion at much greater speed may be taking place. As it was not difficult to adapt the interferometer for this purpose by replacing the pipe p in figure 150 by a long paraffined trough with glass end-plates carrying a solution of zinc sulphate (at maximum conduction) and the coil C by the lighting circuit of 250 volts, the experiment was duly made. The trough pp', figure 151, was 100 cm. long and 7×7 cm.² in cross-section and nearly filled with the solution, the terminals EE' being strips of zinc. The current arriving at I through the key K passed through the ammeter A and the commutator R, thence either in one direction or the other through the trough pp' and back to the lighting circuit at I'. Between N and M pass the rays of light of the self-adjusting interferometer, here made quite coincident, but traveling in opposite directions through the trough pp'. These comprise the corresponding part of the ray parallelogram is figure 150.

There is some difficulty at first in finding the fringes, for the solution is not adequately homogeneous and the slit-images blurred. After about an hour or

more the inequalities have subsided and the fringes are now easily found and can be enlarged at pleasure in the way specified. Naturally they are somewhat sinuous, but quite fixed and remarkably sharp, so that it is possible to estimate within 0.1 fringe. When the current is turned on, the sharpness persists unaltered during the first minute or two; but thereafter the fringes usually enlarge, become more and more vague, and eventually vanish. The lapse of an hour or two nevertheless brings them back again for further trials.

The result of this experiment with fine large fringes was absolutely negative. No effect whatever could be detected (the key K was of course on a quite independent mounting from the interferometer) on closing and again opening the circuit. As the current was fully 4 amperes, the flash of spark on opening was long and care had to be taken to prevent arcing.

The degree to which the electric current and the light-ray are independent may then be found as above. Since $v/c = \lambda/2L$

$$v/c = 5 \times 10^{-5}/200 = 2.5/10^{-7} \text{ per fringe.}$$

But considerably less than the displacement of 0.1 fringe would have been recognized, so that an effect is absent well within 10^{-8}. In other words, v can not have exceeded 500 cm./sec.

EXPERIMENTS WITH THE SELF-ADJUSTING INTERFEROMETER.

43. Apparatus.—This apparatus, described in an earlier report (Carnegie Inst. Wash. Pub. No. 249, part IV, 1919, chap. VII, § 54), is so convenient in many cases that it is worth further study. In figure 152, L is a beam of white light from a collimator, and M, M', N, N' the four mirrors, M being a half-silver, the others opaque. M and M' are attached to a common base, which may be slid nearer to or away from the mirrors N, N', also attached to a common base. In this way the ray systems $abcd$, $a'b'c'd'$ may be brought to coincidence or separated in any reasonable degree, by sliding the system MM' correspondingly. The four mirrors have the usual plane-dot-slot adjustment, and they may be rotated on a vertical axis. Horizontal coincidence of the two component planes entering the telescope at T is thus secured and the fringes then appear at once. They may be enlarged by slight rotation of any mirror, or even by rotating a single plate compensator around a horizontal axis.

But if common plate-glass is used, while the horizontal coincidence of the rays at T is attained without difficulty in any degree, the accurate vertical coincidence of the two slit-images in the telescope is much more troublesome. It results from the fact that the half-silver M, which is twice traversed by each ray, is slightly wedge-shaped and that the deviation of the two rays is not quite the same. Usually it may be eliminated by rotation of the plate M on an axis normal to its face, until the vertical coincidence is perfect. If this fails another half-silver must be selected.

44. Billet compensator.—The Billet wedge compensator may be used at CC', for instance, with entire success. Here C is a very sharp-angled, thick, long wedge-plate capable of being displaced vertically by a graduated micrometer screw, while C' is a similar but short and fixed wedge-plate of the same

average thickness as the other. It is usually necessary to rotate the Billet compensator on a horizontal axis, until slight differences of the deviation of the two rays are wiped out and the fringes are again sharp. I have used the two parts of a Babinet quartz compensator in the same way; but here the wedge angles are rather too large, the deviation of the rays not quite the same, and the fringes as a consequence blurred.

The adjustment is thus at once available for the graduation of the displacement of the wedge in terms of light-waves. For this purpose, T is to be a spectro-telescope and the slit of the collimator is made small enough for the appearance of the spectrum lines. If an arc lamp is used there is an abundance of sodium, and these lines are usually in presence. In this case, if the prism edge of the spectro-telescope is at right angles to the direction of the fringes, they will appear sharply for any width of slit. In general, if great accuracy as to wave-length is not necessary a wide slit under conditions stated may be used. A great advantage in relation to the intensity of spectrum is thus secured.

45. Projection.—In the case of white light from the arc lamp or the sun and bright mirrors, the fringes, if accurately produced, as just explained, are (in the absence of the telescope T) caught on a white screen 10 or 20 feet across the room, still clear, though highly magnified. The supernumerary reflection from the rear of M is lateral and may usually be screened off. The fringes are very stable and fully under the control of the compensator CC'. A lens at T may of course be introduced for projection at closer ranges. The collimator itself may be used for focusing the slit-images for small distances, but this does not necessarily focus the fringes.

If now the beam is passed through a direct-vision prism, provided with a lens if desirable, the spectrum fringes may also be projected in the focus of the lens, on a white screen. Naturally, since the slit must be wide to admit an adequate quantity of light, it is necessary that the edge of the prism be at right angles to the direction of the fringes. Since the fringes seen with white light are in the present apparatus nearly horizontal, the prism edge may then be vertical. When the spectrum fringes become inclined, as they are arcs of large circles, the prism must be rotated correspondingly on an axis normal to its edge.

46. Sliding micrometer with split mirror.—The range of the Billet compensator is too small for promiscuous work. A most serviceable micrometer is obtained by separating the mirror M', for instance, into two parts, $M'M'_1$, with a narrow vertical crevice between them. Both must be capable of slight rotation about a vertical and horizontal (plane-dot-slot) axis. M', moreover, is on a slide micrometer, with its screw in the direction s normal to the face of M'. The two mirrors M and $M'M'_1$ are on a common base, sliding right and left in the diagram.

This device is thus again almost self-adjusting, as follows: MM' is moved until the rays $aba'b'$ are coincident or nearly so, the spot d' falling on the mirror M'. The slit-images are then brought to coincidence horizontally and vertically, whereupon the (horizontal) fringes appear at once. They may be made of any size by rotating M' on a horizontal axis. The system MM' is then to be slid right or left until the spots dd' fall on the separated mirrors M' and M'_1. The latter is now to be rotated around a horizontal and a vertical axis until the two slit-images coincide. Finally, the micrometer screw at s is to be given a few turns, so that M' and M'_1 may be quite coplanar. The fringes just selected will appear. The method is very rapid. Both mirrors M' and M'_1 must be firm in mounting; otherwise the quivering fringes may escape detection.

47. Adjustment for reading vertical displacements.—The scope of the self-adjusting interferometer is much enlarged by reflecting the component rays $aba'b'$ in figure 152 vertically together during a part of their path. For this purpose an obtuse-angled silvered prism P, figure 153, is convenient, together with the plane mirror below, at U. The angle ϕ of the prism need not exceed 100°; but it must be mounted on horizontal and vertical axes, in order that the edge at ϕ may be made nearly parallel to the mirror U and normal to the rays ab.

In much of the present work, U is to be the level surface of one shank of the mercury **U**-tube, and U' the other, originally nearly coplanar with it. If U' is displaced, as in figure 153, over a vertical distance Δh, the component rays afb and $a'f'b'$ will now contain a path difference of

$$n\lambda = 2\Delta h \cos (\phi - 90) = 2\Delta h \sin \phi$$

where ϕ is the prism angle. If the fringes are restored by the slide micrometer $M'M'_1$ of figure 152, with a displacement of Δs,

$$n\lambda = 2\Delta s \cos i$$

where i is the angle of incidence. Thus,

$$\Delta h = \Delta s \cos i / \sin \phi$$

i being nearly 45° and ϕ not far from 90°.

The form of prism used is given by figure 154, where F is a hollow prismatic frame of sheet brass, turned up outward at the edges, so that the silvered-glass plates pp' may be secured by steel clips cc' on both sides of the square faces of F. If p remains fixed to the frame, an excess of angle is given to p' by the thrust of the screw q near the center of the side-face. Att' is a plane-dot-slot device, operating in connection with the stiff central spring S. This prism, P, and its fixed mirror U (fig. 155) must be rigidly attached to the basal slide B of the interferometer, as, for instance, by the bent arm r, clamped at k, the distance PU being approximately chosen. P and U are first roughly adjusted with a broad beam of sunlight, sweeping by P normally to the diagram. The direct beam and the one reflected via PUP are then made to coincide on a

distant wall, by utilizing the play available at the elbow, clamps, and other stiff screws of the framework, as well as the plane-dot-slot (three axes normal to each other). The remainder of the adjustment for coincidence of slit-images is done on the interferometer, which should be in adjustment before the element figure 155 is added. With regard to the three orthogonal axes specified, one may note that rotation around y (normal to fig. 155) moves the reflected spot of sunlight up and down, whereas rotation around x (parallel to edge of prism) and around z moves the spot right and left; hence, if the initial rough adjustment is in good symmetry, the y and x axes suffice, and these are given by the plane-dot-slot machine adequately. Unfortunately, on tilting the prism system PU, the rays afb pass into eee or ccc, figure 153. The incident and emergent beams are thus no longer parallel, but inclined symmetrically to the plane of symmetry of the prism.

When the arm (fig. 155), adjusted by sunlight, is placed on the interferometer, the slit-images will usually appear; but they will not be coincident. Since the interferometer itself is in adjustment, the additional correction is again to be made with the plane-dot-slot device tt'. The fringes are then found easily by first using the spectro-telescope, and they may be changed in size by manipulating the horizontal axes of both M'_1 and M' conjointly. If the slit-images are not parallel, but at an angle with each other, the discrepancy may be corrected by rotating the whole frame 155 slightly, on a horizontal axis normal to the figure. This may be inferred from the ray systems ab, cc, ee in figure 153.

To test the apparatus, a thin silvered magnet mirror was placed on U over one of the light spots. The small mirror was slightly wedge-shaped and on calipering showed a mean thickness of 0.100 cm.$=\Delta h$. But the U plate was unfortunately not an optic flat, so that measurements in the two beams, right and left, included the surface curvature. There was also the annoyance from dust, etc., and the fact that fringes could be read much more accurately than the micrometer could be placed. For this reason I merely estimated the angles $i=45°$ and $\phi=97°$. Interferometer values, from $\Delta h=\Delta s \cos 45/\sin \phi$, were, for example:

TABLE 3.—Self-adjusting interferometer. Factor 0.7124 $i=45°$ $\phi=97°$.

Ray ab	Zero	s	Δs	Δh
	1.0390 cm.	....	....	....
	....	0.8898 cm.	0.1504 cm.	0.1075 cm.
	(shifted)	.8986	.1416	.1012
Ray $a'b'$	1.0415	....	....	....
	....	1.1894	0.1478	0.1053
	(shifted)	1.1814	.1398	.0996
	(shifted)	1.1836	.1420	.1001
	1.0417	....	....	....

The difficulty here is attributable to the curvature of the U-plane, which dislocated the slit-images, modified the fringes, and required some fresh adjustment; but the example is adequate for illustration, the individual measurements being true to 0.0005 cm.

To further test the apparatus, I made a U-gage out of a shallow cylindrical glass dish (*A*, fig. 156) by cementing a vertical glass partition *B* across it on the sides only, leaving the bottom of *B* slightly above the bottom of *A*. A shallow charge of mercury, poured into *A*, would there establish communication between the two compartments. Light glass plates *CC'* were then floated on the mercury. This form of U-gage is objectionable because of the irregular distribution of capillary forces, but it is sufficient for the present purposes. With the slide micrometer already in adjustment, there was no difficulty in finding the fringes, and they were remarkably steady in spite of the mobile mirrors *U, U'*. The adjustment for coincidence of slit-images should be made at the prism *P*, at least very nearly.

The work done with this device, being incidental and serving merely as a test of apparatus, is of no further interest.

CHAPTER IV.

GRAVITATIONAL EXPERIMENTS.

48 Introductory.—As heretofore stated, the present research was begun with the object of reading the deflections of the gravitation needle by interferometry, a project which succeeded without great hardship. The real difficulty was found in the endeavor to interpret what had been measured, for constants several times as large as the constant of gravitation were not unusual. Even with a needle of filamentary framework, in a plenum of air, a constant nearly twice the normal value may result, and this in the summer, in a dark basement room, the mean temperature of which changes but a degree or two per day.

Naturally, the disturbing factor is effectively some kind of repulsive radiation, and the simplest working hypothesis is an assumption that the radiation in question is screened off from a corresponding end of the needle by the large attracting mass on the outside of the apparatus. Consequently, the effect of the radiation is a force always in the same sense as the gravitational attraction to be measured. It is with the object of determining to what degree the radiation discrepancy may be controlled or eliminated under ordinary laboratory surroundings that the preceding and the present experiments have been undetaken, with a full consciousness of the difficulties involved.

The large room in which the experiments were made being of importance as a typical environment, it is necessary to point out that the floor was 3 feet below the ground on the east and 10 feet on the west, the embankment sloping downward from side to side. On the east, therefore, merely the heavy basement wall screened off the sun, if present. On the south there was a large building and on the west a double wall, including the embankment specified. Solar radiation thus has the easiest access on the east, and accordingly the morning observations, whether the weather is clear or cloudy, are always largest and much too large as compared with afternoon and night observations. At the same time it is possible that such small temperature changes as occur in the room are most marked in the forenoon. Similarly, the presence of the observer near the instrument, if prolonged, produces a drift of the needle always toward larger deflections.

49. Apparatus, I.—At the end of my last experiments a form of apparatus was installed, capable of exhaustion and containing a gravitation needle made of wires as thin as possible (phosphor-bronze wire, 0.24 mm. in diameter) compatible with the lead weights, m, at the ends. The object of this was to diminish the radiation effect to an inferior limit, always remembering that the

84

lateral area of the shots m is necessarily in presence. The narrow case (see fig. 157) was a rectangle of brass with reëntrant sides, into which plates of thick glass could be sealed with cement free from air leakage. When the parts of the case were assembled, its inner dimensions were: Breadth 1.2 cm., height 8 cm., length 25 cm., inclosing a needle 22 cm. long. A vertical tube adapted for quartz-fiber suspension arose, in the usual way, from the middle of the top of the brass case. The torsion-head above and the bottom of the tube were sealed against air leakage by the aid of cups, into which resinous cement was poured in the molten state and allowed to solidify.

Each attracting weight M had a mounting quite independent of the case and, acting at one end of the needle only, could easily be moved, between stops, from one side of it to the other by a cranklike arrangement. If M is not too heavy, methods of multiplication are possible.

The half-silver method of reading the deflections of the needle and other details are conveniently shown by the sectional plan (fig. 157), where cc' is the rectangular brass frame holding the glass plates gg', and mm' is the needle with a mirror at n. M is the attracting weight in one alternative position, determined by the stop on the crank mechanism. The half-silver mirror, adjustably attached to the objective of the telescope T, is shown at H. By means of it the divisions of a glass millimeter scale S, illuminated by a tungsten bulb L shining through oiled paper, are reflected upon n and thence through H into the telescope T. The total distance of S from the mirror n was found by steel tape to be $L=447.5$ cm. with allowance for the kink at H. The advantage of the arrangement lies in the halved distance of the telescope from the scale measured along the reflected beam, so that the magnification is doubled; but in view of the loss of light at the half-silver, the (distant) illumination of S must be intense. If S is long, L must be capable of being shifted along a slide. The presence of the observer at T is not to be prolonged.

The masses of the attracted lead balls at the end of the filamentary needle were $m=0.6295$ gram each, though the quartz-fiber would have been strong enough to hold a larger mass with advantage.

The attracting masses M were of different sizes in the several experiments, the smallest being $M=949$ grams, the largest $M=3,368$ grams, with an intermediate size of $M=2,950$ grams used in connection with the latter. Other masses were used later. They were turned spherical.

To determine the distance R of the center of the mass M from the center of the shot m is a difficult problem. Telescopes were used heretofore, but in the present report the best results were obtained, I believe, by calipering. Thus, in the line of centers of the two positions of M, the outside thickness of the case d, the distance of the outer end of the diameter of M and the outside of the glass face on the further side y, and finally the diameter of the ball z are carefully determined for each of the two positions of M. Then $2R=y+y'-x-z$. In this way it was found that for

$M=$ 949 grams. $R=(\,8.27+8.35-2.65-5.48)/2=4.25$ cm.
       3368 grams. $R=(11.17+11.19-2.71-8.30)/2=5.67$ cm.
       2947 grams. $R=(10.81+10.72-2.74-7.93)/2=5.43$ cm.

The shot is thus assumed to lie in the middle plane of the case nearly enough to come within the compensation resulting from the two positions of M. Since R enters as a square, it seems advisable not to make it too small. As R^2 increases with M, the advantage of large external masses is not great, particularly as the small masses are so much more easily and certainly controlled.

The moment of inertia of the needle, $2l = 22.0$ cm. long, between centers of $m = 0.6295g$ has for its main part $2ml^2 = 152.5$ (gcm.^{2}). To this is to be added the moment of inertia of the stem wire ($\rho = 0.0044$ gram per cm.), 3.9; of the oblique wire brace or tie, 1.0; and of the glass filament added for ridigity, 2.0; making a total of $N = 159.4 = 2ml^2 (1 + s) = 152.5 (1 + 0.0452)$ gcm.^{2}

The torsion coefficient of the wire is most conveniently found from the period T_1 of the needle vibrating in a plenum, after reduction to vacuo. This was determined with a stop-watch measuring the interval between two similar passages through the equilibrium position. As T is over 5 minutes, it is necessary that the arc of vibration be relatively large; otherwise the datum is
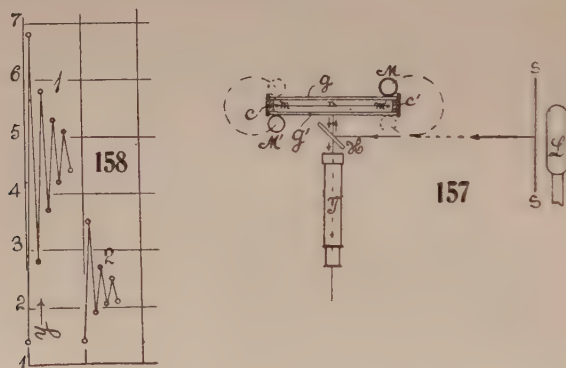
inaccurate to several seconds. It was found that the vibration which occurs immediately after the case is exhausted is very steady and periods were found as follows:

$$T_1 = 311.5,\ \ 310.0,\ \ 312.0,\ \ 311.5,\ \ 311.0,\ \ 311.2.\ \ \text{Mean } 311.2 \pm 0.28 \text{ sec.}$$

Discrepancies result from radiation forces and are practically absent from the method as such. As the quantity T_1 enters in the square, this is not as good a result as I expected.

The value of the logarithmic decrement λ was obtained from observation of consecutive arcs of vibration, as shown in the example (fig. 158), where y is the scale-reading seen on the telescope. Unfortunately, the apparatus had been mounted in October of last year and the mirror in the meantime had become bluish from the sulphur sublimate coming out of the packing. It was therefore difficult to read the scale rapidly as accurately as would otherwise have been easily possible, and the results of figure 158 (series 1 and 2) are not very smooth, but they are sufficient for the present purposes. If the successive arcs are called Δy, $\epsilon^\lambda = 1.35$ in the first and 1.34 in the (better) second

series, which makes $\lambda=0.293$ nearly. Hence the true period T of the needle is

$$T=T_1/\sqrt{1+\lambda^2/4\pi^2}=T_1/1.0011$$

The intervals on the stop-watch, moreover, were found too long (on comparison with a chronometer) by the factor 1.0055. This with the preceding equation gives

$$T=T_1\times1.0044=312.6 \text{ sec.}$$

With the given value of λ, the question may be answered how long it is advisable to wait for an appreciably stationary needle after the position of M is changed. The equation shows that for the nth arc θ_n after the first θ_1

$$\log\theta_n=\log\theta_1-(n-1)\log\epsilon^\lambda$$

The following data suffice for guidance

$n=1$	2	3	4	5	6	7	8	9	10	11
$\Delta y=\theta=1$	0.75	0.56	0.41	0.31	0.23	0.17	0.13	0.10	0.07	0.05

Thus at least an hour should be allowed, and observations taken $T/2$ apart. In the actual case, however, the reduction of arc is for some reason more rapid, for after half an hour the needle is appreciably stationary for any position of M. This is very convenient, though I do not understand the reason. The prolonged presence of the observer at the telescope produced a drift toward larger arcs.

50. Equations.—The approximate equation for the gravitation constant, γ, containing all quantities to be measured when the needle itself is used to find the torsion coefficient of the quartz-fiber, is

$$(1) \qquad \gamma'=\frac{\pi^2N}{LT^2l}\frac{R^2}{Mm}\Delta y$$

Δy being the ultimate double amplitude for the scale-distance L when the attracting weight M passes from side to side of m. T is the period, N the moment of inertia, and l the semi-length of the needle. Finally, R is the effective distance apart of M and m.

Since the stem is also appreciably attracted, a correction must be made for it. If t/τ is the ratio of torques for stem and mass m separately,

$$(2) \qquad \frac{t}{\tau}=\frac{\rho R}{lm}(\sqrt{R^2+l^2}-R)$$

when ρ is the mass per centimeter of the stem. Hence finally the corrected constant is

$$(3) \qquad \gamma=\gamma'/(1+t/\tau)$$

For the case of two attracting masses M' and M'', one at each end of the needle and coöperating, we should have

$$\gamma=\kappa'\Delta y'=\kappa''\Delta y''=\frac{\Delta y'+\Delta y''}{1/\kappa'+1/\kappa''}$$

If Δy is the observed deflection for both conjointly,

$$\Delta y = \Delta y' + \Delta y''$$

whence

(4)
$$\gamma = \frac{\Delta y}{1/\kappa' + 1/\kappa''}$$

κ' and κ'', being the corrected coefficients, are usually not very different in value.

One may note that for measurements at one end of the needle only, while the R datum is corrected for slight asymmetry of the shot m, the $2l$ measurement is not so corrected. With two balls M' and M'' acting, respectively, on m' and m'', the l measurement is also corrected for asymmetry. Thus, if the masses M' and M'' are carefully turned spherical, both the R and l measurements are guaranteed.

If in equation (1) we replace N by $2ml^2(1+s)$, where $s = 0.0453$, a small quantity, is the ratio of the moment of inertia of the filamentary framework to that of the shot, m vanishes from the equation (except in the corrections), which now takes the simpler form

(5)
$$\gamma = \frac{2\pi^2 lR^2}{LM} \frac{\Delta y}{T^2} (1 + s - t/\tau)$$

showing that l virtually enters in the first power only. The term t/τ is of the same order as s ($t/\tau = 0.020$ to 0.024), so that the parenthesis is a correction but little over 2 per cent. Moreover, *caet. par.*, Δy increases at the same rate as T^2, the period of the needle.

With regard to outstanding masses at the crank or at the support of M, let R' be the (oblique) distance of the center of gravity of such a mass μ, under the center of M, from the shot m, so that $R' = R/\cos \phi$, where ϕ is the (large) angle of R' to the horizontal. Thus the additional force component in the horizontal direction is

$$f = \gamma \mu m \cos \phi / R'^2 = \gamma \mu m \cos^3 \phi / R^2$$

and its relation to the gravitational pull F of M is therefore

(6)
$$f/F = (\mu/M) \cos^3 \phi$$

As the angle ϕ will usually exceed $45°$, the weight μ will not enter with more than 30 per cent of its value. By using compensators on opposite sides of the case to the cranks, I assured myself that their presence or absence made no appreciable difference.

---

51. **The radiant discrepancies.**—It is so difficult to make a clear exposition of the relatively large thermal discrepancies which vitiate the otherwise admirable performance of the Boys quartz-fiber suspension that I have endeavored to pass in review brief estimates of the different possible activities involved. To do this it will suffice to compute the speed Δv or v of the convection current needed to produce a force equal to the gravitational attraction of a kilo-

gram ball M, for the shot $m=0.63$ gram, at the distance $R=4.3$ cm., occurring in the above observations.

We may begin with Bernouilli's equation, which for the case of constant energy and practically constant density, ρ, may be written

$$\Delta p = -(\rho/2)\Delta v^2 = -\rho v \Delta v$$

If the initial velocity is $-\Delta v/2$ and the final $+\Delta v/2$, we avoid further particularizing as to v and put

$$\Delta p = \rho/2(\Delta v)^2$$

which is numerically the same as if Δp and Δv were suddenly acquired from rest. If a is the lateral area of the shot (0.159 cm.^{2}) and f the radiant force, $\Delta p = f/a$. If $M=10^3$ grams, $m=0.63$ gram, $R=4.3$ cm., $\gamma=10^{-8}\times6.66$, then the velocity increment (Δv) necessary to produce a force f just equal to gravitational attraction will be ($\rho=0.0013$).

$$(\Delta v)^2 = \frac{2}{a\rho}\,\gamma\,\frac{Mm}{R^2} = 0.022 \text{ or } \Delta v = 0.15 \text{ cm./sec.}$$

If the air is exhausted to 1 cm., the speed would be $\sqrt{76}$ larger, or $\Delta v=1.3$ cm./sec. The latter velocity is out of the question under the circumstances of exhaustion at constant viscosity, and this suggests the advantage of using the needle in vacuo; but that convection currents of at least a fraction of the former velocity (1.5 mm./sec.) may be produced in a plenum can not be so easily gainsaid. The side of the shot fronting M is exceptional, as compared with the three other sides, and it is here that Δv is operative. The fatal difficulty, as it seems to me, is, however, this, that Δv may just as well be deducted from a preëxisting velocity as added to it, so that pressure should rise and the radiant forces become repulsive as well as attractive, whereas the general rule is that these forces are always attractive.

If we assume that the radiant force, equal to the gravitational attraction, is the result of a current of air traveling at speed v from shot toward M, the results are very similar, since

$$f = 10^{-6}\times2.3 = a\rho v^2$$

Thus $v=0.10$ cm./sec. in a plenum and the question arises as to the origin of this current, persistent in relation M.

Again, the viscous drag, across a sphere, of strength f, requires a speed v given by

$$f = 10^{-6}\times2.3 = 6\pi\eta r v$$

where $2r=0.45$ cm. is the diameter of the shot m and $\eta=170\times10^{-6}$ the viscosity of air. Thus

$$v = 10^{-3}\times3.15 \text{ cm./sec.}$$

This datum is very interesting, showing that a relatively small velocity of air current would drag the ball with a force equal to the gravitation applied, and that the two preceding cases are insignificant by comparison. Moreover, f here varies as the first power of v.

7

But the difficulty of accounting for a current which moves persistently from m to M remains the same as before. The effect of the two gravitational fields, that of M and that of the earth, can hardly be conceived as other than static, resulting in slightly displaced isobars, no longer quite plane. One may be tempted to invent a mechanism for a slow current as follows: In consequence of the attraction of M, the air within the case near it is proportionally slightly more dense. One may imagine this air sinking as a consequence, in response to the earth's gravitational field. As the air sinks it is removed from M and consequently expands isothermally with absorption of heat from the environment. As fresh air replaces the denser air which has sunk, the general result is a circulation directed from the shot m toward M and maintained by heat energy. Nevertheless, even if such a mechanism were feasible, it would fail to clearly suggest the dependence of the radiant forces on the temperature changes of the environment.

As a final estimate, one may refer to the light or radiation pressure screened off by M, which simple mechanism has been assumed above for convenience. If p is this pressure, $f = ap = 0.16p$. In the case of full sunlight the energy received is 3 gcal./min. or $10^6 \times 2.1$ ergs./sec. As this resides in a prism 1 cm.^{2} in section and 3×10^{10} cm. long, the energy per cm.^{3} is 7×10^{-5} ergs., and therefore

$$p = 7 \times 10^{-5} \text{ dynes/cm.}^2 \text{ or } f = 1.1 \times 10^{-5} \text{ dynes}$$

This is about five times as large as the gravitational pull ($10^{-6} \times 2.3$) postulated above. In other words, an amount of radiation equivalent to one-fifth of the full solar delivery would have to be screened off by M, which is itself not a cold body. It does not seem that, in a closed room, anything like this can be (differentially) available. Moreover, there is here no clear suggestion why the data should be improved by measurement in a partial vacuum.

In Nature (vol. 108, 1921, p. 40) Professor Boys discusses the same subject, with copious references to original experiments of Bennett (1792), Cavendish (1798), and Joule (1862). It is interesting to note that Cavendish, in spite of his relatively enormous apparatus, encountered similar radiation discrepancies and was fully aware of their nature. Boys and Briscoe (Phil. Mag., vol. 31, p. 59, 1891), in their remarkable development of Joule's convection radioscope, counteract extraneous radiation by a rotating envelope. Unfortunately, this device can not be applied in case of the gravitation apparatus. Boys regards the phenomena, as a whole, to result from convection currents, and no doubt in case of a plenum they largely do so. But inasmuch as the phenomena persist in large part, even at the highest exhaustions applied (within 0.003 mm.), it is difficult to believe that convection can still be operative.

In the light of the above estimates, we may state a probable case conservatively, as follows: During the daytime, M is progressively hotter than m. The result is a circulation of air within the case from m towards M near the bottom and up on the inside of the glass face nearest M. The shot m is

dragged by this current. At night, M is progressively colder than m, and the result is a reversed circulation downward on the glass face and in the direction from M to m near the bottom of the case. In a partial vacuum, while the viscosity of air remains constant, its mass or inertia diminishes, and hence the circulation is reduced. Thus the radiant forces are much smaller.

Nevertheles there are a variety of reasons which make it difficult to accept this view. It is hard to believe that two bodies, M and m, in a room of nearly constant temperature and but 4 to 5 cm. apart, can persistently differ sufficiently in temperature to evoke an air current in the case of the kind required. Again, M acts about as effectively when it is behind the case (between pier and case) as when M is in front, while the solar radiation with which M reciprocates, filtering through the walls of the room, does not come from the rear. Finally, the detailed behavior of the radiant forces does not quite conform to such a straight forward hypothesis. We may therefore regard M as a body screening off external, effectively repulsive radiation from m, at least for convenience of expression.

52. Observations. Small attracting mass M=949 grams.—The constants entering equation (1) for the small body were

$N=159.4$ gcm.^{2} $T=311.6$ sec.* $R=4.25$ cm. $M=949$ g.
$L=447.5$ cm. $l=11.0$ cm. $\rho=0.0044$ g/cm. $m=0.6295$ g.

Hence

$$\gamma'=\kappa'\Delta y=10^{-8}\times9.95\Delta y$$

In equation (2) the ratio becomes

$$\frac{t}{\tau}=\frac{0.0044\times4.25}{11.0\times0.63}(11.79-4.25)=0.02035$$

Hence in equation (3)

$$\gamma=\gamma'\frac{1}{1.0204}=10^{-8}\times9.753\Delta y$$

Hence the deflection to be anticipated should be

$$\Delta y_0'=\frac{\gamma}{10^{-8}\times9.753}=0.68 \text{ cm.}$$

The observations (M operating at one end of the needle only) made in the daytime and even at night on or after a fairly clear day were, as usual, much too large, as shown in figure 159, the needle being in a vacuum of a few millimeters. The points show the successive observations with M alternately in front and to the rear of m. Forenoon, afternoon, and night observations are distinguished by A, P, N, and little circles mark the beginning and end of each series. S denotes sunshine and C cloudy. The values of the double amplitudes Δy are attached to each series. $\Delta y_0'$ ranges as high as 0.80 cm. and the night value is not below 0.70 cm. It may thus be necessary to use the night of

* Earlier datum, left uncorrected here, as it suffices for the paragraph.

cloudy or rainy days to obtain more approximately correct values ($\Delta y_0 = 0.68$). Both elongations drift somewhat, and it is probable that in the course of a more prolonged interval of measurement both values would have been obtained, the present set being at best 3 per cent too large in their γ value. I did not, however, persevere, as I had but one of these balls ($M = 949$ grams). The l asymmetry is thus left uncompensated, which would in any case leave the interpretation in difficulty. Finally, $\Delta y = 0.7$ cm. is too small to furnish more than a corroborative value.
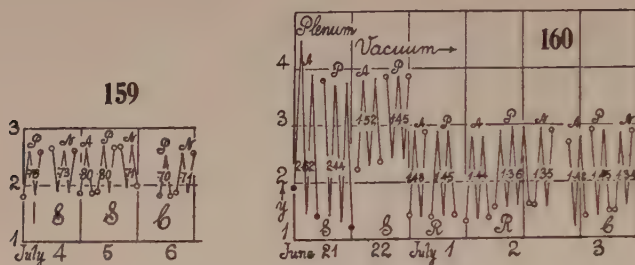
This relatively light ball M is interesting, as it is so easily moved and may therefore be used in a method of multiplication. If λ is the logarithmic decrement, and x the maximum deflection obtainable when the ball M is passed from side to side synchronously with and in a way to continually amplify the motion, we may write

$$(7) \qquad e^\lambda = \frac{x + \Delta y/2}{x - \Delta y/2} = \frac{2x + \Delta y}{2x - \Delta y}$$

as the M effect, in this case, is merely to change the position of equilibrium and Δy is a double deflection in $\gamma = \kappa \Delta y$. Hence

$$(8) \qquad \Delta y = 2x \frac{e^\lambda - 1}{e^\lambda + 1}$$

In view of the long period of over 5^m, the method is tedious; but with the above $e^\lambda = 1.34$ and $\Delta y_0 = 0.69$,

$$2x = 0.69 \frac{2.34}{0.34} = 4.8 \text{ cm.}$$

nearly. I satisfied myself as to the feasibility of this procedure by actual trial, but did not complete it, because of the eye-strain involved in reading the scale reflection in the dull mirror already specified.

53. Observations. Large attracting mass M = 3,368 grams.—The crank mechanism was still rigid enough to control this massive body without additional complications. Greater care had to be taken with the adjustment at the stops. The constants entering equation (1) are the same as before, so far as the needle is concerned; the new data are

$$M = 3{,}368 \text{ grams.} \qquad R = 5.67 \text{ cm.}$$

Hence the following relations result:

$$\gamma' = 10^{-8} \times 4.960 \Delta y$$

In equation (2)

$$\frac{t}{\tau} = 0.0241$$

which in equation (3) gives

(9) $$\gamma = 10^{-8} \times 4.844 \Delta y$$

so that the deflection along a horizontal scale should be

$$\Delta y_0 = 1.375 \text{ cm.}$$

Similarly the computation by equation (5) gives

$$\gamma = 10^{-8} \times 4.841 \Delta y \text{ and } \Delta y_0 = 1.376 \text{ cm., since } (1 - s + t/\tau) = 1.0212$$

The observations (mapped out consecutively, as in § 52) were begun (fig. 160) in a plenum of air on June 21. The consecutive points give the scale readings at intervals, one-half to three-quarters of an hour after turning, for alternate positions of the attracting mass M. The mean values of Δy are attached to each group of forenoon, afternoon, and night observations. Since the anticipative value of Δy_0 is but 1.37 cm., the plenum deflections ($2^h 62^m$ a. m., $2^h 44^m$ p. m.) are liable on a clear day to reach almost twice the normal value, and this in spite of the filamentary framework of the needle.

The conditions are at once improved in the observations with the needle, in a vacuum of a few millimeters, on July 22 ($\Delta y = 1.52$ a. m. and 1.45 p. m.), though clear weather still prevailed.

The improvement is enhanced on July 1, 2, 3, when the sky was heavily overcast, with much rain (R), viz,

	July 1.	July 2.	July 3.
Forenoon (A)............	$\Delta y = 1.48$	1.44	1.42
Afternoon (P)...........	1.46	1.36	1.45
Night (N)...............	....	1.35	1.34

The morning deflections almost always exceed those of the afternoon, owing, as already intimated, to the structure of the building, which has but one thick wall in the east and two with an embankment of earth in the west to shut off solar radiation. We may conclude from figure 160 that the apparatus is seeking thermal equilibrium and eventually attains or even surpasses it. In other words, it appears as if at night the radiation discrepancy was reversed and became negative, for Δy is often below the normal value. It will be seen that these low values are associated with excessive drift; thus, on the night of July 3, the first doublet is $\Delta y = 1.37$ cm., followed by a sudden displacement at the lower reading. A similar drift spoils the afternoon observation on the same day. Furthermore, as the weight is on one side only, the l asymmetry is not eliminated. For these reasons these observations, like the preceding, were continued but a few days, for corroborative evidence.

From another point of view, the set of the needle for the night observations is truly remarkable. The difference from the normal deflection is but 0.2 to 0.3 mm. on an effective radius of 8,950.0 mm.; $i.$ $e.,$ an average angle of $\frac{2}{89,500} = 0.000028$ rad., or about $6''$ in the twist of the quartz-fiber is in question.

54. Observations. Two large attracting masses M' and M'' coöperating.

—The pull of these masses being exerted at the two ends of the needle, respectively, the advantages of equation (4) accrue to the work. The first of the masses was the same as that used in § 53, so that in $\gamma = \kappa' \Delta y$, $\kappa' = 10^{-8} \times 4.843$. The second was a little smaller, viz, $M'' = 2,947$ grams and $R = 5.43$ cm. The latter was determined by calipering as explained, so that $R = \frac{1}{2}(10.81 + 10.72 - 2.74 - 7.93)$, 7.93 cm. being the diameter of the ball and 2.74 cm. the outside thickness of the case. Hence the approximate value of κ'' is $10^{-8} \times 5.198$. The value of t/τ is 0.0236, so that in view of the factor $1/1.0236$

$$\gamma = \kappa'' \Delta y = 10^{-8} 5.078 \Delta y$$

and the normal deflection for this ball alone should be $\Delta y_0 = 1.31$ cm. Again, since $1 + s - t/\tau = 1.0453 - 0.0236 = 1.0217$, equation (5) gives

$$\gamma = 10^{-8} \times 5.076 \Delta y \quad \text{and} \quad \Delta y_0 = 1.31 \text{ cm.}$$

If the balls are taken together and act in the same sense for the deflection Δy,

(10)
$$\gamma = \frac{\Delta y}{1/\kappa' + 1/\kappa''} = \kappa \Delta y = 10^{-8} \times 2.479 \Delta y$$

which is practically the fourth part of $\kappa' + \kappa''$. The normal deflection should be

$$\Delta y_0 = \gamma/\kappa = 2.687 \text{ cm.}$$

which is the same as

$$\Delta y' + \Delta y'' = 1.375 + 1.312 = 2.687$$

The observations, begun on July 7 and continued for some time, three times daily, forenoon (A), afternoon (P), and night (N), with periods of from 30 minutes to 1 hour between consecutive observations, are given in figure 161.* The ultimate set of the needle at any observation was remarkably consistent, the reading being repeated at least twice, $T/2$ seconds apart. In fact, the decisive set of the needle in so delicate an instrument is profoundly impressive, the only difficulty being to decipher what is being so faithfully recorded. The scale-readings also were now clear to 0.1 or 0.2 mm. It is necessary, however, for the observer to keep as much as possible away from the instrument, even though sitting in a symmetrical position as remote as possible. On loitering near the telescope for some time (15 minutes and longer), gradual deflections

---

* To secure better vision the scale was slightly shifted on July 13.

of 1 mm. or more may be recognized, due no doubt to bodily heat radiation, as they gradually quite vanish again.

In figure 161, the mean value of Δy is inscribed on each group of observations. As the normal value should be $\Delta y = 2.69$ cm., it is obvious that only the night (N) observations are acceptable. On July 7, the apparatus, which had just been set up, was slowly approaching thermal equilibrium. On July 9, during the period of exceptional rain-storms, there was a dense fog at night, which may account in some way for the high night value. On other nights the needle showed a tendency to drift slightly, always toward larger deflections. The following is the mean record for 10 days:

June.	7	8	9	10	11	12	13	14	15	16
	cm.	cm.	cm.	cm.	cm.	cm.	cm.	cm.	cm.	cm.
Forenoon (A)...	....	2.90	2.77	2.73	2.79	2.72	2.94	2.94	....	2.98
Afternoon (P)..	2.84	2.79	2.74	2.79	2.71	2.74	2.77	2.76	2.66	2.76
Night (N)......	2.71	2.67	2.74	2.66	2.67	2.68	2.66	2.69	2.66	2.70
Weather.........	C	C	R	R	C	$C_1 S$	S	S	$C_1 R$	S

On July 15, a cloudy day of even temperature with a mild rain at the end, the data were nearly normal throughout the day. This is in strong contrast to the data of the clear day following, in which the radiation conditions were bad. Nevertheless, the last night doublet is $\Delta y = 2.66$ cm., so that further observations would have been normal. Similarly on July 14 the last night doublet is $\Delta y = 2.67$ cm.

If, therefore, we exclude the first night datum, as the apparatus was too fresh, and the exceptional datum during the fog of July 9, and take the last doublets specified, the mean of the eight deflections is $\Delta y = 2.666 \pm 0.0017$ cm. Therefore

$$\gamma = 10^{-8} \times 2.479 \Delta y = 10^{-8} \times 6.609$$

which is as near the normal value as one may hope to get, seeing that the small individual deflections, Δy, must be read off on a millimeter scale. If the values for the night observations (excepting June 7, 9, 16) be taken as they stand, the mean is

$$\Delta y = 2.674 \pm 0.0032 \qquad \gamma = 6.629$$

Night observations made on an exhausted gravitational apparatus therefore seem to give promise of trustworthy results, particularly if a season of uniform temperature is chosen and a relatively finer quartz-fiber is inserted. While the exhaustion here in question has not been carried further than a few milli-meters, the experiments are all aiming at the final test under complete exhaustion.

55. Apparatus II.   New thin quartz-fiber.—The encouraging results obtained in the last paragraph indicate that for further development a much more sensitive quartz-fiber suspension will have to be installed. Search was therefore made for a finer quartz filament and one was eventually found giving a deflection Δy of over 13 cm. with the same needle and attracting bodies similarly placed. In compensation for this advantage, however, the period T of the needle was over 12 minutes and the logarithmic decrement very large (about $\lambda = 0.9$), so that the determination of T was to be the marked difficulty encountered in the work.

The case of the apparatus was new, but consisted of a recessed brass rec-tangle like the preceding, closed with thick glass plates, sealed in place. Resinous cement, in the molten state, was poured into the crevice between glass plate and brass rim, and subsequently remelted several times locally, with a hot, flat metallic strip, to obviate leakage. Yet with all the care taken, it was not easy to get the case quite tight.

The needle being the same as before, the mass of each shot was 0.6295 gram and the length of needle (determined by a distant telescope and new scale) $2l = 22.05$ cm., the moment of inertia $N = 159.4$, about as above.

The masses and distances between centers for the two attracting bodies were

$M' = 3.368$ grams. $R' = \frac{1}{2}(11.63 + 11.58 - 8.29 - 3.12) = 5.89$ cm.
$M'' = 2.947$ grams. $R'' = \frac{1}{2}(11.20 + 11.12 - 7.92 - 3.13) = 5.63$

the latter determined by calipering, as above explained.

The scale-distance from mirror, found by steel tape, was $L = 445.8$ cm. The same half-silver device for reading was employed, a movable frosted tungsten lamp, sliding behind the distant glass scale, to illuminate the particular part of it needed in the reading.

As the deflection Δy is large, it was sufficient to pass the weight M from one side to the other, to obtain arcs large enough for the measurement of the logarithmic decrement. An example of two such experiments is given in figure 162, the needle being in a vacuum of about 0.5 cm. The needle comes to rest after about eight semiperiods, practically therefore within an hour, so that this time will have to be allowed between the readings for Δy.
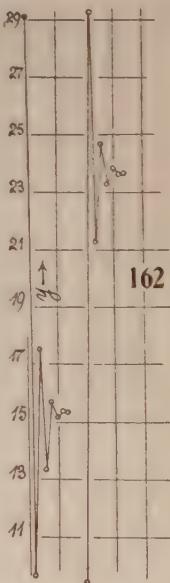
The logarithmic decrement is unfortunately no longer constant. If computed from observations 3 elongations apart, the values come out for the two graphs

$$e^\lambda = 2.41 \qquad e^\lambda = 2.44$$
$$2.44 \qquad 2.45$$
$$2.48 \qquad 2.53$$

As the period T is to be determined from the first two arcs on passing the weight M from side by side, the corresponding values of $e^\lambda = 2.47 = 2.49$ were computed. These make $\lambda = 0.909$ on the average, and hence the period is

$$T = T_1/\sqrt{1+\lambda^2/4\pi^2} = T_1/1.010$$

T_1 being the damped period. This is to be increased by the correction, here 1.0056, for the stop-watch, so that $T = T_1/1.0047$.

The value of T_1, like the value of λ, is variable in a vacuum of a few millimeters to an unexpected extent and therefore very difficult to ascertain, possibly even with a complete and rigorous exhaustion. For this I was not quite ready. The method here, as above, consisted in finding with a stop-watch the interval of time elapsed between two similar passages through the known position of equilibrium. The reading itself was certainly accurate to the fraction of a second, but the periods found were liable to vary from about 12 to 13 minutes, and this apparently quite irrationally. Sometimes two consecutive periods would be nearly the same; at other times quite different. In this dilemma the only recourse seemed to be the very tedious process of determining T_1 for each exchange of the position of the weight M. After this had been done for a time, it was found that the periods depended to a surprising extent on the accurate selection of the position of equilibrium, the error being of an order of 5 seconds per millimeter of departure of the assumed equilibrium from the true position of equilibrium on the scale. Moreover, if y is the true zero and y_T the convenient value assumed in measuring T, then falling from the high elongations, if $y - y_T$ is positive, T is low, rising from the low elongations, if $y - y_T$ is positive, T is high, and vice versa. Fortunately the y's are nearly known, being the limits of the Δy sought. Hence if $y - y_T$ has the same sign and value at both elongations, the mean T, for the two elongations, is the correct value. After prolonged trial this method also proved to be far from satisfactory. Some independent radiation discrepancy often intervenes, because of which two consecutive observations are respectively too large and too small, so that the mean value of the pair is probably the closest approach to T obtainable, always supposing that $y - y_T$ is very small (1 or 2 mm.). The following example may be cited:

	July 18.		July 19.			July 20.		
High elongation..	$12^m 29^s$	$12^m 35^s$	$12^m 3^s$	$12^m 22^s$	$12^m 12^s$	$12^m 4^s$	$12^m 11^s$	$12^m 18^s$
Low elongation..	12 15	12 17	12 11	12 19	12 31	12 48	12 28	12 30
Mean	12 22	12 26	12 17	12 20	12 20	12 26	12 20	12 24

Naturally, the final mean, $T = 742$ sec., is still quite deficient. Thus, in addition to the high value of λ, variations in the radiating forces during a period are fruitful sources of discrepancy. One may therefore anticipate better

results from the measurement of semiperiods. The motion of the needle is throughout faster, and small departures of the fiducial mark from the true position of equilibrium will represent smaller time-errors. In fact, consecutive values of T were here also liable to be too large and too small, respectively, so that their mean is the closest approach to T obtainable. The value of $y-y_T$, if small, did not seem to show more than a qualitative basis for discrimination. Since there is drift, the actual value of y is not sharply determinable. The following is an example of the mean values of T, found from semiperiods:

TABLE 4.—Doubled semiperiods, $T/2$.

Date.	P	Mean.	N	Mean.
	sec.	sec.	sec.	sec.
July 21.......	746	756	752	753
	766	.	754	
	736	749	...	...
	762		...	
July 22.......	756	758	742	759
	760		776	
	750	760	774	762
	770		750	
July 23.......	758	753	754	756
	748		758	
	764	755	766	...
	746		...	
July 24.......	750	750	754	766
	750		778	
	758	762	762	772
	766		782	
July 25.......	...	...	761	761
	...		762	
	...	...	770	766
	...		762	
Mean		755		758

On July 21 there was too much drift, so that the results are unsatisfactory. One may note that the high and low individual values often change places. Moreover, even widely different individual T values, if consecutive, are symmetrical to the mean, approximately; for instance (semi-periods).

$$\left.\begin{array}{l} 7^m\ \ 4^s \\ 5^m\ 53^s \end{array}\right\} 6^m\ 28^s \qquad \left.\begin{array}{l} 7^m\ 19^s \\ 5^m\ 30^s \end{array}\right\} 6^m\ 24^s$$

These are usually observed in the forenoon and are worthless, both in T and Δy. Obtained in this way, the mean of eight afternoon doublets was $T=755$ seconds and of eight night doublets $T=758$ seconds, both derived from semiperiods. This is much in excess of the datum (742 seconds) obtained from the observation of whole periods above. In this dilemma, the only way out seems to be to adopt temporarily the mean value $T_1=750$ seconds for the damped period, until the apparatus can be rigorously exhausted for the measurement of T.

If the value of $T_1=750$ seconds is thus provisionally accepted, the period is $T=T_1/1.0047=746.4$ seconds.

Finally, the correction for the stem attraction $t/\tau=(R\rho/lm)\,(\sqrt{R^2+l^2}-R)$, where $\rho=0.0044$ $g/cm.$ and $m=0.63$ gram, comes out $t/\tau=0.0247$ for the larger M' and 0.0241 for the smaller M''. The factor $(1+s-t/\tau)$ in equation (5) thus becomes

$$(1.0453-0.0247)=1.0206 \text{ and } (1.0453-0.0241)=1.0212$$

in the two cases. Further, if $\gamma=\kappa\Delta y$

$$\kappa'=10^{-9}\times 9.781 \text{ for the larger } M' \text{ and } \Delta y$$
$$\kappa''=10^{-9}\times 10.218 \text{ for the smaller } M'' \text{ and } \Delta y''$$

and finally,

$$\gamma=\frac{\Delta y}{1/\kappa'+1/\kappa''}=10^{-9}\times 4.997\Delta y$$

so that the normal deflection is $\Delta y_0=13.33$ cm., with the understanding that κ and Δy_0 are merely provisional, like the T_1^2 which they embody.

56. Observations Thin quartz-fiber. Large M.

—The new observations are given in figures 163, 164 and were all obtained in a vacuum of a few millimeters (2 to 5). Throughout a single group, forenoon, afternoon, or night (A, P, N), the scale is left untouched, but in different groups slight changes are often advantageous. On July 17, soon after the apparatus was set up, and the following day there is considerable drift, while the apparatus seeks thermal equilibrium with its environment. So the values of Δy (marked on each group) are high, even at night. On July 19, 20, the night observations have apparently become normal $(\Delta y=13.43, 13.40)$. On the following day, July 21, there was a fall of atmospheric temperature and a peculiar behavior of the apparatus, particularly at night. There is excessive drift at the lower elongations. If all observations are taken, $\Delta y=13.14$ cm., a datum below the normal value and suggesting a reversal of radiant forces. Their effect is here for the first time definitely repulsive, whereas, as an almost uniform rule, they act as an increment to gravitational attraction. If the exceptionally low observation (9.55) is excluded, the mean would be $\Delta y=13.38$ cm., or nearly normal. If the smaller observation (9.00) is excluded, the mean is but $\Delta y=12.88$ cm., excessively low. Although there is nothing else against the exceptional reading (9.55), it is an isolated case thus far, though it occurs again below, for it would mean that the usual radiation from without inward turns with quick fall of atmospheric temperature into a radiation from within outward, reversing the radiant forces. Very high deflections are in evidence during the forenoon of July 23 and the radiating forces dissipate slowly. On July 26 (fig. 164), it was thought desirable to restore the position of the scale, on account of the continuous seasonal drift which the needle had experienced. This drift is without consequence, as it is probably due to the slow yielding of the cement by which the hooks on the needle and torsion-head are fastened to the hooks at the ends of the quartz-fiber, to obviate all sudden accidental dis-

placements at these contacts. It was similarly present in early experiments and finally reached a limit. It is always marked in a fresh apparatus, in the beginning. The isolated low value of Δy found on July 21 is again repeated on July 31, after the violent thunderstorm had suddenly cooled the atmosphere. As a result, even the afternoon observations are nearly normal; but the first
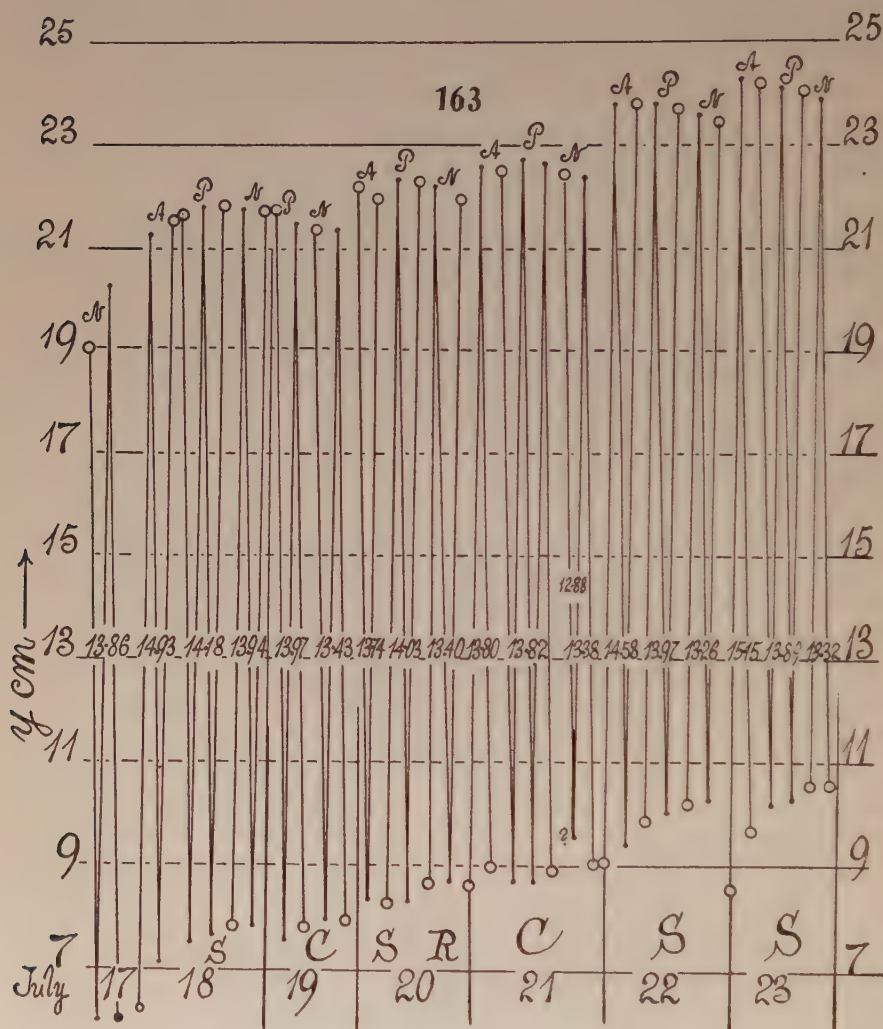
doublet at night is as low as $\Delta y = 12.66$, the mean value being 13.24 for all observations. There can be no doubt, therefore, that the radiation forces are here repulsive, a condition which is short-lived and soon vanishes, as in the preceding case. If, therefore, we look at the cause of the usual discrepancy as an effectively repulsive radiation from without, screened off by the mass M (attraction incremented), we here meet with a radiation contributed by the mass M (attraction decremented), because of the deficiency from without, a

sudden fall of atmospheric temperature being in question. Thus the phe-
nomenon is of rare occurrence.

On August 1 and 2 there is actually a nearly symmetrical drift, and the
night data found under these circumstances would seem to be the more trust-
worthy. They make a strong contrast with the irregular drift on August 3,
when atmospheric temperatures at night were low and their effect exaggerated
by an accidentally open window in the laboratory. The night mean falls as
low as $\Delta y = 13.01$ cm., with the least doublet but 12.42 cm. On August 5 the
scale was shifted; but low values continue, here as well as on August 6, with
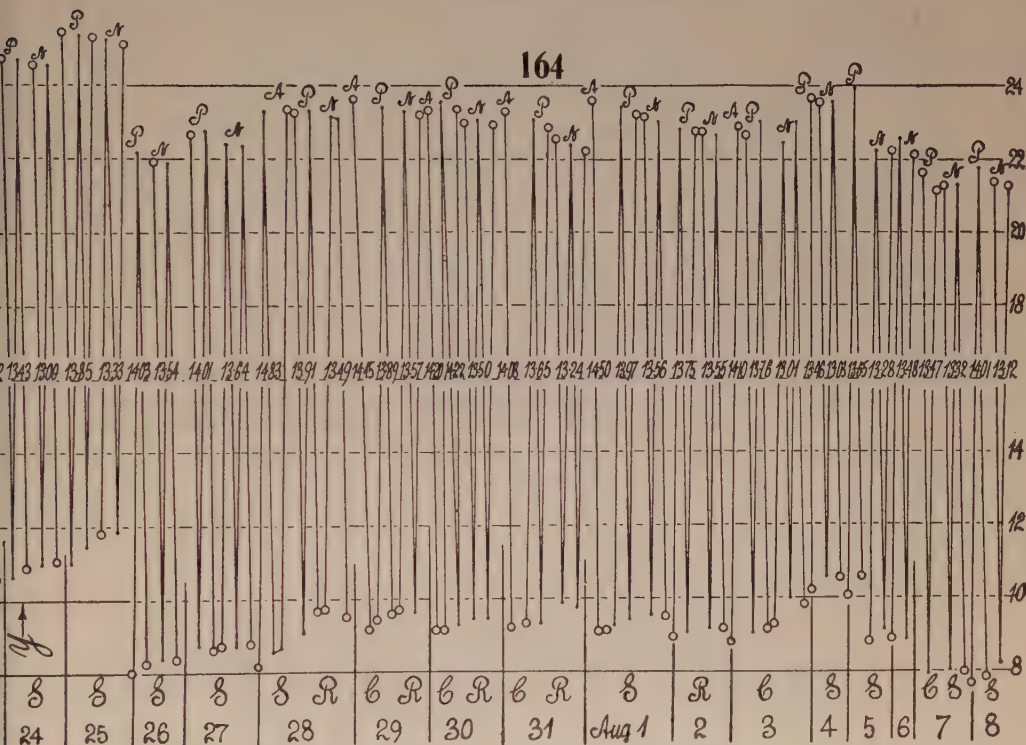
a minimum doublet of 13.29 cm. Low night values are still the rule for the
remainder of the curve. These are, in my opinion, due to the relatively cool
nights during this season; but on August 4 a new air-pump was installed,
giving vacua below 1 mm., and this may have contributed to reduce the data
for Δy, though I do not think so.

If we regard the observations on August 1 and 2, under good conditions,
again, it is probable that the full-drift curves for an interval of 24 hours
would be bow-shaped and concave upward at the upper points, concave down-
ward at the lower points of elongation.

It is curious to note that the diurnal drift (scale reset July 26 because
of it) is always larger on a given day at the lower points (where the eastern

8

mass M' is in front, or on the south side of the case) than at the upper (M' north side of m). The drift below is in the opposite direction to that in which M' pulls, and it is chiefly here that the radiation discrepancy vanishes. This very much resembles a viscous effect, since any given pull of M acts on the viscous deformation produced, left by the preceding opposite pull. The upper points show the reciprocal effect, only less pronounced. The seasonal drift vanishes for old needles (as in the experiments, February 5), but the diurnal drift does not, and it is always more pronounced at the lower points.

When the eastern mass M' is behind the case there is less protection from the outside southeastern (solar) radiation. Since the diurnal drift would respond to such a radiation, we infer that it is rather this mechanism than viscosity which is operative. There is, however, an uncertainty in superposing the diurnal on the seasonal drift. If we suppose the latter to be upgoing for both upper and lower points and superpose on this a diurnal drift upgoing below and downgoing above, we will most nearly reproduce the actual occurrences in figures 163 and 164 or figure 161.

57. Mean results.—Returning to the laboratory in September, I made a few supplementary night observations on the now well-seasoned apparatus. They are given in full in table 5.

TABLE 5.—Example of the values of successive scale readings y and deflections Δy, observed at night.

Date.	Time.	y	Δy	Date.	Time.	y	Δy
		cm.	cm.			cm.	cm.
Sept. 8........	5ʰ 45ᵐ	28.78	13.58	Sept. 12........	6ʰ 40ᵐ	28.30	13.56
	7　15	42.30			7　50	41.88	
	8　15	28.75			8　45	21.35	
	10　00	42.38			9　45	41.89	
Sept. 9.........	7　00	41.58	13.55	Sept. 13........	6　20	41.70	13.25
	8　00	27.95			7　10	28.46	
	9　00	41.58			8　00	41.72	
	10　00	28.02		Sept. 14........	7　40	42.58	13.52
Sept. 10........	6　45	28.25	13.47		9　00	29.06	
	7　45	41.73		Sept. 15........	6　15	27.30	13.41
	8　45	28.26			7　35	40.84	
	9　45	41.72			8　15	27.55	
Sept. 11........	7　00	41.82	13.50				
	8　00	28.47					
	9　00	41.82					
	10　00	28.37					

Obtained during a season of more equable temperature with an old apparatus, the earlier of these data for Δy are probably the most trustworthy of the lot, but later divergencies appeared. Whenever the Δy is derived from triplets, etc., it is included in table 6 to find the mean value.

In figure 165 I have constructed most of the data for Δy, investigated both for the morning and afternoon observations (a. m. observations are incomplete and erratic), as well as the atmospheric temperature in degrees Fahrenheit

for the successive days in July, August, and September. Though there are a few divergencies (July 30 for instance), the graphs for afternoon and night run closely alike, the former being naturally above the latter throughout. Correlative peaks and depressions may be picked out in turn. The correspondence with the temperature graph θ is not so striking, though some relation is perceptible. A comparison with the daily change of temperature was also made, but the resemblance is less close. Hence the warm days contribute the larger radiant forces, and they vanish with the day to about the same limit, both in warmer and colder summer weather.

The current deflections Δy obtained in the course of 24 days' examination, together with 8 observations of a later date, are given in table 6.

The forenoon observations, being excessive, particularly on sunny days, were eventually discontinued. The afternoon data are still much too large. The

TABLE 6.—Deflections Δy on successive days. Case exhausted to a few millimeters.

Date.	A	P	N	Date.	A	P	N
	cm.	cm.	cm.		cm.	cm.	cm.
July 17	.....	.....	13.86	August 1	14.50	13.97	13.56
18	14.93	14.18	13.94	2	.....	13.75	13.55
19	.....	13.99	13.43	3	14.10	13.76	13.01
20	13.74	14.03	13.40	*4	.....	13.46	13.03
21	13.80	13.82	13.38	5	.....	13.65	13.28
22	14.58	13.79	13.26	6	.....	.....	13.48
23	15.15	13.89	13.32	7	.....	13.47	13.32
24	.....	13.93	13.50	8	.....	14.01	13.12
25	.....	13.85	13.33	9	.....	14.33	13.70
26	.....	14.03	13.54	Sept. 8	.....	.....	13.58
27	.....	14.01	13.64	9	.....	.....	13.55
28	14.83	13.91	13.49	10	.....	.....	13.47
29	14.45	13.89	13.57	11	.....	.....	13.50
30	14.20	14.22	13.50	12	.....	.....	13.56
31	14.08	13.65	13.24	13	.....	.....	13.25
				14	.....	.....	13.52
				15	.....	.....	13.41

* New air-pump.

night observations, after the first two days in which a steady state is approached, seem to oscillate about a normal value. The mean values of the 30 night observations after July 18 are, in decades, $\Delta y = 13.429$, 13.354, 13.466 cm., which when averaged * give

$$\Delta y = 13.416 \pm 0.033$$

* Taken individually, the mean error would be 0.0312.

whence
$$\gamma = 10^{-9} \times 4.997\Delta y = 10^{-8} \times 6.704$$

This result is obtained by introducing the provisional period $T = 750$ sec. of § 55, which thus appears to be too small, as the γ obtained is too large. If the mean whole-period observations $T = 742$ sec. had been accepted, the result would be larger still. With the mean afternoon half-period observations, $T = 755$ sec., the result comes out $\gamma = 10^{-8} \times 6.615$, which is about as much too small. For the mean night half-period observations $T = 758$ sec., the result, $\gamma = 10^{-8} \times 6.563$, is thus much too small. It will therefore be the chief burden of the succeeding paragraphs to endeavor to find a more trustworthy value of T, if possible, and this should apparently closely approach $T = 752$ sec.

One may notice in passing that the introduction of the finer quartz-fiber, in spite of the larger deflection Δy, has been of no material benefit in the accuracy of the data for either Δy or T.

58. Higher exhaustion.—The endeavor was now made to reach more perfect vacua, with the object of reducing the logarithmic decrement λ of the needle. The latter was put in vibration by exchanging the positions of the large weights M.

At the stage of exhaustion for 0.1 or 0.2 mm., the logarithmic decrement, λ log e, fell for the needle from the original value of 0.385 to λ log $e = 0.331$, 0.344, etc., in experiments made on different days. The needle still stuck to the glass face (east shot forward, west shot rearward) for some time after the exhaustion had ceased. It usually had to be gently tapped off and then gradually swung freely. The radiant forces are thus much in excess when the shot are near the glass plates, and the needle, taking always the same oblique position during exhaustion, must be not quite symmetric to the case.

Another curious result was the occasional occurrence of large differences between logarithmic decrements, according as the first swing was from large or from small scale-readings, y; *i. e.*, according as the eastern M is in front (F, here associated with small values of λ) or in the rear (R, associated with large values of λ). The value of λ log e for the latter case being as above, of the order of 0.34, the former values (readings falling from low y) were even as small as λ log $e = 0.28$ in two successive tests.

This shows that the values of λ are in some way closely associated with the occurrence of radiant forces. The successive arcs of vibration sometimes give evidence of asymmetry of field of the same kind. Thus at higher exhaustions and in two consecutive cases (M positions exchanged),

Δy	λ log e	Δy	λ log e
10.50	0.2638	19.60	0.3454
5.72	.3560	8.85	.2841
2.52	.1634	4.60	.3661
1.73	.2838	1.98	.2714
.90	....	1.06	....
Mean...	.267	....	.317

the needle falling from low and high values of y, respectively. It is obvious, therefore, that the vibration is associated with a persistent drift of the needle, so that arcs would be described with mean velocities, $v \pm v'$, v' being impressed by the drift. The latter is a residuum of the agencies which during exhaustion fix the bodies m to the glass plates of the cases.

The vacuum was now increased to a few thousandths of a millimeter as tested by the McLeod gage (0.001 to 0.005 mm.), and observations made in the course of time to test the leakage of the case of the needle. The mean values of $\lambda \log e$ conveniently found from four arcs $y_1 \ldots y_4$ in the form $\log (y_1 - y_2) - \log (y_3 - y_4) = 2\lambda \log e$ were

Time.......	0	1	4.5	8	29	hours
$\lambda \log e$......	0.293	0.320	0.352	0.365	0.434	

In another of the many experiments made,

Time.......	0	1	31	hours
$\lambda \log e$......	0.267	0.317	0.455	

These results, constructed in curve a, figure 167, are discouraging, for neither is the case and appurtenances * adequately tight for exhaustions of this severity nor is the logarithmic decrement small enough to be fully available for computing T. If the pump is kept running with the case open, the needle shows a tendency to stick to the case, and there are other interferences. Experiments of this kind were carried on for several weeks, introducing a great variety of improvements, but not with any appreciably greater success.

59. Telescope at a distance.—In determining the gravitational deflections, there is no objection to the nearness of the telescope to the needle, as the reading requires but the momentary presence of the observer after the position of the needle has been fixed. For this reason the advantage gained by anchoring the telescope on the same pier which carries the case is available. But in measuring the period T and the logarithmic decrement λ, even if both are roughly known, a longer stay at the telescope is necessary. Thus the radiation from the body of the observer becomes appreciable and some of the drift in the above work is due to this cause.

Hence the telescope is to be removed to a considerable distance from the case (8 to 10 feet), and if a stable support can there be located, the appropriate modification of the above method is feasible in the way shown in figure 166. Here S is the scale at the distance $L = 447$ cm. from the mirror m in the case C, H being the half-silver. Near it is placed the lens L of long focus ($F = 185$ cm.), and at further long distance ($L' = 261$ cm.) the telescope T, the line of vision Tm being at right angles to the direction of the impinging light SH. The latter is screened off as far as possible. Without the lens L the millimeter divisions for a telescope of moderate magnifying power (focal length $= 22$ cm.) would be so small as to be useless; but with the lens the definition is admirable and there is abundance of light if S is illuminated by a tungsten burner, as above.

---

* The leak was eventually located in the rubber-tube connections.

With this arrangement measurements of λ were carried out from five successive elongations y or four arcs Δy. Nevertheless the zigzag march of the consecutive values of λ had not been eliminated. Two series, for instance, gave

$$\lambda \log e = 0.351 \qquad 0.360$$
$$.328 \qquad .316$$
$$.338 \qquad .337$$

Mean... .336   .332

but the mean values (found as above) agree more closely than heretofore.

The case was now freshly exhausted to 2.6×10^{-3} millimeters of pressure. Measurements of λ were made from five elongations throughout consecutive days. The mean results of each quintuplet were as follows:

Time......	0	3	23	37	hours
λ log e......	0.280	0.276	0.322	0.345	
		.276		.341	

Though the individual values still zigzagged, the mean results are satisfactory and trustworthy. At the outset (0 hour), λ is naturally uncertain

166

167
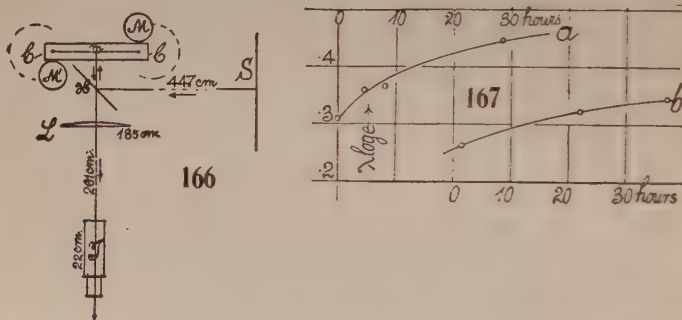
and happens to be larger than the 3-hour value. These data are summarized by the graph b, figure 167, and resemble the other curve (167, a). The increase of λ is, again, due to the slow infiltration of air through the rubber tubes, which still made up the connections. The graph suggests a method of finding the viscosity of air at extremely high exhaustions, presently to be further developed.

Together with the trustworthy values of λ thus obtained, it was hoped that definite values for T, the period of the needle, would be determinable, but all such attempts, though made with the greatest care, failed utterly of yielding adequate data. The results were no better than those recorded in § 55, table 4, under much smaller vacua, and are therefore not worth reproducing here. The reason for this seems to be that the needle is not vibrating under simple harmonic conditions, for besides the torque of the fiber there are the variable field of radiant forces and probably a not quite uniform gravitational field, by all of which the moving needle is influenced. Moreover, when the torque is so small as in the present case, the two other agencies are more nearly of the same order and the data correspondingly irregular. In the above experiments, § 54, with a thicker fiber, the larger torques and smaller deflec-

tions both produced a more nearly normal environment for the vibration of the needle.

60. Removal of the gravitational field.—This is done by placing the masses MM' in the neutral position during observation. The plan is thus to deflect the needle from rest to the maximum elongation by placing MM' in either of the extreme positions and with the needle so deflected for an instant to quickly put the weights in the neutral position again, *i. e.*, in the plane of the case prolonged. It is thus possible to determine both the period T of the needle and the logarithmic decrement, the former by timing successive passages through the equilibrium position with the stop-watch and the latter by reading the elongations. After a group of observations for M in front and M in the rear respectively have been completed, the approximate data for all subsequent series are given, a convenience which greatly facilitates the work. The zero-point was nearly constant. For example (equilibrium at $y = 36.00$ cm.),

y	Δy	$\lambda \log e$	y	Δy	$\lambda \log e$
25.55 cm.	14.19 cm.	0.341	46.90 cm.	14.94 cm.	0.349
39.74	5.80		31.96	6.08	
33.94	2.80		38.04	2.86	
36.74	1.27		35.18	1.27	
35.57	...		36.45	...	

The arcs are smaller than in the above work, but the needle comes to rest sooner and the radiation is taken symmetrically from both sides. The periods are found from observations between the first and second and the second and third elongations. So far as the method goes, the values of T and λ are quite accurately found in this way, the difficulty being in the interpretation, as the needle does not swing under simple harmonic conditions. Table 7 is a list of the data obtained, the work being continuous with that of § 59.

The table also contains a second series of data made in October during the few available days in which the steam heat was shut off. In the warmer months it had made little difference whether the needle moved from the front (F, southern exposure) or from the rear (R) of the case in its first and longest arc of vibration. In the second group of experiments, however, there is considerable difference, as is indicated by the letters F and R. In table 7 these give the temporary position of the eastern weight M, which starts the vibrations as explained, or of the first elongation of the eastern end of the needle. Apart from the cold rainstorm at the beginning, the F period is always much larger than the R period immediately following. Since the needle has two ends, radiation forces necessarily act differentially; but in some way the effective radiation urges the needle into increased vibration in the F case and retards it, or acts like an elastic buffer, in the R case. The enormous differences observed are quite astonishing. They are therefore omitted from the discussions below.

The observations for λ, together with those of the last paragraph antedating them, are given in figure 168 (later data crossed) in terms of the time elapsed

after an exhaustion to 2.6×10^{-3} mm. As a whole, they seem to be trustworthy, though strongly modified by the radiant forces. As the air slowly leaks in through the rubber tubes, λ increases gradually from day to day, the vacuum remaining within 0.1 mm. even at the end. Unfortunately, at the highest vacuum applied, $i.\ e.$, immediately after exhaustion, the logarithmic decrement is still too large for the purposes of precision. The curve suggests that for vacua within 2×10^{-3} mm. λ will decrease rapidly; but it also accentuates the need of the highest vacua attainable. So far as determinable in a heated room, the plenum value of $\lambda \log e$ was estimated as 1.

TABLE 7.—Successive values of the semiperiod $T/2$ and the logarithmic decrement λ, in the morning (A), afternoon (P) and at night (N). Original exhaustion to 2×10^{-3} mm., very slowly decreasing in the lapse of time.

Time.		$\lambda \log \epsilon$	$T/2$		Time.		$\lambda \log \epsilon$	$T/2$		
hours.					*hours.*					
N	44	....	6m 43s		P	262	.383	6m 19s		
	45	....	3		N	265	.400	5 50		
A	61	.341	5 43		P	1.5	.262	6 16	F	
	62	.349	45		†P	2.5	.279	5 13	R	
P	63	.346	5 55		*P	4.0	.272	5 56	R	
	65	.355	6 15		P	75	.359	6 15	F	
	67	.354	6 4		P	76	....	5 34	R	
N	69	.355	6 6		N	79	.371	5 29	R	
A	85	.370	5 5		N	80	.365	6 31	F	
P	88	.363	5 50		*A	92	.381	6 2	F	
	91	.361	6 21		P	171	.387	5 53	R	
N	94	.362	6 1			172	.408	6 31	F	
A	108	.381	5 1		A	189	.412	4 38	R	
	109	.392	5 21		P	190	.408	5 28	F	
P	113	....	6 22			196	.412	6 5	R	
*P	115	....	6 37		N	197	.428	6 25	F	
P	162	.380	6 34		P	268	.447	5 12	R	
N	166	.390	6 1			269	.457	6 17	F	
N	167	.368	6 36		N	271	.443	5 28	R	
A	256	.399	4 56			272	.443	6 28	F	
P	258	.383	5 20							

* Steam heat on thereafter; later again turned off. All observations made during the prolonged absence of steam heat.
† Cold storm.

Unlike λ, the values for the period T (fig. 168) show no marked improvement as the vacuum increases. They rather vary with the time of day, being smallest in the morning and largest toward the end of the day, and they drop off at night (A denoting forenoon, P afternoon, N night). The latitude of values is enormous, ranging from less than 10 minutes to over 13 minutes. The former cases (low T) are usually encountered in the morning, and probably indicate repulsive radiant forces acting from the plates toward the middle plane of the case, like an elastic buffer, whereby the period is shortened. The large values of T found in the late afternoon might in the same way be supposed to result from radiant attractions, which by a reversed procedure lengthen the period. But this is improbable. In all cases the screening masses M are quite out of the way, and, curiously enough, the zero-point is

relatively steady, changing scarcely 1 or 2 mm., while the static gravitational deflection alone is over 130 mm.

Finally, there seems to be little promise, in case of T, of modifying the unfavorable conditions by higher exhaustions. It is not, therefore, the large logarithmic decrement λ (adequately determinable, but without relation to T), but the radiant discrepancy, which vitiates the meaning of the otherwise accurately measureable values of T. In other words, the effect of the changes of λ on T is nearly negligible in comparison with the enormous fluctuations of T resulting from modified environmental radiation.

Furthermore, whereas the deflections Δy are largest in the morning and least at night, the T values pursue a nearly opposite course, increasing from morning to afternoon, except that the night periods again drop off (fig. 168). Hence the value of γ if computed in the morning with $\Delta y/T$ would be enormously too large, both factors conspiring in the same direction. As the day progresses, both approach normal values, so that with $\Delta y/T$ the γ rapidly decreases. It is rather a pity that there is no compensation in the march of these occurrences. There is, however, one very promising inference to be
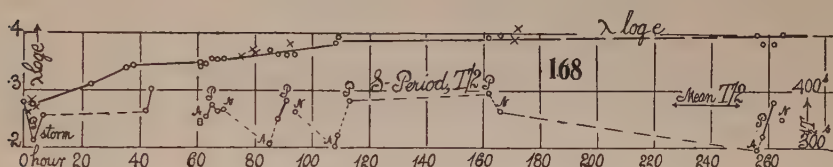
drawn from the behavior of T, in its passage through a maximum in the afternoon, as shown in figure 168; for it seems obvious that, both when the environmental temperature is gradually increasing (morning) and when it is gradually decreasing (night), small values of T, the period of the needle, occur. This was also shown strikingly during a violent rainstorm, in which the atmospheric temperature dropped about 20° F. rather suddenly. Periods were observed at that time, as follows:

Exhaustion, 3×10^{-3} mm.		
Before storm.....	$3^h 15^m$ p. m.	$T = 752$ sec.
During storm.....	4 15	626
After storm......	6 00	712

Under the high exhaustion in question, the T discrepancy can scarcely be identified with anything else than some form of radiation pressure. Since M is out of the way, there is an exchange of radiation between the inner walls of the case and the needle. If the case is warmer, the needle meets repulsive agencies toward the center from the excess of radiation inward. If the masses m at the end of the needle are the warmer, the needle radiates toward the case outward and therefore experiences a repulsive reaction which functions just like the preceding instance of a hotter case. Now, if this field of radiant repulsive force were symmetrical and uniform, no effect would be produced; but if it increases toward the walls of the case, the effect will be virtually

an increase of the torsion coefficient of the quartz-fiber, so that T comes out smaller. That the radiant field is far from uniform is evidenced by the tendency of the needle to stick to the glass plates of the case whenever the latter is freshly exhausted and even when the exhaustions are high throughout. The needle usually has to be tapped free. It is further evidenced by the good γ values obtained when the excursions of the needle end are relatively small, as in §§ 53, 54 ($\Delta y = 1.34$ cm. and 2.66 cm. as compared with $\Delta y = 13.5$ cm.; shot excursions, $\Delta x = 0.016$ cm., 0.032 cm., and 0.16 cm.).

It would then follow that the large deflections are obtained when the radiant field is nearly uniform and that the larger values of the period T are the more nearly correct. Excessive values of T would then correspond to a radiant field increasing from the plates of the case to the needle, and this, as one would naturally suppose, is a rare occurrence, as in figure 168. The inference is also in keeping with the γ values thus obtained.

Finally, the deflections Δy are modified and complicated by the screening effect of the presence of the masses M, which in the T experiments are absent.

61. Estimate of radiation temperature differences.—With the data of the preceding paragraph, it will now be possible to get some idea as to what the temperatures of case and needle between which radiation takes place would have to be. Although the glass plates are impervious to dark radiation from without, the heat will nevertheless accumulate in them, to be radiated in turn from the inside towards the needle. Thus the plates are merely a temporary obstacle to the passage of radiation, eventually acting much like a relay.

Let us suppose that the radiant repulsion from case to needle, the elastic buffer effect explained in § 60, can be expressed as an increment a_r of the modulus of torsion a of the needle. Then, if the two periods with and without radiation forces are T' and T, the equations will be ($N = 2ml^2$ being the moment of inertia of the needle):

(1) $$T' = 2\pi \sqrt{\frac{N}{a + a_r}} \qquad T = 2\pi \sqrt{\frac{N}{a}}$$

from which

(2) $$a_r = 8\pi^2 ml^2 \Delta \frac{1}{T^2}$$

m being the mass of the shot and Δ a symbol of finite differences. Furthermore, if f_r is the radiant force at each end and $\Delta y_r / 4L$ half the double deflection in radians (Δy_r distance between elongations; L distance of scale from mirror):

$$a_r = 2f_r l / \left(\frac{\Delta y}{4L}\right) = 8f_r lL / \Delta y_r$$

If we equate these values of a_r

(3) $$f_r = \pi^2 \left(\frac{ml}{L} \Delta \frac{1}{T^2}\right) \Delta y_r$$

where the quantity in parenthesis is the virtual modulus of the radiant forces, f_r, and Δy_r the double deflection referable to it. To find Δ_1/T^2, the least and maximum T found in vacuo in the last paragraph, *i. e.*, $T'=5$ minutes and $T=6.5$ minutes, may be inserted, so that $\Delta(1/T^2)=4.5\times10^{-6}$, nearly. As $m=0.63$g, $l=11$ cm., $L=450$ cm., the modulus is 70×10^{-8}, nearly.

To determine the radiation forces in vacuo, it will be necessary to postulate the case of black body, or full radiation, *i. e.*, to assume Stefan's law, so that if θ and θ_0 are the absolute temperatures between which radiation takes place and E the energy radiated (ergs per cm.^{2} per sec.)

(4) $$E=K(\theta^4-\theta_0{}^4)=4K\theta^3\Delta\theta$$

as $\theta-\theta_0$ is relatively small here. The value of θ may be taken as $300°$ and $K=5.3\times10^{-5}$ is the datum found at the Reichsanstalt. Thus,

$$E=4\times5.3\times10^{-5}\times(300)^3\Delta\theta=10^3\times5.7\Delta\theta \text{ ergs./sec.}$$

This radiation may at the outset be supposed to reach the needle from a single cm.^{2} of each plate situated on the normal to needle and plate, as shown in figure 169. There are two coöperating hemispheres cen-

169

tered at s and s', so that $2E$ is contained with a sphere whose radius is the velocity of light. Let ρ be the energy density at a distance r from s or s', implying

(5) $$\rho=\rho_0/r^2$$

and

$$2E=\int_0^c \rho_0/r^2 \cdot 4\pi r^2 dr=4\pi\rho_0 c$$

whence

(6) $$\rho_0=E/2\pi c$$

This energy density ρ_0 is thus the light pressure at a distance of 1 cm. from the element s or s'. If we suppose (as is nearly the case) the shot m of frontal area A to be situated there, the force f_r upon it will be

(7) $$f_r=\rho_0 A=EA/2\pi c=\frac{10^3\times5.7A\Delta\theta}{2\pi c}$$

where $A=0.16$ cm.^{2} Hence

$$f_r=10^{-9}\times4.8\Delta\theta$$

for the square centimeter of plate taken. There is an inconsistency in equation (1) as compared with equation (5), which does not condition simple harmonic motion. It must be supposed, therefore, that for small excursions the equations would not be materially altered.

If now we equate the values of f_r in (3) and (7),

(8) $$70\times10^{-8}\Delta y_r=10^{-9}\times4.8\Delta\theta$$
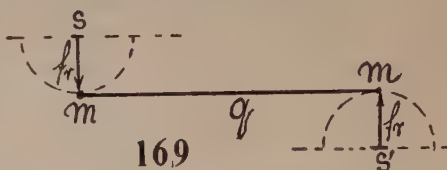
or
$$\Delta\theta = 145\Delta y_r$$

if but a single square centimeter on each glass face radiates toward m. As there are a number of such square centimeters contributing radiation, a second integration is implied, by which the coefficient of (8) would be decreased 10 or 20 times; but this detail is beyond the purpose of the present estimate. One may conclude, I think, that $\Delta\theta$ and Δy_r are numerically not of the same order, or that an increment of deflection of $\Delta y_r = 1$ cm. should be equivalent to a temperature difference of the order of $10°$ C. between plates and shot m. This is too large a value to persist in a room of practically constant temperature in the summer. It is thus more than probable that at a vacuum of 10^{-3} mm. or 1.4 dynes per cm.^{2}, or a force $1.4 \times 0.16 = 0.22$ dyne on each shot, so small a part as 10 or 20 times the $10^{-8} \times 70 \times \Delta y_r$ instanced in equation (3) may remain fluctuating in value, with small changes in the thermal environment. In fact, from this point of view, a vacuum of 10^{-3} mm. is still an enormous agency as compared with the small radiation discrepancies involved.

The conclusion would, then, be that it is not light pressure but a radiometer effect which militates against the experiments, and that its complete elimination, even at the highest exhaustions attainable, would not be feasible.

62. Measurement of γ in terms of the viscosity of air.—This method was tested in the last report (Carnegie Inst. Wash. Pub. No. 310, § 94) with the rather unpromising case of a straw-shafted needle, but the results obtained were surprisingly good. Uniform motion at a distance from the turning-points is the usual occurrence. For the present needle with a filamentary suspension, the equations for the spheres m and m' are known and the results therefore more trustworthy.

The experiment is made in a plenum of air, therefore, of known viscosity. A maximum deflection of the m balls is produced by temporarily placing the M balls in position. When this is attained, the latter are reversed and the velocity v with which the needle passes through the equilibrium position is measured with a stop-watch. The M balls are then again reversed and the measurement of v repeated, etc. In a plenum, the motion of the needle through the zero-point is practically uniform and therefore the frictional force is equal to the gravitational pull. Moreover, if two points of the scale near to and equidistant from the zero-point are selected for releasing and arresting the stop-watch, the torsion of the fiber acts to the same degree to produce an acceleration and a retardation and is thus eliminated.

The frictional resistance encountered by either round mass m of radius r is by Stokes's equation $6\pi\eta r v$, where η is the viscosity of air. The velocity v of the balls m is

$$v = \Delta x/\Delta t = (l/2L)\Delta y/\Delta t$$

l being the semi-length of the needle and L the scale-distance from the mirror. Δy is the telescopic excursion in the time Δt, symmetrically to the position of

equilibrium, and the latter must first be found by putting M and M' in the neutral plane. We obtain

$$\gamma \frac{mM}{R^2} = 6\pi\eta r \frac{l}{2L} \frac{\Delta y}{\Delta t}$$

whence

$$\gamma = \frac{R^2}{Mm} \frac{3\pi\eta rl}{L} \frac{\Delta y}{\Delta t}$$

If we insert the values for the first weight M

$$M = 3,368 \text{ grams.} \qquad R = 5.67 \text{ cm.}$$
$$m = .6295 \text{ grams.} \qquad \eta = .00019.$$
$$L = 447.5 \text{ cm.} \qquad r = .23 \text{ cm.}$$
$$l = 11.0 \text{ cm.}$$

$$\gamma = 10^{-7} \times 1.536 \Delta y'/\Delta t$$

For the second weight,

$$M = 2947 \text{ grams.} \qquad R = 5.43 \text{ cm.}$$

whence

$$\gamma = 10^{-7} \times 1.609 \Delta y''/\Delta t$$

Hence, when both coöperate

$$\gamma = 10^{-7} \times 3.145 \Delta y/\Delta t$$

Unfortunately, the steam heat had been turned on permanently in the building and further measurement of γ was therefore out of the question. The position of equilibrium of the needle continually shifted. Nevertheless, I was anxious to test the equation, to see how far the results would diverge from a normal value, even under these extremely unfavorable conditions. The time taken by the needle to pass over $\Delta y = 2$ cm. of scale near the zero-point were

Rightward ...12	13	15.8	12.2	sec.
Leftward 16	16	15.5	16.0	sec.
Mean $\Delta y/\Delta t = 0.15$	0.14	0.128	0.145	cm./sec.
$10^8 \times \gamma = 4.6$	4.4	4.1	4.6	

These values are of course small, which may in part be due to the rough values of y and r inserted or to an absence of corrections for the framework or the equations. It is chiefly due to the presence of relatively enormous and varying radiant forces. By no other method would it have been possible to get a value of γ under these circumstances anything like as near as this, and the reason is that all radiant forces of fixed direction are eliminated. Those effective are the ones which shift with the weights M.

INTERFEROMETER EXPERIMENTS IN ACOUSTICS AND GRAVITATION

PART III

By CARL BARUS, Ph. D., LL.D.

Hazard Professor of Physics and Dean of the Graduate Department in Brown University

PREFACE.

The following papers contain the experiments made in this laboratory during the last two years, chiefly with the aid of the mercury U-gage, the rise and fall of the free surfaces of which are read off with the interferometer. In most cases relative values of the small pressures in question are alone of interest, and as these are proportional to the corresponding fringe displacements with white light, it suffices to report the latter graphically. Unfortunately, the range of the gage is restricted by the tendency of the surfaces of mercury gradually to lose parallelism in their reciprocal motion. This has been partially counteracted by making the free mercury surfaces of large (10 cm.) diameter, by filling the gage in vacuo, etc. The success of these devices is but partial. Moreover, pressures within 5×10^{-4} cm. of mercury are liable to be more or less distorted by capillary forces and thus not registered in the surface depressions of the gage. Finally in a closed region with rigid walls, small pressure increments, if accruing in the lapse of time, are not determinable, owing to coincident relatively enormous temperature discrepancies which may supervene. The hope of measuring slowly accumulating pressure increments easily and directly, a frequent desideratum in physical chemistry and biology, has not borne fruit, as shown by a number of typical examples in Chapter I.

If, however, the walls of a region are elastic in such a way as to determine a definite small-pressure increment within, the temperature difficulties vanish. Thus the measurement of variations of surface tension by the pressures observed within a bubble works out nicely, though it must be acknowledged that the work requires both patience and expedition. It is possible to trace the increase of surface tension in this way almost as far as the solid state. The experiments succeed not with soap-bubbles only, for colloidal solutions are very generally available. An interesting result, moreover, is the possibility of thinning out of a soap solution to a degree approaching pure water with continually increasing surface tensions.

In the case of gases, there are many measurements to which the U-tube interferometer lends itself. Thus it is easy to find the viscosity of a gas from very small pressure increments, though here the temperature discrepancy referred to above is already menacing, in spite of the small times of transpiration. In the case of efflux, I have not been able to produce a hole small enough to admit of trustworthy results. The large increase of gas viscosity, produced by the heat of a flame carried at the end of a fine jet, is strikingly noticeable. The flame thus virtually plugs the gas-jet; and since the plug is removed with the flame, there is here a mechanism favorable to turbulency in flames.

A most promising application of the **U**-gage was found in the endeavor to measure the density and diffusion of gases. For here it is merely necessary to determine the pressures at the end of a long tube in the lapse of time. I have, therefore, investigated this subject at some length, using a variety of gases and with special reference to the gage discrepancy already stated. The densities found may be shown to conform satisfactorily with known data. The diffusion coefficients come out consistently for all lengths and widths of tubes; but for some reason which I have not ascertained, the coefficients found are larger than the standard data. From measurements of the pressure at the top of hot gas columns, the coefficient of expansion may be derived approximately, and more precisely as the pipe is longer. The attempt to find the hygrometric state of the air, however, failed, probably from the difficulty of actually drying the tube and appurtenances adequately.

In Chapter IV, I have returned to the pressures generated acoustically when pin-hole probes are placed at the nodes of vibrating systems. These pin-holes, which are ideally salient and reëntrant cones, respectively, with a prescribed size of hole, are always used in pairs; for in such a case the fringe displacement of the tube interferometer is nearly doubled. If a region of pulsating air has access to still air through a pin-hole probe only, the pin-hole being placed at the boundary, the resulting stream-lines point from the apex to the base of the pin-hole cone. Their strength varies with the diameter of the pin-hole (critical maximum of efficiency), the obliquity of the walls, and the intensity of the pulsation (node). The result is a pressure increment or decrement, respectively, in the pulsating region. The first part of the paper describes the vibration in branched pipes excited by a telephonic siren, as it were, or by paired sirens in unison. The pipes are of different diameters, but the branched region is closed and preference is given to quill tubes. The character of the motion within is mapped out both with the telephones in sequence (plate displacement respectively in and out) and in phase (plate displacement in and out together) for a great variety of tube-lengths. If the survey is made in pitch, the maxima of fringe displacement (crests) show the pipe-notes in any given case. The endeavor is then made to distribute the observed pipe-lengths determined by the crests in relation to the free wave-length of the pipe-note. A curious feature in all this work is the appearance of strong low-frequency crests (2 and 4 foot octave) in connection with pipes less than 10 cm. long, and the repeated occurrence of multiple resonance.

Among the allied results, the use of currents arising in the electromagnetic mechanism of a loud-speaker horn, receiving diapason pipe-notes from different distances, may be mentioned. The most interesting method of exciting vibration, however, is the small spark-gap placed at one end of a doubly capped tube. For in such a case, in addition to the acoustic resonance (frequencies of the tube) the electromagnetic frequency of the coil, if low enough, may also be recognized by an anomalous crest, the pitch of which is controlled by the capacity and inductance of the coil.

In Chapter V, I have collected such experiments as grew out of the work incidentally and seemed to require further investigation. Thus, when Mayer's phenomenon of acoustic pressure is evoked by telephones, it shows a systematic distribution of both attractions and repulsions along the pipe axis, and these are best exhibited when the resonators or disks are swung from a bifilar mechanism or a torsion balance. In the work done with interferometers, the peculiar asymmetrical sequence of fringes produced by the aid of the extraordinary ray of a calcite rhomb used as a compensator is noteworthy. A suggestion for the use of long-distance interferometry in connection with earthquake phenomena to detect slight changes of shear is given a preliminary trial, etc.

In the last chapter I have put together the work done on the constant of gravitation. The chief purpose of this chapter is to compare the night observation for the Newtonian constant made under reasonable laboratory surroundings, in 1922, throughout a number of months in the summer, with corresponding data obtained in 1921. The result is disappointing; for the mean data of the two series differ in spite of all precautions by nearly 2 per cent. Incidentally, it is shown that the static displacement of the needle, its period, and logarithmic decrement are interdependent, all being similarly influenced by the presence of dominating radiant forces, which it was found impossible to bring under adequate control. They are considerably reduced by the partial exhaustion of the needle-case and all observations were made in rarefied air; but they are increased again by high exhaustions, and the anomalous results obtained under these circumstances, where attractions are frequently inverted and repulsive forces appear, are a curious incident in the work. For this reason, the endeavors to interpret the motion of the needle in terms of the viscosity of the gas, etc., are illusory, since the chief resistances are radiant forces. In fact, the blight which seems to descend upon the apparatus after high exhaustion, reversing all normal behavior for days, is an astonishing phenomenon. I have been tempted at times to find more in it than a mere consequence of the law of cooling to ultimate equilibrium.

My thanks are due to Miss Mildred E. Carlen for her efficient assistance in preparing this volume for the press.

<div align="right">CARL BARUS.</div>

BROWN UNIVERSITY,
  Providence, Rhode Island.

CONTENTS.

CHAPTER I.

MODIFIED INTERFEROMETER U-TUBE WITH APPLICATIONS.

1. Apparatus.—The mercury U-tube heretofore used, at the end of a long interval of time, developed increasingly annoying viscous discrepancies, probably due to the aging of the mercury; at least, on cleaning and refilling the apparatus with fresh mercury they vanished. The other difficulty, however, was not so overcome; *i. e.*, the two free surfaces of mercury do not rise and fall rigorously in parallel. They remain practically so only within a small displacement (dh), usually not exceeding 50 fringes. This not only reduces the limits within which the gage may be used, but introduces an error of obliquity. All methods used hitherto to overcome this failed, and even the practically unavailable naked mercury surface is not free from the discrepancy.

A method of at least improving the gage by enlarging the area of the free surfaces suggests itself as promising. This is done in the apparatus shown in figure 1, where AB is an iron block containing two shallow cisterns about 9.5 cm. in diameter and 2 cm. deep. They are joined by the canal C made by the junction of two oblique $\frac{1}{8}$-inch drill-holes. This is narrow enough to guarantee nearly aperiodic and sufficiently rapid deflections at the interferometer, so that a vertical screw to choke off C, partially, is needless. Mercury is poured into the cistern to a depth of less than a centimeter and covered by the two equally thin glass plates, g, g', beveled at the edges. These not only make admirable mirrors, but they almost completely dampen the natural quiver of the mercury surface in an agitated environment. The cisterns are closed by the equally thick glass plates (G, G'), laid upon the flat surface of iron and sealed with molten soft sealing-wax at their edges when the block is warm. A linear gas-flame from a pin-hole is very serviceable for the purpose. This simple method of closing the shanks of the U-tube is preferable to the use of reëntrant receptacles in the iron, because the plates GG' may be so easily removed and very low pressures or partial vacua alone come in question. Access for pressure measurements to either cistern is obtained through the two tubulures (t, t') in front. The two beams of the quadratic interferometer a, b, about 10 cm. apart, are reflected from the mercury mirror, so that glass thicknesses must be nearly equal.

The gage constructed in this way, and used in connection with the fringes of white light, behaved admirably within the field of the ocular micrometer, *i. e.*, within about 200 or 300 fringes. Beyond this, however, the growing obliquity of surfaces gradually puts a stop to further measurement. Possibly anchoring small plates (g, g') with fibers of silk in the middle of the pools of mercury would be a further remedy; but the exposed surfaces of mercury

would then be free to quiver annoyingly. With the further aid of the slide micrometer on the interferometer, supplementing the ocular plate micrometer, I was able to carry the pressure measurements as far as 0.2 mm. of mercury before the fringes became too vague to be easily recognized. The useful interval lies between 10^{-4} mm. and 0.1 mm., the size of fringes (usually within 0.1 mm. in the ocular) being modified to suit the experiment. The ocular micrometer should be placed in the wide slit-image of the *collimator,* in which case the telescope is free to move to and fro. If one of the shanks of the U-tube is closed or communicates with a closed region, the U-gage becomes a very sensitive air thermometer. Hence, if pressure measurements are in question, it is necessary to work in an environment of practically constant temperature; for spurious pressure increments in millimeters would be interpreted numerically over twice the actual temperature increments.

2. **Mercury charged in vacuo.**—Some time after this, in endeavoring to use the U-tube as a vacuum gage, I noticed that the tendency of the plates
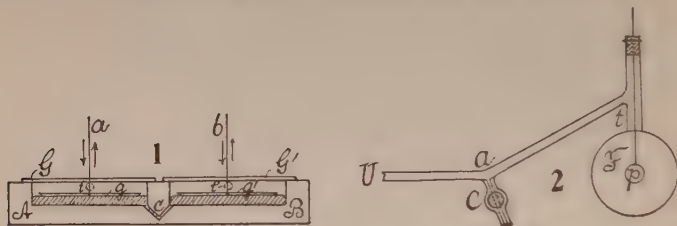
to lose accurate parallelism on measuring relatively high pressure differences (0.02 mm. to 0.1 mm.) had disappeared. The inference is that in order to give the gage the largest possible range, the mercury charge must be added in vacuo. When the gage which has been filled in a plenum is exhausted, air-bubbles are apt to rise and cling to the lower face of the glass plate, from which they are difficult to remove, particularly if the mercury is no longer quite clean. This succeeds, however, with a trigger arrangement by which the plates may be tilted and manipulated, through the rubber-tube connections, in vacuo. It is not uncommon to find the cast-iron cistern (*AB*, fig. 1), though perfect as a mercury container, apparently leaky under exhaustion, so that large bubbles appear under the glass plate when the internal pressure falls to a few millimeters. It is even probable that films of air between glass or iron and the mercury may on exhaustion be thrown into a bubble-shape and become appreciable. The experiments which show this are convincing. Thus, if the gage is kept exhausted for 1 or 2 hours, no bubbles appear under the plate *g,* the mirror remaining smooth. If, now, air is allowed to enter and plenum is retained for a few hours, large bubbles half an inch in diameter will separate out as soon as the gage is again exhausted. After the lapse of a day (the gage being open to the air), the air-bubbles formed on exhaustion will cover the lower face of the plate. Thus, the bubbles date back to the plenum, and they arise from the infiltration of air between mercury and the

glass or iron surfaces, previously exhausted. The next exhaustion merely exhibits the result by expanding the air.

The largest crop of such bubbles was obtained on exhausting the gage in the presence of saturated water-vapor within. Removing the water-tube and exhausting again, the plate was fairly deluged with bubbles, and the effect only ceased after the complete removal of water-vapor by successive exhaustion.

The vacuum-filled gage will be used for a variety of experiments below, where relatively long-range pressure increments are demanded. With very pure mercury charged in the way stated, the annoyances of separating slit-images were found to be absent. Nevertheless, in the lapse of time they reappeared and the range was correspondingly shortened. This aging seems to introduce a peculiar error to be discussed in §§ 37, *et seq.*, below, under the name of capillary error; for it appears that the whole pressure is not expressed in the displacement of the mercury surfaces g, g', but that a correction term, nearly constant in a given series of measurements, must be added, even when the zero of the gage (*i. e.*, the fringe position for no pressure) is quite fixed.

<div align="center">APPLICATION.</div>

3. **Gas evolution and absorption.**—It was hoped that the interferometer **U**-gage might here be of some interest, particularly in chemical and bacteriological researches; but the work is delicate, inasmuch as it calls for rigorous constancy of temperature. Specific pressure production within rigid walls is probably not measurable. For not only is the closed **U**-region with appurtenances an air thermometer, but the vapor-pressure of a solution, if present, also changes. If we write $dp/p = d\tau/\tau$, the spurious pressure increment is more than double the discrepant temperature increment. Moreover, for an aqueous solution at 25° C., $dp = 1.5 d\tau$ millimeters of mercury. Thus together, $dp = \left(\dfrac{760}{300} + 1.5\right) d\tau = 4 d\tau$, nearly. Hence $d\tau = \dfrac{\lambda/2}{4} < 10^{-4°}$ C. is a sufficient temperature discrepancy to produce a spurious pressure discrepancy (0.0003 mm. of mercury) equivalent to one fringe. Such experiments are, therefore, essentially summer basement work. Nevertheless, it seemed to me desirable to give the apparatus a preliminary trial under winter conditions.

The experiment first performed was very simple and consisted in mounting a small boiling-flask 3 cm. diameter (*F*, fig. 2) connected with the **U**-gage at *U*, and the stopcock *C* by a branch tube. The absorption agency *p* was placed in the tube with *C* open and the fringes at zero, by aid of a rubber stopper. Thereafter *C* was quickly closed and the march of fringes observed with a stop-watch.

The test was made with phosphorus, pressed between bits of wire gauze about 1 cm. square. A variety of these experiments was tried, the typical example given in figure 3 corresponding to the following results:

Time = 0	.5	1	2.25	3.25	4.25	5.42	minutes.
Deflection = 0	.11	0	—50	—100	—150	—210	Scale parts, *s*.
$\Delta p \times 10^3 = 0$	+.7	±0	— 3.1	— 6.3	— 9.4	— 13.2	mm. Hg.

Within the first minute pressure rises to a maximum (sometimes 2×10^{-2} mm.) after which it falls regularly at a rate of about 0.03 mm./minute, within the available interval of observation almost linearly. The rise is the excess of the air-thermometer action of the flask F, registering the heat of the phosphorus oxidation or the desiccating effect of the P_2O_5 produced, over the cotemporaneous absorption. Since the air is initially moist, the latter may be the greater heat contribution. After 1 minute the pressure reduction resulting from oxygen absorption supervenes.

As the reduction in pressure after 5 minutes is but 0.13 mm., out of the many centimeters of mercury available, it might seem as if the motion of oxygen through the quill tube Uat, figure 2, had hardly begun, the oxygen in F sufficing. For this quill tube was only about 0.3 cm. in diameter and 10 cm. long, apart from the elbow and rubber joints, which contributed an additional 5 cm. of length and 0.5 cm. in diameter. To obtain results more definitely bearing on such a diffusion-like contribution, the volume of F should be as nearly as possible deleted. This device is shown in figure 4, where the stopper F has a phosphorus grid or the like on its front face and
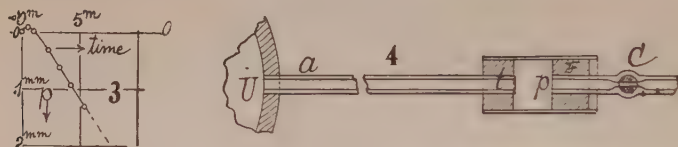
may be moved quite up to the quill tube Uat. The air within the **U**-gage at the other end thus becomes practically the sole oxygen reservoir. The cock C is open on adjusting the tube in place (to avoid turbulence on compression) and closed immediately thereafter.

In the following examples a rough disk of phosphorus had previously been placed between t and p of figure 4 and the grid dispensed with. The oxygen consumption was now apparently slower than before, the diffusion-tube being 17 cm. long and 0.5 cm. in diameter. Nevertheless, because of the limits of the **U**-gage, the experiment had to be made in successive sections and the slide micrometer ($\Delta x \cos i = \Delta h$) used. The range of the ocular micrometer was too small, and its middle 50 merely served as a fiducial point to bring the fringes back to their starting-point. The cock C was opened after about 10 or 12 minutes for about 6 or 7 minutes and the new stage of the experiment begun afresh. This is of course an interruption of the experiment, as fresh air enters at C. As it does not penetrate beyond the large charge of phosphorus, its effect on the oxygen contribution from U should be secondary, but for the fact that it seems to wear out the efficiency of the phosphorus surface. At all events the graphs given in figure 5 are distinctly curved from the beginning and the rates of diffusion persistently diminish, viz:

First stage, 0–10^m	Second stage, 16–28^m	Third stage, 35–47^m
Initial $dp/dt = -0.023$	-0.011	-0.009 mm./min.
Final $dp/dt = -.012$	$-.010$	$-.006$ mm./min.

Much of this distortion, since thermal and absorption effects act differentially, is no doubt due to temperature irregularities. The total pressure reduction may be estimated as not much above 0.5 mm. of mercury, so that the oxygen exhaustion in U is insignificant. The retardation in rates is thus to be ascribed to the diminished effectiveness of the phosphorus surface just referred to, which was no doubt already too much tarnished in the beginning.

4. **Water absorption.**—In this case a tube similar to figure 4 was used, without phosphorus, the cork F being withdrawn towards the rear and the space filled with dry P_2O_5 behind a loose cotton plug as a partition. After at was attached to U, the cock C was closed again. The diffusion of the residual water-vapor in U through the quill tube at (15 cm. long, 0.5 cm. in diam.), into the desiccator F, is here an apparently very slow process, as shown in figure 6. The absorption proceeds at a gradually accelerated rate within the first 100 minutes; but thereafter it is again retarded. The latter must occur
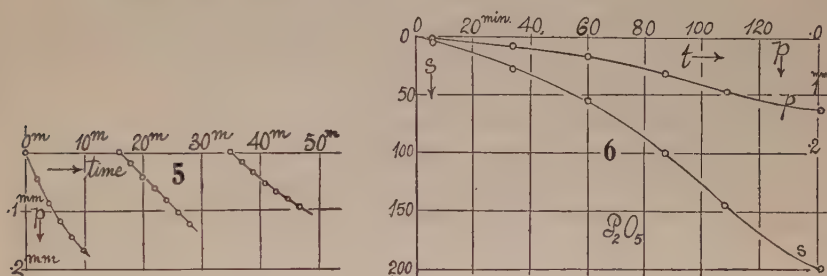
eventually from deficiency of moisture in $U;$ yet it is rather difficult to account for earlier acceleration. The mean results are:

Time $= 0$	6	34	60	87	109	141	minutes.
$\Delta s = 0$	6	26	52	100	148	200	s. p.
$\Delta p \times 10^{+2} = 0$	.4	1.6	3.3	6.3	9.3	12.6	mm. Hg.

Though there was not much moisture in U, the slow drain is rather unexpected, the rates during successive half-hour sections being about

$$10^5 \times dp/dt = 47 \quad 65 \quad 115 \quad 136 \quad 103 \quad \text{mm./min.}$$

The complications here are much like those discussed in the case of phosphorus, with the addition of the variable humidity of U. There must also be a large counteracting thermal effect.

5. **Water evaporation.**—On replacing the phosphorus in F, figure 2, by a wad of wet filter-paper at p and then closing C, data were obtained in which the first trial showed larger evaporation pressures than the second, taken an hour or more later. It was thought that the flask, after the phosphorus experiment, was initially drier. The maximum pressures appeared about 5 minutes after closing C, and they were but 0.044 and 0.026 mm. of mercury respectively. Thus it seemed as if the increase of pressure were confined to the inside of the flask F, the diffusion of water-vapor through Uat having

scarcely begun. After the occurrence of the maxima, the pressures in both cases dropped off.

Using an apparatus of the form of figure 4, in which the stopper F (phosphorus removed) was pushed toward the rear and a wad of wet filter-paper placed between F and the end of the tube at, much more definite results were obtained, as shown in figure 7, curve a. The tube was here 16 cm. long and 0.5 cm. in diameter and the cock C closed immediately after the adjustment had been made; nevertheless there are complications in the pressure increments (h mm. of Hg) within the first 10 minutes. Recovering thereafter, they show an almost linear progress at the rate of 0.0016 mm. per minute within the ensuing 90 minutes, as follows:

Time = 0	15	39	63	87	minutes.
$\Delta p \times 10^3 = 0$	2.1	6.7	10.4	14.4	mm. Hg.

Unlike the complicated case of phosphorus, the present experiment may possibly be modified into a real exhibit of diffusion, and therefore seemed deserving of further trial. Nevertheless, it is essential to bear in mind that slow, incontrollable elevation of room temperature, increasing both the air-pressure and vapor-pressure in the closed region, would give rise to a march of pressure indistinguishable from those obtained. Furthermore, since the saturated vapor-pressure is independent of volume, it is a question whether the occurrence of diffusion would leave any pressure record in U, at all; for the whole region $Uatp$, figure 4, is from the outset under pressure $p_{air} + p_{vapor}$, the latter certainly being saturated at tp. If the vapor advances at all it can do so only by depressing the mercury in U, which would thus become interpretable evidence for diffusion, provided discrepancies of the kind enumerated above can be eliminated.

The repetition of the experiment with a shorter diffusion-tube of the same diameter ($l = 7$ cm., $a = 0.2$ cm.^{2}) gave the results (fig. 7, curve b):

Time = 0	23	26	56	minutes.
$\Delta p \times 10^3 = 0$	2.6	3.1	7.2	mm. Hg.

and a rate of but 0.0014 * mm. per minute. In other words, for a tube less than half as large as the preceding, the coefficient dp/dt is smaller. Thus, unless the air in U was less dry in the present case as compared with the preceding, for which there was no evidence, the experiments being made some time apart, the interpretation of these experiments in terms of diffusion only is out of the question. Moreover, the extreme smallness of the coefficients dp/dt falling within 0.08 mm. per hour, when the saturated pressure is over 15 mm., points in the same direction. What was observed could at best be a residual diffusion, after the pressure gradient had all but vanished. Similarly, adverse results are given in figure 7, curves c and d, obtained from tubes 9 cm. long and respectively 0.5 cm. and 0.17 cm. in diameter. The former shows a high coefficient $10^{-3} \times 3.3$ mm. per minute, while the latter, in spite of its small bore and length, is not inferior in its coefficient ($10^{-3} \times 1.6$) to the case a.

---

* Corrected for change of size of fringes.

There is a further consideration: Like the case of phosphorus above, it is possible that what is at present being measured is the rate of evaporation from a surface. Pieces of thick, wet blotting-paper, 1 cm.² and 3 cm.² in area, were therefore selected as sources of moisture and inclosed between the end of the tube t and the stopper F of figure 4.

The results of figure 8 were obtained in this way, at intervals of about 1 hour apart in a warm, dry room. The attempt to desiccate the volume v of U showed no advantages. As to the observations (both fringe displacement Δs and the slide micrometer Δx being employed), they are remarkably good, with only an occasional lag in the U-tube, which later soon recovers itself. The zero-point was always nicely regained at the end of each experiment, and accidental changes of fringe-breadth were allowed for. The same tube,
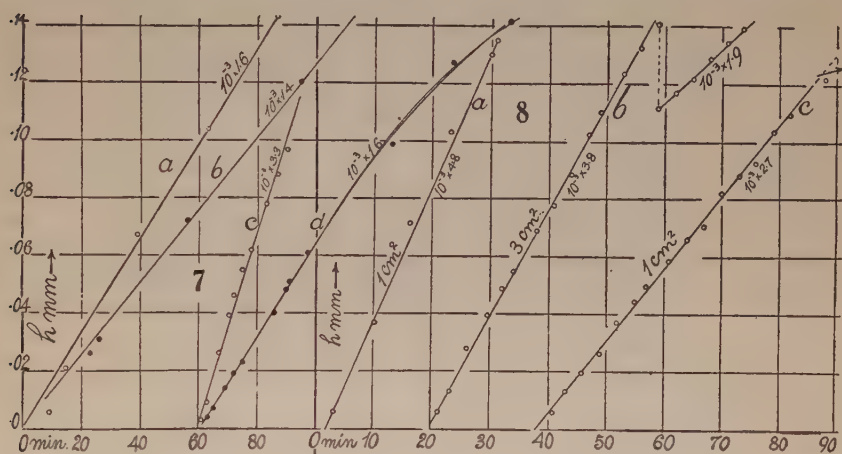
8 cm. long and about 0.4 cm. in diameter ($a=0.13$ cm.²), was used in all cases. The successive rates obtained are thus

Experiment	(a)	(b)	(c)	
Area evaporating	2	6	2	cm.²
$10^5 \times dp/dt$	4.8	3.8	2.7	mm. Hg/min.

From the first and second experiments, it is seen that the area evaporating is of no consequence, for the area 3 times the larger has the smaller coefficient.

In the second and third curves of figure 8, a peculiar feature presents itself. In the former, after 40 minutes, the rate suddenly breaks down to 19×10^{-4}; in the latter after 50 minutes the break is even more pronounced, falling to 6×10^{-4} (data not given). This looks as if the pieces of blotting-paper had become dry; but from the small amount of water evaporated such a result is impossible. Again, if it were a question of vanishing gradient, the evanescence would not occur abruptly, as the observations imply.

One is thus eventually driven to the conclusion that what is being observed is in large measure the result of thermal expansion, inasmuch as the closed region is necessarily an air thermometer, exposed in a room of not rigorously

2

constant temperature. For if we take the largest of the coefficients just obtained, $dp/dt = 5 \times 10^{-3}$ mm./min., and if the **U**-region is the bulb of an air thermometer of constant volume at about 27° C.,

$$(dp/dt)/p = (d\tau/dt)/\tau$$

or,

$$d\tau/dt = \frac{5 \times 10^{-3}}{760} \, 300 = 2 \times 10^{-3\circ} \text{ C./min.}$$

Thus an increase of the mean temperature of the massive apparatus of only about 0.1° C. per hour would suffice to account for the higher results obtained. To this the vapor-pressure increment of the evaporating water further contributes.
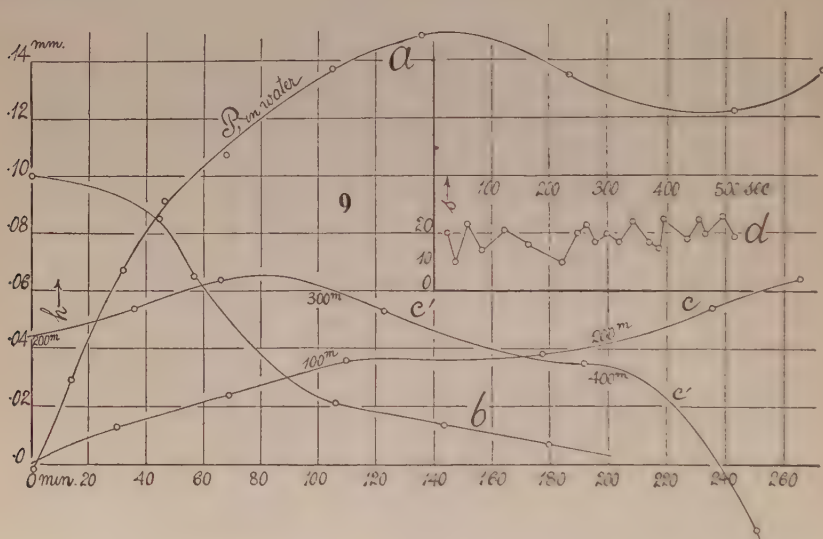
In spite of these discouragements, I made a number of further experiments with the object of capturing a coefficient, actually negative. Small coefficients were rather frequent; but the only negative value obtained is given in figure 9, curve *b*, for the case of a tube 9 cm. long and 0.17 cm. in diameter. The curve is not straight (the usual result), but is such as would be expected in a room slowly cooling, eventually at a decreasing rate. Again, figure 10, the two shanks of the **U**-tube were joined by a short piece of rubber hose which was then closed in the middle with a pinch-cock. But for the almost complete recovery after 420 minutes, the results (fig. 10) would suggest a slight leak in one shank, which was thus not present. On opening the pinch-cock, the zero at once reappeared. Thus the **U**-tube alone makes some contribution to the pressure variations for reasons rather difficult to understand, seeing that the mercury wells are close together in a block of iron.

The pressure decrement in figure 10, where both shanks of the **U**-tube are closed, scarcely exceeds 0.03 mm. The test will be much severer if but

one shank of the tube is closed, the other freely communicating with the atmosphere. Results of this kind, recorded through 450 minutes, are given in figure 9, curves c and c'. These would be in conformity with slowly increasing room temperatures to a maximum at about 300 minutes and a fall thereafter, eventually relatively rapid. In the main, pressure increments exceeding a total of 0.06 mm. of Hg are present. In the same figure (curve a), I have given (by way of contrast) the results observed on joining the same shank to a tube containing phosphorus *submerged* in water. The phosphorus tube must be kept in a water-bath. From this arrangement I anticipated pressure decrements resulting from slow phosphorus oxidation under water. The results (maximum, 0.15 mm. of Hg) reproduced in curve a, however, compare with the largest pressure increments recorded, and the high values, though fluctuating, are sustained for over 270 minutes. The rise is less abrupt than in figures 7 and 8.

When one shank of the **U**-tube is closed, the other being open, atmospheric-pressure variations on a micrometric scale are very well indicated. I have
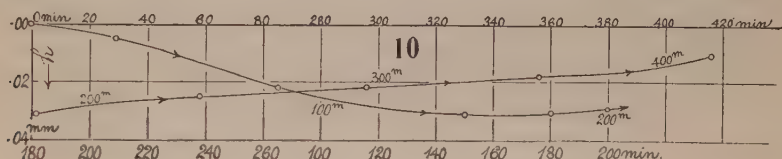
given an example of such cases in the jagged curve d of figure 9, the behavior being followed within 500 seconds. On a windy day these rapid fluctuations of the mercury surface are very marked. In the figure the mean displacement may be taken as within $\Delta s = 10$ scale-parts, or $\Delta p = 0.006$ mm. of mercury. It is not impossible that a micrometric registry of this kind may be of meteorological value.

6. Differential experiments.—In addition to the above work, a number of experiments were made by using the **U**-tube differentially. Thus, figure 11 (inset), a dilute solution of KCl ($\rho = 1.1184$ at 20°) and pure water, were joined respectively to the two shanks of the **U**-tube, the liquids being kept in a water-bath, W. A glass three-way cock, to shut off atmospheric connection, and to separate the KCl chamber from the water chamber, is necessary. I shall give but one example, figure 11, summarizing four successive experiments. It is seen (1) that pressures in the right shank, which happens to be the KCl solution, increase faster; but the rate soon falls off. On exchanging the liquids, (2) pressure still increases faster in the right shank, about at the final rate of the case (1). On again exchanging the tubes (curve 3), the final increase on the right is maintained. The left side was now placed in contact (4) with a small closed P_2O_5 drying-tube in the place of the water (removed). The curve, however, except at the beginning, shows no striking rates, which are throughout inferior to curve (1).

Thus it seems that secondary occurrences, to be associated with temperatures, completely obscure the results looked for, whether of diffusion or vapor-pressure, and that it is only in the summer time, in a non-heated room, that interpretable data can be expected. Meanwhile, the graphs show the extent of annoyances to be guarded against.

7. Summer experiments.—During an interval of steady summer temperature I gave these experiments with pressure increments another trial, using the method indicated in the inset of figure 11. The first test was made with a solution of KCl ($\rho = 1.1184$ at $20°$) compared with water. The results (time t, pressure increment h mm. of mercury),

$$t = 0 \quad 17 \quad 37 \quad 82 \quad 117 \quad 400 \text{ minutes.}$$
$$10^4 h = 0 \quad 15 \quad 20 \quad 15 \quad 15 \quad -25 \text{ mm.}$$
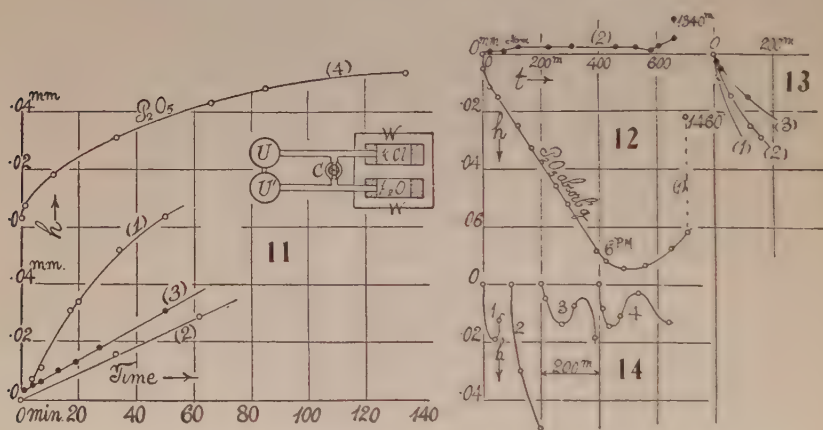
are merely incidental errors. Similarly with a solution of $CaCl_2$ ($\rho = 1.19650$ at $20°$),

$$t = 0 \quad 30 \quad 63 \quad 228 \text{ minutes.}$$
$$10^4 h = 0 \quad 10 \quad 0 \quad -220 \text{ mm.}$$

actually show an apparent excess of pressure over the solution. This can only indicate a temperature difference at the two shanks of the U-gage. It seems to me probable that the walls of the gage in such experiments are soon covered with a film of distilled water and that this contributes the effective equality of vapor-pressure, the surface of solution in the tube being relatively inactive.

These experiments are thus inconclusive. I therefore made a further trial of the water-vapor absorption of P_2O_5, the two tubes containing water and P_2O_5, respectively, being placed as in figure 11. The initial test (graph 1, fig. 12) at first proceeded with vigor; but after 400 minutes' absorption ceased and the reaction is apparently reversed. The tubes were then exchanged. The resulting graph 2 merely shows that water absorption is practically absent. The same was true when the tubes were again exchanged.

The P_2O_5 was therefore replaced by a fresh sample. The graphs 1, 2, 3, figure 13, were now obtained on successive exchanges of the water and P_2O_5 tubes. These graphs are consistent as to absorption, but the reactions are nevertheless so slow and the general run of the curves so complicated with secondary issues and so difficult to interpret, that I abandoned the work as unpromising. In figure 14 a few supplementary results are given with the tubes separated, the water tube being open to the atmosphere. The sinuous curves obtained in the successive changes of tubes show that the temperature discrepancy is prohibitive, even in summer.

Finally I tested the same method (inset, fig. 11) with the U-gage exhausted, comparing H_2O and the $CaCl_2$ solution specified in a vacuum of the vapor-pressure of water. With the cock between the H_2O and $CaCl_2$ tubes open, the fringes were easily found and steady. With influx of air they remained nearly fixed and could be recognized, even through a fog which often formed. On closing the cock between the tubes, however, so that each liquid operated alone, the fringes speedily vanished, too rapidly for control. The method is further objectionable, inasmuch as any slight leak through the glass exhaustion-cocks, etc., would have the same effect. It was therefore not pursued further because of its difficulty. It required four successive exhaustions subsequently to free the gage of the water-vapor which had filtered in between the mercury and the solid parts of the gage, large bubbles forming under the glass plate.

CHAPTER II.

PRESSURES IN CONNECTION WITH SURFACE TENSION.

Soap, Glue, and Sugar Bubbles.

8. The pressure within a soap-bubble.—If both surfaces of the bubble cooperate, this pressure (p) is written $p=4T/r$, where T is the surface tension and r the radius of the bubble. The ease with which p may now be measured by the interferometer **U**-gage suggests a number of observations. One may ask, for instance, whether both surfaces cooperate with unimpaired strength until the bubble bursts from excessive thinness; whether T increases or decreases as the result of concentration of the film during evaporation; or the value of T in modified soap solutions may be read off, etc. If the quadratic interferometer is used with plates at an angle $i=45°$, for reading the displacement Δh of the free surface of the mercury in the **U**-gage, we may write as above

$$T=(\rho gr\cos i/4)c\Delta s$$

where Δn is the number of fringes of wave-length λ passing, and Δx the displacement of the slide micrometer, at an angle equivalent to i, the screw being normal to the displaced mirror. Hence

$$4T/r=\rho g\cos i\cdot\Delta x=(\rho g\lambda/2)\Delta n$$

or

$$T=(\rho gr\cos i/4)\Delta x=(\rho g\lambda/8)\Delta n$$

If the ocular micrometer is used, a trial measurement would give $\Delta x=c\Delta s$ cm., where c is the value of Δx corresponding to one ocular scale-part (0.01 cm.), so that finally

$$T=(\rho gr\cos i/4)c\Delta s$$

The apparatus used is simple, consisting of a bent glass tube $tt't''$, figure 15, about 5 or 7 mm. in diameter, from one end t'' of which, the soap-bubble B is blown. The other end t communicates with one shank of the **U**-gage U, closed by glass plates G, g being the floating plate. The other shank of the gage is in free communication with the air. One of the interferometer beams is shown at b. Pressure is applied at p, the air being blown in through a cotton wad or a capillary tube to avoid excessive vibration (relatively speaking) of the mercury. When
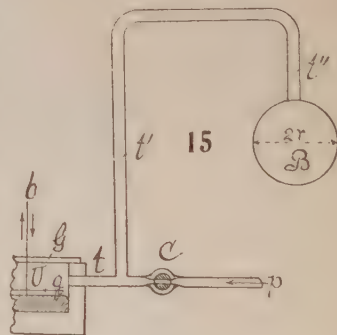
the requisite size of bubble is obtained, the cock C is closed and the displacement of fringes read off. The difficult measurement in relation to the equation

12

is the diameter ($2r$) of the bubble. In the present experiments I contented myself with a projection against a white centimeter scale closely behind the bubble. This is a rough method, but it suffices for the present tentative purposes.

9. Observations.—The micrometer test showed $\Delta x = 1.07 \times 10^{-4} \Delta s$ cm. (in later work 1.03×10^{-4}, or $\Delta h = 7.3 \times 10^{-5} \Delta s$ cm.), so that $\Delta h = 7.6 \times 10^{-5} \Delta s$ cm., $\imath$ being 45°. The results taken in succession were ($T = 0.24 r \Delta s$, etc.)

$2r =$	9	7	9	6.5	4.5	3.0	4.2	2.5	3.0	6.0	cm.
$\Delta s =$	25	30	25	33	50	70	50	85	74	37	s. p.
$10^3 \Delta p =$	19	23	19	25	36	51	36	62	54	27	mm. Hg.
$T =$	28	27	28	27	27	25	26	26	27	27	dyne/cm.

The irregularity here may be due to the r measurement, which is necessarily inadequate and too large; but the different samples need not be identical. The soap mixture was a commercial solution adapted for blowing persistent bubbles; nevertheless the order of value found for T is surprisingly small. Data of the same value were also obtained from fringes only. The pressure seemed to be sustained until the bubble burst, when the fringes fell back to zero. Changes of pressure resulting from deformations of the bubble were easily shown.

In later experiments better results for r were obtained by the shadow of the soap-bubble as cast by a distant electric lamp, on a white centimeter scale. The fringes were somewhat large, $\Delta h = 8.9 \times 10^{-5} \Delta s$ mm., $T = 0.21 r \Delta s$. I found—

$2r =$	3.0	3.0	5.0	5.0	cm.
$\Delta s =$	80	80	50	50	s. p.
$10^3 \Delta p =$	71	71	44	44	mm. Hg.
$T =$	25	25	26	26	dynes/cm.

Here a definite increase of Δx was registered while the bubble slowly dried out to the bursting-point, the increase of T being 6 to 10 per cent. Though the soap-bubble is the bulb of an air thermometer, and slight changes of temperature produce passing fluctuations of fringe positions, on the whole the registry is good, as r accommodates itself to the pressures.

Common commercial soap solution, not intended for soap-bubble experiments, was also tried. The bubbles here burst much more rapidly and bubbles larger than about 4 cm. could not be obtained comformably with quiet fringes. The results were (the preceding fringes being used, $T = 0.210 r \Delta s$):

$2r =$	4.5	3.0	4.0	4.0	3.0	cm.
$\Delta s =$	67	100	75	73	100	s. p.
$10^3 \Delta p =$	60	89	67	65	89	mm. Hg.
$T =$	31.7	31.5	31.5	30.7	31.5	dynes/cm.

Thus the tension is definitely larger here, there being no extra ingredients.

A small quantity of liquid glue was added to this soap solution, the mixture thoroughly shaken up, and tested the next day. Bubbles were now much more persistent, and they shrank to an iridescent viscid soap-glue film (with evaporation of water), which gradually crumpled up. The mean surface tension

found was $T=25$ dynes/cm., so that the T had decreased by the admixture of the glue. It also slightly increased at first on evaporation to about 6 per cent, after which, with the crumpling of the film, T decreased relatively fast but regularly (while the bubble shrank) to about one-third of its original value (not allowing for the r). Here the viscid bubble usually broke and the fringes fell back to zero. The occurrence of a much reduced size of viscid bubble with temporarily stationary but relatively small surface tension may be regarded as evidence in favor of Kelvin's suggestion, viz, that the film puckers to accommodate the energy-content in view of diminished surface tension. Probably in shrinking with deformation, the bubble becomes fissured and springs little leaks, but in such a way that pressure diminishes gradually and regularly. Diffusion would be a slower occurrence. With a broken bubble the fringes instantly fall to zero.

Diluting the glue-soap solution to one-half, the bubbles usually burst; but occasionally one would be captured which shrank, being pervious, in the manner just described.

A variety of further experiments were made with the glycerine-soap solution, using greater care in the measurement of $2r$ (shadow); but not much improvement was observed in the data, probably, I think, because the colloidal structure or phase mixture of successive bubbles is not exactly the same. Taking the means of about 5 observations for each diameter $2r$, the results were (internal pressures decreasing from about 0.015 to 0.0016 mm. of Hg):

$$2r = 1.16 \quad 2.0 \quad 4.9 \quad 7.0 \quad 8.8 \quad 10.4 \quad \text{cm.}$$
$$10^8\Delta h = 15 \quad \cdots \quad \cdots \quad \cdots \quad \cdots \quad 1.6 \quad \text{mm. Hg.}$$
$$T = 28.7 \quad 29.6 \quad 29.3 \quad 29.8 \quad 32.7 \quad 31.8 \quad \text{dynes/cm.}$$

so that T (fig. 16) seems to increase about $\Delta T = 0.4$ per centimeter of increase of the diameter of the bubble. In the same way, T here increased slightly at all diameters, just before the bubbles burst. This would be in keeping with the enormously greater effect observed with glue-bubbles in the next paragraph.

Some time after, the contrasting behavior of common liquid soap and the soap mixture prepared for bubbles was taken up again. The common soap in its T values, for example,

$$T = 32.7 \quad 31.7 \quad 32.7 \quad 32.7 \quad 32.4 \quad \text{mean } 32.4,$$

was usually very constant; but the bubbles lasted only 10 or 20 seconds, not long enough to detect variations. With the prepared mixture, however, the life of 2-cm. bubbles was at times nearly 10 minutes. During this time the drop at the bottom was gradually absorbed, the film showing continual agitation in these parts, while T regularly increased. The following is a good example observed up to the bursting-point.

$$\text{Time} = 0^m \quad 8^m$$
$$T = 27.7 \quad 31.7$$

When the bubble burst, therefore, its T was nearly that of the common soap solution. The lowest value obtained in a number of experiments was 27, the rate of increase dT/dt being 0.5 per minute. Thus, the effect of concen-

tration during evaporation, though not nearly so marked, resembles the behavior of the glue-bubbles below. Other persistent soap mixtures were tried and give about the same rate. For instance, after adding glycerine to the liquid soap aboye, T changed from 28.4 to 30.8 in 5 minutes; in another case from 30.3 to 32.4 in 3 minutes, the rates dT/dt being thus 0.5 to 0.7 per minute. Similarly in a glue soap, T increased from 27 to 28.4 in 4 minutes; again from 27 to 28.9 in 3 minutes. The rates dT/dt are thus 0.4 to 0.6 per minute.

The rate is slower if a drop is at the bottom of the bubble, and faster as the drop vanishes. After this the bubble bursts. Thus

0^m	29	0^m	28	0^m	28
3	32	9	31	1.5	29
		12	33	2	30

the second sample holding a large drop, the colors throughout being in agitated motion. With increasing T operating on a film gradually growing thinner, conditions favorable to bursting increase (*cf.* celluloid bubbles, below).

10. Glue-bubbles.—Common liquid glue was dissolved in 5 to 10 parts of distilled water, thoroughly warmed, shaken, and allowed to stand for a day or more. The bubbles obtainable in this way rarely exceed 2 cm. in diameter and most of them break before the measurements of $2r$ and Δh can be completed. The work, therefore, is an exercise of patience, for only occasionally a result is obtained. Still more rarely (I succeeded only twice in many hundred trials), a bubble is obtained which actually solidifies to a film of gelatine, highly iridescent and lasting indefinitely.

Samples of dilute glue are apt to vary widely in T. Thus, for instance, $2r=2$ cm., $T=32$; $2r=1.5$ cm., $T=43$ were obtained from short-lived bubbles of the same solution. Longer-lived bubbles suggest the reason for this variability. In the case of bubbles bursting after 2 minutes, the data were:

Persistence:	0	1	2 min.	
T	28.3	39.7	34.1	First case.
T	30.4	36.9	49.9	Second case.

In the first example T passes through a maximum before the bubble bursts; in the second, T has enormously increased and is apparently still growing.

But the full exhibition of these phenomena was not reached until one of the bubbles, $2r=1.7$ cm., actually dried to a solid iridescent spherical film of glue. The drop at the bottom of the bubble, in this case, evaporated very slowly, but without marked distortion of the shape of the bubble. When dry and detached it was quite flexible and robust but sticky, the folds easily cohering.

Table I and figure 17 (1), give a full account of the observations made in the lapse of about 4.5 hours, after which the internal pressure excess had nearly vanished. It will be seen that there were successive stages marked a, b, c, d, e in the graph at which the pressure was temporarily stationary. The successive intervals of stability decreased, and the one at d was very short, prior to the persistent stage e. One would be inclined to infer that these

stages represent successive phases or types of colloid, each with its appropriate T. But it is obvious from the mottled color-fields on the bubbles that at each stage a large number of phases must contribute to the temporary equilibrium. At f, at the limit, the colloid is probably solid. Thereafter the nearly regular decrease of T between 20 and 265 minutes is merely apparent, and to be ascribed to the continued diffusion of air outward, from within the thin solid sphere at a pressure excess, into the atmosphere. The water has first largely evaporated and the air follows after, probably along the same channels between the colloidal molecules.

In the preceding case the surface tension of the phase conglomerate a ($T=30$) has nearly doubled ($T=57$) in the phase e. In the present experiment, figure 17(2), the initial surface tension ($T=35$) is more than doubled

TABLE I.—*Dilute glue-bubbles evaporating to the solid state.*

Bubble.	Time.	$10^3\Delta h$	T	Bubble.	Time.	$10^3\Delta h$	T
	min.	cm. Hg			min.	cm. Hg	
Sphere	0	12.7	29.8	Sphere	0	10.6	35.2
$2r = 1.7$ cm.	2	11.2	31.5	$2r = 2.0$ cm	1	11.3	37.4
	4	11.9	33.4	becoming	2	13.3	44.2
	6	12.5	35.3	pear-shaped	5	25.2	83.4
	8	20.4	57.3	1.7 × 2.0 cm.	10	25.2	83.4
	20	20.4	57.3		12	24.5	81.1
	35	17.3	48.7		15	24.1	79.9
	40	16.7	47.0		21	22.6	74.7
	45	16.1	45.4		95	11.7	38.8
	65	13.3	37.4		150	.5	1.7
	75	12.3	34.5				
	80	10.6	29.8				
	110	7.9	22.3				
	140	5.0	14.3				
	165	1.3	3.5				

($T=83$) in the persistent phase. Here, however, the drop at the bottom of the bubble later expanded on its own account, so that the solid bubble was symmetrically pear-shaped, while the top diameter in the final distortion shrank from about $2r=2$ to $2r=1.7$. The data are thus complicated by change of form. Moreover, the phenomenon ran through its cycle from the minimum at a' to the maximum at b', much more rapidly, so that only these two temporary stages could be recognized. Here and in the preceding experiment, however, there may be phase equilibria antedating the first observation; for it takes some time to set the fringes with the slide micrometer and to measure the diameter $2r$. Beyond c' the phenomenon is the same as before, indicating diffusion of air outward through the solidifying film. In the present case the diffusion after everything is dry is apparently accelerated; but this is probably thermal discrepancy.

Between e and f or b' and c', the film is still liquid and contractile and the values of T obtained are probably true surface tensions. Beyond f or c' the film is less and less contractile and the values of T cease to have a meaning.

One can not argue, therefore, that T has been measured quite into the solid state; but it has been measured as far as a highly viscous, but still liquid, film of glue.*

Promiscuous work with the glue-bubbles led to no further striking results. I shall therefore give mean values. Four experiments with the original solution, after long standing, showed ($2r=2.1$ cm.) $T=25$; warming and shaking the solution, $T=26.8$. Two drops of soap solution were now added to 10 c. c. of the glue. The mean results with small bubbles ($2r=2.2$) were $T=27$; with four large bubbles ($2r=4.4$ cm.), $T=28.7$. These differences are merely incidental, the glue-soap mixture being perhaps more expansible.

Again, a drop of caustic soda in solution was added to the original gelatine. Three tests gave ($2r=2.3$ cm.) $T=26.8$. The alkaline glue solution was then diluted over one-half, an advantageous procedure, for large persistent bubbles were now very easily obtained. The mean result of six tests ($2r=4.7$ cm.) was $T=28.2$. The latter solution, further diluted to more than one-half, was

TABLE 2.

Successive dilution.	$2r$	T	Remarks.
1/8	4.2	29	
1/16	4.8	28	Colors not striking, just before breaking.
1/32	4.3	30	Colors absent, nearly.
1/64	4.1	41	No color.
1/128	4.2	53	Do.
1/256	2.7	55–62	Very variable in T.

found to be equally available, 3 large bubbles ($2r=4.7$) giving $T=29.1$. At this stage the usually promiscuous grouping of drifting interference colors began to conform to well-developed broad, horizontal color-bands, still in motion, however. In fact, surging, broad color-patches, which keep moving till the bubble bursts, are the noteworthy feature of these glue-bubbles. It is indicative, of course, of the high degree of heterogeneity, which has not been eliminated even in these excessively thin films. In a further dilution to over one-half, the bubble became more fragile. Incidentally T had decreased, the mean of four cases being ($2r=4.6$ cm.) $T=26.8$. All this is still far remote from the T of pure water. After allowing the last solution to stand for some time, the following mean results (4 to 5 tests each) were obtained for successive further dilutions (table 2).

Thus (fig. 18) T shows no tendency to increase, except in the last three cases. Nevertheless, the bubbles had been continually growing more fragile. Interference colors are quite absent when the marked increase of T begins, as the relatively thick bubbles only can withstand the rapidly increasing capillary stress. In the last solution, the original liquid glue was diluted nearly

---

* From another point of view, the arrest at e and b', respectively, may be regarded as evidences of incipient solidification, so that the growth of T ceases.

1.500 times and the T found was very variable, jumping from bubble to bubble, between 55 and 62. The colloidal content is thus irregularly distributed. It should be noted that whenever T is large, it is also very variable in one and the same bubble, decreasing rapidly till the bubble bursts. The decrease occurs so rapidly that a contamination of the surface seems unlikely though this may be among the reasons. I am inclined to think that a redistribution of phases involving expenditure of potential energy is more probable. Colloidal molecules are being marshaled on the surface.
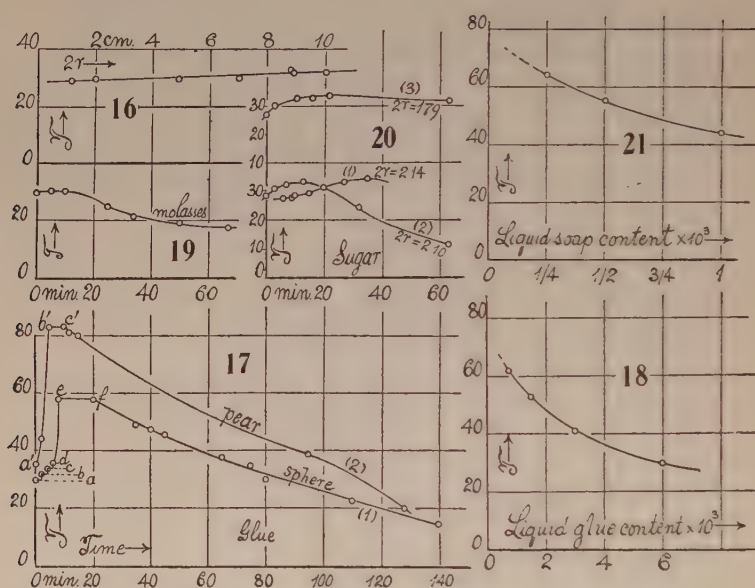
11. Molasses.—Bubbles of diluted molasses are far more difficult to obtain without admixtures than glue-bubbles. I captured but one of the requisite persistence; but this gradually shrank from a diameter of 1 cm. to 0.9 cm., and after 70 minutes it had become distorted to a viscid pendant. Being a viscous liquid, the values of T are probably trustworthy, apart from the changes of form. The mean diameter of the bubble was 0.90 cm. and the data for T, as given in figure 19, were:

Time	....	0	5	9	25	34	50	67 minutes.
T	....	30	31	30	25	21	19	17

The spherical form persisted at least 50 minutes; but at 67 minutes the bubble had become bean-shaped, the drop at the bottom remaining. After 9 minutes, the loss of internal pressure from diffusion of air outward is in excess of any further increase of T, owing to concentration by evaporation.

12. Sugar.—With sugar solutions (0.1 gram per cm.^{3} of water) I was unable to secure any adequately persistent bubbles, after many trials. If,

however, 1 or 2 drops of common soap solution are added to 10 c. c. of the 10 per cent sugar solution and the mixture thoroughly stirred, bubbles at least as large as 2 cm. are easily obtained. Many of them survive through a number of observations and some actually pass into the solid state. Smooth, iridescent bubbles of solid sugar were in fact detachable, having lasted under pressure one or more hours. Success is usually assured when the solutions are freshly put together. After standing a day they are liable to become turbid and the bubbles burst. Additions of 1 or 2 drops of fresh soap solution, however, is apt to clarify the mixture and restore its usefulness. A drop of dilute caustic alkali (NaOH) has the same effect. Curiously enough, neither from the soap solution nor from the sugar solution can adequately persistent bubbles be obtained. The advantages of adding sugar to soap solutions is of course well known; but what I here wish to accentuate is the profound effect on T of a mere trace of soap. But this, too, is not out of keeping with the nature of T.

In the first experiment, figure 20(1), the zero of fringes was accidentally shifted and the absolute data may be slightly displaced. The relations, however, are trustworthy, and they indicate a marked increase of T during the first half hour. After about 40 minutes the pressure was removed, whereupon the bubble shrank in its lower half (drop). The attempt to blow it out again broke it. This bubble, like all the rest, was vividly colored in bands parallel to the equator. The next experiment, figure 20(2), proceeded satisfactorily. There was no appreciable change of diameter $2r=2.10$ cm. After about 2 hours the solid bubble broke off under the pressure. The film, smooth (without puckering) and iridescent, remained so indefinitely (days) thereafter. As the curve shows, T rose regularly from 28.7 to 33.6, after which the leakage from diffusion of air outward supervenes. Next day the solution had become turbid and persistent bubbles were not obtainable. The addition of 2 drops of soap solution restored it and the data, figure 20(3), were thus obtained. The maximum, $T=33.6$, happens to be the same as before; but the final apparent decrease of T does not occur (temperature discrepancies). After the observations of figure 20(3), the following were successively taken:

Time	85	112	153 minutes.
T	..........28.9	31.2	31.5

which probably indicate thermal fluctuations. This bubble shrank somewhat in drying to the solid state. With another fresh solution the results

Time	 0	3	6 minutes.
T	..........29.6	31.5	31.5

are of the same nature. In a great variety of individual experiments (10 cases), with similar solutions, initial values of T from 26 to 29 were obtained, the mean value being $T=27.9$.

The endeavor was now made to obtain bubbles of sugar solution by adding 2 drops of caustic-soda solution, but none persisted. On supplying 2 drops of soap solution, however, bubbles were again obtained, but in this case they

remained colorless and lasted only a few minutes. The following examples may be given:

$$2r = 2.10 \quad 2.05 \quad 2.20 \quad 2.10 \quad 2.05 \text{ cm.}$$
$$T = 36.2 \quad 37.1 \quad 37.1 \quad 38.8 \quad 36.7$$

Thus the surface tension in these thick bubbles has been increased in marked degree. It was, moreover, found to decrease in the same bubble ($\Delta T = -0.0012$ per minute being observed) in the lapse of time; but the bubble did not last long enough for adequate tests.

Tried again next day (means of three observations each), the data were $T = 35.6$; with 2 more drops of soap solution, $T = 34.1$; with further 2 drops of soap solution, $T = 34.1$; with 2 more drops of NaOH solution, $T = 34.2$. The bubbles remained relatively brittle and colorless. Finally, diluting the solution one-half, the mean results were $T = 35.8$; with 2 drops of soap, $T = 35.4$. Thus throughout all these modifications, the solution retained about the same high T, with bubbles that throughout were clear, thick, and of slight persistence, as compared with the same solutions (approximately) above.

To meet this dilemma fresh sugar solutions were taken and tested with 2 drops of soap solution. It was astonishing to find that T had increased further in all of the 7 tests made, to over $T = 40$. Moreover, T fell at first and later usually rose again. Thus, for example:

$$\text{Time} \ \ldots\ldots\ 0 \qquad 2 \qquad 4 \quad \text{minutes.}$$
$$T \ \ldots\ldots\ldots 43.5 \qquad 38.8 \qquad 41.4$$

The bubbles ($2r = 2.1$) were uniformly thick, colorless, short-lived, and T a continually variable quantity.

This experiment suggested that probably the soap solution, kept in a covered glass and remaining perfectly clear, was nevertheless continually undergoing change owing to exposure to the air. Fresh soap solution from a supply in a stoppered bottle was therefore taken and two drops of it added to fresh 10 c. c. of the sugar solution. The result was immediately decisive and the highly colored bubbles with low T were again obtained. For example:

TABLE 3.

$2r$	Time	T
cm.	min.	
2.21	......	28.7
1.95	3	23.3
	6	25.6
2.30	1	30.1
	2	27.5
	3	24.9
	4	26.3
etc.		

Notwithstanding the occasional occurrence of solid-sugar bubbles, it thus seems as if the sugar had very little to do with the T values, these being determined in the above tests by the 2 or 3 drops of progressively changing

soap solution. To test this, 2 drops of soap solution were added to 10 c. c. of distilled water, care having been taken to clean all apparatus until distilled water itself produced no results. The bubbles obtained with these dilute mixtures were naturally short-lived, bursting within a minute or two. The surface tensions in 10 successive tests, though consistent in a single test, were very variable, ranging from $T=35$ to $T=50$. The feature throughout was the marked and rapid decrease of T, for the same bubble, within a minute of its life. For example, with bubbles each $2r=1.1$ cm., the T values successively obtained were

42.1	42.1	49.8	36.9	43.9	46.5
39.2	29.5	44.6	31.7	41.4	42.5
36.9	34.8	...	29.1	...	...

The bubbles were all thick and colorless. Some of them could be blown to a diameter of even 4 cm., but they burst before any color appeared.

The interesting question paralleling the above experience with glue solutions may now be asked, as to the degree of approach to the surface tension of pure water which may be reached by successively diluting soap solutions. Mixtures were therefore prepared of 10 c. c. distilled water with 1 drop of soap solution. Estimating the drop as less than 0.01 c. c., the dilution of the solution is greater than 0.001. The first of these gave the values

10 c. c. $H_2O + 1$ drop: $2r = $ 2.2 2.1 2.2 1.9 cm.
$T = $ 36 36 31 31

which are unexpectedly low. The tube and other parts were therefore further cleansed and a fresh solution prepared showing (successive values of T)

10 c. c. $H_2O + 1$ drop: $2r = $ 2.0 1.90 2.00 2.10 cm.
$T = $ 41 39 48 48
36 37 45 43

which is an improvement. The bubbles last less than a minute, and during this time T regularly falls. The solution was now diluted one-half, giving

10 c. c. $H_2O + 0.5$ drop: $2r = $ 1.90 1.90 2.20 1.90 1.80 cm.
$T = $ 52 59 60 54 58
50 54 58 50 56

T decreasing as usual. The preceding solution on further dilution to one-half gave

10 c. c. $H_2O + 0.25$ drop: $2r = $ 1.90 1.80 1.80 cm.
$T = $ 63 64 66
61 63

A final dilution to one-half was also tried, but the bubbles were now too short-lived for one observer to manipulate. One bubble was caught showing about $T=62$. This was a late and low value. With two observers there would have been no difficulty, but the experiment similarly made in §10 with glue is much less trying.

The mean data, viz, 1 drop, $T=44$; 0.5 drop, $T=55$; 0.25 drop, $T=64$, have been constructed in figure 21. A linear extrapolation for pure water would make T somewhere near 70; a quadratic extrapolation nearer 80. Since

T decreases rapidly, since it takes time to blow the bubble and set the fringes with the slide micrometer, even the first T observed is itself probably low. At all events, the data are in good accord with the surface tension of a clean surface of water.

As to the cause of the rapid decline of T after the bubble is blown, two reasons may be adduced. In the first place, the outer surface, at least in contact with air, becomes contaminated, or again, colloidal matter within the bubble may accumulate at the surface. In the second place, we may suppose the forces embodied in T act not merely at the surface of the film, but throughout its cross-section. Hence if this cross-section decreases in thickness from evaporation, the thinning of the walls is expressed in a continued reduction of T. The water-bubbles are throughout colorless; but if with continued addition of soap solution one eventually reaches the iridescent stage of film, one should expect the least values of T (such as found) to accompany the thinnest bubbles.
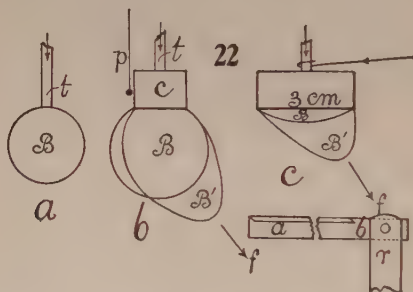
13. Charged bubbles. Sparkless sparks.—The initial experiments, in which the bubble was charged by a micrometer screw electrophorus, showed no appreciable fringe displacement for the available potentials. It was necessary to use a small Wimshurst machine to electrify the bubbles. The first of these were blown from a 0.25-inch tube t, figure $22a$; but on charging they were too easily pulled off the tube along the lines of force. A similarly charged plate below and a drop at the bottom of the bubble to weight it down, however, were the means of obtaining a few preliminary results. The internal pressure of the uncharged bubble, 10^{-3} 6.4 cm. Hg, fell to 10^{-3} 5.5 cm., developing a difference of $p=9\times10^{-4}$ cm. Hg before the bubble was torn off. Since for the potential V the charge is $Q=rV$, where $r=2$ cm. is the radius of the bubble,

$$p=2\pi(Q/4\pi r^2)^2=V^2/8\pi r^2 \quad \text{or} \quad V=r\sqrt{8\pi p}$$

Thus

$$V=2\sqrt{25.1\times9\times10^{-4}\times13.6\times981}=35 \text{ electrost. units or } 10{,}500 \text{ volts}$$

nearly. Very high potentials are therefore needed even in these simple performances.

The purpose of the experiments, however, is the nearly complete removal of internal pressure and with this in view the device, figure $22b$, with a cylin-

drical funnel tc and therefore a larger base of attachment, was adopted. The bubbles are now no longer spherical, at least when charged. A pith ball p may be added to indicate the rise or drop of potential. The cylinder c was about 3 cm. in diameter and 1.5 cm. deep. Larger sizes up to 6 cm. were also tried, and abandoned, as it would have been much less easy to produce the large number of films needed. The effect of gradually charging the exposed bubble B is to draw it out into a blunt spindle B' along the incidental lines of force f, to a maximum of distortion; at a definite potential, however, the stretched bubble suddenly, almost spasmodically, returns to the form B, usually with vigorous quivering, right and left. B' may even touch objects and be discharged; but frequently the bubble parts at an unstable constriction and the end flies off. The aerial discharges take place in free air and at each such discharge the repelled pith ball falls back slightly toward the vertical. The discharges from the bubble, in spite of the violent jerking, are thus only partial, just noticeable with the pith ball and probably within 10 per cent. At the same time the reduced pressure rises. Potential must be increased very gradually coincidently with the slow expansion. This means, therefore, that at each jerk some of the lines of force f break loose with an outrush of ions from the film. The phenomenon is very interesting, as it takes place without any light effect even in the dark, so far as I could observe, and without noise. Such a result, when occurring with metal electrodes, is usually estimated as equivalent to an electrical pressure of $p = 2\pi\sigma^2 = 68$ dynes/cm.^{2} The forces are thus of the same order as those depending on the surface tensions $T = 30$ dynes/cm. It may, therefore, be anticipated that they will be observable together.

With the larger part of the bubble B outside, as in figure 22b, the experiment is short-lived, as the bubble soon parts and the pressure within can not be wholly removed. To accomplish this, only a small segment of the bubble must protrude, as in figure 22c. The radius of such bubbles may be estimated as 4 to 3 cm., for a depth of the protruding part of 0.6 to 1 cm. These bubbles are also drawn out along the lines f, to return with a jerk, and the experiment may now be repeated 10 to 50 times before the bubble breaks. During the earlier spasms all superfluous water is thrown off, so that at the end the film is very even throughout, more actively stimulated, and requiring higher potentials to contend with the effective surface tensions. At first there is perhaps little more than a flutter.

Using the small Wimshurst machine, giving a spark within 1 cm., the run of pressure in a large number of experiments was typically as follows:

Discharged	$10^3p = 4.9$	4.9	4.9 cm. Hg.
Charged	$10^3p = 1.4$	1.4	1.0
Kept charged.....	$10^3p = 3.5$	3.5	3.5 etc.

the same bubble being successively discharged at the poles of the machine and then gradually charged again. Pressure here falls off to a minimum; but on further continued play of the machine this rises as if the potential were being dropped by brush discharge or other increasing leakage of ions. The potential

3

was scarcely sufficient to remove all pressure, nor to reach the jerking stage. Frequently the T of the uncharged bubble regularly increased by this successive charging and discharging, as, for instance,

Discharged ..... $10^3p =$	4.9	5.2	5.4	5.5	5.5	5.6 cm. Hg.
Charged .... $10^3p =$	1.7	1.7	1.7	1.7	1.7	1.4
Kept charged.... $10^3p =$	2.8	2.8	2.1	2.8	2.8	2.8

Common soap solution behaved similarly, except that but 1 or 2 discharges were possible before the bubble burst, and the pressure could not be so fully reduced; thus, uncharged $p \times 10^8 = 5.6$; charged $10^3p = 2.1$; later $10^3p = 3.5$.

The charge here was negative, the positive pole being put to earth. The latter pole was less efficient as a charger and there was no rise in pressure in time; thus, uncharged $p \times 10^3 = 4.9$; charged, $p \times 10^3 = 3.5$ (minimum permanent).

The above peculiar minima may of course be attributed to the bubble, its T changing under electrification; but they are more probably to be ascribed to the machine. So also the inferior efficiency of positive charge is more liable to be a defect of the machine. To elucidate this point, a large Holtz machine was installed, operating on a holder of the form figure 22c. With common soap solution pressures were brought down from 4.9×10^{-8} to 0.7×10^{-8} cm. Hg. Drops being shed in the earlier flutters, the bubble after the final violent oscillation soon broke, however carefully and slowly the potential was increased.

With the prepared soap solution, the whole of the internal pressure of the uncharged bubble, if low enough, was easily removed, on very slow rotation of the machine, and the resultant pressure even became negative; as for example, uncharged $p \times 10^3 =$ below 4; charged $p \times 10^3 = 0$; later $p \times 10^3 = -0.7$ cm. Hg. There was now no minimum p with subsequent recovery. The pressure, even below $p = 0$, could be maintained indefinitely by very slowly rotating the machine. It was not always possible, however, to bring the internal pressure down to zero. Selecting a few cases (fig. 22c), the run in successive shallow bubbles was

Uncharged .... $10^3p =$	5.1	5.2	4.7	4.9	4.9 etc. cm. Hg.
Charged .... $10^3p =$	1.7–1.6	1.4–1.0	0.7	1.0–0.7	0.7–0.5

the charged bubble jerking continually with but slight change of pressure or voltage. Large bubbles were liable to break apart prematurely with differences less striking, as for instance,

Charged .... $10^3p =$	4.1	4.2	3.0 etc. cm. Hg.
Uncharged ..... $10^3p =$	2.1–1.8	2.1–1.8	1.4

The differences in the first instance were on the average about $10^3\Delta p = 4.0$ cm. of mercury. With the machine at rest, p slowly rose, owing to the leakage. Both poles behaved alike. Discharge effects in pressure and potential, produced by the jerks as above, were slight when compared with those produced at the poles of the machine.

The correctness of the theory of partial discharge may be proved by an aluminum electroscope (*abr*, fig. 22c) below the bubble. The electroscope

consists of a horizontal hacksaw blade against which a very thin (0.03 mm.) elastic strip of aluminum foil *ab*, 8 inches long, is appressed, both being carried by the hard-rubber stem *r*. To give the strip *ab* rigidity, it is bent at right angles throughout its length, except at the end *b*, where the flexure is to take place when the strip is charged and diverges from the saw-blade. This simple contrivance works admirably; the slightest spasm of the bubble *B′* communicates an increment of potential and increases the divergence to a final maximum. Meanwhile the pith ball *p* only just changes its obliquity to the vertical at the successive jerks. The amount of outrush or intermittent current thus depends on the supply of removable ions at the outer surface of the soap-bubble. Possibly a skin layer of molecules free from surface tension (T counterbalanced by $2\pi\sigma^2$) strips off bodily, seeing that $2\pi\sigma^2$ like electric charge can reside only on the surface molecules. On the same plan all drops, etc., are removed at the beginning. Successive molecular layers thus exfoliate till the bubble breaks.*

Owing to the distortion of the bubble, computations are not easily possible. As the form *B′* (fig. 22c) becomes more spindle-shaped, the surface density at the blunt point rapidly increases. It is here, therefore, that the inward components of the surface tensions are first balanced by the rigorously superficial outward electric pressures. At the beginning, when there is a drop, etc., at the bottom of the bubble, the excess of moisture is shed at once and the pressure reductions needed are below 25 dynes per square centimeter. Later, when the bubble has become very even and thin, pressure reductions (as instanced above) of the value of 55 dynes per square centimeter are registered at each exfoliation. It is here, therefore, that the surface tensions proper compete with the electric pressures. Hence the surface molecules slide off with much greater difficulty at the end of the experiment. If the pressure needed to produce a spark be estimated at 68 dynes/cm.², the lines of force might seem to break off to this extent with greater ease of slip from a liquid than from a solid surface; but from the variable curvature of the bubble the inference is not warranted. The difference only of internal and external pressures is constant throughout and is observed.

OIL BUBBLES.

14. Oil and rubber surface tensions.—Sweet oil was first tested; but the bubbles producible, 1 to 2 cm. in diameter, broke at once. No value of T (single observer) could be obtained after many trials. A drop of soda solution, warming, etc., rather made the behavior worse. Drops or small quantities of liquid soap were also unavailing; but on adding a larger quantity of soap solution (10 to 20 per cent) and shaking, opaque bubbles were easily obtained from the emulsion, with surface tensions $T = 25, 28, 27, 29, 26$, etc. Another

---

* This type of exfoliation has recently been discussed by Sir W. H. Bragg (Nature, Feb. 21, 1925) in relation to the work of Perrin and of Wells, with evidence given by X-ray investigation.

emulsion behaved similarly, showing mean $T=26$. The oil was not present as a merely neutral body, however, for a reduction of T from the normal value 32 is in evidence. The white bubbles, originally opaque, cleared to films decorated with white patches, during which time T decreased markedly; for instance, in a later experiment after heating, originally, $T=29.6$; just before bursting, $T=23.7$; another trial giving the same result.

The behavior of paraffine (vacuum) oil, both alone and with admixtures of small quantities of soap solution, was the same. With larger admixtures of liquid soap, the oil in emulsion behaved rather more like a neutral body than sweet oil. Bubbles over 5 cm. in diameter were easily produced and the surface tensions obtained from the opaque bubbles had a mean value $T=30$. On standing (days) the emulsion separated into clear oil below and a long column of pasty emulsion above. From this after weeks of standing a short layer of clear soap solution appeared on top.

The question now arises whether the phenomenal reduction of the T of pure water by addition of soap solution is an isolated case, or whether something similar can be done with oil on addition of another suitable colloid. Pure rubber (not vulcanized) was therefore dissolved in the paraffine (vacuum) oil by heating and digestion, the oil becoming distinctly more viscid. Bubbles were now easily produced even over 2 cm. in diameter and lasting 1 or 2 minutes. Good values of surface tension were thus obtainable, viz ($2r=2$ cm. throughout), $T=30.7$, 31.9, 31.4, 30.7, etc., and these values were constant till the bubbles burst. The colloid can thus have had very little effect on T (Magie's value for sweet oil, for instance, is 32); but it does contribute in marked degree to the persistence of bubbles, as in the case of soap.

Rubber dissolved in a mixture of sweet oil and paraffine oil gave the same order of results, $T=30$ to 31.

Rubber dissolved in kerosene (illuminating oil) was much less available, the bubble bursting almost before the fringes came to rest. The value of T obtained in several experiments was of the order $T=26$; but this is merely an estimate.

The partial success of these results induced me to test other oils, with a view to obtaining the surface tension of pure rubber, if possible. For this purpose a gasoline solution seemed specially adaptable, for with the speedy evaporation of gasoline a rubber film would remain. It is necessary to use a gasoline solution thick enough to only just flow. Even then the bubbles are too short lived for the successive measurements of $2r$ and Δx. After many trials, three cases occurred in which the fringes were glimpsed in position. The estimate so obtained ($2r=1.5$ cm., $\Delta x=0.0170$ cm.) was $T=30$, which is the usual order of values for the preceding colloid solutions.

15. Canada balsam.—This substance seemed particularly favorable for T measurements, as the bubble remains viscous for a long time. The solution in turpentine, however, failed of success, the bubbles bursting almost at once.

The viscid liquid itself was therefore tried, warmed to facilitate the blowing. The results obtained for T are shown in figure 23, in a scale of minutes. The first series is the most complete and indicates the uniform occurrence of a rise of T during the first 5 or 10 minutes, after which T regularly but slowly decreases. This is to be ascribed, as I think, to the diminished contractility or incipient solidification of the tissue with loss of the air within the bubble. At 74 minutes the original clear iridescent bubble was found to be opalescent or opaque. It had roughened and shrunk from 2.3 to less than 2.2 cm. in diameter. At 85 minutes it had shrunk further to 2.0 cm. Breaking it at 102 minutes, it was still flexible, but very tough. In series 2, the bubble became opaque after about 60 minutes and then broke of its own accord. In the series 3, the bubble sprang a leak (?) early, but seemed afterward to have resealed itself again.

As the production of persistent bubbles is thus easy with this substance, a thick solution of Canada balsam in chloroform was next tested, and the data obtained are given in figure 24. As a whole, they show a close resemblance to figure 23. The results of the first series are low; but it was found that the lower end of the tube had become choked with an excess of the solution, a danger to be guarded against in all these experiments. The diminution is thus a thermal effect and T eventually runs into negative values. The second series, however, is trustworthy, the data being

Time	0	3	12	26	38	53	66	170 minutes.
$10^3 \times \Delta h$	17.4	13.5	11.8	9.6	7.7	5.7	4.8	4.8 cm. Hg.
T	49.1	49.4	43.2	35.1	28.1	20.8	17.4	14.3

At 170 minutes the originally clear iridescent bubble was found to be opalescent with a satin-like luster. It had decreased in size from a diameter of 2.2 cm. to 1.8 cm., but was otherwise quite intact. Observed next day, it had shrunk further to a white dry pendant, but was still whole, giving an apparent value of $T=3.6$. The bubble crumbled at the touch, however, to a white, chalk-like powder. It is noteworthy that between 66 minutes and 170 minutes there was no difference of internal pressure, the reduction of apparent T being due to shrinkage. In the third series the initial T is somewhat smaller, but the general behavior is the same, remembering that the fall of T during incipient solidification can not be independent of temperature. The data were

Time	0	3	6	12	29	48	79	117	129	360 minutes.
$\Delta h \times 10^3$	12.3	12.9	12.6	11.7	9.5	8.1	5.3	4.6	5.0	4.8 cm. Hg.
T	43.6	45.9	44.6	41.6	33.8	28.7	18.9	16.4	17.6	16.9

After 117 minutes this bubble had also become opalescent and stringy, showing creases on the surface; though the bag was still whole, for after 360 minutes scarcely any change of internal pressure was observable. In this respect, therefore, series 2 and 3 are in accord; for long periods (hours) after incipient opalescence, the internal pressure remains nearly fixed.

In the case of series 4, the bubble obtained was a very thin, highly iridescent sphere, and it was with regret that the observations could not be extended

beyond 50 minutes. They are separately given in figure 24, and are (bubble clear throughout) :

Time	0	3	7	15	36	52 minutes.
$10^3 \times \Delta h$	14.4	15.1	14.0	11.9	8.3	6.0 cm. Hg.
T	47.7	49.8	46.3	39.2	27.5	20.0

From the initial high T value, there is a rapid descent similar to the case of series 2. Next day this bubble had shrunk to a white bag about 1.3 cm. in diameter. The internal pressure was zero, suggesting a rent.

The surface tension of these thick chloroform solutions differs but little (as a whole) from the behavior of warmed Canada balsam. The difference of viscosity is thus merely incidental. Since the fall of T following the rise during the first 3 or 4 minutes occurs while the bubble is perfectly clear and therefore probably still a viscous fluid, and since the pressure within the opaque bubble remains constant for hours, I am in some doubt whether the reference
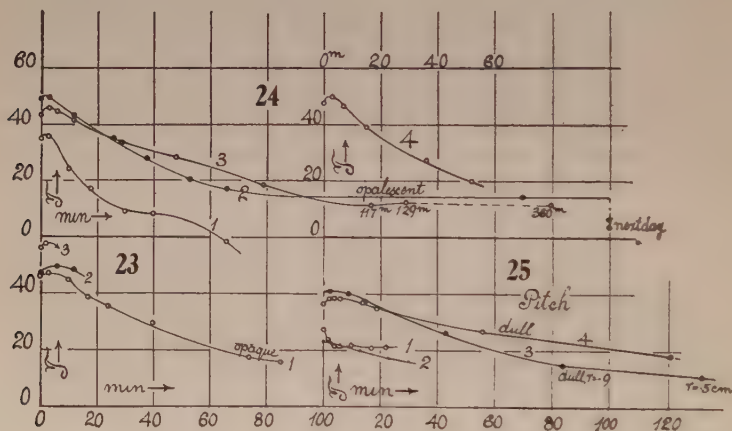
of this feature of the experiment to diminished contractility is quite warranted. The assumption of incipient solidification is thus merely a reasonable hypothesis, for the air does leak out. Under the microscope patches of the white, solid, friable chalk-like bubble residues appear minutely cellular, like transverse sections of wood, but more finely porous. A measurement of the pores (granting that they may be the illusion produced by a rough surface) showed them no longer than 0.0001 cm. in diameter and evenly distributed. If we consult again curve 1, figure 23, and particularly curves (2) and (3), figure 24, it will be seen that the fall of T (which means escape of air and a leaking bubble) occurs while the bubble is clear and iridescent, whereas the nearly constant low values of T thereafter (bubble now impervious to air) occur when the bubble has become opalescent and rough, or white, and opaque. During the clear stage the bubble does not appreciably shrink. It does so during the opaque stage, keeping the pressure nearly constant within. The decrease of T in the graphs as stated is purely due to this fact. Thus the bubble is impervious when the liquid solvents (chloroform, etc.) have prac-

tically evaporated, but not so when they are present and the bubble clear and glass-like. One may infer that the diffusion of the high-pressure air within the bubble outward is conditioned by the presence of a liquid solvent. Furthermore, that toward the end of the evaporation, at least, the resin and the solvent separate so that the latter occurs in an indefinite number of minute droplets, not exceeding 0.001 mm. in diameter, throughout the tissue of the resin. It may have been so distributed throughout, but the separated resin and solution in some measure recalls the ejection of the solute on the freezing of a salt solution. In the final bright white residue, air only is present in the pores. To resume: The clear bubble leaks, but does not appreciably shrink and pressure within diminishes; the opaque bubble often shrinks in excess of the leakage, if any, and the internal pressure may be constant or even rise.

With mastic in alcohol similar experiments were tried at length, but failed in all cases. Bubbles were producible, but they did not last.

16 Pitch.—The sample used was rather old and stiff and it was necessary to blow the bubbles warm, after the fusion of the pitch. The results for T in the lapse of minutes are summarized in figure 25, graphs 1 and 2. In both cases the surface tensions are low values, even at the beginning, and they apparently decrease as usual in the lapse of time. The bubble of No. 2 was elliptical and the absolute results of the graph are therefore too low. It was curious to note that the bubbles remained black throughout, but were initially glossy.

This sample of pitch was therefore diluted with a small addition of turpentine, fused, and stirred. With the nearly cold mixture a bubble was blown and examined for over two hours. The graph, figure 25, No. 3, summarizes the data. It will be seen that they show a very close resemblance to the behavior of Canada balsam throughout, even as to the absolute values, which were

Time	2	9	15	43	83	132	minutes.
$\Delta h \times 10^3$	13.1	12.8	12.0	8.4	5.1	5.5	cm. Hg.
T	41.1	40.2	37.8	26.3	15.0	12.4	

At 83 minutes the bubbles had assumed a dull surface, with shrinkage from diameter 1.9 to 1.8 cm., and at 132 minutes it had shrunk further to a black paper bag, as it were, about one-half its original diameter. The pressure within had actually increased. We have here the same tendency to maintain constant pressure inside the bubble that characterized the opaque stage of Canada balsam, and the same inferences might be drawn.

Further turpentine was now added; but it was not possible to obtain bubbles from the solution until the greater part of the turpentine had been boiled away. The bubble finally obtained was small, $2r = 1.7$ cm. After about 120 minutes it had shrunk to 1.6 cm., with a dulled surface; after 180 minutes to 1.4 cm. with distortion, the dull bubble being more or less cushion-shape, embraced by a bright ring around the edge. The data were (curve 4)

Time	0	2	4	6	14	19	56	121	180	212	minutes.
$\Delta h \times 10^3$	13.1	13.7	13.8	13.7	13.2	12.4	9.6	6.8	6.2	5.5	cm. Hg.
T	36.7	38.5	38.8	38.5	37.1	35.0	27.0	18.1	14.6	12.7	

The relative constancy of pressure during the long period of shrinkage (121 to 212 minutes, dull surface) is again noteworthy, so that while the glossy bubble does not shrink appreciably, the dull bubble sometimes shrinks in excess of leakage, if any. Pitch of course remains viscous, never becoming solid.

17. Nitrocelluloid.—With thick collodion, bubbles are easily producible, but they last but 1 or 2 seconds. Occasionally one is caught which solidifies; but on so doing it shrinks to a puckered cylindrical tube, by shrinking equatorially and additionally blowing out liquid adhesions like the drop at the bottom. All is complete in a few seconds. Under these circumstances the pressure goes up many fold and is beyond the range of the U-gage interferometer. I caught but one measurable bubble, $2r = 1.5$ cm., iridescent and spherical. The internal pressure was $\Delta h \times 10^3 = 11.4$ cm. Hg and $T = 30$. Thus the colloidal solution presents no abnormal values, however the tough solid resulting may behave. With celluloid varnish (thick), bubbles are also producible, but none of them persist.

Celluloid thus differs from the preceding colloids in speed and intensity of reaction. Speed is referable to the volatile solvents, and a determination of the air leakage of the clear bubble is thus out of the question. In the second stage, with evaporated solvent, the period of shrinkage is similarly rapid. Pressures, instead of remaining constant as heretofore, actually increase impulsively many times and they furnish only a lower limit of value for the cohesional forces in action. In other words, while the solid residues of Canada balsam are brittle and friable, those of nitrocelluloid are flexible and tenacious, and we have thus an interesting transition from the surface tension of the liquid bubble to the elastic forces (probably) of the solid film.

In a corroborative experiment some time later, a bubble $2r = 1.4$ cm. in diameter showed an initial $T = 29$. It shrank in a few seconds to an elliptical puckered solid bubble, which later became rounded to a crumpled sphere, about $2r = 0.7$ cm. in diameter. Pressures were increased about 5 times after shrinking, which after 7 minutes (leakage) became 3 times, after 22 minutes 2 times, after 39 minutes and long thereafter once the pressure in the liquid bubble. If we compute the solid data as surface tension, $T = 74$, necessarily a lower limit. The size and form changed no further. Under the microscope no structure was detected in the crumpled bubble. Certain parts of it were iridescent, but as a whole it was free from the colors seen on the liquid film.

CHAPTER III.

VISCOSITY, DENSITY, AND DIFFUSION OF GASES.

VISCOSITY AND EFFLUX.

18. Viscosity of air.—The observation made above, of a more rapid trans-
piration of air through one pin-hole as compared with the other, in case of
a common pressure difference, suggested an actual measurement of the
viscosity η of air, by capillary-tube method. For this purpose (inset, fig. 26),
it is merely necessary to attach such a tube, by a piece of pure rubber tubing,
to one shank of the **U**-gage, the other remaining open to the atmosphere. On
pushing the tube in question inward slightly, the pressure will rise from p
(atmosphere) to P a little above (excess of the order of 0.05 mm. of mercury),
and this is indicated by the displacement, s, of fringes. The change of s in
the lapse of time is, then, to be measured with a stop-watch. Thus the method
is extremely simple and capable of indefinite repetition, either for $P > p$ or
$P < p$. Any other gas may replace air on the side of the **U**-tube in question.
The serviceable equation for this purpose was deduced long ago by O. E.
Meyer,[*] in the form

$$(1) \qquad \eta = \frac{\pi}{16} \frac{P^2 p^2}{p_1 V_1/t} \; \frac{R^4}{L}\left(1 + 4\frac{\zeta}{R}\right)$$

where P and p are the pressures at the two ends of the capillary tube of
length L and radius R, and V_1/t is the volume of air transpiring per second
at the mean pressure p_1. The coefficient of slip, $\zeta = \eta/\epsilon$, (the ratio of internal
and external friction) will have to be neglected. In this equation $P + p$ may
be written $2P$, since $P - p$ is very small compared with $P + p$. But $p_1 V_1/t =
R(m_1/t)\tau$, if m_1/t is the mass of air transpiring per second; and since this
comes out of the closed volume V of air, of mass m, of the shank of the **U**-gage,

$$(2) \qquad m_1/t = -dm/dt$$

Hence if the volume V is preliminarily taken as constant, while the pressure
P decreases,

$$(3) \qquad p_1 V_1/t = R(m_1/t)\tau = -R(dm/dt)\tau = -V dP/dt$$

so that the equation (2) now becomes

$$(4) \qquad \eta' = -\frac{\pi}{16} \frac{R^4}{LV} \frac{2P(P-p)}{dP/dt} = -\frac{\pi}{8} \frac{R^4}{LV} \frac{P(P-p)}{d(P-p)/dt}$$

as p is the constant atmospheric pressure without. Therefore,

$$(5) \qquad \eta' = -\frac{\pi}{8} \frac{R^4}{LV} \frac{P}{d(\log (P-p))/dt}$$

[*] O. E. Meyer: Pogg. Ann. CXXVII, p. 269, 1866.

31

But since $P-p$ is proportional to the fringe displacement s, the logarithmic time differential is simply $d(\log s)/dt$. Hence finally,

$$(6) \qquad \eta' = -\frac{\pi}{8}\frac{R^4}{LV}\frac{P}{d(\log s)/dt}$$

V being supposed not appreciably variable. Thus $d(\log s)/dt$ is constant, and it is merely necessary to record the decrease of the fringe displacement s in the lapse of time, after the capillary tube is affixed under slight pressure, $P-p$ to the U-gage on one side.
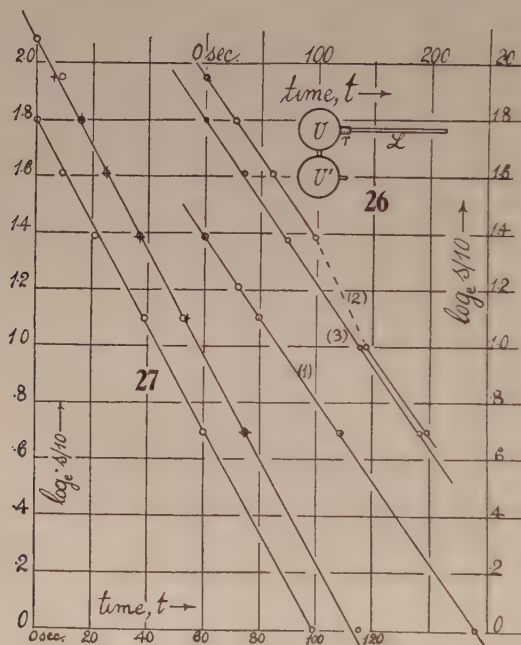
Equation (6) is incomplete, inasmuch as V, though very nearly constant, nevertheless varies in the same order as P, so that $p_1V_1/t = VdP/dt + PdV/dt$. It is desirable, however, to test (6) preliminarily, in order to ascertain to what degree the method is feasible.

19. Observations.—The first tube selected had a length of 15.1 cm. and an internal diameter (as found by the microscope) of 0.0354 cm. Attached by an inch of pure rubber tube to one shank of the U-tube with a slight pressure excess, the relations of $\log_e s$ (or for convenience $\log_e s/10$) in the lapse of time were such as shown in the three graphs of figure 26. Of these, No. 1 is as nearly linear as may be expected, seeing that no attempt was made at precision, the time t being taken when the fringes passed successive equidistant scale divisions of the ocular micrometer. The same is true for the third graph. The second is for some reason irregular, owing possibly to an accidental

small displacement of the zero at 100 seconds (about). The mean rates in the three cases are respectively

$$10^3 d(\log s)/dt = 5.74,\ 5.84,\ 5.79$$

giving a mean value of 0.00579, as a whole.

The volume V of the closed shank of the U-gage was about 70 cm.³, the reduced barometric height $B = 75.4$ cm. Hence the equation

$$\eta' = -\frac{\pi}{8}\frac{R^4}{LV}\frac{B\rho g}{d(\log s)/dt}$$

or

$$\eta' = \frac{\pi}{8}\frac{10^{-8}\times 9.81}{15.1\times 70}\frac{75.4\times 13.6\times 981}{.00579} = 0.00633$$

Thus, while the logarithmic variation is sustained, the incomplete η' is enormously too large. This implies that most of the air is pushed bodily through the capillary tube by the advancing piston U, at nearly constant pressure.

The second tube was of larger bore, the diameter being 0.0454 cm. and the length 11.7 cm. The three graphs of $\log s/10$ and t obtained for this tube are much steeper and shown in figure 27 in a different scale. Here all three graphs are as nearly linear as may be expected from the straightforward method of record. The individual mean rates are respectively

$$10^3 d(\log s)/dt = -18.8,\ -17.9,\ -18.5$$

with a mean rate therefore of 0.0184. Applying the preceding equation to this case

$$\eta' = \frac{\pi}{8}\frac{10^{-7}\times 2.65}{11.7\times 70}\frac{75.4\times 13.6\times 981}{0.0184} = 0.00696$$

an order of value about the same as the preceding case, while the logarithmic variation is again substantiated.

It is therefore necessary to complete the equation for η, which is easily done by replacing VdP/dt by the full coefficient. If a is the area, H the normal depth of the cylindrical volume V, at U, and if the mercury head is h,

$$V = a(H + h/2)\ \text{or}\ dV = adh/2$$

and

$$p_1 V_1/t = R(dm/dt)\tau = VdP/dt + PdV/dt = (V\rho g + aP/2)dh/dt$$

If B is the barometer height, since $P - p = h\rho g$ and $V = aH$ (nearly),

$$\eta = \frac{\pi}{8}\frac{R^4}{LV}\frac{B\rho g}{(B/2H+1)d(\log s)/dt}$$

since $d(\log h)/dt = d(\log s)/dt$, s being the fringe displacement from zero. Thus

$$\eta = \eta'/(1 + B/2H) = \eta'/(1 + 75.4/2) = \eta'/38.7$$

as $H = 1$ cm. in the apparatus. Hence in the two cases,

$L = 15.1$ cm.; $2R = 0.0350$ cm.; $\eta = 0.00633/38.7 = 0.0000164$
$L = 11.7$ cm.; $2R = 0.0454$ cm.; $\eta = 0.00696/38.7 = 0.0000180$

Both values are now correct in order; but the first, in which the transpiration is much slower, has been more influenced by the concomitant and inevitable changes of temperature in the U-gage reservoir V. It is obvious that the difficulties of Chapter I enter. For this reason, a more accurate determination of R, etc., and a consideration of the initially adiabatic temperature increment in V after compression, is of no interest, except in connection with observations made under very constant temperature conditions in summer.

20. Efflux through pin-holes.—This apparently simpler experiment does not succeed by the present method. In the first place, the hole must be considerably finer than 0.1 mm. or finer than can be punctured by the most delicate cambric needle. It will not, therefore, be round, and its area a' would have to be estimated. In the second place, the equation for this case $(v=\sqrt{2(P-p)/\rho})$, reduces in the same notation to

$$\frac{dh}{dt}\cdot\frac{d\log h}{dt}=\left(\frac{a'}{a}\right)^2\frac{2R^2\tau^2\rho_a}{H^2\rho_m g(1+B/2H)^2}$$

where R is the gas constant, τ the absolute temperature, ρ_a, ρ_m the densities of the gas and of mercury, and a the area of the U-gage. Thus neither of the rates are linear, and the head h must be known throughout, since $(dh/dt)^2/h$ is constant. Using the equations, the rates would be (hole $2r=0.027$ cm., $h=10^{-5}\times6.3s$)

50 s. p.	$dh/dt =$ 0.00439	$ds/dt =$ 69 s. p./sec.
25		310	49
12.5		219	35
6.2		155	25
3.1		110	17

which is too rapid for observation, as I found.

The equation if written in the form

$$(dh/dt)^2=Ah$$

is integrable and becomes

$$\sqrt{H}-\sqrt{h}=\sqrt{A/2}t$$

and thus, curiously enough, terminates in $h=0$, thereafter to increase again in the lapse of time, indefinitely.

I endeavored to get further light on the subject by inserting a fine wire $(2r=0.02$ cm.) into the above pin-hole $(2r=0.0272$ cm.), whereby the flow became sufficiently slow to be observable; but the efflux conditions of the experiments are thereby spoiled by the friction along the wire. Examples of the curves obtained are given in figure 28, a, b, still difficult to observe, and which differ materially from each other, depending on the initial rapid fall before observation is possible. They are not in numerical conformity with the equation or otherwise, as may be seen by using the constants $10^5a=267$; $a_\tau=70$; $(1+B/2H)=39$; $\tau=300°$; etc., which makes $\sqrt{A}/2=0.0179$ quite out of proportion. The actual efflux is much too slow as compared with the

equation, so that Torricelli's law in case of efflux into air, instead of vacuum, and a very small pressure difference, is here not warranted.

21. Sensitive flames. Adjustment.—The disposition of apparatus is shown in figure 29, where UU' is the interferomoter **U**-gage, r and s the reëntrant and salient pin-holes, t the quill tube, and F the fine conical gas-jet about 1 mm. in diameter (salient outward) for the sensitive flame. F is preferably placed vertically. The gas inlet G is at the middle of t, so that r, s, and F may function as nodes. G is provided with a stopcock to vary the gas-pressure. Since this pressure acts at both U and U', it is only the acoustic pressure due to vibration within the quill tube which will influence the gage U.
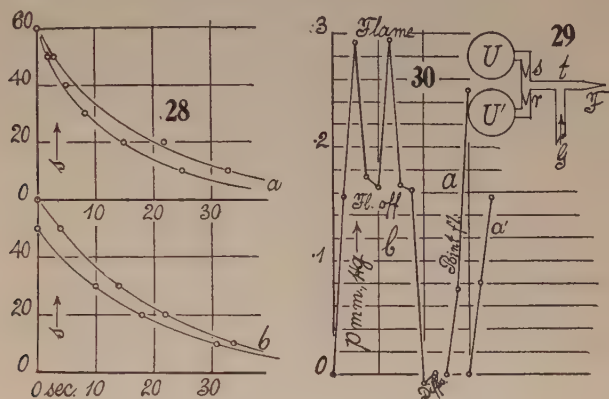
The pin-holes rs are rarely quite of the same diameter. Hence the fringes will move for any sudden change of pressure at G, temporarily, but they soon return to zero. The flame F was very sensitive, but no acoustic pressure under any conditions could be observed. There was no effect even when the flame was purposely made turbulent by high gas-pressure. Thus the sensitive-flame phenomenon must be considered to exist outside of the quill tube tF and there is no corresponding vibration apparent within.

22. Same. Telephonic excitation.—On removing t from rs and the gage and joining the open end of t to a telephone mouthpiece, excited by a little induction coil with a break of variable pitch, one gets a beautiful exhibition of König's flames at F. In this case a small, sharp flame, 2 or 3 cm. or less, is of course desirable. However, the attempt to detect the resonances in the quill tube in this way failed. The method may, however, be useful in detecting the harmonies of the telephone plate and appurtenances.

23. Apparent flame pressure * and viscosity.—Joining the quill tube t with the shank U only (s, fig. 1, may be left in place, as it does not function, r, also

---

* Prof. A. T. Jones (Thesis, Clark Univ., 1913) seems to have first come across these phenomena and is inclined to accentuate the flame-pressure aspect (Science, LX, 1924, p. 315).

inactive, must be open to the atmosphere), one observes an increased pressure within t (cæt. par.), whenever the flame F is ignited. These pressures are in excess of the normal registry of the gage, so that small flames, from a point like a split pea to 2 or 3 cm., are to be used. Figure 30 gives examples of the results. The curve a (points spaced horizontally to show different conditions) beginning with no pressure (millimeters of mercury), when the cock is closed, registers about 0.075 mm. with the cock just open, owing to the resistance at the jet, and 0.25 mm. after the flame is lighted. At a', the lower graph, is a less well chosen adjustment. The point flame, therefore, acts like a stopper, virtually narrowing the jet. Figure 30b gives a more extended series, with a flame 2 to 3 cm. long. Hence the gas-pressure at t in the absence of flame is larger, about 0.16 mm. With the flame lighted, the pressure reaches nearly 0.3 mm. It is not, however, relatively as much larger as in the case of the point flame. When the flame is blown out, the intermediate gas-pressure is restored, first at a rapid rate, finally very gradually, the progress obviously corresponding to a case of cooling of the mouth of the jet. The phenomenon is remarkably steady, and the experiment may be repeated indefinitely, two cases being given in figure 30. When the gas is finally shut off, the fringes dip below zero, which, however, is regained in the lapse of time. This is optic (refraction) evidence of the diffusion of hydrocarbon gas into the U-gage and of the subsequent diffusion outward; or in accord with the next sections, it may be due to the density difference at U and U'.

24. Inferences.—I was at first inclined to believe that an actual pressure increment within the flame locus had been observed. What happens, however, is probably no more than a large increase of the viscosity of the gas at the jet. Because of the high temperature there, the jet with the flame lighted temporarily conveys a much more viscous gas-current. Thus the asymptotic cooling effects in figure 30 are accounted for (hot-jet tube), as well as the striking steadiness of the phenomenon when the flame is on, and the disproportionately great effect of point flames. For in the latter, the colder blue base is lacking.

It follows from the above that if for any reason the flame is removed, there is an instantaneous excessive *outrush* of gas from the jet. When the flame is restored this excess is at once cut off. Here, then, is a mechanism that contributes to periodic motion of flame and must be effective in turbulent flames. Since pin-holes are sensitive at nodes, I have supposed that temperature occurrences might here be effective also; but this can not be the case in a phenomenon which is symmetrically either positive or negative, depending on the slope of the pin-hole.

With regard to the pin-hole probe itself, however, which is virtually a hollow cone, it would seem that on compression towards the point the adiabatic increase of temperature is accompanied by diminished flow outward, whereas

on dilatation from the point, there is a corresponding rapid flow of air inward. The result must be an excess of flow inward until the increased air-pressure within the closed region compensates for the viscosity differences at the point. Reversing the pin-hole, therefore, reverses the sign of the pressure, just as observed. Relaying is a failure, because adequate motion after the first pin-hole is quenched.

DENSITY AND DIFFUSION OF GASES.

25. Apparatus.—The present method, which in practice is singularly expeditious and simple, should nevertheless, it was hoped, eventually be capable of giving results well within 1 per cent. I have carried it through preliminarily to exhibit its entire feasibility, the plan being to compare the pressure of a column of gas with that of the surrounding air. A diagram of the apparatus is given in figure 31, where tt is a quill tube 68 cm. long, in which the gas (here supposed lighter than air) is to be stored. This communicates by the three-way stopcock C with one shank (10 cm. diameter, 1 cm. deep) G of the interferometer U-gage. M shows the flat charge of mercury, p the sealed cover-glass, and L one component beam of the interferometer. The other shank of the U-tube (not shown) is open to the atmosphere.

With C set as in the figure, the gas arriving at g is passed in excess through tt. After a few minutes the plug in C is suddenly rotated 90° and the pressures produced at M read off by the fringe displacement in the telescope of the interferometer. The zero of the scale may be set by the slide micrometer. It is desirable to repeat this operation many times, as in the first instance there is a large throw of fringes. After this, with the tube filled with gas, the fringes are more steady and may be read off within 5 seconds or less. Diffusion, though relatively slow, nevertheless sets in from the beginning, the gas escaping both at the bottom and the top of tt, to be regularly replaced by air. If a stop-watch is started when the gas is definitely turned off, the progress of the diffusion phenomenon is registered by the displacement of fringes from minute to minute. To keep the gas within tt, the channel in C must be slightly above the tubulure in G, so that the connector s rises toward the left. This adjustment of diffusion from top and bottom is advantageous in requiring but very little gas; but for precision it is far preferable to so design the apparatus that the gage G and tubes sCt are filled with gas, and diffusion can take place out of the bottom of tt only.

26. Equation and data for density.—If Δp denotes the pressure difference on the two sides (gas and air), Δh the difference of heads of mercury of density ρ_m and Δx the corresponding displacement of the mirror on the screw slide-micrometer, for an angle of reflection θ of the rays of the quadratic interferometer

(1) $$2\Delta h = 2\Delta x \cos \theta$$

(2) $$\Delta p = \Delta x \cos \theta \rho_m g$$

Similarly, if $\Delta\rho$ is the difference in density of the gas examined and the known density of the surrounding air,

(3) $\Delta p = H\Delta\rho g$

H being the length of the quill tube tt used. Thus

(4) $\Delta\rho = \rho_m \cos\theta \Delta x/H$

The tube was 68.4 cm. long and θ (which is difficult to measure) was taken as 45°. It was, however, frequently convenient to read the fringe displacement Δs off on the ocular micrometer, where by preliminary comparison

(5) $\Delta x = 10^{-5}\, 2.25\Delta s$ cm.

Accepting this provisionally

(6) $\Delta p = 9440\Delta x = 0.2122\Delta s$

and

(7) $\Delta\rho = 0.1415\Delta x = 10^{-6}\, 3.184\Delta s$

The linear relation of Δx and Δs must also be tested.

For convenience, ordinary coal-gas was first taken. The results are adequately given in the graphs figure 32, a, b, c, and figure 33 d, e, where the abscissas denote the time of observation in steps of 1 minute each. The initial time (o minute) is frequently indicated. In curves a and b, 2 and 1 minutes, respectively, passed before the fringe reading could be taken. In curves d and e, however, with the advantage of the method of repeated filling, the reading could be made within 5 seconds, to this extent eliminating the initial diffusion. One may note that the curves are as a rule regular; but that certain discontinuities occur in the places marked by the arrow. They may be due to release from the surface viscosity of the mercury, as the gage was not tapped; or they may result from different components of the coal-gas diffusing out at different rates. Thus, in the curve d there are three branches, the last being nearly straight. In curve e, however, there is an actual break at br and some adhesion and slip in the gage under so gradual a release is more probable. It would seem to make little difference here; for the densities are determined from the beginning and the diffusion coefficients from the ends of the curves. In case of curves c, d, e, rubber-pipe connectors were so far as possible avoided.

As the curves a, b, c (fig. 32) begin with initial diffusion (1 to 2 minutes), they are less available than figure 33, d and e, for these (multiple filling) begin with the same pressure (equivalent to $s = 168$ scale-parts of displacement) and after 15 minutes show respectively $s = 83$ and 81 scale-parts of pressure, and this in spite of the break in curve e, which must have been in the gage. From equations (5 to 7), $\Delta x = 0.00425$ cm. whence $\Delta p = 35.7$ dynes/cm.², and $\Delta\rho = 0.000535$. The density of air being (at 25° and 76.4 cm.) $\rho' = 0.001190$, it follows that the gas density observed is $\rho' - \Delta\rho = 0.000655$; or under normal conditions about $\rho = 0.000712$. This is correct in order of value, but as yet

problematical. To improve it, θ in equation (4) must be measured and the interpolation equation (5) tested. The other curves (b, c) gave values of the same order, after the initial diffusion was estimated.

The endeavor was now made to correct both the provisional values of Δx and $\cos \theta$. In the latter case the angle between incident and emergent rays was 3.6° in excess of 90°, so that the values of $\theta = 46.8°$. This is equivalent to a diminution of ρ by 3.2 per cent. Again a long-range comparison was made between Δx of the slide micrometer and the Δs of the ocular micrometer, by applying steps of pressure to one shank. These results are given in figure 34 for increasing and decreasing pressures. It is interesting to note that the ratio is the same, but the lines differ by a lag of two or three ocular scale-parts, or a little over a fringe. I at first inferred this to be merely a question of the time needed for the final flow to equilibrium as the pressure vanishes. To have waited for its full disappearance would have introduced temperature
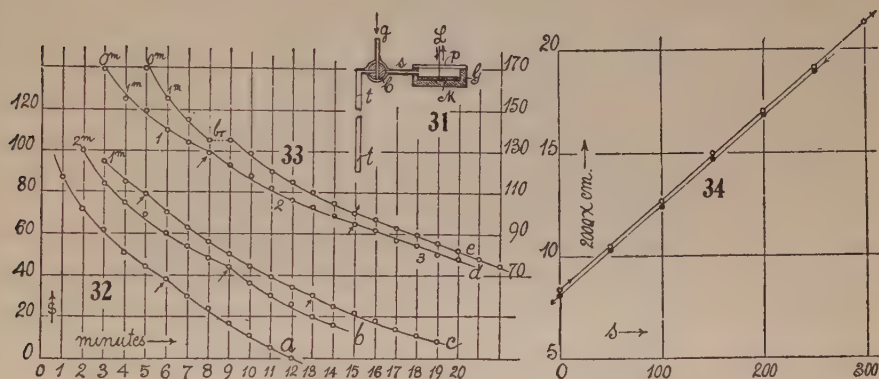
disturbances into the closed region. The ratio given by the new graph is $\Delta x = 10^{-6} \, 21.5 \Delta s$, which accounts for an addition 4.4 per cent. Thus the difference becomes $\Delta \rho = 10^{-6} \, 2.94 \Delta s = 0.000494$, whence $\rho = 10^{-6} \, 696$, or, reduced to normal conditions, $\rho = 0.000757$.

Some error may reside in a frictional temperature effect of the gas passing tt, and temperature should preferably be measured in the tube; but the following paragraphs indicate pronouncedly that a static error referable to surface tension of the mercury in the gage needs attention.

A few incidental results on different days may be recorded. The first at 23.5° and 75.1 cm. of the barometer gave $\Delta s = 166$, whence the reduced $\rho = 0.000758$. Another at 22.5° and about the same barometer gave $\rho = 0.000755$. In all cases it is best to set the screw micrometer so that the displaced fringes may be nearly at zero. Measurement is then made directly in terms of Δx, while Δs is a small correction. This avoids the serious use of the relations Δx and Δs of the two micrometers, a quantity which varies with incidental conditions of fringe size. It is even better to take the limit of the ocular throw of fringes as the zero of the slide micrometer.

4

27. Equations for diffusion.—If $\partial\rho/\partial t = A^2\partial^2\rho/\partial x^2$, where ρ is the density of the gas at a time t and at a distance x from the end of the tube, the coefficient of diffusion is a^2 in [cm.^{2}/sec.]. The problem in case of the tube is practically that of diffusion in one direction in infinite space bounded on one side by a plane, at which $\rho=0$ at all times. Initially $\rho=\rho_0$ was constant throughout all gas-filled space. The general solution, given by Riemann (see Partielle Differentialgl., Hattendorf, 1876), for the present particular case leads to

$$(8) \quad \rho = \frac{2\rho_0}{\sqrt{\pi}} \int_0^{x/2a\sqrt{t}} e^{-\beta^2}d\beta = \frac{2\rho_0}{\sqrt{\pi}}\left\{ \frac{x}{2a\sqrt{t}} - \frac{x^3}{3(2a\sqrt{t})^3} + \frac{x^5}{5.2(2a\sqrt{t})^5} - \cdots \right\}$$

Since for the vertical tube $dp = \rho g \cdot dx$, the pressure value is found on integration for a tube-length x to be

$$p = \frac{2\rho_0 g}{\sqrt{\pi}}\left(\frac{x^2}{2(2a\sqrt{t})} - \frac{x^4}{12(2a\sqrt{t})^3} + \frac{x^6}{60(2a\sqrt{t})^5} \cdots \right)$$

or, on replacing $\rho_0 g x$ by p_0, the initial pressure,

$$p = \frac{p_0}{\sqrt{\pi}} \frac{x}{2a\sqrt{t}}\left(1 - \frac{x^2}{24a^2 t} + \frac{x^4}{480a^4 t^2} - \cdots \right)$$

Thus, if l is the tube-length,

$$a = \frac{1}{\sqrt{\pi}} \frac{p_0}{p} \frac{l}{2\sqrt{t}}\left(1 - \frac{l^2}{24a^2 t} + \frac{l^4}{480a^4 t^2} - \cdots \right)$$

seeing that approximate values of a suffice in the correction terms.

A subsidiary explanation is needed here. If ρ' is the air density and ρ the density of mixed air and gas in the tube tt', $\Delta\rho = \rho' - \rho$, where $p = Hg\Delta\rho$ at the **U**-gage. But $\rho = \frac{B-B_h}{B}\rho' + \frac{B_h}{B}\rho_h$, if ρ' and ρ_h are the gas densities at the barometric pressures B, whereas B has fallen for the gas to B_h by diffusion. Hence $\Delta\rho = \frac{B_h}{B}(\rho' - \rho_h)$, and therefore

$$p = Hg\Delta\rho = H\frac{B_h}{B}(\rho' - \rho_h)$$

$$p_0 = \qquad H\frac{B}{B}(\rho' - \rho_h)$$

whence

$$\frac{p}{p_0} = \frac{B_h}{B} = \frac{\rho_h t}{\rho_{h0}}$$

The ratio of **U**-gage pressures is the same as the ratio of the barometric pressures which determine the dilution of the gas after t seconds of diffusion at constant temperature. It is here tacitly assumed that the a's for diffusion of H_2 into air and of air into H_2 are the same. The subject is resumed in § 41.

But since p is nearly proportional to the fringe displacement s, the first term reduces finally to

$$a = \frac{1}{\sqrt{\pi}} \frac{s_0}{s} \frac{l}{2\sqrt{t}} (1 - \text{etc.})$$

It is thus merely necessary to observe the initial fringe displacement s_0 and a final displacement s_2, after say 15 minutes, to obtain a^2, the diffusion coefficient.

In the above experiment, however, diffusion takes place at both ends of the tube, which is equivalent to using two tubes of length $l/2$. This reduces the main term one-half (since p_0 and l are both reduced), so that

$$a = \frac{1}{\sqrt{\pi}} \frac{s_0}{s} \frac{l}{4\sqrt{t}} \left(1 - \frac{l^2}{96a^2t} + \frac{l^4}{7680a^4t^2} - \right)$$

would be used in the experiments.

28. Data for diffusion.—The curves, figure 33, d or e, are available. Taking the former with $t = 15$ minutes $= 900$ seconds, $s_0 = 168$; $s = 83$; $l = 68.4$ cm., the first term is

$$a' = \frac{1}{\sqrt{\pi}} \frac{s_0}{s} \frac{l}{4\sqrt{t}} = \frac{1}{1.77} \frac{168}{83} \frac{68.4}{4 \times 30} = 0.6508$$

whence

$$a'^2 = 0.4236$$

The term

$$-l^2/96a^2t = -(68.4)^2/(96 \times 0.42 \times 900) = -0.1278$$

The term

$$l^4/7680a^4t^2 = (68.4)^4/7680 \times (0.42)^2 \times (900)^2 = 0.0196$$

And the correction therefore

$$1 - 0.1082 = 0.8918$$

so that $a = 0.580$ and $a^2 = 0.337$.

The datum is again of the right order of value, but probably in need of the same kind of corrections already instanced in the preceding paragraph. In particular, the diffusion from both ends not strictly identical is objectionable.

29. Hydrogen. Density.—The next test made was possibly too severe for the method, for the very rapid initial diffusion of hydrogen will facilitate an escape of gas from the quill tube before the fringes come to rest (5 seconds). Whether from this cause or whether from some other error still to be detected, the hydrogen data for ρ came out much too large. It is curious that the initial fringe displacements in any given experiment are remarkably constant (to about 1 part in 300), even when the quill tube is successively refilled 25 to 50 times.

The hydrogen was generated by sheet zinc with dilute H_2SO_4 in a Kipp apparatus and passed directly through a cotton filter into the quill tube. An example of results obtained on different days follows. ρ' refers to air, ρ to hydrogen corrected for moisture,* ρ_0 refers to normal conditions. Tube-length 68.4 cm. (Table 4.)

---

* In winter for dry air and wet H_2, $\rho_h (B - \pi)/B = \rho_a - \rho_w - C\Delta x$; in summer for wet air and H_2, $\rho_a - \rho_h = (BC/(B - \pi))\Delta x$.

The values of ρ_0 are thus about twice too large and vary erratically from day to day. The presence of 3 or 4 per cent of H_2S would account for the excess value, but so much is improbable. Temperature, which should be measured in the quill tube, would account for some slight variations. The optic flatness of the plates of the interferometer may not have warranted the large Δx displacement. A value of $\theta = 40°$ in the first three experiments in place of $46.8°$ taken would have given a correct order of value, but this is out of the question. The rapidity of initial diffusion, already referred to, may be mentioned in explanation. The compression of the volume of air in the gage is negligible. The displacement of fringes on opening and closing the cock did not exceed $\Delta s = 10$ or $\Delta x = 10^{-6} \times 215$ cm. Hence if the gage reservoir is 10 cm. in diameter and 1 cm. deep, while the quill tube is but 0.3

TABLE 4.

Date.	Temp.	Bar.	$\Delta x \times 10^3$	$\Delta p \times 10^6$	$p' \times 10^9$	$p \times 10^6$	$\rho_0 \times 10^6$	$10^3 \Delta x$ deficient.
	•	cm.	cm.					
Feb. 18	26.0	77.0	7.25	993	1196	179	193	0.87
Feb. 20	24.5	75.2	7.30	999	1174	155	170	.66
Feb. 21	23.5	75.3	7.06	966	1179	195	211	.94
Feb. 22	23.8	76.0	†7.10	1005	1189	163	178	.60

† θ changed to $45°$; $\Delta p = 0.1415 \Delta x$ here; in other cases $\Delta p = 0.1370\Delta x$.

cm. in diameter, the equivalent length Δl of quill tube would be $\Delta l \times 0.07 = 10^{-6} \, 78 \times 215$ or $\Delta l = 0.24$ cm. when the total length is $l = 68.4$ cm.

Taking the behavior as a whole, it appears, in spite of these minor misgivings, as if the initial pressures or thrusts were not fully given by the gage, but in part resisted, for instance, by capillary counterforces of the mercury surface. Moreover, the mercury was old and no longer quite bright. In fact, if we compute backward from the known density of hydrogen (ρ_0), the values of Δx in the table are on the average 0.00077 cm. too small. This is the Δx equivalent of the capillary reaction, and since $\Delta h = \Delta x \cos \theta$, the corresponding pressure would be 0.00054 cm. of mercury. In § 31 below a reaction of the same order is encountered in measuring the relatively small Δx observed when warm air is compared with cold air, so that the reaction is actually in a measure static. It was thus necessary to recharge the **U**-gage with fresh pure mercury preliminarily, as the reaction would seem to be associated with the dulled surface of the metal.

30. Diffusion of hydrogen.—Two series of experiments made several days apart are given in figure 35, the ordinates being ocular scale-parts s, equivalent to 21.5×10^{-6} cm. each ($\Delta x = 10^{-6} \times 21.5\Delta s$). Considered as a whole, the agreement is quite satisfactory, although the former hold and release of the gage is again apparent. One of the series was prolonged 57 minutes, the fringe displacement being still 50 scale-parts. Even after several hours, the presence of H_2 in the open tube was quite apparent. If the observable initial density

is too large and the initial pressure therefore too small, the coefficient of diffusion will also come out too small, and that is the case. We shall have in the two cases for a time interval of 15 minutes

$$t=0 \text{ sec.} \quad s_0 = 334 \quad t=900 \text{ sec.} \quad s=153$$
$$328 \qquad\qquad\qquad 152$$

The $l=68.4$ cm. is the same as above. The ratio s_0/s is thus 2.18 and 2.16 respectively, so that the mean 2.17 may be taken. This gives for the first term of the diffusion equation $a'=0.698$, whence $a'^2=0.487$. The first term in the correction is -0.1112; the second $+0.0148$, whence $a=a^1 \times 0.904=0.631$ and therefore $a^2=0.398$. This, as was anticipated, is too small, the standard value being near 0.66. The initial s_0 falls short, as before, but the essential
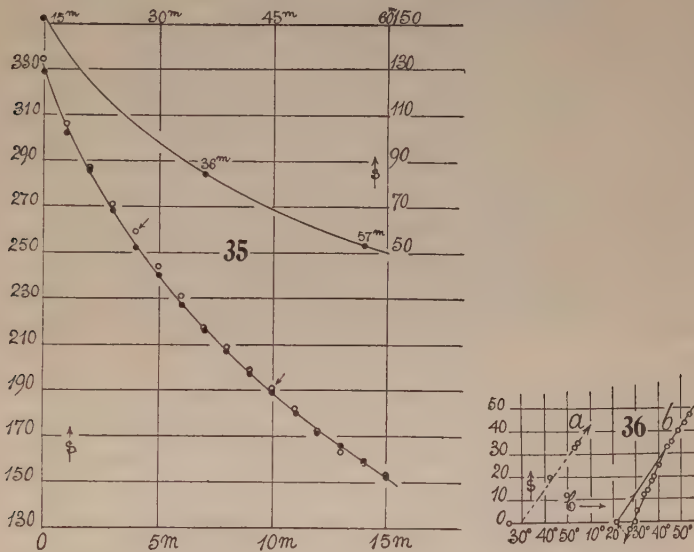
discrepancy lies in the hypothesis, i. e., the upper mouth of the quill tube is too much constricted by the stop-cock and hence the assumption of two identical half tubes is not valid. The true value of a must therefore lie somewhere between $a=0.631$ and twice this value. It is actually 0.81, which indicates the diminished diffusion (one may estimate it as only about 17 per cent) at the top. Again, when a and l increase together, the value of the parenthesis in the equation for a remains unchanged. Computed for diffusion at the lower end only, the result after 15 minutes is $a=1.396 \times (1-0.1112+0.0148)$ $=1.262$; after 30 minutes, $a=1.544(1-0.0454+0.0024)=1.544$; after 60 minutes about $a=1.9$. The equation, therefore, does not here respond adequately to the observed occurrences, as a whole, in the lapse of time.

31. **Coefficient of expansion of air.***—By surrounding the tube tt', figure 31, with a water or steam jacket, the expansion of the air within the quill

---

* §§31, 32, 33, are a digression, and contain experiments made to throw light on the gage discrepancy in question. The subject is resumed in §34.

tube should be determinable. This was accordingly tried, using a heavy brass tube 2 cm. in diameter for the jacket and placing a thermometer and stirring apparatus within the brass envelope. The mixture was made more thorough by siphoning the water from lower to higher levels.

In the first experiment (fig. 36, graph a) the outside of the brass jacket was directly heated by a burner and readings taken in steps of temperature at the ocular micrometer. Contrary to expectations, this curve is roughly linear, but its slope is only 1.4 scale-parts per degree centigrade. In this case the fringes were larger than above, so that $\Delta x = 10^{-6} \times 15 \Delta s$, where (if a is the coefficient of expansion)

$$a = \frac{\Delta \rho / \rho_0}{\Delta t} = \frac{\rho_m \cos \theta}{\rho_0 H} \frac{\Delta x}{\Delta t} = 109 \frac{\Delta x}{\Delta t} = 10^{-3} \times 1.63 \frac{\Delta s}{\Delta t}$$

Thus the coefficient found is but $a = 0.0024$.

A number of subsequent experiments indicated that a was always small if measured in a temperature-rising series, but approached a normal value if measured on cooling. Figure 36, curve b, shows a case of this kind. To guard against incidental temperature disturbance, the compensating cold-air tube was placed at a distance and connected with $\frac{1}{8}$-inch lead pipe with its shank of the U-tube. It will be seen that in the up-going branch the curve rises with almost the same slope as before, so that $a = 0.0024$ here also. The down-going slope soon becomes steeper. Hence $\Delta s / \Delta t = 2.15$, so that $a = 0.00163 \times 2.15 = 0.0035$, which is a closer approach to the standard value, but still definitely short of it.

Although the curve b runs below $s = 0$, on further cooling in the lapse of time, the micrometer zero was nevertheless quite regained. Thus there is something here cyclic and viscous in character. As one can hardly fancy any difficulty for the heat to get through the thin quill tube, the thrusts on the mercury surfaces in the gage are met by an apparent static resistance there. On cooling these relations are reversed. What is rather striking is the parallelism of the up-going curves a and b in spite of the deficiency, particularly as all the other experiments behaved similarly.

Taking the work as a whole, it seems as if the above capillary resistance to thrust is effective here also, so that the pressures, if increasing, are not fully registered in a depression of the surface of the U-gage. A few experiments were thereafter made with a steam jacket. In the first the heating was done too near the interferometer, so that a displacement of fringes occurred. The zero was therefore taken after the exposure to 100°. The results were $\Delta x = 0.00171$ cm. for a rise of temperature from 25° to 100°, so that

$$a = 109 \frac{0.00171}{75} = 0.00248$$

In the second the fringes returned to zero before and after the exposure to 99.7° (boiling-point); but the fringe displacement was only equivalent to $\Delta x = 0.00145$, so that

$$a = 109 \frac{0.00145}{72.7} = 0.00218$$

Both values are as usual too small. Curiously enough, no fault could be found with the technique in the second, which is the smallest, the heating apparatus, etc., being placed at a distance. The fringe displacement should have been equivalent to 0.00247 cm. or 4.94 scale-parts in place of the 2.9 obtained. The deficiency is thus 2 scale-parts or $\Delta x = 0.001$ cm.

This difference tends to be static. If we turn again to the case of hydrogen (§ 29, with the same constants), $\Delta\rho$ is roughly 10^{-4} too small, so that the observed Δx is $10^{-4}/0.1415 = 0.7 \times 10^{-3}$ cm. short of its true value, which is even less than the discrepancy just considered, although the hydrogen Δx is 5 times larger.

32. Vapor pressure. Hygrometry.—A few other incidental experiments were made with the old gage, as follows: To determine the atmospheric vapor-pressure, dry air and wet air were alternately pumped through the tube tt', figure 31. In the latter case the air was passed in a tube over wet filter-paper. As but a small fringe displacement is to be expected, the method is not good, for there is considerable commotion of fringes incidental to the pumping, so that the zero is not quite trustworthy. Many alterations of the kind specified gave a mean value of about 4 scale-parts as the excess pressure for wet air at 23.8° and 75.3 cm. of the barometer. Hence $\Delta\rho = \rho' - \rho = \rho' - \left(\dfrac{p-\pi}{p}\,\rho' - \rho_w\right)$ if π is the vapor-pressure and ρ_w the saturation vapor density of water-vapor at 23.8°. Thus

$$\Delta\rho = \frac{\pi}{p}\,\rho' - \rho_w = \Delta x \cos\theta\rho_m/H = 0.1415\Delta x = 10^{-6}\,2.1\Delta s$$

if $\Delta x = 10^{-6}\,15\Delta s$, as here found. Hence for $\Delta s = 4.5$, $\Delta\rho = 10^{-6}\,2.1 \times 4.5 = 10^{-6}\,9.4$, and

$$\rho_w = \frac{2.22}{75.3}\,0.00118 - 10^{-6} \times 9.4 = 10^{-6} \times 25$$

The actual saturation vapor density is $10^{-6} \times 22$, which is as close as one can expect to come.

Repeating these experiments at some length in the summer time, no certain fringe displacement could be detected equivalent to the alternate passage of dry air ($CaCl_2$) and of wet air (bubbled through water) through the tube. The computed displacement should have been over $\Delta s = 20$ scale-parts. I failed to detect a reason for this persistently negative result, unless it is much more difficult to dry the tube than I anticipated. Heating the tube was of course out of the question.

33. Gage tests by direct compression.—Measurements of this kind were made when I first used the interferometer **U**-gage (Carnegie Inst. Wash. Pub. 310, p. 2, 1921), but only cursorily. The method consists in closing one shank of the **U**-tube and compressing the air within by advancing a fine-threaded thin screw by a definite number of turns. Unfortunately, the closed region is a sensitive air thermometer and the results obtainable in a steam-

heated room will show a cyclic progress due to the slight change of temperature. Figure 37 gives data of this kind, the abscissa showing the number of turns of screw and the ordinates Δx the displacement of the slide micrometer to bring the fringes back to zero. Ascending and descending series are indicated by arrows. I worked as quickly as the micrometer could be set, and though the zero in Δx was finally nearly regained, the curves are cyclic.

Figure 38 (decreasing pressure positive) summarizes corresponding results when the room was unfavorable. In the ascending branch the rate is $10^{-6}\,575$ cm. per turn before the break at a, where the fringes were incidentally shaken. In the return branch there is initially a kind of back-lash, after which the uniform rate $10^{-6}\,680$, much higher than before, appears. Many other examples of the same kind might be given, of which figure 37 is the best available.

The screw had a pitch of $\Delta l = 0.073$ cm. and its mean section was $a = 0.204$ cm.² Thus for one turn the volume decrement of the region is $dv = 0.204 \times 0.073 = 0.0149$ cm.³ On the other hand, the area of the shank was (diameter 9.5 cm.) $A = 70.9$ cm.², and its volume excursion therefore $dV = 70.9 \Delta x \cos \theta/2$, since but half the total head $\Delta h = \Delta x \cos \theta$ is allotted to one side. At constant temperature we may write

$$-\frac{dv}{V} + \frac{dV}{V} = \frac{dp}{p} = \frac{dh}{H} = \frac{\Delta x \cos \theta}{76}$$

if V is the total volume of the closed region and H the barometric height. If now we eliminate the common area

$$-\frac{dV}{V} = \frac{dh}{2h}$$

where h is the height of the cylindrical volume of the shank. If h can be estimated

$$V = \frac{adl}{\Delta x \cos \theta} \frac{1}{1/2h + 1/76}$$

where dl is the advance of the screw of cross-section a. This gives a fairly good value of V; but the height h is difficult to measure for the closed shank. If, on the other hand, h is not introduced, the equations lead to

$$-V = (76A/2)\left(1 - \frac{2adl}{A\Delta x \cos \theta}\right)$$

but the observations are not sharp enough to accurately evaluate the last factor, which is nearly zero. Thus, in the experiment and from figure 37, per turn of screw $a = 0.204$ cm.²; $dl = 0.073$ cm. (pitch); $\theta = 45°$; $A = 70.9$ cm.²: $\Delta x = 0.000595$ (cm./turn); whence

$$2adl/A\Delta x \cos \theta = 0.9986$$

and the parenthesis is thus but 0.0014 and is made up of errors of observation in the relatively large number 0.9946. In other words, the small piston a and the large piston A have moved as if the air were an incompressible fluid, if figure 37 is used for Δx.

In fact, if one accepts an estimate of $V = Ah = 70.9 \times 1.5$ cm.³, the corresponding value of Δx comes out $10^6 \Delta x = 571$ cm. Figure 37 shows that this lies quite within the range of thermal variation and could easily have been taken. Hence no discrimination can be carried out in this way unless the temperature conditions are ideal. Moreover, figure 37, while containing thermal cycles, curiously enough suggests no static effect in the values of Δx observed. Thus this leaves the whole question at issue open, and I am at a loss how further to approach it, except possibly with the change of apparatus indicated.

34. U-gage with fresh mercury.—The disquieting feature of the above work with hydrogen, viz, that the deficient pressures might be referable to
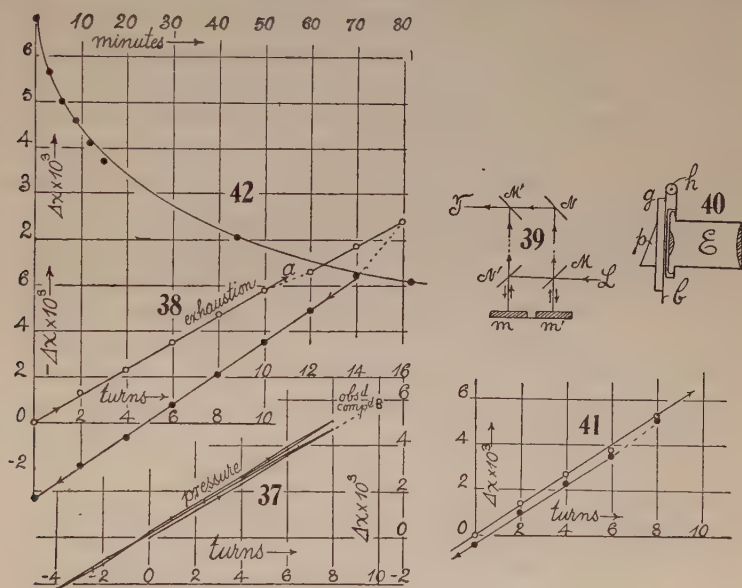
viscous or capillary resistances in the old mercury of the **U**-gage, induced me to introduce a fresh change of distilled mercury. A larger quantity, moreover, was taken, which makes the mercury more mobile than the shallow disk-like charge. The fringes are thus harder to read, but the quivering mercury surface is more liable to conform to a true reading. The fringes were at first hard to find. In the quadratic interferometer the spectrum fringes (in view of the fact that the component rays pass through the half-silvers M, N', M', fig. 39, twice) are too faint to be seen if very small and if a prism grating is used in front of the objective of the telescope at T. The visibility can be very greatly improved, however, by placing the grating in front of the ocular. For this purpose prism grating pg, figure 40, is attached to a brass plate hinged at h to a second plate clamped to the edge of the ocular. The plates are perforated. When not needed, the grating pg is therefore swiveled

out of range and the fringes of white light become available. When pg is used the collimator is provided with a slit parallel to the edge of the prism. In the case of white light the slit is widened at right angles to the fringes, so that they may play across the plate micrometer which now replaces the slit. An ocular plate micrometer is not desirable, as the telescope must frequently be shifted.

The advantage of the spectrum fringes, or channeled spectra, lies in their range of visibility. They are easily identified long after the white fringes have left the field. The type of spectrum fringes which usually appear in this adjustment is fan-shaped, as they open out from violet to red. Those of maximum size and coinciding with the white fringes are normal to the slit. From this they diverge on both sides symmetrically, growing continually finer, until the hair fringes are nearly parallel to the slit.

The behavior of the new gage when tested with the air-compressure screw was apparently better than the old gage. One example of results is given in figure 41, in which the ascending and descending rates are $\Delta x = 0.00067$ cm. and 0.00066 cm. per turn of screw. Nevertheless, between the two graphs there is something akin to the former back-lash, which amounts on the average to nearly $\Delta x = 0.0005$ cm. Granting that by reason of the inevitable thermometer errors of a closed region these data are not very searching, the breadth of loop here obtained is nevertheless of the order of the discrepancy of the data in tables for H_2 gas (§ 29), the mean deficiency in the old gage for thrusts being $\Delta x = 0.00077$. It thus begins to look as if an increment of the order of about 0.0005 cm. of mercury (say 7 dynes/cm.^{2}) is not a gravitational resistance when obtained with the mercury gage, owing to the appearance of capillary and similar surface forces. This critical question will have to be left for conditions of constant temperature such as occur in the summer only.

35. New quill-tube experiments with hydrogen. (Fresh mercury.)— The endeavor was now made to obtain better results for hydrogen by aid of the new gage. In the first series the glass quill tube ($l = 68.4$, $2r = 0.3$ cm.) was again used, a number of useful improvements having been added. The essential data are given in table 5.

TABLE 5.

Bar.	t	$\Delta x \times 10^4$	$\Delta \rho \times 10^6$	$\rho_t \times 10^6$	$10^6 \rho_0$	Deficiency $\Delta x \times 10^4$
cm.	.	cm.				cm.
74.9	23.6	68.5	969	183	201	8.6
	24.0	70.5	998	151	160	5.9
	24.0	70.0	991	158	174	6.5
	24.0	70.0	991	158	174	6.5
	24.0	68.0	976	173	190	7.8

The mean of these results, taken independently at different times of the day, is $\rho_0 = 0.000181$, practically the same value as that obtained above (§ 29,

$\rho_0 = 0.000188$), the difference being referable to the cos θ of the interferometer, which is here newly adjusted. Hence the change of gage, the supply of fresh pure mercury, etc., has made no appreciable difference in the run of density values obtained. The mean deficiency in Δx is again about 0.71×10^{-3} cm., which compares closely with the 0.77×10^{-3} cm. above. This means that a pressure of about 5×10^{-4} cm. of mercury is borne by the capillary forces of the U-gage and does not appear in the gravitational or fringe displacement of the surfaces of the mercury.

In case of the first experiment of the table, the diffusion of the gas in the quill tube into the air was followed for over 80 minutes. The results are given in figure 42. The slide micrometer alone was used, the fringes being brought back to the fiducial mark in the ocular at the times given in the figure. It is interesting to note that after an hour and a half considerable hydrogen pressure is still evident in the charged tube. The coefficient of diffusion from both ends of the tube would naturally be low as before; but the constants of the curve (fig. 42), if taken for diffusion from the bottom of the quill tube only, were much nearer the correct datum, 0.81 (the coefficient being a^2), than heretofore. The march of a in the lapse of time, though still apparent, is reduced. The data are

$t = 15^m$	$a = 1.160 \ (1 - 0.161 + 0.031) = 1.009$	$\Delta x_0/\Delta x = 1.80$
$t = 30^m$	$a = 1.133 \ (1 - .084 + .008) = 1.046$	2.49
$t = 60^m$	$a = 1.434 \ (1 - .025 + .001) = 1.434$	4.56

One may note in relation to the sequel, §§ 43, 46, that a has not fallen below 1.

36. Experiments in wider and longer tubes (gas-pipes).—The results obtained when $\frac{1}{8}$-inch and $\frac{1}{2}$-inch iron gas-pipes held the charge of hydrogen were as follows:

Tube.		Bar.	t	$\Delta x \times 10^4$	$\Delta \rho \times 10^6$	$\rho_t \times 10^6$	$\rho_0 \times 10^6$
$2r = 0.5$ cm.	$l = 70.5$ cm.	75.1	25.1	72.5	996	151	168
1.6 cm.	74.0 cm.	75.1	26.2	75.0	975	157	174

These data for about the same length of tube as before are of the same order of value. It was interesting to note that even for the wide tube (diameter 1.6 cm.), the experiments as such proceeded smoothly. The question of a more critical import, however, would be answered by longer tubes; for with these the true density should be approached more closely as the length is greater, seeing that the static character of the capillary error had been retained. This proved to be the case, as shown by the next table.

Tube.		Bar.	t	$\Delta x \times 10^4$	$\Delta \rho \times 10^6$	$\rho_t \times 10^6$	$\rho_0 \times 10^6$	$\dfrac{\Delta p}{\text{cm. Hg.}}$
$2r = 0.5$ cm.	$l = 158$ cm.	cm. 75.2	20	170.0	1,034	141	153	0.0120
		75.2	20	173.5	1,056	119	129	.0122

In the first experiment the freshly made hydrogen probably still contained a little air. As stated above, the pipe was repeatedly refilled by turning the three-way cock. Fringe displacements of such readings are remarkably constant; but even if the cock is closed for but a minute, there is considerable throw of fringes on opening, showing that the initial diffusions, together with temperature accommodations, are marked.

Unfortunately, to accommodate this long tube below the interferometer, it was necessary to poke it through the floor into the basement. As a result the temperature (winter) varied from $15°$ below to $25°$ above the floor, so that a mean value was taken. The static discrepancy is of the same order as before, about 0.0005 cm. The total pressure difference is roughly $\Delta p = 0.012$ cm. of mercury here.

Thus it seems that for pressures below $\delta h = 0.0005$ cm. of mercury, or the corresponding Δx increments, little can be done but to add this discrepancy δx to the Δx obtained. This δx in other words is the capillary or viscous resistance which attaches itself to the gravitational resistance of the depressed mercury column of the U-gage. Hence our equations would read at the given temperature t (ρ_t to be corrected for vapor-pressure)

$$\rho_t = \rho_a - C(\Delta x + \delta x) - \rho_w$$

where ρ_w is the density of water vapor at t, if present, ρ_a the density of air, and $C = \rho_m \cos \theta / H$ for the tube-length H. In the last series ($\delta x = 0.0006$ accepted)

$$\rho_t = 0.001192 - 0.0608(0.0173 + 0.0006) - 0.000017 = 0.000083$$
$$\rho_0 = 0.0000897$$

which is nearer than one would expect to come, considering the variable temperature $15°$ to $25°$ of the pipe, the non-rigorous purity of the gas, and the capricious character of the correction δx, the latter being not smaller than 0.0005 cm. as taken, and may run to 0.0007. The correction for vapor-pressure would reduce ρ_0 a few per cent. To minimize the capillary effect, the diameter of the shanks of the U-tube was made large (10 cm.). There may be a further advantage in diminishing the size of mirror (glass plate) anchored in the middle of the vat. Another feature is not to be overlooked, viz, in a gage, like the present, not filled in vacuo, the mirrors do not move rigorously in parallel. Hence a small obliquity error is introduced.

If the mirror on the slide micrometer is not quite plane parallel, but a wedge of small angle ϕ, a path difference of $(\mu - 1) \phi \tan \theta \cdot \Delta x$ would be introduced. This, however, from the smallness of both ϕ and Δx, is negligible.

37. **Capillary gage correction, δx, in case of hot air.**—It has already been inferred that this correction is the same in the hydrogen and hot-air experiment, though the pressures Δx are widely different, relatively. The measurement of the coefficient of expansion of air is thus an extreme test; for here the δx is over one-third as large as Δx. Conformably with the data already obtained (§ 31), the coefficient must thus come out much too small. If we write

$$-(d\rho/\rho)/d\tau = 1/\tau \text{ and } 1/\tau_0 = (1/\tau)(\rho_0/\rho)$$

at constant pressure, where the subscript refers to zero centigrade, the coefficient of expansion may be computed as

$$I/\tau_0 = (\rho_0/\rho)(d\rho/d\tau)/\rho = a$$

A new apparatus was used, consisting of a vertical $\frac{1}{8}$-inch gas-pipe 70 cm. long, open below and communicating with the **U**-gage above, as in figure 31. This pipe was surrounded by a steam jacket of $\frac{3}{4}$-inch gas-pipe, the whole firmly screwed together, with an addition of other improvements.

In the first experiment with the room temperature at $27°$ and $\delta x = 0.0006$ cm. accepted, the data were $\Delta x = 0.0015$, $\Delta x + \delta x = 0.0021$ cm., $\Delta\tau = 73°$, $\rho/\rho_0 = 0.90$, $\rho = 0.00117$; whence $\Delta\rho = 0.137(\Delta x + \delta x) = 0.000288$; $(\Delta\rho/\Delta\tau)/\rho = 0.0034$, $(\Delta\rho/\Delta\tau)/\rho_0 = 0.0037 = I/\tau_0 = a$, which is as near the coefficient of expansion as one may hope to approach conformably with the micrometer reading to $\Delta x = 10^{-4}$ cm. An error of 3 or 4 per cent in the coefficient of expansion is to be expected from this source alone.

In a variety of subsequent experiments, values of a rather higher than the one given were found, so that capillary discrepancies as low as $\delta x = 0.0004$ cm. may have been operative. But as the whole the presence of this quantity, of the order of values given, may in this particular work be regarded as substantiated, even for such small total density increments as are here in question ($\Delta\rho = 3 \times 10^{-4}$; $\Delta p = 2 \times 10^{-3}$ cm. of mercury).

38. Diffusion in one direction only.—In the above work, two discrepancies were left outstanding. One related to the diffusion from the top and bottom of the vertical quill tube under conditions not identical. Here, moreover, the possibility of practically exhausting the tube of its charge of hydrogen at its middle point is not to be overlooked. The other is the error of Δx, resulting from quasi-capillary phenomena at the mercury surface of the **U**-gage. These were counteracted by adding a correction δx to the Δx observed, and the group of experiments made seemed to conform to a nearly constant positive value of δx.

Two methods were now employed in the endeavor to remove these disturbances. These consisted in filling the whole system tCG, figure 31, of diffusion tube and shank of **U**-gage with the gas (hydrogen) to be tested; or if this should be inadvisable, to diminish the bore of the cock C to a mere crevice, while increasing the bore of the diffusion tube tt. In such a case loss by diffusion at the top could be considered negligible.

The modification of the apparatus (fig. 31) is shown in figure 43, in plan, where H is the source of hydrogen, U one shank of the **U**-gage (closed),

C the three-way cock, t the vertical diffusion tube. The influx pipe is branched at b and provided with two glass stop-cocks c and c'. If C is adjusted as in the figure, c and c' open, the gas fills the gage U first and then by the branch de and C, enters the diffusion pipe t and leaves at its open lower end. On completed filling, c' is permanently closed, after which t may receive H_2 via bf by properly turning the cock C, and may be alternately
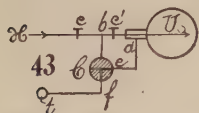
placed in connection with U only, as in figure 43 (c' being closed). The cock c' is as fine in bore as possible, as is also the cross-branch in C, thus preventing the rapid influx of gas into U, which might dislocate the fringes. Other devices were tried, but figure 43 sufficiently indicates the general method.

The attempt to flood the **U**-gage with hydrogen, no matter how carefully done, always resulted in a large displacement of the zero-point of the gage; and to my astonishment this displacement was now in the *opposite* direction to that obtained in the preceding (§ 37, etc.) paragraphs; *i. e.*, δx had changed from positive to negative values. In other words, Δx was now too large. This occurred so consistently that I was inclined to refer the effect observed to changed capillary properties of a mercury surface in an atmosphere of H_2 as compared with the same surface in an atmosphere of air. But as these effects are always accompanied by a marked distortion of fringes, meaning that the mean inclination of the surface has changed, it is difficult to reach a trustworthy conclusion.

39. Incidental results. Density.—As all the diffusion experiments were preceded by density measurements, it is of interest to give these results separately, at the outset. In place of the density ρ_h, however, it will here be preferable to compute the micrometer displacement (Δx), which should have been obtained for the hydrogen density 89.6×10^{-6} under normal conditions of temperature and pressure. The equation reads, at t degree,

$$\rho_h \frac{B-\pi}{B} = \rho_a - \Delta\rho - \rho_w = \rho_a - C\Delta x - \rho_w$$

whence

$$C\Delta x = \rho_a - \rho_h(B-\pi)/B - \rho_w$$

where B is the barometric pressure and π the vapor-pressure of saturated water-vapor, ρ_a, ρ_h, ρ_w the densities of air, hydrogen, and vapor all at the same temperature t. If ρ_a as in the following experiments is also moist, ρ_w disappears and

$$\Delta x = \frac{B-\pi}{BC}(\rho_a - \rho_h)$$

Thus it appears also that the rate at which ρ_h varies with Δx is roughly $-C$. Hence if the error of Δx is 10^{-4} cm. and C is about 0.13 in these experiments, the effect on ρ_h would be $10^{-5} \times 13$. Since the density of H_2 is below $10^{-6} \times 90$, this is an error of nearly 15 per cent. It will therefore be best to report the values of Δx as found, together with the value computed, as has been done together with the relevant data in table 6.

Thus the effect of flooding the **U**-gage with hydrogen is a relatively enormous displacement of the zero of fringes before and after the operation. Whenever this occurs, moreover, the Δx observed for the density measurement is correspondingly changed, and in the present case (unlike that of the preceding

experiments) in the direction of an increase of Δx, $i.$ $e.$, δx is negative.* As has been stated, this effect or the reversal of sign of δx might seem to be attributable to the behavior of a mercury surface in an atmosphere of hydrogen; but the experiment is so complicated and the data so capricious that no confidence can be placed in such an inference. When Δx is found without flooding and the zero before and after the measurement is the same, the values are reasonable. In two cases, series IV, third experiment, and series VI, first experiment, Δx is practically correct. In one case, series II, experi-

TABLE 6.

Tube 2.	Series.	Initial zero $10^4\Delta x$.	Final zero $10^4\Delta x$.	Observed $10^4\Delta x$.	Computed $10^4\Delta x$.	$\dfrac{\rho_a\times10^6}{\rho_h\times10^6}$	$\dfrac{(B-\pi)}{B}$ C	Remarks.
		cm.	cm.	cm	cm.			
$l=71$ cm. $2r=0.7$ cm.	I	134	101	86	79	1,177 81.5	0.972 .1354	After diffus.exp't, H at U-tube.
	II	113	113	75	80	1,191 82.6	.974 .1354	Separate exp't, air at U.
	II	113	108	82	80	1,189 82.4	.974 .1354	After diffus.exp't, H at U.
	III	77	80	82	80	1,193 82.8	.975 .1354	Separate exp't, air at U.
	IV	107	83	82	80	1,192 82.7	.971 .1354	Separate exp't, H at U.
	IV	111	111	82	80	1,192 82.7	.971 .1354	After diffus.exp't, air at U.
	IV	121	121	78	78	1,183 82.1	.964 .1354	Sep. exp't, next day, air at U.
$l=74$ cm. $2r=1.7$ cm.	V	119	119	84	81	1,179 81.8	.962 .1300	Separate exp't, air at U.
	V	119	120	84	81	1,179 81.8	.962 .1300	After diffus.exp't, air at U.
	VI	123	123	83	83	1,187 82.4	.974 .1300	Separate exp't, air at U.
	VI	127	57	91	83	1,187 82.4	.974 .1300	After diffus.exp't, H at U.
	VI	87	87	88	84	1,198 83	.975 .1300	Sep. exp't next day, air at U.

ment 1, Δx is deficient as in the earlier results. Usually it is in excess by 2×10^{-4} or 3×10^{-4} cm. After vigorous flushing, with much inevitable commotion of fringes (series I, and series VI, experiment 2) the excess may reach 8×10^{-4} cm. In the latter case the excess had not even vanished on the ensuing day ($\delta x=4\times10^{-4}$), though as a rule there is an apparent recovery after the hydrogen atmosphere around the mercury has been dissipated. When the zero is much displaced, the recovery is very obvious during the march of the ensuing diffusion and the fringes show increasing distortion. The diffusion data are then erroneous, as will presently be seen.

Obviously, therefore, the method of flooding the U-gage with hydrogen is not safely available. It is thus necessary to use a very fine perforation in

---

* Since the U-gage has two surfaces, this merely means that δx is now positive on the other shank.

the cock C at the head of the diffusion tube and to make this as wide as practicable. In table 5 the second tube used had a diameter of 1.7 cm. and an area enormous in comparison with the crevice in the stop-cock above. A capillary-tube connection would be even preferable, if available.

40. The same. Diffusion.—The diffusion curves, of which seven examples are given in figures 44 to 50, require more searching examination. The curves, as a whole, when considered in relation to the behavior of an interferometer **U**-gage, with the fringes successively placed at zero by a slide micrometer (displacement Δx at $\theta=45°$), are remarkably regular. When studied with more critical detail, however, they present many anomalies. Table 7 presents a number of these peculiarities.

In the first and second series, the cocks were of about 1 mm. bore as compared with the tube diameter of 7 mm. Curiously enough, the data here obtained are nearly as good as any of the following, in spite of later improve-

ments. The pressure ratios at the beginning and end of 50 minutes of diffusion are 3.18 and 3.30 respectively, pressures being proportional to the initial and final Δx.
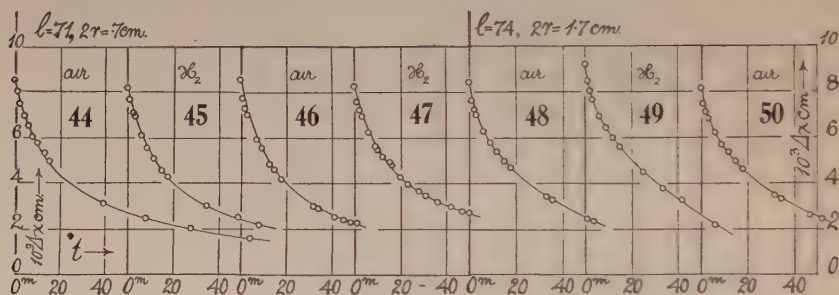
In series III and IV the bore of the cocks was reduced to mere crevices, the same diffusion pipe being retained. In series III there must have been some incidental dislocation of fringes (marked †). The effect of this as it gradually vanishes is to increase the diffusion-rates spuriously. The same effect appears in the drop of Δx in 50 minutes.

In series V and VI, retaining the same fine-bore cocks, a wide diffusion tube was substituted. Series V is among the best of the lot. In series VI the commotion due to influx of H_2 produces a condition similar to that in series III, but more marked. Series VII was made later. If we omit the cases marked (†), the ratio of H_2-pressure at the beginning and end of 50 minutes of diffusion has the mean value 3.19 for the thin pipe. It is rather disappointing that the laborious work of flooding the **U**-gage and using fine-bore cocks has evidenced so little improvement on the results.

Inasmuch as the series VI is not trustworthy, a special series (VII) was investigated, using the original method of figure 31, but with a fine-bore

cock C. The attempt was made to connect C and U by metallic and by glass capillary tubes. It was found that diameters up to 0.5 mm. could not be used because of the viscosity of the gas. In fact, the U-tube behaved like a closed region with a wandering zero (Chap. I), and the results were worthless. A connecting-tube with a diameter exceeding 1 mm. was found essential. To guard against transpiration leakage, all rubber-tube connections, though used sparingly throughout the experiments, were painted over with soft sealing-

TABLE 7.—*Data of diffusion measurements.*

	Series.						
	I	II	III	IV	V	VI	VII
Initial zero, $x \times 10^4$ cm.	135	113	77	108	119	127	85
Final zero,* $x \times 10^4$ cm.	101	108	80	83	120	52	86
Temperature, ° C....	23.2	22.9	22.0	22.3	22.9	23.1	21.2
Initial reading, $\Delta x \times 10^4$ cm. obs.	86.0	82.0	†85.5	82.5	84.0	†91.5	81.0
Initial reading, computed	79.2	80.0	80.4	80.3	82.6	83.2	83.5
Final reading, $\Delta x \times 10^4$ cm., obs. after 50 minutes	27.0	24.8	22.5	26.7	25.0	26	25.0
$10^4 \times \Delta x$ drop in 50 minutes	59.0	57.2	63.0	55.8	59.0	65.5	56.0
Pressure ratio in 50 minutes	3.18	3.30	†3.80	3.10	3.36	†3.52	3.24
Mean a (50 minutes).	1.111	....	....	....	1.201	....	....
Atmosphere at U-gage	Air	H_2	Air	H_2	Air	H_2	Air
Pipe-length, l cm....	71	71	71	71	74	74	74
Pipe-diameter, $2r$ cm.	.7	.7	.7	.7	1.7	1.7	1.7
Glass-cock bore, cm..	.15	.15	crevice	crevice	crevice	crevice	crevice
Reading ($\Delta x \times 10^4$ cm.) after 15 minutes	50.0	46.0	45.5	47.5	49.5	55.5	49.5
$\Delta x \times 10^4$ drop in 15 minutes	36.0	36.0	†40.0	35.0	34.5	†36.0	31.5
Pressure ratio (15 minutes)	1.72	1.78	†1.88	1.74	1.70	†1.65	1.64
Mean a (15 minutes)	1.039	....	....	....	1.037	....	.....

* The final zero, of course, was taken for the Δx data.   † Referred to in text.

wax. Under these circumstances the observations of series VII (fig. 50) proceeded faultlessly, as appears in the zeros, which before and after the diffusion are practically the same. The displacement or pressure ratio 3.24 at the beginning and end of 50 minutes is nevertheless the same as the mean of series I and II. Hence the additional care taken seems to have been superfluous. Series V has an equally fixed zero; hence the pressure ratio 3.30, the mean of series V and VII, may be taken as holding for the wide diffusion tube (bore 1.7 cm.).

5

To compute the coefficient of diffusion, a^2, when the escape of hydrogen takes place at the lower mouth only, the equation

$$a = \frac{\Delta x_0}{\Delta x} \frac{l}{2\sqrt{\pi t}} \left(1 - l^2/24a^2 t + l^4/480a^4 t^2 - \right)$$

is available. The series converges slowly, unless t is large, and for this reason the time interval $t = 50$ minutes was taken throughout. The pressure ratio $p_0/p = \Delta x_0/\Delta x$, where Δx_0 and Δx are the slide-micrometer displacements at the beginning and end of $t = 3,000$ seconds. For the case of series I, II, IV we therefore have $l = 71$ cm., $t = 3,000$ seconds, $\Delta x_0/\Delta x = 3.19$, whence uncorrected $a' = 1.167$. The term $-l^2/24a^2 t = 0.0515$ and $l^4/480a^4 t^2 = 0.0032$, which makes the full correction $1 - 0.0483$; whence $a = 1.167 \times 0.9516 = 1.111$ and $a^2 = 1.234$. For the case of series V and VII obtained with the wide tube, $l = 74$ cm., $t = 3,000$ seconds, $\Delta x_0/\Delta x = 3.30$; whence $a' = 1.258$ and the correction terms -0.0481 and $+0.0028$, respectively. This makes $a = 1.258 \times 0.955 = 1.201$ and $a^2 = 1.440$. The mean of these values, $a^2 = 1.337$, is about twice as large as the value for hydrogen (0.66) usually given. It thus becomes a question to search for the cause of this large divergence.

In view of the tendency of the values of a to rise in the lapse of time, I also made the computation for an interval of 15 minutes. The data are inserted in the bottom of table 6. It is very interesting to note that the run of the ratio of pressures, $\Delta x_0/\Delta x$, for narrow and wide tubes is about the same (excluding the first exceptional value marked) and that it is smaller for the wide tubes. This eliminates the appreciable occurrence of convection errors. The results came out as follows:

$2r = 0.7$ cm., Series I, II, IV: $a = 1.168$ $(1 - 0.1709 + 0.0351) = 1.009$
1.7 cm., Series V, VII: $a = 1.176$ $(1 - 0.1832 + 0.0403) = 1.008$

Thus the values of a for the $\frac{1}{8}$-inch and $\frac{1}{2}$-inch gas-pipe happen to coincide. They are, however, smaller, as was anticipated, than the values for a lapse of 50 minutes; but they agree admirably with the values obtained with very long tubes below.

The further decrease of a does not occur; for if $t = 7.5$ minutes, the computation shows

$2r = 0.7$ $a = 1.342$ $(1 - 0.260 + 0.081) = 1.10$
$2r = 1.7$ $a = 1.368$ $(1 - 0.271 + 0.088) = 1.12$

Thus a has risen; but the t-interval is now too small.

41. Inferences relative to equations.—In spite of the minor discrepancies, the mean value of a found for long tubes of all diameters, from quill sizes to tubes over 0.5 inch in bore, for 50-minute intervals, is of the order of value $a = 1.1$ to 1.2; and this is about 50 per cent larger than the value $a = 0.8$, estimated. So much can not be accounted for in terms of any of the capillary distortions, δx, discussed above. Moreover, they are not observed to vanish between the initial Δx_0 and the final Δx 50 minutes later. They merely account for the differences of value in a obtained in the different series. With tubes

of so many diameters, moreover, the effect of leakage or diffusion at the top must be negligible, else the thin pipes would have shown it.

The effect produced by the rise of the mercury surface in the **U**-tube during diffusion produces a slight current down the diffusion tube. Since $\Delta x = 0.0057$ about, the rise of mercury surface may be put $\Delta h = 0.004$ cm., which is equivalent to a decrement of volume of 0.31 cm.[3] This air passes through the diffusion tube of a diameter 0.7 cm. or greater. Hence the total displacement of the air column in the diffusion tube is about 1 cm. In the wide tube (diameter 1.7 cm.) the displacement would be 0.14 cm. Both may be here disregarded, as the experiments show.

Though the attempt has already been made (§ 27) to treat the concomitant effect of the influx of air at the bottom of the tube, it is necessary to examine this occurrence from the point of view of diffusion. If we denote by ρ_0' the density of air at the atmospheric temperature and pressure of the experiment and by a', the corresponding diffusion coefficient of air into hydrogen, the problem becomes an inversion of the case for hydrogen and thus leads to

$$\rho' = \rho_0'\left(1 - \frac{2}{\pi}\int_0^{x/2a'\sqrt{t}} e^{-\beta^2}d\beta\right)$$

where ρ' is the density of the air at t seconds at x cm. from the end of the tube. Expanding the integral as before, and integrating for the length l of tube,

$$\rho' = \rho_0'(1 - (l/2a'\sqrt{\pi t})(1 - l^2/24a^2t + l^4/480a'^4t^2 -)$$

where ρ' is the mean density at t seconds of the air left in the tube.

If we add the corresponding mean density of hydrogen at the same time, the total mean density $\bar{\rho}$ of the mixed gas in the tube is

$$\bar{\rho} = \rho_0' - (\rho_0'l/2a'\sqrt{\pi t})(1 - \dots) + (\rho_0 l/2a\sqrt{\pi t})(1 - \dots)$$

Ignoring the correctives temporarily for brevity, this may be converted into pressures, $p = gl\bar{\rho}$, etc., whence

$$\bar{p} = p_0' - (l/2\sqrt{\pi t})(p_0'(1 - \dots)/a' - p_0(1 - \dots)/a)$$

If we solve this for a, the reduced result is

$$a = \frac{ap_0'(1 - \dots)/a'p_0 - (1 - \dots)}{p_0'/p - 1} \frac{l}{2\sqrt{\pi t}} \frac{p_0}{p}$$

apart from the correctives in both terms of the first numerator. The expression may also be written

$$a = \frac{l}{2\sqrt{\pi t}} \frac{(a/a')(p_0' - p_0) - p_0(1 - a/a')}{p_0' - p}$$

If now, $a = a'$ nearly,

$$a = \frac{l}{2\sqrt{\pi t}} \frac{p_0' - p_0}{p_0' - p} = \frac{l}{2\sqrt{\pi t}} \frac{\Delta x_0}{\Delta x}$$

the expression used in the above computations with the inclusion of the correctives. But if a differs from a', the value so found is not correct. If we call the above original value A,

$$1 = \frac{A}{a'} + \frac{p_0}{p_0' - p} \frac{l}{2\sqrt{\pi t}} \left(\frac{1}{a'} - \frac{1}{a} \right)$$

a single equation with two variables, $1/a'$ and $1/a$.

Thus, if $a^2 - 0.66$ or $a = 0.81$, the value of a' computed from $A = 1.111$ from series I, II, IV above, would be $a' = 1.126$, somewhat lower than the A found. In this equation it is necessary to reduce p_0 to its equivalent in (Δx) by the equation $(\Delta x) \cos \theta \rho_m = l\rho_h$, where ρ_h is at atmospheric temperature. This makes $(\Delta x) = 0.000609$ cm. The Δx equivalent of $p_0' - p$ is given in table 6 above, and the mean value of $\Delta x = 0.00573$ cm.

The question is thus brought to a rather unsatisfactory conclusion; but I have not been able to find any further reason for corrections. True, there may be a release in capillary strain of the kind discussed when Δx_0 falls to Δx. Since, however, the zeros are often quite the same at the beginning and end of 50 minutes of diffusion, there is little probability in this assumption. A final device, viz, to contrast a very long and a very short diffusion tube, is still worth trying.

42. Diffusion in case of a longer tube.—Whatever the reason for the outstanding difference may be, it will be reduced by using the longest vertical tube available in the present installment. This was of length $l = 157$ cm. and diameter $2r = 0.7$, being $\frac{1}{8}$-inch iron gas-pipe. All rubber connections were waxed. The fringe displacement is thus about twice a slarge as the preceding. Unfortunately it was accompanied with considerable distortion. This distortion completely vanished in the course of the first series of data for diffusion (fig. 51), in which the observation was carried on for 3 hours. After 2 hours the diffusion curve is practically linear at a rate of $\Delta x / \Delta t = 30 \times 10^{-6}$ cm./min. Some H_2 would thus be left after 6 hours. The curve, in view of the fact that fringes were placed by the slide micrometer (displacement Δx), is remarkably regular. The error of Δx is now again negative as originally, or the correction $\delta x = +0.0008$ cm. (about 0.0006 cm. of mercury head) compatibly no doubt with the observed distortion. The constant $C = \rho_m \cos \theta / l$ is here $C = 0.0612$ and $\Delta \rho = C \Delta x$. This constant enters the density measurements only, the diffusion data being independent of it, and hence of θ.

The following values (table 8) enter into the density measurement conformably with $\Delta x = (B - \pi)(\rho_a - \rho_h)/BC$, where B is the barometric pressure and ρ_a and ρ_h refer to it and the temperature $\theta = 22.8°$.

TABLE 8.

Tube.	B	θ	π	$\rho_a \times 10^6$	$\rho_h \times 10^6$	Computed $\Delta x_0 \times 10^4$.	Observed $\Delta x_0 \times 10^4$.	Diff.
	cm.	°	cm.			cm.	cm.	cm.
$l = 157$ cm., $2r = 0.7$ cm.	76.34	22.8	2.07	1,197	83.1	177	169	0.0008

With the observed $\Delta x = 0.0169$, the density of hydrogen under normal conditions would come out $\rho_0 = 143 \times 10^{-6}$, corresponding to the long-tube values discussed above (§ 36).

Since the diffusion rates are necessarily slower for long tubes, larger time intervals t will be desirable to avoid excessive correctives. The data in table 9 (22.8°) are relevant, a' being uncorrected.

TABLE 9.

t sec.	a'	$l^2/24a^2t$	$l^4/480a^4t^2$	Factor.	a	a^2	Initial and final zero $\Delta x \times 10^4$.	$\dfrac{\Delta x_0}{\Delta x}$ observed.	$\dfrac{\Delta x_0}{\Delta x}$ computed.
3,000	1.270	0.2123	0.0112	0.799	1.015	1.030	112	1.57	1.64
6,000	1.124	.1356	.0221	.887	.996	.992	112	1.06	2.06
9,000	1.111	.0924	.0103	.918	1.020	1.040	...	2.38	2.50

Thus the mean values $a = 1.010$ and $a^2 = 1.021$ have apparently been brought somewhat nearer the usual tabulated values (0.81 and 0.66), but they are still in marked degree above them. Part of this might be supposed to result from the release of capillary strain virtually complete after 100 minutes; but as the computed $\Delta x_0 = 0.0177$ is *larger* than the observed $\Delta x_0 = 0.0169$, all the values of a would be 5 per cent larger, viz,

$$
\begin{array}{lll}
t = & 50 \text{ minutes} & a = 1.066 \quad a^2 = 1.137 \\
& 100 \text{ minutes} & 1.046 \quad\quad 1.095 \\
& 150 \text{ minutes} & 1.071 \quad\quad 1.147
\end{array}
$$

which actually brings these results nearer the short-tube values again. In the latter case one may notice that the wide-tube values, in spite of the smooth diffusion, are the largest. Hence it might seem probable that convection has something to do with the high results. Convection within the tube should accelerate diffusion or be favorable to loss at the lower end and the effect would be marked with tubes both wide and short. This inference is made untenable by the behavior of quill tubes which show the same large a, but in which convection must be negligible.

I am obliged to conclude, therefore, that values of the diffusion coefficient of hydrogen into air below $a^2 = 1$ have not been attainable by the method pursued. In figure 51a I have drawn the curve which should be observed if $a^2 = 0.66$, since $a \propto \Delta x_0/\Delta x \propto 1/\Delta x$, if the correctives are small. This may be assumed to occur for values of t greater than 100 minutes. The mean difference is about 0.0020 cm. in Δx. The occurrence of such a discrepancy resulting from capillary forces is out of the question, as it must have been detected in the large number of density measurements made, where δx falls below ± 0.0008; one would have to assume that the mercury surface of the gage in contact with the atmosphere is always supported, or that the closed shank in contact with hydrogen is always depressed by an equivalent capillary pressure. A unilateral effect of this size has nowhere been put in evidence.

43. Diffusion. Very long tube.—As the mean values of the coefficient a had fallen from $a=1.1$ or 1.2 to $a=1.010$ when the tube-length was doubled, the question arises whether a real limit has been reached. Accordingly the tube-length was again increased, this time to over five times the original length. To accommodate the new tube, $l=386$ cm. and $2r=0.7$ cm., it had to be placed *at a slant,* the top being at the influx cock C, 94.5 cm. above the floor, while the far end rested in the distance on the floor. Hence for the density measurements, $l=94.5$ cm., whereas for diffusion measurements $l=386$ cm. Far from being disadvantageous, this disposition has much to recommend it. The constant $C=\rho_m \cos\theta/l=0.1018$, since $l=94.5$ cm. In fact, the density measurements came out flawlessly at once, as, for instance:

Length radius.	Series.	Initial zero $x\times10^4$.	Final zero $x\times10^4$.	$\Delta x_0\times10^4$ observed.	$\Delta x_0\times10^4$ computed.	$\rho_a\times10^8$	$\rho_h\times10^8$	Temp. pressure.	τ
		cm.	*cm.*	*cm.*	*cm.*				*cm.*
$l=386$ cm. $2r=.7$ cm. } IX		112	112	105	105	1,187	82.7 { 23.5° 75.80 cm. }		2.15

In other words, the observed and computed fringe displacement, Δx_0, corresponding to the hydrogen pressure, are identical, which implies the standard hydrogen density.

The diffusion measurements are given (with the *doubled* time-scale marked near the curve) in the graph *b,* figure 51, and as a whole are also remarkably smooth. At the beginning, however, there is always some irregularity which I refer to inevitable convection at the free end, just after the tube is filled. This amounts to $3/105$ of the initial displacement Δx_0. One would be tempted to take the second point and a shortened tube-length, but such a selection would nevertheless be arbitrary.

Owing to the unusual length of tube, the diffusion proceeds very slowly, so that a long period of observation is necessary, if the diffusion equation is to converge rapidly. Observations were made throughout about 700 minutes on the same day and were continued the next day; but the latter were thrown out, as the zero had changed (temperature) during the night. I shall give these data as an example in full, in table 10, t being the time in minutes and Δx the corresponding micrometer displacement which brings the fringe back to zero. One may note that after 26 hours about 17 per cent of the original hydrogen pressure is still left in the tube.

Table 10 shows that 200 minutes is not sufficient for the practical convergence of the diffusion equation, but that after 400 minutes this may be assumed. I have, however, in the table given the mean of all results, as less arbitrary. Dropping the first a, the mean of the others is $a=1.002$. The mean might be diminished 3 per cent if the first observation were removed for the reasons given.

If, now, we compare the values of a obtained ($l=35$ cm. from next section) for different tube-lengths, viz,

	50-minute intervals.				10-minute interval.		10-minute interval.
		cm.	cm.		cm.		cm.
$l=71$ to 74		157	386	71	74		35
$a=$ 1.111 to 1.201		1.010	1.043	1.009	1.008		1.045
$a^2=$ 1.234 to 1.440		1.021	1.092	1.018	1.016		1.092
$2r=$ 0.7 to 1.7		0.7	0.7	.7	.7		1.7

remembering that the last could be reduced about 3 per cent, it is obvious that a limit has been reached within the errors of method and measurement. So far as I see, therefore, it does not seem possible to reach the relatively low values ($a=0.81$) usually quoted for the diffusion of hydrogen into air by the present apparently straightforward procedure. The results for wide tubes ($2r=1.7$ cm.), in which convection is most easily possible, are highest; but if the data for 15-minute intervals be taken, the first set ($l=71$, $2r=0.07$ and $l=74$, $2r=1.7$ cm.) leads to identical a values, 1.009 and 1.008, which fit the above data very closely.

TABLE 10.—*Diffusion of H_2 into air. Zero at $x=0.0112$ cm.*

[Long tube: $l=386$ cm., $2r=0.7$ cm., barometer 75.80 cm., temperature 23.5°.]

t	$\Delta x \times 10^4$	Δt	a'	$l^2/24a^2t$	$l^4/480a^4t^2$	a	a^2
min.	cm.	min.					
0	105	200	1.413	0.2600	0.0811	1.160	1.346
1	102						
2	101.5	400	1.192	.1824	.0400	1.018	1.036
3	101						
6	100	600	1.118	.1385	.0230	.989	.979
11	97.5						
30	95	700	1.118	.1188	.0169	1.004	1.008
58	89						
60	89			Mean		1.043	1.092
131	81						
181	76.5						
251	71						
291	68.5						
351	65						
393	62.5						
447	60						
591	54						
702	50						
(next day *) 1,485	19.5						
1,564	18						

* Zero at $x=0.0098$ cm.

44. Diffusion. Short tube.—By way of contrast, diffusion experiments with a short tube were finally made. They, moreover, serve as an introduction to the promiscuous experiments with gas-pressures made elsewhere. The tube

in question had the dimensions $l=35$ cm. and $2r=1.7$ cm., being half-inch iron gas-pipe. As the fringe displacements are small, they were read off directly (s) and then reduced if necessary to slide-micrometer values (x) by the equation $\Delta x = 10^{-6} \times 668 \Delta s$. The observed data are reproduced in figures 52 and 53, respectively, in Δx cm. and also in Δs, which are arbitrary
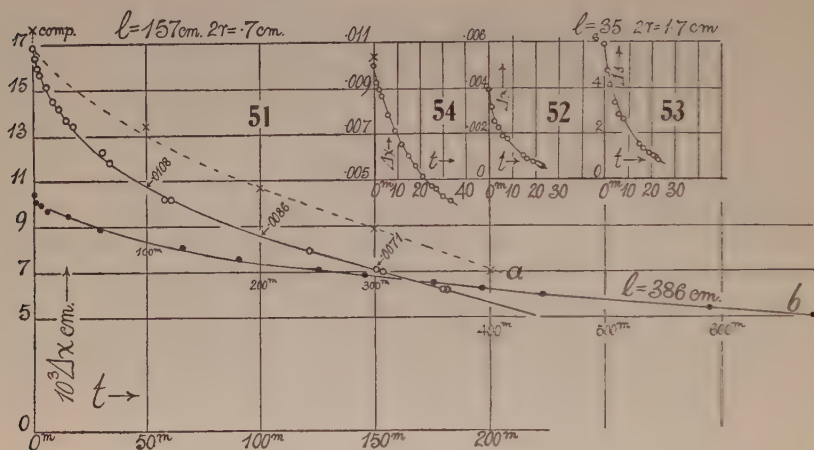
ocular scale-parts. In view of the shortness of the tube, the diffusion is rapid and relatively small time-intervals suffice to converge the equation, 10 to 20 minutes being deemed sufficient. As a further advantage of the small displacements, the zero remained quite the same before and after the diffusion experiment. The results of the measurement for density were ($C = \rho_m \cos \theta/l = 0.2747$) $l=35$ cm., $\Delta s_0 = 5.8$, $\Delta x_0 = 0.00389$ cm. (observed), $B = 75.41$ cm., $2r=1.7$ cm., $\Delta x_0 = 0.00388$ cm. (computed), $\theta = 23.5°$. Thus the normal density of hydrogen appears here at once and there happens to be no appreciable capillary correction.

For the diffusion coefficient it is convenient to take the s values directly, since

$$a = \frac{l}{2\sqrt{\pi t}} \frac{\Delta s_0}{\Delta s} \left(1 - l^2/24a^2 t + l^4/480a^4 t^2 - \right)$$

At $t=0$ second, $\Delta s_0 = 5.8$, and the curve gives further (temp. 23.5°),

l	t	Δs	$\Delta s_0/\Delta s$	a'	$l^2/24a^2 t$	$l^4/480a^4 t^2$	a
cm.	min.						
35	10	2.10	2.76	1.120	0.0678	0.0006	1.045
35	20	1.05	5.50	1.568	.0346	.0014	1.516

The diffusion thus increases for some reason, probably thermal convection, in the lapse of time. The mean value $a=1.28$ is too large, as was anticipated. It would probably have been better to use a narrow tube, seeing that at

10 minutes the corrections are small and the a value obtained closely in accord with the preceding long-tube values.

45. Quill tube.—Contrawise, the concluding experiment (fig. 54) with a long vertical glass tube ($l=94$ cm.) and a relatively fine bore ($2r=0.15$ cm.) accentuated the leak at the top, in spite of the crevice-apertured stop-cock employed. The density results came out fairly well, viz, bar., 75.34 cm.; temp., 25.0°; $\rho_a \times 10^6$, 1,174; $\rho_h \times 10^6$, 81.5; computed Δx_0, 0.01035 cm.; observed Δx_0, 0.01005 cm., the placement of the slide micrometer being too small by 3×10^{-4} cm., a return to the original sign of δx.

The diffusion data are also smooth, but rapid. The constants were

$$15 \text{ minutes} \ldots \ldots a = 1.480 \ (1 - 0.1867 + 0.0428) = 1.269.$$
$$30 \text{ minutes} \ldots \ldots a = 1.478 \ (1 - 0.0936 + 0.0421) = 1.401.$$

Again a increases in the lapse of time, which can not now be referred to convection, seeing that the bore of tube is only 1.5 mm. There seems no way of accounting for this, except in terms of the crevice-leak, on top, in relation to the small volume of gas in the vertical tube and of the gas expulsion from the tube below, where the mercury surface of the **U**-gage rises. The latter, since $\Delta x_0 = 0.01$, may be estimated at $\Delta h = 0.004$ cm., equivalent to a volume of 0.31 cm.³ Since the area of tube is 0.018 cm.², the displacement would be 17 cm. for the 94 cm. of tube. This is no longer negligible.

46. Conclusion.—Thus, finally, if we include the values for a found above for quill tubes, and use the smallest t compatible with a reasonably convergent equation, the results at about 22° to 23° are

l......	35	68.4	71	74	157	386	cm.
$2r$......	1.7	.3	.7	1.7	7	.7	cm.
t......	10	15	15	15	50	400	minutes.
a......	1.045	1.009	1.009	1.008	1.010	1.002	cm./√sec.

CHAPTER IV.

PIN-HOLE PROBE EXPERIMENTS, CHIEFLY WITH BRANCHED TUBES.

BRANCH PIPES.

47. Branch adjustments.—The simplest of these tube combinations is shown in figure 55, where U, U' are the two shanks of the mercury **U**-tube, the deplacements of the heads of which are read off by a vertical interferometer. The cylindrical spaces above U, U' are closed by glass plates and these spaces are coupled with telephones T, T' by quill tubes tt and $t't''$, the whole forming a closed region. The tube tt carries a T branch, into the free end of which the salient pin-hole s is inserted, short ends of pure-rubber tubing being available for junctions. Similarly, the tube $t't''$ is provided with the reëntrant pin-hole r. Thus U responds to T, U' to T', and the effect of either telephone may be quite removed by withdrawing the corresponding pin-hole adjutage. The telephones may also be examined together by coupling s and r with a short length of rubber tubing at a. In such a case either may be examined separately (T for instance) by closing the quill tube (here to be short) t''. If s and r are not coupled, but open to the air, a branch a' from t to t'' makes the registry impossible, the fringes remaining stationary at all frequencies.
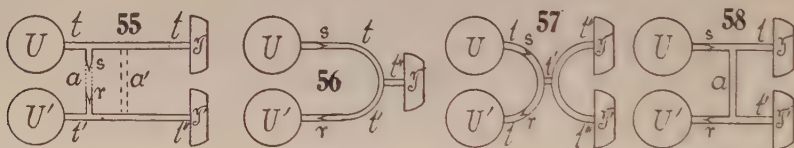
High-resistance radio telephones are preferable. A small inductor, with 20,000 to 40,000 non-inductive resistance in the secondary and one or two storage cells in the primary, is convenient for actuating the telephones. A break of variable frequency (usually c to c'') places the note. Small interference fringes, measuring 0.01 cm. in the ocular, are usually sufficient in sensitiveness.

Figure 56 is an arrangement for a single telephone T. The quill tubes t and t', carrying the salient and reëntrant pin-holes s and r, are joined by a **T**-branch at t'', with the telephone T. In figure 57 the same arrangement is duplicated at $t''t'''$, so as to receive the sound-waves from both telephones T, T'. The curious feature about this arrangement is the low pitch (c', d') which it harbors at the maximum, even when the unbroken tubes used are short (10 cm.). Finally, figure 58 shows the **H**-branch already tested in the preceding report, with a cross-tube a. By stopping off the quill tube t', T alone is tested, as in the case of figure 55.

64

48. Experiments.*—It will not be possible to give more here than a few examples, as the results are often involved and too complicated for reproduction. Among these the case of a single telephone and connection, TtU, figure 55, with $T't''t'U'$ removed, deserves mention. The length of rubber tubing between s and T to be called l (right insert, fig. 59) was successively increased and the intensity s and pitch of the maximum found for each value of length l. Figure 59 is a summary of the results, with 4×10^4 and 2×10^4 ohms in the telephone circuit, and the intensities s are exhibited in relation to n, the frequency of the maximum. The length l is also inserted at each point. Halving the resistance does not quite double the fringe displacement s. Within the limits of error s is proportional to n directly. One would be inclined to attribute this to an induced electromotive force e, varying with n; but as the mean value of e depends on the speed of breaking the circuit and not on the number of breaks per second, this explanation is not tenable. Since e
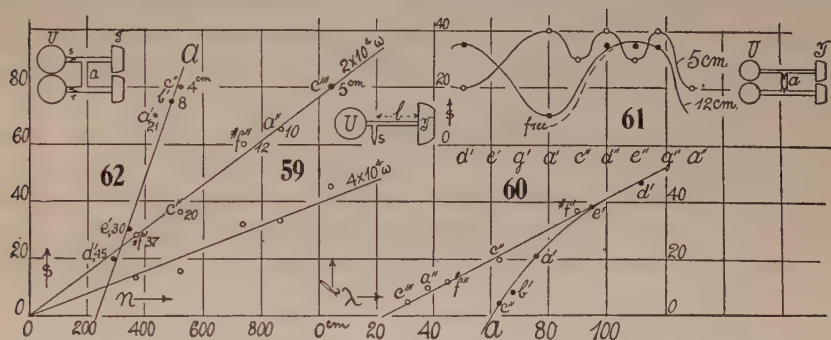
must be regarded as constant, therefore, the cause is to be sought in an acoustic pressure favored by frequency.

Another aspect of these results is reproduced in figure 60 (upper curve) in which the inserted length l and the wave-length λ, corresponding to n, are compared. Here also there is proportionality; but it is no longer direct, since the nearest equation would read

$$2(l+12)=\lambda$$

In other words, the length l acts as if it were 12 cm. longer, or 12 cm. are supplied by the short but irregular length sU of the pipe UT. Since at the maximum the pin-hole is located at a node, it is difficult to understand this result.

If the combination of figure 55 be taken with a junction-pipe a, of small length, 5 cm., maxima are redundant and closely crowded, as in figure 61. The pipes have no sharp tune. If the length of the cross-piece a is increased to 12 cm., the high maxima become more definite. Finally, if the pin-holes are free (a removed) the same conditions are enhanced. Thus a junction, a,

---

* As relative intensity of sound is alone of interest, the fringe displacement, s, as directly observed, is used as the ordinate of most of the graphs.

longer than 12 cm., is ineffective. The best conditions are naturally reached if UT and $U'T'$ have the same harmonics.

In this respect the combination (fig. 56) with but a single telephone has advantages and shows high sensitiveness. The pitch, however, is liable to be different with different telephones of the same kind. Thus, at 40,000 ohms, $s''=50$ with a c'' crest, and $s=43$ with a $\flat b'$ crest, appeared. The design (fig. 57) is quite sensitive, in spite of low frequency. Thus with $t=15$ cm., $t'=8$ cm., t'', t''' each 16 cm., $s=70$ was obtained at the low-pitched crest e'. In all cases there must be provision for flux of air. If in figure 57, $Tt''t'sU$ and $T't'''t'sU$ make a closed region, U' being left open and the r pipe closed, there is scarcely any response; but if s on a T-branch juts into the atmosphere, the system is very sensitive.

The importance of the cross-piece a of length l in figure 58 has already been indicated. Relevant data are also given in figures 61 and 62, graph a. Naturally there is no direct proportionality of s and n; and the relation of l and λ (black dots in fig. 60) is a curved line, which seems to merge into the simpler relations (open dots) of the design (fig. 55), when l is large.

49. Multiple resonance; narrow tubes. Location of pin-holes.—Some time after, the H-branch-tube was taken up again (see inset 62 or fig. 58), largely in relation to multiple resonance * which has recently gained increasing attention. A variety of examples have been given in my earlier reports; but in the present case other matters not then treated are to be considered. These are the strong resonances of very low pitch obtainable in very short tubes; the effect produced by reversing the action of one of the two telephones on the same circuit; the adjustment of salient and reëntrant pin-holes in relation to each other and to the U-gage; and finally the behavior of H-tubes of large diameter (2 cm.) and of doubly capped straight tubes.

I began the work with thin tubes (fig. 63, inset, t, t') about 6 mm. in diameter joined by the cross-piece A of the same diameter. The telephones T, T' at the ends of t, t' were of the common pattern, and supplied with the same current in series, but one of them (T) was provided with a switch C by which its current could be reversed with reference to T'. At the other ends of t, t' the salient (s) and reëntrant (r) pin-holes were inserted and joined to the shanks U, U' of the U-gage by the shortest tubing admissible. The results obtained are summarized in figures 64 to 66. For the curves marked S, the telephones cooperated, the plates presumably advancing and retreating in amplitude, respectively; i. e., telephone plates vibrating in opposed phases, being concave and convex, respectively, at the same time. For the case P the current of one was reversed, so that both plates advanced or retreated together (vibration in the same phase, both convex or both concave). The telephones were actuated by a small induction coil with over 2,000 ohms in the

---

* An interesting digest of the subject in reference to the work of Paget, Boys, Paris, is given in Nature, 1923, Feb. 24, p. 254, by Mr. P. Rothwell.

telephone circuit and an appropriate break-circuit device (electric siren), as heretofore explained (*cf.* § 75).

The difference of behavior for the two adjustments are given in figure 64, the ordinates showing the fringe displacements, *s*, proportional to the acoustic pressures at the different stages of pitch indicated by the abscissas. One observes the very striking presence of notes of the 2-foot octave in case of quill tubes but 16 cm. long. When the telephones are in sequence *S*, the high notes (*e''*) of the 1-foot octave resonate far more intensely than the low notes *d' . . . . . e'*. These being here at the limits of performance of the siren were difficult to locate, but the resonance interval is a little over the octave *e'* to *e''*, with the *e''* very abrupt.
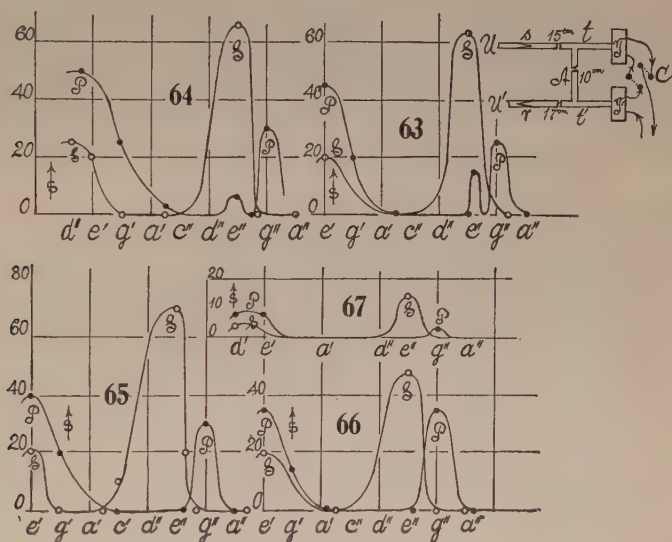
For the case *P* with the telephone plates in phase, the low pitches (*d'* to *e'*) are far more intense than the high pitches (*g''* with an uncertain *e''*). This specific difference in the two telephone adjustments makes it quite improbable that the high pitches are in all cases called out by the upper harmonics of the telephone note, *i. e.*, that the fringe deflection, etc., is merely apparent and called out by the harmonic *e''* in *e'*. It is more reasonable to assume that both *e'* and *e''* correspond to distinct modes of vibration of the H-pipe.

The endeavor was now made to test each pipe *t* and *t'* separately. Accordingly, *t'* was detached from the U-gage and closed with a plug, so that *tAt'* now became a closed region communicating with *U* by the salient pin-hole *s*. No fringe deflection whatever was obtainable in this way, a result corroborating my earlier experiments of an analogous kind. Similarly, when *s* was detached from the U-gage and closed, *r* communicating with *U'*, no deflection was obtained at any pitch. Thus the slender closed region needs an additional vent to generate acoustic pressure. This was secured by leaving *s* attached to *U*,

while r was detached but not closed, so that r freely communicated with the atmosphere. The results are summarized in the graphs (fig. 63) for the S and P switching of the telephones. These curves are almost identical with the corresponding cases of figure 64, not merely in pitch, but even as to intensity; and fluctuating e'' in the P graph is now very definite. Since the plates here vibrate in phase, it is probably the residue of the overtone of the strong e'. The alternative case of the reëntrant pin-hole r joined to U' and s communicating with the atmosphere is given in the graph (fig. 65). The curves again are a close reproduction of figures 63 and 64; the e'' in the R curves does not appear, but the e'' intensity in the S curve is the highest obtained. These results (fig. 63, 65) contrasted with the first (fig. 64) are illuminating; if s communicates with U, there is no advantage in having r communicate with U', contrary to what would naturally be supposed. The air-space above the shank U' acts merely like any other atmosphere, the acoustic-pressure difference s, r being constant, like an electromotive force on open circuit. This recalls the impossibility of relaying a series of pin-holes discussed in a preceding report (Carnegie Inst., Washington, Pub. 310, 5, 1923).

To further elucidate this question, I closed t' at r with a plug and put the reëntrant pin-hole r in the cross-branch at A, salient outward. The results obtained in this case are given in figure 66, and they differ from the preceding graphs in intensity only, but all the relations are preserved. A still more striking result was obtained by detaching s from U and r from U' and joining the cross-piece at A with U by a short tube. The results are given in figure 67, in which the intensities are naturally low, but all features reappear identically. Thus excess pressure exists throughout the pipe. Had both pin-holes been placed at A, the P graph would have evidenced a strong overtone here, and it is suggested that paired pin-holes at a prospective node will secure the largest values.

50. The same. Wide tubes.—The above arrangement did not admit of the examination of the tubes t and t' individually and the closed region gave no response. It seemed probable that this difficulty could be overcome by widening the tubes as in figure 68 (inset), where the pipes t, t' are 2 cm. in diameter and all 15 cm. long. They were also placed farther apart to accommodate the individual telephones T, T'. The latter were first put in communication with t and t' by short rubber tubes and the high-resistance radio-telephones used; but no fringe displacement was thus obtainable. The pipes t, t' were therefore directly mounted with cement on the mouthpieces of common telephones, as shown, and T' provided with a switch C. The far ends of t and t' were closed with well fitting perforated corks and connected with the pin-holes s and r and the shanks of the U-gage with rubber tubing. Reducing the resistance to 1,000 ohms, fringe displacements were obtained, which were enhanced by placing s and r as near U and U' as possible (short connectors). Thus I obtained for telephones in sequence, S, pitch e'', $s=40$ scale-parts; telephones

in phase, P, pitch f'', $s=53$ scale-parts; and it made little difference whether the vent at A (1 cm. nearly) was open or closed.

The reëntrant pin-hole was now detached and closed, the salient pin-hole being the sole communicator with the U-gage. This is the case of a closed region. The s pin-hole was similarly treated, in succession, and the results were: Salient pin-hole only: telephones in sequence, $s=70$, be''; telephones in phase, $s=45$, be''. Reëntrant pin-hole only: telephones in sequence, $s=38$, e''; telephones in phase, $s=60$, f''. Thus it appears that the closed region of sufficient volume responds, and this even more actively than when both pin-holes are used conjointly as originally. This seems to be due to the curious result that for the salient pin-hole alone, the telephones in sequence (S) are more active, whereas for the reëntrant pin-hole the telephones in phase (P) are the more so.

With the adjustment shown in figure 68 (inset), the occurrence of multiple resonance is very neatly shown, both for the case where the telephones are in sequence (S), figure 69, and for the case P, figure 68. The two pin-holes were first used together as in the figure. The full curves marked $r+s$ were

TABLE 11.

Pipes and tele-phones.	Pin-hole.	Switch.	Pitch.	s	Tele-phone.	Pin-hole.	Switch.	Pitch.	s
t, T	s	S	bd''	85	T'	s	S	bd''	80
t, T	s	P	..	5	T'	s	P	..	0
t', T'	r	S	d''	80	T	r	S	d''	80
t', T'	r	P	g'	5	T	r	P	..	0

thus obtained with 1,000 ohms in the telephone circuit. The two tubes responding with the salient and the reëntrant pin-holes were then successively detached and plugged, so that the fringe displacement of one tube only was recorded. The curves marked s (salient pin-hole) and r were so obtained, for each switching (S, P) of the telephones. In the low-pitch values (fig. 69) the component resonances are nearly the same in frequency, and the compound curve is of the same type. The high-pitch components, however, are some distance apart (f'' and a''), but their compound curve is an active coalescence throughout the whole of this interval. In figure 68 for telephones in phase (P) the low-pitch resonances are obscure. The high-pitch resonances (e'' and a'') for r and s are also less intense than in the preceding figure, but they merge in a plateau-like curve which shows sustained intensity between e'' and a''.

When the pipes t and t' were opened (corks withdrawn) and the pin-holes at the end of 6-inch quill tubes used as probes and inserted close to T and T', the behavior of each pipe was about the same as presented in table 11 (resistance in circuit, 1,000 ohms).

When the pin-holes were used conjointly ($s+r$), the result was here summational, so that a double resistance (2,000 ohms) had to be inserted into

the telephone circuit, giving S, d'', 80 scale-parts, P, g', 20 scale-parts. This experiment was now repeated with the tubes t and t' closed (as in fig. 68) with a perforated tube, through which the pin-hole probes were thrust loosely to within a centimeter of the plate of the telephone. The results are given in table 12.

The telephones switched into phase (P) gave no result at any pitch. As the fit at the perforation was not snug, it was next waxed, giving data shown

TABLE 12.

Telephone.	Pin-hole.	Switch.	Pitch.	s
T and T'	s and r	S	a'	60 scale-parts.
T	s	S	..	35
T'	r	S	..	33

in table 13, which is practically the same result. In these cases it made little difference in pitch or intensity whether the vent in the cross-piece A was open or closed. The low-resonance pitch a' in the tube closed at both ends contrasts very strikingly with the high pitch d'' for the same tube closed at one end only. In the former a'' is inactive, no fringe displacement resulting.

Thus it appears that a salient and reëntrant pin-hole probe on separate tubes communicating with the shanks U and U' of the U-gage may probably be used together in the same pipe; and this proved to be the case. For instance: Tubes t, t' closed at both ends, $r+s$ in t, pitch ♭b', switch S, $s=50$ scale-parts;

TABLE 13.

Telephone.	Pin-hole.	Switch.	Pitch.	s
T and T'	s and r	S	a'	55 scale-parts.
T	s	S	..	26
T'	r	S	..	30

tube t closed, t' open, $r+s$ in t, pitch c'', switch S, $s=50$ scale-parts. In all these cases when the telephones were switched in phase no appreciable fringe displacement was obtained.

The exploration of the closed tubes t, t' (fig. 68, inset) in depth, by passing the respective pin-holes through the perforated corks to different distances from the telephone plates, proved to be a difficult experiment both for a single pin-hole in each tube or a double pin-hole in a single tube. Pressures seemed to fall off from the plate or the cork at the end of the tubes toward the middle, but there were frequent discrepancies traced to the adjustment of the pin-hole. The telephones in adjustment P were quite ineffective; when in sequence (S) the resonant pitch was sharply a'. The following data finally obtained are trustworthy for the pipe t and the salient pin-hole at 1 cm. from

plate, $s=65$; middle of t pipe, $s=40$; 1 cm. from corked end, $s=68$. The t' tube showed no certain difference of deflection for any position of the reëntrant pin-hole from the plate to the corked end of the pipe t'. Thus it made no difference whether both pin-holes were attached to their respective shanks of the U-tube, or whether one was free. Both could be detached, moreover (fig. 70), and the middle of the cross-tube A, figure 68, joined to the U-gage as in the preceding experiment (fig. 67), showing a small residual fringe displacement of $s=15$. Curiously enough, with both pin-holes saliently inward at the corks, the deflections for the usual attachment were liable to be negative ($s=33$). With one tube (t') quite closed and the other joined
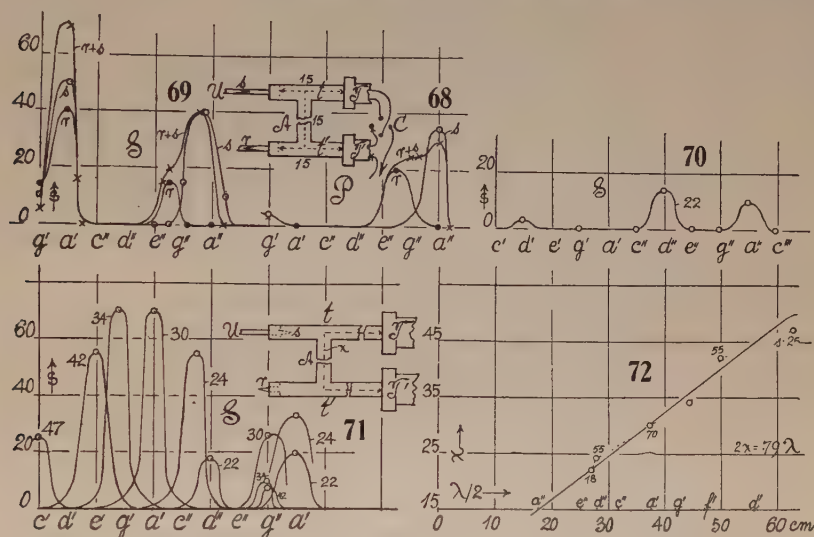
to the U-gage, there was no displacement at any pitch, the fringes merely wandering in response to temperature.

51. Modes of vibration within the H-tube.—From what has preceded, the character of the possible vibrations in the H-tube (fig. 68, inset) is now clear. At low pitch the ends of the t and t' tubes are nodes, from which the acoustic pressure diminishes upward 40 per cent toward the middle of each and thence to the middle of the cross-pipe A, where it nearly but not quite vanishes (reduced 80 per cent). Hence the middle of the branch A (fig. 68) is an antinode and the motion in t and t' is bifurcated towards the two ends of each, as shown in the diagram. The high pitch, however, is an individual vibration, probably arising in each doubly closed tube t and t'. The pitch here will usually differ but slightly, and hence if sounding together the graphs coalesce.

To test this matter further and deduce an equation, the pipe (fig. 71) was prepared, in which an expansible branch A could be increased in length at pleasure. The fringe deflections for the upper and lower pitch are given in

6

table 14 and constructed for the case of telephones in sequence (S) in figure 71. For the telephones in phase (P), the upper resonances are practically the same as when the telephones are in sequence, but the lower resonances only appear in the latter case (sequence, S). Moreover, while the upper pitch remains nearly the same for all values of length A (marked in centimeters on the graphs), the lower resonances are very sharp and move rapidly into lower pitch (d'' to c') with increase of the A length. Moreover, the upper resonances are usually strong when the lower are less intense. Both pass through a maximum, particularly the lower resonances, which rise from about $s=20$ at d'' to 70 at g' to a' and then fall to 25 at c'.

TABLE 14.—*Resonances of the* H-*tube.*

[$x=$ axial distance from plate to plate of telephones. Distance in tubes t and t', 15 cm. Fringe displacements, s.]

x	Telephones in sequence (S).				Telephones in phase (P).			
	Pitch.	s	Pitch.	s	Pitch.	s	Pitch.	s
		scale-parts.		scale-parts.		scale-parts.		scale-parts.
47	c'	25	..	..	..	..	..	..
42	e'	55	g''	8	e'	2	g''	10
34	bg'	70	g''	10	bg'	4	g''	10
30	a'	70	$\sharp g''$	25	g'	4	g''	20
24	bd''	55	a''	33	g'	4	g''	25
22	d''	18	a''	18	g'	3	a'''	20
Single tube	..	..	a''	30	..	..	..	..

In figure 72 I have given the length x from plate to plate of the telephones, along the axes of the tubes tAt', in terms of the semiwave-length $l=\lambda/2$ of the given pitch in free air. These points make a coherent grouping quite as close as the ear can well estimate pitch. It is therefore probable that a linear equation

(1) $$x=(x_0/\lambda_0)\lambda=(x_0/l_0)l$$

is applicable and the the graph (fig. 72) shows $x_0/l_0=0.79$. Hence

(2) $$x=0.79l=0.40\lambda$$

instead of $\lambda/2$, which would hold in the absence of viscosity. The independent data of figure 69 would give $2x=0.81\lambda$, and the other incidental values on the average also $2x=0.79\lambda$.

With this it is now very interesting to compare the data of figures 64 to 67 for a pipe about but 0.6 cm. in diameter (apart from the expansion at the telephones), and a prevailing lower harmonic e'. Here

$$x_0/l_0=25/50=0.5 \text{ or } x=0.5l=0.25\lambda$$

In other words, the internal friction for these narrow tubes is enormously larger, so that for a given pitch but half the normal length suffices. This accounts for the striking occurrence of very low frequencies in connection with these short pipes.

The equation given by Helmholtz for the open organ-pipe and discussed by Rayleigh (Sound, Chapter IX) is

$$u = v(1 - \sqrt{\eta/2n\rho}/R$$

where u is the velocity of sound within the pipe of radius R under conditions of viscosity η, v the free velocity in air of density, ρ, and n the frequency. If we convert this into wave-lengths λ' corresponding to u and λ to v at the same n,

(3) $$(\lambda - \lambda')/\lambda = \sqrt{\eta/2n\rho}/R$$

In equation (4) if $2x = \lambda' = 0.79\lambda$, the corresponding value comes out experimentally

(4) $$\frac{\lambda - \lambda'}{\lambda} = 0.2$$

and is, so far as figures 71 and 72 show, not appreciably dependent on frequency n within the interval c' to c'' under observation. Since the diameter of pipes is $2R = 2$ cm., the quantity $R(\lambda - \lambda')/\lambda = 0.2$ (here experimentally constant) has the same value.

To compare this with the narrow tube of figures 65 to 67, which has unfortunately the telephone mouthpieces as terminals and possibly a tube not adequately smooth (because of the rubber-tube junctions), we may regard $2R > 0.6$ cm., the diameter of brass pipe. The pitch at e' descended to $\flat d'$. Thus $\lambda' = 0.5\lambda$ or $(\lambda - \lambda')/\lambda = 0.5$ and $\lambda' = 0.47\lambda$ or $(\lambda - \lambda')/\lambda = 0.53$ occur. Hence $R(\lambda - \lambda')/\lambda = 0.15$ to 0.19 are reasonable estimates, the latter showing a tendency to conform with this part of equation (3).

Returning to the wider tube $R = 1$ cm. and figure 71, one may inquire whether a reasonable value of η is approached at any of the pitches d'' to c' tested, since

$$[R(\lambda - \lambda')/\lambda]^2 = 0.04 = \eta/2n\rho$$

The values so obtained range from $\eta = 0.06$ at pitch d'' to $\eta = 0.027$ at c', and are thus quite out of keeping with the viscosity of a gas. The individual values computed from equation (3) directly are $(R = 1$ cm.) (table 15).

TABLE 15.

Pitch.	d''	$\flat d''$	a'	$\flat \bar{g}'$	e'	c'
$R.\Delta\lambda/\lambda$	0.21	0.20	0.19	0.24	0.16	0.25
n	590	550	440	370	330	260
η	.070	.057	.042	.055	.022	.044

Thus the mean friction here in evidence (0.049) would be about 270 larger than the viscosity of the gas.

It has been assumed that the lower maxima in figures 69, 68, and 71 occur when the telephones are used in sequence, i. e., when the plates are

respectively convex and concave at the same time, for the alternating vibra-
tion should be stimulated by an advance of one plate, coinciding with a
retreat of the other. Not wishing to injure the telephones, this interpretation
of S and P has not been directly investigated. Moreover, in figures 64 to 67
both commutations of the telephones are definitely active at the lower
resonance, though one is about twice as much so as the other. However,
it will be shown below that the P position evokes overtones, and this may
be taken as adequate evidence.

At the high pitch there should be no difference, since in the case of the
wide tubes each vibrates separately. For the quill tubes (fig. 64 to 67), where
the best adjustment for the lower pitch is the worst for the higher, through-
out, the relations are again less clear.

52. Continued. Deep resonances.—To refer the high-pitch data at g''
and a'' to the individual tubes t and t' (fig. 71, inset), experiments were made
at some length by elongating one or the other of these tubes. The results
were unsatisfactory, and no multiple resonances or coalescences of graphs
were obtained. In fact, a third tube closed at both ends was inserted between
t and t' and parallel to them on the cross-piece A, without any effect worth
recording. The third tube merely lowered the lower resonances and modified
amplitudes. Its own vibrations, if occurring, were not appreciable at the
U-gage.

A more promising method of procedure, keeping the telephones always in
sequence, seemed to be that of cutting down the outer lengths of the tubes
t and t' as shown in the inset, figure 73, until the pin-hole lay very close
(1 to 2 cm.) to the cross-tube A. The reduced effective length of each tube
was now but 9 cm. A very extended survey from c to c''' was carried out,
but at first no marked resonances at all were detected. With greater care
in tightening all joints and reducing the effective telephonic resistance to
one-third, the graphs of figure 73 were traced, and they refer to a total axial
length x of 24 cm. and 29 cm.

At $x=24$ cm. (cross-piece A, 9 cm.) the resonances are very weak in spite
of the low resistances, both at d'' and at a''. The d'' has the proper frequency
in relation to x, but the a'' appears here as in figure 71, and it even occurred
(g'' to a'') when the tubes t, t' of that figure were elongated 3 cm. Thus the
a'' frequencies can hardly be associated with the tubes tt', but are referable
to the telephones, which have remained the same throughout.

At $x=29$ cm., $i. e.$, for an increase of length of the cross-piece A from 9 to
14 cm., the graphs show highly increased sensitiveness with the b' pitch
properly salient and the a'' located as before. This increase of sensitiveness,
through a maximum as A increases, has already been shown in figure 71 and
thus corroborates an interesting result.

The new resonance d' for $x=24$ is probably evoked by exciting the over-
tone d''. Similarly, b for $x=29$ excites the overtone b', as the telephone note
is not a simple harmonic.

The novelty in the graphs for $x=29$ is the low $\sharp d$ (frequency about 150), for which the free semi-wave-length would be over a meter. This is very salient and distinct, though the exact location of pitch between d and e is a little difficult to ascertain. With pipes but 9 cm. long and a maximum axial distance not exceeding 29 cm., the origin of this note is an interesting problem. To suppose that it awakens a'' as its second overtone is not in keeping with the fixity of a'' above stated.

The subtlety of the relations involved is well shown by the graphs (figs. 74 and 75), in which the pipes t and t' as above are prolonged by quill tubes t'' and t''', with the pin-holes (as before) near the U-tube. The cross-pipe A was short ($x=25$). The a'' maximum has its usual fixed position and the $\sharp c''$ maximum, figure 74, corresponds to x; but these two maxima now show a strong tendency to coalesce. The $\sharp c'$ maximum might be associated with $\sharp c''$. One observes the multiple resonance below $\sharp c'$. The $\sharp g'$ maximum here, as compared with figure 73, is new.
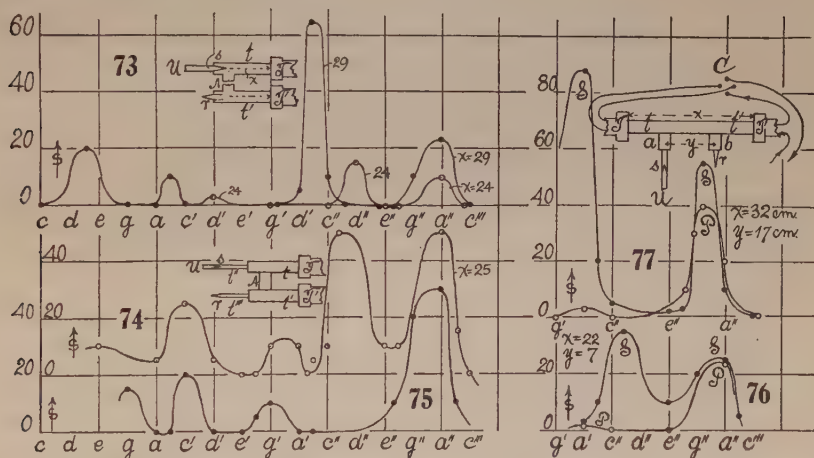
In case of figure 75, the quill tube t''' was removed and the pin-hole attached directly to t' as before. The resonances near a'', g', c', and even below, remain nearly intact, but the strong $\sharp c''$ resonance has been quite obliterated. Hence this maximum would seem to be referable to the quill tube t''' acting independently. Similarly, the new maximum near g', as compared with figure 73, should be associated with the quill tube t''. The maximum near c', though more pointed in figure 75, is present in both figures and might therefore originate with the tube-length $t''tAt'$. Granting the uncertainty of these conjectures, there is nevertheless a suggestion that by connecting quill tubes with the nodal ends of the pipes t, t', a variety of multiple resonances might be obtained. Experiments made at some length along these lines, however, gave me nothing more than highly ornamented graphs, containing secondary maxima. I obtained no contrasts quite so clear as those of figures 74 and 75, though on lowering the resistance in the telephone a number of subsidiary maxima varying with t'' and t''' were readily picked out.

STRAIGHT AND TRANSVERSE PIPES.

53. Straight tubes 2 cm. diameter.—The inset, figure 77, shows the new adjustment with the telephones TT' at the ends of the pipe tt'. The latter is provided with adjutages a and b, y cm. apart, when the total length of tt' is x. The salient (s) and reëntrant (r) pin-holes are here attached. The telephone current in T may be reversed at c.

The graphs, figures 76 and 77, are the results of two surveys in pitch, for $x=22$ cm., $y=7$ cm., and $x=32$ cm., $y=17$ cm., respectively, the adjutages being about 7 cm. from the telephone plates. The results conform closely with figure 71 for bent tubes, as would be anticipated. The chief maximum near c'' in figure 76 and near a' in figure 77 being strong in the S position, but practically absent in the P position of the switch. Moreover, the intensity of this maximum increases in marked degree with x, being over twice as high for $x=32$ as for $x=22$.

If the adjutages ab are placed nearer the telephone plate, the fringe displacements s may be enormously increased. Thus in figure 82 (below), $x=32$, $y=25$, so that the plane of the pin-holes is about 3 cm. from the respective telephone plates. It was necessary to put 1,000 ohms in the telephone circuit, so that the a' maxima are here over 3 times as high as before. The pin-holes may be inserted at a and b (fig. 77), or side by side in a, b being closed. If the reëntrant pin-hole is at the middle of tt', a smaller displacement s is obtained, as indicated (fig. 82).

The fixed maxima near g'' are as usual present in all cases, and here they also increase in intensity with x. In figure 82, however, they have not been raised in the same ratio as the a' maxima.

54. Transverse tubes, 2 cm. diameter.—The tube tt' was now provided with a cross-branch in the middle, shown at mn in the inset, figure 79. This not only makes it convenient to search for the occurrence of nodes midway between the telephone plates, but (as will presently appear) with the telephones in phase (P), a complete succession of nodes may be invoked in these transverse pipes without changing the position of pin-holes. The length z of the cross-branch in relation to the length x of pipes tt' modifies the intensity of vibration obtained, though it seems to change the pitch very slowly at first.

The graphs traced in the frequency surveys are given in figures 78 and 79, for $z=4$ and 13, respectively. In both a new maximum at c'' is strikingly developed. This maximum is very high in figure 79, conformably with the large $z=13$ cm. It occurs, moreover, for the P position of the switch and not at all for the S position, as do the maxima belonging to the ends of tt' hitherto studied. There is thus an opposition in the phase of the telephone plates in the two cases of experiment.

While the strong a' maximum has vanished, the g'' maxima are still remarkably strong at the middle of tt'. In figure 78 the salient pin-hole was at the m end, but near the U-gage, while the reëntrant pin-hole was put in the cork at n. Adding a quill-tube adjutage here in the interest of greater

symmetry, the e'' maximum was but slightly enhanced, but the g'' maximum considerably, as the figure indicates. In figure 79 the pin-holes were tentatively placed side by side in a doubly perforated cork. In this case the g'' was not marked and had coalesced with the excessive e'' maximum. Placing the reëntrant pin-hole at n decreased the e'' somewhat, but brought out the g'' maximum more sharply, as indicated more fully in figure 80.

To produce a node in the middle of the pipe tt', the telephone plates must be in the same phase, whereas for a neutral segment here they should be in opposite phases. It is thus curious to note the pitch a' in the latter case, as compared with the pitch e'' of the former middle node, a difference interval of but a fifth. This, however, is conformable with the expansion of tube at mn, figure 79.
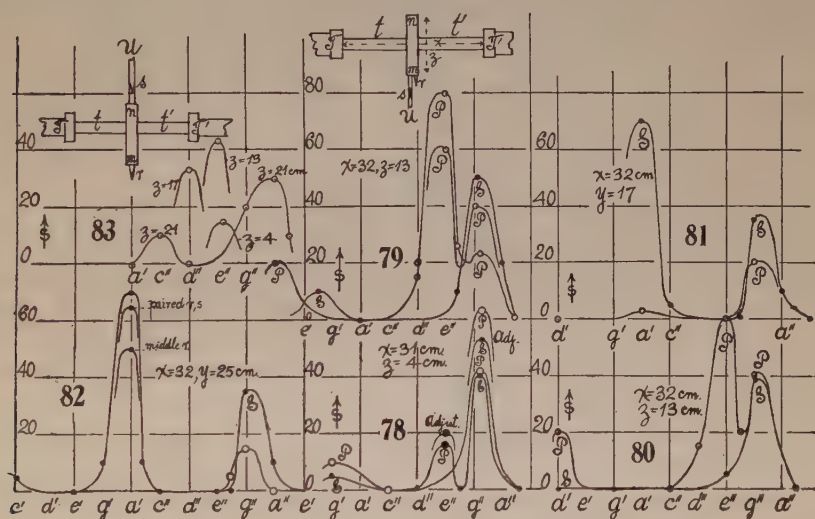
Figure 81, finally, is a repetition of the case of figure 77 ($x=32$ cm., $y=17$), but in the presence of the cross-branch ($z=13$ cm.). The character of the graph is unchanged, though with reduced intensity. It thus contrasts sharply with figure 79, except at the common fixed maximum at g''.

The effect of the expansion in z in intensity and pitch was next investigated, as shown in figure 83 (inset). The pin-holes were here placed at the opposite ends, m and n, m being elongated. The graphs obtained for the different adjustments ($z=4$, 13, 17, 21 cm.) are indicated, showing that here there is also an optimum in length at $z=13$ cm., about, while the pitch changes from $\sharp e''$ to c''.

The arrangement, however, is far more sensitive if the adjutage m is closed and the two pin-holes r and s are placed side by side in n, s communicating with the U-gage. The pitch and intensity of the maxima found in the different adjustments is given in figure 84, the z lengths (4, 9, 14, 16, 21, 22 cm.) in round numbers being attached. The locus rises rapidly to the optimum and then decreases, fast at first but eventually less so, the distribution being much

as in figure 71. In the adjustment of figure 84, the pin-holes necessarily lie at the node.

The full resonance curve for the length $z=9$ cm., given in figure 84, is interesting, 1,000 ohms being in circuit, telephones in phase (P). All the e's (e, e', e'') are active. Probably the e and e' as given by the telephone plate contain the dominant e'' as an overtone. Similarly, g, g', g'' coalesce with e, e', e'', more or less, so that except at a', c'', c''' there is response throughout. In the case S, with the telephone plates not vibrating in phase, there is moderate response at g'' only.

55. Comparison of constants for wide tubes.

—If we collect the data of figure 71 for the tube-length x and corresponding intensity of note or fringe displacement s, and compare them with figure 84 for the transverse tube-length z and its fringe displacement s, the following correspondence appears:

Longitudinal tube
$x=$	22	24	30	34	42	47	cm.
$s=$	18	55	70	70	55	25	scale-parts.
	d''	bd''	a'	bg'	e'	c'	

Transverse tube
$z=$	4	9	14	16	21	22	cm.
	25, 32	75, 100, 120	95, 100	60	40	35	scale-parts.
	bf''	e''	$\sharp c''$	b'	a'	g'	

These curves are given in figures 85 and 86. The x values of s could have been increased several times by placing the pin-holes nearer the telephone plates (as was done in the work of figure 82) under high resistance; but it is merely the relative values or configuration curves which are here in question. The cusplike rapidity with which the optimum is reached and lost in the case of transverse pipes (pin-holes in the middle between plates) is in contrast with the more leisurely progress in the case of longitudinal pipes; but a preferable length in z or in x is none the less clearly present in both cases. Thus a length most favorable to response exists, and for this it is not easy to account. True, the transverse tube is associated with the longitudinal tube (inset, fig. 86), so that the vibration is from T to m and T' to m simultaneously, making m a node; but the longitudinal tube is alone, the transverse section being removed.

If we use the above equation (2) in x and λ obtained with bent pipes

$$x=0.4\lambda$$

and apply it to the axial length of the semi-wave-lengths T to m and T' to m (deducting the n protuberance $z''=2$ cm. from z so that $z'+z''=z$), the following data appear:

Observed $z'+x/2$......	18	22	27	29	34	35
Pitch......	f''	e''	$\sharp C'$	b'	a'	g'
Computed $z'+x/2=0.4\lambda$......	19	20	24	27	30	34

These values, though too small in the computed data, nevertheless show that the vibration form is correctly assumed, the node of both T and T' being at m and receding with m. The true coefficients here would be 0.44, 0.45, 0.43, 0.45, between e'' and a', or $x=0.44\lambda$ on the average.

Thus is seems probable that additional resistance was introduced in the above experiments ($x=0.4\lambda$) by the two right-angled bends in the tubes. The experiment was therefore repeated with straight tubes 2 cm. in diameter (inset, fig. 87), with the results given in the graph of that figure, 1,200 ohms in the telephone circuit. If x is the length from plate to plate of the telephones, the data range as follows (fig. 87):

Observed x 21	27	32	39	51	62 cm.	
Observed pitch ....d''	b'	ba'	f'	d'	a	
Observed $\lambda/2$ 28	33	40	47	56	75 cm.	
Observed s 70	83	60	53	25	35 scale-parts.	
Computed $\lambda/2$ 24	31	37	45	59	71 cm.	
Computed pitch ....f''	c''	a'	f'	bd'	a	
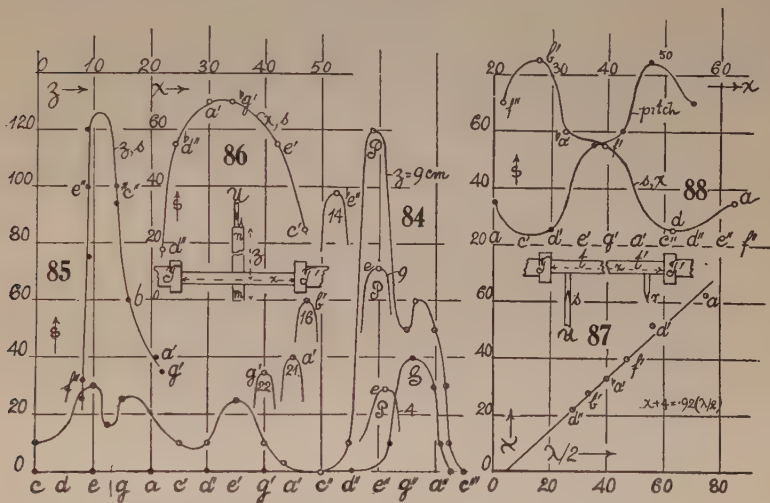
The mean coefficient obtained from these results, $x=0.43\lambda$, agrees very very nearly with the data for transverse tubes. Though this graph is the best obtained, the equation is inadequate, as may be seen by computing the λ from the observed x, in which case the higher notes $d''b'ba'$ would be too far off to have deceived the ear of the observer. In fact, an equation of the form $x=-a+b\lambda$ must at the outset be much more satisfactory; for the a is referable to the space in the telephone mouthpiece. Thus, for instance, $x+4=0.92$ ($\lambda/2$) would give the data:

$x=21$	27	32	39	51	62 cm.
$\lambda/2=27$	34	39	47	60	72 cm.
Observed pitch$=d''$	b'	ba'	f'	d'	a
Computed pitch$=d''$	b'	ba'	f'	$\#c'$	a

which is perhaps as near as the pitch obtained under chromatic conditions can be recognized. Thus there is no experimental evidence here of an effect of pitch in relation to viscosity within the octave and a half surveyed.

Figure 88 shows the fringe displacement s for the different pipe-lengths x, as well as pitch. There is also an optimum length here at $x=30$ approximately, though the curve later (at a, $x=80$) shows signs of recovery. Much depends

in such cases on the steady efficiency of the contact-breaker; so that inferences here must be made with caution. The possibility of a harmonic distribution of points is not, however, improbable.

56. Telephones in parallel.—A number of experiments (tubes straight, 2 cm. in diameter, as in fig. 77) were made with the telephone circuit in parallel, so adjusted that one of the currents could be reversed. The distribution of s in pitch was naturally not modified, but the sensitivity was usually much smaller. A single telephone sufficed to bring out the resonant note almost in full strength, which was quite audible, $s=0$, with the telephones in opposition. Thus at pitch e'', $s=40$ scale-parts, appeared with one telephone or both telephones cooperating $s=0$ when they counteracted each other. In the alternative case, $s=30$ for one and $s=40$ for two telephones was obtained, while $s=0$ appeared with the telephones antagonistic.

The experiments were made with the object of gradually modifying the phase of one telephone plate with reference to the other, and from this viewpoint the design is of great interest; but nothing worth recording was obtained.*

QUILL PIPES, CAPPED AT BOTH ENDS.

57. Vibration in closed straight quill tubes. Straight tubes.—Though some work of this kind was done above, it was thought well to carry it through more systematically and with thinner tubes. The plan of the apparatus is shown in the inset, figure 89, with the pin-holes s, r close to the telephones T, T' and the ends of the t, t' tubes extending very nearly to the telephone plates. A full survey from c to d''' was made both for the shortest available length, $x=9$ cm., and for the longest, $x=29$ cm. The results are summarized in the graphs, figures 89 and 90, both for the S and P telephone relations.

With the telephone plates vibrating in the same phase (P, currents in sequence), the two curves are practically identical, except in intensity distributions. Thus the maxima near $a''-b''$, $d''-\sharp d''$, $a'-b'$, $d'-\sharp d'$, below a are present in both. Below a in the 4-foot octave, the graph is still of high intensity, s, and practically horizontal, almost to c. The pipe is in resonance with any pitch of the 4-foot octave. The intensities of the a'', a', a of the pipe are in excess when $x=9$ cm., the intensity of d'', d slightly in excess when $x=29$ cm.

When the telephone plates vibrate in opposite phases (S, current in contrary), the single strong movable note corresponding to the length x of the tt' pipe appears. This is at a' in figure 90, $x=9$ cm., at g-a in figure 89, $x=29$ cm. and in both cases very outspoken. The steady maximum near b'' is now stronger for $x=29$ cm.; that near c'' coalesces below ($x=9$ cm.) with the large a' maximum; that near a below ($x=9$ cm.), with the large a maximum above ($x=29$).

---

* This has since succeeded both with resistance and inductance leading to interesting deductions to be given in the Proceedings of the National Academy of Sciences for May et seq., 1925.

When the plates are in phase (P), the pipe is rarely silent; not at all for $x=9$ cm. It presents a remarkable case of multiple resonance. It is possible that the lower pitched maxima all evoke the strong upper harmonic near b''.

In figures 91, 92, and 93 the resonance pitch corresponding to different lengths of pipe x have been recorded. The experiments were completed at different times and in figures 91 and 92 the graph appears to be curved, as if an effect of pitch in relation to viscosity of air were here discernible; but in figure 93, which was made with great care in view of this question, there is no such effect appreciable. The discrepancy is thus referable to the difficulty of locating the very flat maximum of the 4-foot octave.

The curves have a common characteristic. Compared with figure 87 for 2 cm. pipes, their mean slope is very much less, $2x=0.35$ being the mean

result. All the curves, however, demand an initial constant, as if referable to the space in the telephone mouthpieces. This is at present relatively large, so that (fig. 93) the equation $x+10=0.51(\lambda/2)$ is a more suitable form. The results are now:

Observed x	9	15	20	25	29 cm.
Observed s	70	80	90	85	50 scale-parts.
Observed pitch	a'	e'	d'	b	a
Observed $\lambda/2$	37	50	56	67	75 cm.
Computed $\lambda/2$	37	49	59	69	76 cm.
Computed pitch	a'	e'	bd'	b	a

These data are in places again disappointing as to pitch. In the case of somewhat flickering chromatic intervals, the ear occasionally overestimates its precision.

The data of figure 93 are given as to intensity and pitch in figure 94. The optimum appears as usual. The rapid drop of frequency (a' to e') for the first small elongation, $x=9$ to $x=15$, is noteworthy.

If we take the equation $x+a=b(\lambda/2)$ and compare the coefficients for tubes 2 cm. in diameter and the present quill tubes 0.4 mm. in diameter, the

respective coefficients are 0.92 and 0.51. Thus, while the ratio of diameters has gone down five times, the ratio of coefficients is but $0.92/0.51=1.8$. If we write the equation in u and v, § 51,

$$\frac{(x+a)-\lambda/2}{\lambda/2} = -\frac{1}{R}\sqrt{\frac{\eta}{2n\rho}}$$

Since no relation to n has been detected, this conforms to

$$\frac{(x+a)-\lambda/2}{\lambda/2} = -(1-b)$$

Thus for the two diameters $2R=2$ cm. and 0.4 mm. the coefficients are $1-b=0.08$ and 0.49, respectively. Hence, while R has decreased five times $(1-b)$ has increased about six times and $R(1-b)$ is no longer constant. Without violence to the observations this differential coefficient $1-b=0.08$, however, might be put 0.09 or even larger, in view of the difficulties in fixing pitch above pointed out. The discrepancy is therefore not decisive, except in the absence of the frequency effect $\sqrt{\eta/2n\rho}$.

58. Vibration in transverse quill tubes.—The adjustment is shown in figure 95 (inset), t'' being the transverse quill tube activated when the telephone plates vibrate in the same phase. A difficulty is here encountered, inasmuch as the conical pin-hole tubes r and s are no longer negligibly small in comparison with the pipe t''. With 200 ohms in the telephone circuit, the response is good and figure 95, a shows that an optimum is probable, as usual. The rapid march of the note (e'' to b') for the first small elongations ($z=7$ cm. to $z=12$ cm.) is noteworthy, here as in the above data (compare fig. 94, a' to e'). While for telephone plates in opposite phases there was no response, a fringe displacement of 60 scale-parts was observed for like phases.

If the transverse length is called z (see fig. 95), the coefficient in $z+a=b(\lambda/2)$ here comes out astonishingly large, and in figure 95, curve a conforms closely to $z+12=0.85(\lambda/2)$. This value for these thin quill tubes ($2R=0.4$ cm.) recalls the value for tubes 2 cm. in bore. The work was repeated later (figs. 95 and 96, curve b) with modifications; but the results are of the same order, $z+13=0.89(\lambda/2)$ so far as the coefficient is concerned.

In figure 97 the survey was repeated in such a way as to obtain large fringe displacements throughout (see fig. 98); but the mean coefficient is here even larger, the equation reading $z+16=0.96(\lambda/2)$. If the whole distance to the telephone plate $t+t''$ or $t'+t''$ is taken, $z+23=0.96(\lambda/2)$ would adequately reproduce the data, which procedure does not, of course, modify b.

On comparing figure 97 for transverse pipes with figure 93 for straight pipes (longitudinal vibration), one notices that the frequency in the latter case is about an octave lower; but there is a full octave in figure 93 and more than an octave in figure 97. Yet no suggestion of a frequency effect appears. Moreover, the respective coefficients b are in the inverse order in which they should occur, for it is the higher octave (fig. 97) which has the largest

coefficient. The cause of this anomalous result will be considered in the next section.

Figure 98, indicating the large intensities s in relation to transverse-tube-length z and the observed pitch, imply an optimum within the smallest available tube-length $z = 10$ cm. Apart from this, the graphs of figures 98 and 94 are not dissimilar. Moreover, one would expect an optimum here when $z = x/2$, i. e., for three equivalent resonators. I refrain from putting stress on the absolute magnitude of the s data, as they are subject (as already intimated) to the play of the contact breaker and this is liable to vary in efficiency. Thus,
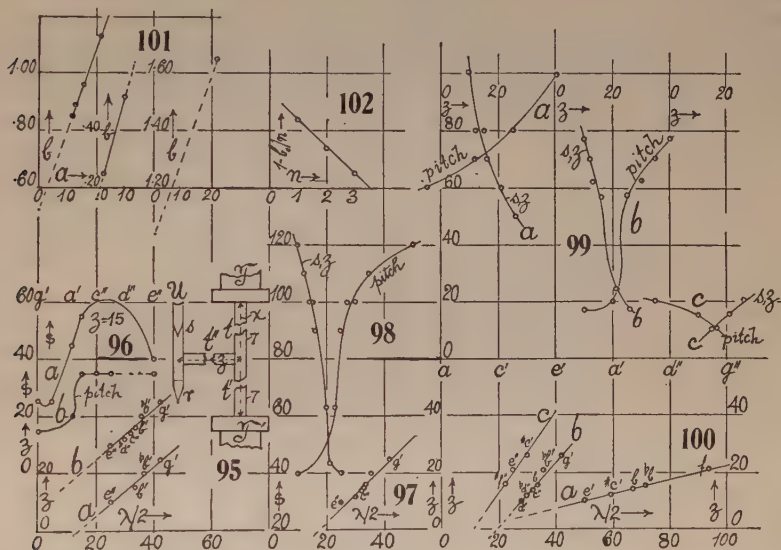
in figure 96, the curve b has probably encountered some such discrepancy, from which the curve a is free.

59. The same. Overtones. Viscosity effect.—After obtaining the anomalous results stated, I overhauled the apparatus as a whole, chiefly with regard to slight leakages at the telephone plates and elsewhere. The result was a considerably increased sensitivity (s), as shown in table 16, 1,000 ohms being in circuit (see fig. 99). The slopes of the given series (fig. 100, curve b) has even increased, so that now $z + 22 = 1.13(\lambda/2)$. The observations as a whole were more regular. At the same time, however, I detected the graph (c), a scant fifth above (b) and reproduced by the equation $z + 22 = 1.65(\lambda/2)$. Clearly this was the third harmonic of the transverse tube, so that the fundamental might be looked for an octave lower. The graph (a) in figure 100 was accordingly sought and found. The initial tube-length a here is, as usual, smaller and the equation $z + 2.5 = 0.25(\lambda/2)$ adequately reproduces the data. The present coefficient $b = 0.25$ is thus astonishingly small, being but one-half of the preceding coefficient, $b = 0.51$, for vibrating air filaments in straight tubes.

If one conceives the vibrations to take place along $Ttt''s$ and $T't't''r$ (fig. 95, inset) and return, the structure in the tube t'' (area of filament reduced one-half) and the expansion in the tube sr may have something to do with the increased resistance; but the initial lengths a seem to be adjusted by the tube itself in an arbitrary manner, being but $a=2.5$ cm. for the graph a, and $a=22$ cm. for the overtone graphs b and c. Unfortunately, in the case of curve a, the fringe displacements below f are nearly constant (compare graphs 89 and 90), so that resonances are continuous and can no longer be picked out. Figure 99 shows, however, that in curves a and b the optimum should lie below 10; and since the straight pipes t and t' (fig. 95, inset) are each 7 cm. long, this result would be consistent if the resonance of the $x/2$ and z air filaments contributes to this end. Contrariwise, the optimum in the overtone graph c would lie considerably above 26 cm. (fig. 99), and for this there seems to be no suggestion at hand.

TABLE 16.

$z =$	10 cm.	12 cm	14 cm.	16 cm.	21 cm.	26 cm.
B Pitch	d''	bd''	c''	b'	bb'	g'.
B $\lambda/2$	28	30	32	33	35	42 cm.
B s	77	70	62	57	24	17 scale-parts.
A Pitch	e'	$\sharp c'$	b	bb	f?	(continuous).
A $\lambda/2$	50	59	67	71	94?	cm. (continuous).
A s	100	80	80	70	60	50 scale-parts (continuous).
C Pitch	..	..	..	$\sharp f''$	e''	$\sharp c''$.
C $\lambda/2$	..	..	..	22	25	30 cm.
C s	..	..	..	10	15	20 scale-parts.

The apparatus is active even if but one telephone is used, the other being silent. Thus at d'', $s=75$ fell to $s=35$ with one telephone excluded. Care to guard against even small leakages is very necessary, or s will fall off.

With the graphs a, b, c, figure 100, another method of approaching the frequency correction becomes available. Since the first three harmonics are in question, the pipe-lengths $z+a$ are respectively equivalent to $\lambda'/2$, $2\lambda'/2$, $3\lambda'/2$, where λ' is the wave-length within the quill tubes, and not to $\lambda'/2$, as was postulated in the equations $z+2.5=0.25(\lambda/2)$, $z+22=1.13(\lambda/2)$, and $z+22=1.65(\lambda/2)$. Thus, if the corrected coefficients b are called b, b', b'', respectively, the following relations appear for the relative frequencies n;

Curve (a) freq. ratio, $n=1$ $b=0.25$ $b=0.25$ $1-b=0.75$ $(1-b)\sqrt{n}=0.75$.
Curve (b)   2 1.13 $b'=.56$ $1-b'=.44$ $(1-b')\sqrt{n}=.62$.
Curve (c)   3 1.65 $b''=.55$ $1-b''=.45$ $(1-b'')\sqrt{n}=.78$.

In the preceding section for straight tubes, $x+10=0.51(\lambda/2)$ was obtained, so that $b=0.51$ is more probably the coefficient for the fundamental. True, figure 90 contains an a maximum below the a'; but it is to be considered incidental and at all events too low for development. Thus it appears that a coefficient of this order could be identified with the data $b'=0.56$ and $b''=0.055$

for the second and third overtones in the table. But such a procedure leaves the datum $b'=0.25$, here found, still more anomalous.

From the theoretical equations, as above put,

$$(\lambda/2-(z+a))/(\lambda/2)=1-b=\sqrt{\eta/2n\rho}/R$$

$(1-b)\sqrt{n}=$const. should follow for a given radius of tube R. These data have also been tabulated, and it is now the second harmonic which is inconsistent. There are, however, three earlier values (figs. 95 and 97) for this coefficient, respectively, $b'=0.45$, 0.43, and 0.48, and if their mean be taken $(1-b')\sqrt{n}=0.77$, which would fit in better with the table.

The subject therefore is quite involved. Within the range of the separate graphs, figures 95, 97, and 100, no frequency effect can be detected. From the group of graphs for successive overtones, such a relation can not, however, with confidence be rejected. It seems more plausible that $b=0.51$ given by straight tubes is trustworthy and that, therefore $(1-b)\sqrt{n}$ is not constant, whereas b probably is nearly so.

What is particularly puzzling is the interdependence of a and b. As obtained in different experiments, a and b vary proportionally for incidental causes not detected. Thus in figures 95, 97, and 100 for the octave

$$
\begin{array}{cccc}
a=12 & 13 & 16 & 22 \\
b=\;0.85 & 0.89 & 0.96 & 1.13
\end{array}
$$

In figures 93 and 100 for the fundamental

$$
\begin{array}{cc}
a=10 & 2.5 \\
b=\;0.51 & 0.25
\end{array}
$$

while the fifth in figure 100 stands alone. These data are constructed in figure 101 and the graphs are seen to be consistent and not very different for the fundamental and the octave.

TABLE 17.

	Freq. ratio, $n =$		
	1	2	3
b_0	0.16	0.52	1.05
b_0/n	.16	.26	.35
$1-b_0/n$ .... $\Big\{$	.84	.74	.65 observed.
	.84	.74	.64 computed.

It is thus worth while to attempt to eliminate the a from the equation, if the incidental influences modifying b are to be removed. This may be done by estimating the b_0 which holds for $a=0$ in an equation $b=b_0+\beta a$, and since the slope for the octave is not very different from the fundamental, the slope for the fifth may be taken as the same as that of the octave. Thus the data are given in table 17.

The last values are given in figure 102 and comform very nearly to the equation $1 - b_0 n = 0.94 - n/10$, as given by the table; or if b_0 be computed, the results are

$n = 1$	b_0 (observed) 0.16	b_0 (computed) 0.16
2	.52	.52
3	1.05	1.08

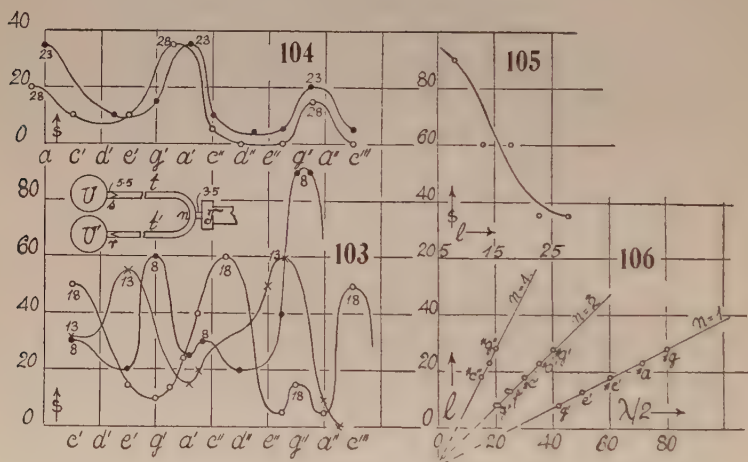The method pursued has thus been as follows: From $x + a = b(\lambda/2)$ the equation

$$x + a = (b_0 + \beta a)(\lambda/2) \text{ or } x = b_0\lambda/2 - (\beta\lambda/2 - 1)a$$

was inferred. This for $a = 0$ gives

$$x = b_0\lambda/2, \text{ where } x = n(\lambda'/2)$$

n being the frequency and λ' the wave-length under friction. Thus

$$\lambda' = (b_0/n)\lambda \text{ and } \frac{\lambda - \lambda'}{\lambda} = 1 - b_0/n = 0.94 - n/10$$

as computed above. In so far as this b_0 or null method is valid, a frequency effect must be recognized; but it does not follow the theoretical equation $(\lambda - \lambda')/\lambda = \sqrt{\eta/R^2 2\rho n}$ in these severe quill-tube tests. It will probably be safer, however, to confine the attention to the non-reduced b, as in the following section.

60. **The same. Single telephonic exciter.**—The preceding methods with two cooperating telephones introduce certain complicating inconveniences. In the case of straight tubes (longitudinal) the paired pin-holes must be displaced to follow the nodes of the overtones. In transverse quill tubes the pin-holes are fixed, but their tube-length is a material addition to the remaining tube-length. In this respect the adjustment given in figure 103 (inset) has advantages. A single telephone T here actuates the paired quill pipes (0.35 cm. in bore) sn and rn, n being a node. With fixed pin-holes r and s, one should expect all the overtones to appear in succession; but for some reason the

fifths are deleted. The results, however, are very much smoother than heretofore and three successive octave groups are available for exploration.

The survey in pitch is summarized in figures 103 and 104, the telephone, small inductor, and circuit together constituting the electric siren. The lengths l are measured fròm s or r to n. Beginning with $l=8$ cm. in the bend, l is increased in steps of 5 cm. on each side. Corresponding maxima are tabulated in table 18.

The chief maxima thus reappear at octave intervals. The optimum (see fig. 105) lies within 8 cm. There are small secondary maxima which it is difficult to construe.

The relations of l and λ are given in figure 106, with the pitch added at each observation. Their disposition is again as nearly linear as the ear can guarantee, the three lines $n=1$, 2, 4 belonging to the successive octave groups. Each again demands an initial tube-length, but this ($l=12$, 12, 13 cm.) is here nearly the same in the three cases, or is at least without systematic change.

TABLE 18.

l	Pitch.	$\lambda/2$	Pitch.	$\lambda/2$	Pitch.	$\lambda/2$	Remarks.
		cm.		cm.		cm.	
8 cm....	..	..	g''—$\sharp g''$	21-22	g'	42	Minima, a', d'', a''
Computed				20	..	41	Sec. max., b'.
13 cm....	..	..	e''—f''	24-25	e'	50	Minima, a' $\sharp a''$
Computed				25		50	
18 cm....	$\sharp c'''$	15	$\sharp c''$	30	$\sharp c'$	60	Minima, g', f'', a''
Computed	..	15		30	..	60	Sec. max., g''
23 cm....	$\sharp a''$	18	$\sharp a'$	35	$\sharp a$	71	Minima, $\sharp d'$ (c'', d'', e'')
Computed	..	18	..	35	..	69	
28 cm....	$\sharp g''$	20	$\sharp g$	40	$\sharp g$	80	Minima (c', d', e') (d'', e'', g'')
Computed	..	20	..	40	..	79	

One might suppose that the tube ends Us and $U'r$ are implicated, but their length is but 5 to 6 cm. The equations of the lines for the frequency ratios n may be written

$$n=4 \qquad l+12=2.0 \ (\lambda/2)$$
$$2 \qquad l+12=1.0 \ (\lambda/2)$$
$$1 \qquad l+13=.52 \ (\lambda/2)$$

The above shows the computed values which, on the whole, are about as near as the ear may expect to come. A few divergences could doubtless be resolved on repetition. Thus the viscosity here expresses itself in the coefficient together with an additional tube length.

A question presents itself, whether these octaves (of which the middle one is the most conspicuous) are not stimulated by overtones in the telephone-note. Thus when for $l=8$ cm., the telephone sounds g', it may be the g'' evoked which produces the g' maximum; for $l=18$ cm. the telephone note near c' may be active through c'', g'', c''' in the overtones, etc. In such a case, the above equations would be repetitions of each other. It is, however, improbable that the overtones should be of the observed intensity, and more important

7

still, the telephone overtone can only be operative if b is fractional. Thus $b=0.25$ is the only case which could be evoked in this way. Consequently we may write with assurance as in the preceding section (if λ' is the wavelength under friction), taking the graph $n=1$ as the fundamental:

$$
\begin{aligned}
n=1 \quad & (\lambda'/2)=l+13=0.52(\lambda/2) \quad & \lambda'=0.52\,\lambda \\
2 \quad & 2\,(\lambda'/2)=l+12=1.0\ (\lambda/2) \quad & \lambda'=\ .50\,\lambda \\
4 \quad & 4\,(\lambda'/2)=l+12=2.0\ (\lambda/2) \quad & \lambda'=\ .50\,\lambda
\end{aligned}
$$

in the general form $n(\lambda'/2)=l+a=b(\lambda/2)$. Since the constant a is here the same (nearly) throughout, the coefficient b is probably less in need of reduction in relation to a. At all events, no observations could be devised to elucidate this dependence.

Thus it appears that the relations are simpler than in the preceding section, $b=0.51$ being constant for the three octave groups $n=1, 2, 4$ in frequency ratio. The values heretofore found were for straight tubes of about the same section $b=0.51$, $a=10$ cm., $n=1$; for transverse tubes, $b=0.25$, $a=2.5$ cm., $n=1$; $b=0.56$, $a=22$, $n=2$; $b=0.55$, $a=22$, $n=3$. These are all of the same order of value, excepting the case $n=1$ for transverse tubes, where $b=0.25$ has but one-half its anticipative value. Thus in the four octave groups $n=1, 2, 3, 4$, b does not vary, if the exceptional case specified, associated with the exceptional $a=2.5$ cm., can be explained. The endeavor to reduce b to b_0 for $a=0$, by the constants of figure 101, leads to no trustworthy results in the single telephone experiments; b_0/n (0.27, 0.31, 0.31) comes out more nearly constant than $1-b_0/n$. Tentatively, one may postulate that the transverse pipe on sounding its fundamental vibrates like a closed organ-pipe or that

$$
\frac{n}{4}\lambda'=0.25(\lambda/2)
$$

whence $\lambda'=0.50\lambda$, in keeping with the six other octave groups. The result remains none the less difficult to understand, and one more easily concedes here that it is the first overtone of the telephone-note which evokes this apparently low octave group. To make sure of its occurrence, I repeated the two telephone experiments (fig. 95, inset) and obtained for the transverse pipe somewhat differently mounted:

$z=$	8	13	18 cm.
Pitch $=$	$f'\text{-}g'$	c'	a
$s=$	35	30	50 scale-parts.
Observed $\lambda/2=$	45	63	75 cm.
Computed $\lambda/2=\begin{cases}\\ \\\end{cases}$	45	63	82 cm.
	$f'\text{-}g'$	c'	$\sharp g$

results given by the equation $z+4=0.27(\lambda/2)$. The difficulty here, already foreshadowed in figures 89 and 90, lies in the plateau-like character of the low-pitched maxima; but the order of $b=0.27$ is none the less definite.

A final question relative to the need of joining the pin-holes s and r to the respective shanks U and U' of the gage, deserves attention. In the inset, figure 107, the pin-hole r is disconnected and open to the atmosphere. Another telephone was used, but the endeavor was made to insert a tube-length $l=8$

cm. so far as this can be done. The graph thus obtained (fig. 107) is closely
similar to the graph for $l=8$ cm. in figure 103, a little shift necessarily result-
ing from the l-difference. In figure 107, however, the secondary maxima were
more carefully traced, showing one at g'' which is ignored in figure 103. The
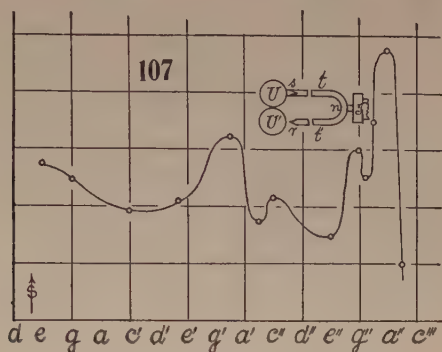
curve below g' in the 2- and 4-foot octaves was also followed at closer
intervals. It is astonishing to find a strong 4-foot e in these short ($l=8$ cm.)
quill tubes, and the whole curve presents a case of multiresonance which only
terminates at b''. Nowhere else is the response absent. It is conceivable that
the g'' and a'' maxima may belong to the tubes t and t' separately.

61. The same. Single telephone and single tube.—The final method
tested (shown in the inset of fig. 108), though apparently the simplest, failed
to give data as clear cut as was expected. Here the quill tube tt (0.35 cm. in
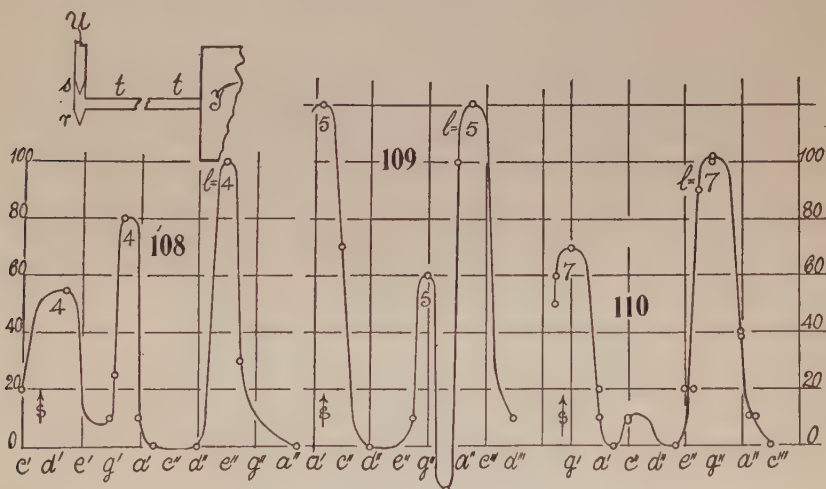
diameter) extends at one end to the plate of the telephone T, while the other
carries a **T**-branch holding the salient and reëntrant pin-holes r, s. The latter
is joined with a short end of tubing to one shank of the interferometer **U**-gage
and r is open to the atmosphere. In this case the quill tube tt may be made

very short, and the graph (fig. 108) was obtained with tt less than $l=5$ cm. With 2,000 ohms in circuit the strong maxima near e'', $\flat a'$, and $\flat e'$ appeared. There is marked response even at c' for this 4-cm. tube. It is possible, of course, that this low pitch may be evoked by the upper harmonics of the telephone-note, though one would not anticipate the observed intensity in such a case. The maxima obtained do not fit in with the results below, which, however, is not surprising, as the diameter for the short length was irregular.

A repetition of the work, with a quill tube slightly longer ($l=5$ cm.) and of uniform bore, gave the data of figure 109, with two definite maxima at $\flat b''$ and $\flat b'$ and peculiar behavior near $\flat a''$, which I did not stop to investigate. Acoustic pressure here came out definitely negative, and this is the only case of negative pressure obtained in this group of experiments. Figure 110 shows
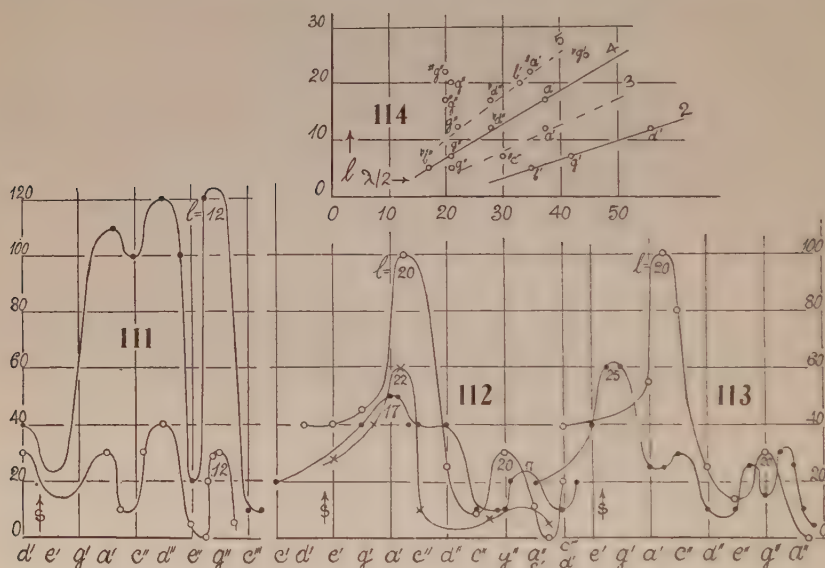
the results for a tube-length (tt) of $l=7$ cm., with two marked maxima about an octave apart and a minor one. In figure 111 the tube-length is increased to 12 cm. and two different intensities of current were used, producing similar but unequally developed curves.

Beyond this the graphs for $l=17$, 22 cm. gradually fall out of agreement. Resonance is continuous over large intervals and the appropriate maxima are harder to recognize. The crest near a' for $l=17$ cm. is still acceptable, but the one for $l=22$ cm., which should be at f', is absent.

A repetition of the last case with $l=20$ cm. and somewhat larger intensity is also given in figure 112. It closely resembles the graph for $l=22$ in character, and the pitch of the chief but spurious maximum is about the same. Hence the orderly sequence of maxima stops at $l=17$ cm. and between 17 and 22 cm. there is little progress. Between $l=20$ and 25 cm. (fig. 113) the

sequence of maxima seems to recommence, though the details of the graphs for these long tubes naturally increase.

In figure 114, the l and $\lambda/2$ values for the chief crests have been constructed. The values which may be taken as belonging together are (curve 4):

Pitch.	l	$\lambda/2$
bb''	5 cm.	17.5 cm.
g''	7	21
d''	12	28
a'	17	37

conforming adequately with $l+5.5=0.60(\lambda/2)$. The lower octaves are less definitely (curve 2):

Pitch.	l	$\lambda/2$
bb'	5 cm.	35 cm.
g'	7	42
d	12	56

and their coefficient $b=0.32$ agrees roughly with the preceding, if reduced. Both coefficients are larger for some reason than in the above experiments with double tubes, while the two maxima in figure 113 would correspond to a coefficient of less than $b=0.5$. Thus the conditions here are much more complicated than heretofore and a number of prominent crests (curves 3 and 5) can only tentatively be grouped together; the graphs are probably untrustworthy, even though their coefficients are roughly in the ratio of 2, 3, 4, 5. The crests near g'', which together lie nearly on a vertical for all values of l, are clearly to be referred to the resonance of independent vibrator like the telephone-plate.

62. Reversal of pin-holes, etc.—If the pin-holes are reversed at the same shank of the U-tube, so that, in figure 108, inset, s and r both point toward U, the graphs obtained are throughout negative. Pressures have been changed to dilatations within tt. The arrangement, however (see also fig. 115 at UT), is usually much less sensitive, and, what is more important, the resulting graphs are quite different in the disposition of their (negative) crests from the original case. Thus, for instance, the persistent g'' crest (fig. 116 showing the direct and fig. 117 the reversed pin-hole adjustment, with two graphs for large and small intensity at $l=10$ cm.) is quite absent ($s=0$) in the reversed case, and similarly with other crests. In fact, these graphs are liable to be without harmonic character, showing response everywhere from a' to a'', with a maximum at about c''. The conditions under which reversal proceeds are

thus quite complicated and difficult to investigate; but they may be of con-
siderable importance in their bearing on the phenomenon as a whole.

A number of other experiments of reversal were made, resulting in graphs
of the same character as figures 116 and 117, which need not therefore be
given. As in case of the curves for $l = 10$ cm., notes which fail in some adjust-
ments come out in others, a result probably similar to difficulties of intonation
in musical instruments. The amplitudes increase more rapidly than the electric
currents actuating the telephone. The chief difficulty of comparison, however,
lies in the unequal lengths of the tubes for reversed pin-holes, if the adjustment
of figure 116 (inset) is used. I therefore returned to the adjustment of figure
108 (inset) where the pin-hole tubes are in the transverse branch. Results
so obtained (length $l = 10$ cm.) are given in figure 118, the upper curve
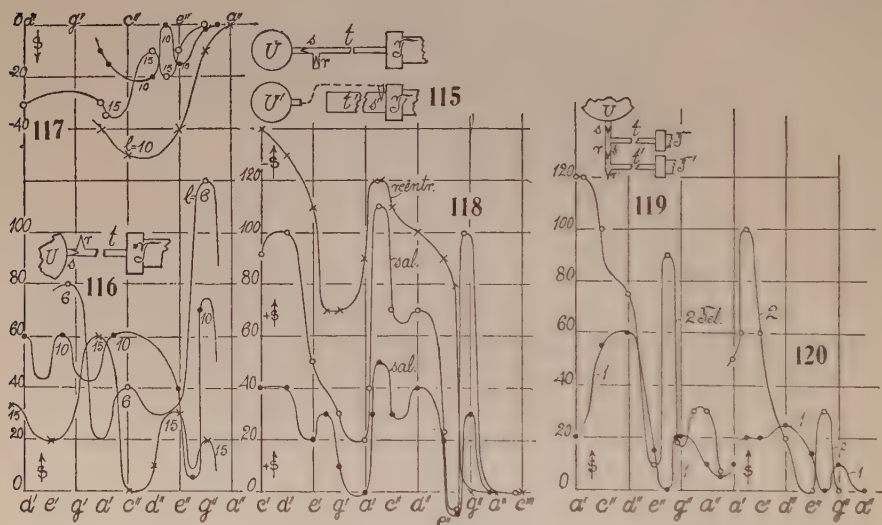
showing the acoustic dilatations ($-s$ charted upward) and the two lower the
acoustic pressures ($+s$ upward), for pitches from c' to c'''. In the latter cases
($+s$), fringes of different size were used in the two curves. Hence the
difference of intensity. In figure 118 there is an obvious correspondence
between all the graphs. Thus, the b' crest is a definite feature of all, as is
also the march toward a lower maximum somewhere near b. In their details,
however, the $+s$ and $-s$ graphs differ, particularly at the crest near g'', which
comes out strongly with salient pin-holes, but is silent for reëntrant pin-holes,
as already found in figure 116. Hence, while in the above I associated this
persistent note with the telephone-plate, it now seems more probable that
it is to be referred to the pin-hole tubes. That these in the salient position do
respond quite appreciably I showed in an earlier report (Carnegie Inst. Wash.
Pub. 310, § 25, figs. 34, 35, 1921). Similarly the negative f'' in the salient
cases does not appear in the reëntrant graph.

If the pin-hole between U and tt (fig. 116) is removed, so that a single pin-hole salient outward remains, the tube tt is virtually open at one end. The graphs are, of course, essentially different and the sensitiveness is liable to be very low unless the size of pin-hole is judiciously chosen.

Since in case of the use of two pin-holes r and s but a single shank of the U-tube is required, the other with reversed pin-holes may be used for any other acoustic purposes at the same time. Thus in figure 115, the quill tube t is set for acoustic dilatation, while the pin-hole s' salient as to U' measures the acoustic pressure in the wide tube t' open at one end, the telephones TT being in parallel. In this way, if t or t' is adjustable in length, the lengths of t and t', which correspond to the same crest, may be directly compared. The fringe displacements are nearly summational; thus:

Tube t (alone) s equals 30; t' (alone) 45; $t+t'$ (together) 70 scale-parts. The difficulties in tuning such pipes are, however, greater than I anticipated.

63. Successive telephones in cascade.—In the earlier reports the endeavor was repeatedly made to obtain increased acoustic pressure from a succession of pin-holes in series; but no relaying of this kind occurs. There should, however, be a definite result if (as in fig. 119), between each pair of pin-holes sr, $s'r'$, etc., a telephone T, T', etc., is introduced. For the case of two identical telephones in parallel, the graphs (fig. 119) show this to be the case. But while the intensity for two telephones is as a whole much larger than for one, the positions of the crests and troughs is by no means the same. The two quill tubes t and t' do not behave identically. Thus near f'', while one telephone evokes a trough, the combined effect of two is a pronounced crest. Even in a repetition of the experiment with slightly altered tube-length tt' (fig. 120), this inversion at f'' is sustained. The conditions are further complicated, inasmuch as the relative efficiency of the pin-holes enters fundamentally into the result. If the current in one telephone is reversed, the sum is also liable to be reduced.

It is not surprising, therefore, that with three telephones adjusted on the plan of figure 119, inset, an increase of the acoustic pressure produced by two (all left in parallel) is not as a rule attainable; at least I did not, after many trials, obtain a single marked result, and in many cases there was a reduction.

64. Experiments with high resistance (binaural) telephones. Apparent hysteresis.—In testing the radio telephones, the H-branch of figure 58 above was used for convenience, the cross-tube a being provided with a short branch and stopcock, so that the air within the H-branch could be partially exhausted. To make the telephones air-tight, a gasket of card-board, previously soaked in hot oil to expel air, was interposed between the cap and the telephone-plate.

Very small fringes, less than 0.5 scale-part of the ocular micrometer (1 cm. divided in 0.1 mm.), were used to admit of larger pressure ranges. Tested

with the slide micrometer Δx, at $\theta=45°$ $(2\Delta x \cos \theta = n\lambda = 2\Delta h)$, the coefficient was at first $\Delta x = 10^{-4} \times 1.07$ cm. per scale-part (Δs); or $\Delta h = 7.6 \times 10^{-5}$ mm. per ocular scale-part. The coefficient changed to $\Delta x = 10^{-4} \times 1.03\Delta s$, in the course of the work.

The small inductor of varying frequency (electric siren) actuating the telephone gave about 50 scale-parts (s) of deflection at resonance, with 40,000 ohms in the telephone circuit. Between 20,000 and 40,000 ohms, sR was nearly constant; as, for instance,

$$s= \quad 100 \quad 66 \quad 52 \quad \text{scale-parts.}$$
$$10^{-4}\ R= \quad 2 \quad 3 \quad 4 \quad \text{ohms.}$$

An example is given in figure 121, taking $\dfrac{1}{s} = \dfrac{1}{e}R$. The figure also gives data for single telephone, either the tube t or t' being stopped in this case. Usually, larger deflections were obtained with loose rubber connections than with very tight rubber connections at the branches, a result probably to be referred to the pressure introduced in making the latter connection, as will presently be shown. Closing the cross-piece a (fig. 58, or insert, fig. 121) with a screw pinch-cock, gradually cut off all deflection. If there is a slight leak in the **U**-gage the deflections are scarcely reduced; but a continuous air current now passes against resistance from U' at lower pressure through a to U at higher pressure, in virtue of the acoustic mechanism. For the acoustic pressures at the pin-hole valves demand an excess of pressure of U over U'.

An interesting result is the detection of what appear to be hysteresis phenomena in the telephones. The **H**-branch method (fig. 121, inset) was again used. The deflections s were found to be smaller for gradually increasing telephonic currents than for decreasing currents to the extent of 5 or 10 per cent. Example of each result is given in figure 122, constructing the fringe deflections $s = e\left(\dfrac{1}{R}\right)$, both for the interval between $R = \infty$ and 20,000 and between ∞ and 30,000 ohms. As the **U**-gage returns strictly to zero when the current is broken, the phenomenon can not easily be referred to the gage. It may therefore be in the telephone, which here appears more sensitive if it has recently been more highly stimulated. The effect quite disappears after the current is broken. It is, moreover, as might be expected, somewhat capricious, so that it varies in amount in different telephone adjustments and may even be absent. However, it is not improbable that the difficulties encountered in the density work (above, § 37, etc.) are producing similar discrepancies here.

65. Telephonic effect at different air-pressures.—The above result suggested the desirability of testing the telephone with a partial vacuum in the **H**-branch and the apparatus (fig. 121, inset), therefore, was made moderately air-tight, as above explained. Increased air-pressure on the front face of the plate wiped out all fringe deflection.

On removing the air from a (fig. 121, inset) through a side-branch with stop-cock by gentle suction, it was very curious to note that the mouth cavity frequently responded by resonance loudly to the telephone pitch, the latter being otherwise practically inaudible under the circumstances (distance, closed region). The run of experiment was usually something like this, remembering that a slight air leak remained in the telephone: Starting with a deflection of about 40 space-parts, this fell off to very small values immediately after suction and closing the stop-cock. In the lapse of time, however, the deflection increased, finally rapidly, until it reached even 85 or 90 scale-parts, i. e., more than double the original value. The latter is a maximum; and on further waiting, it slowly decreased, more and more so, as it got smaller. To reach the original deflection again sometimes took an hour. Putting a mercury gage in connection with the closed region, it was found that the whole march of rapid increase and decrease of s occurs very nearly at atmospheric pressure. Thus one would naturally refer the occurrence to the telephone, the plate of which is successively spaced and momentarily conforms to maximum sensitiveness. The reason, however, for the long retention of increased sensitiveness, when once impressed, is by no means clear to me, though there is probably a connection between the present result and the preceding. In fact, both phenomena may vanish
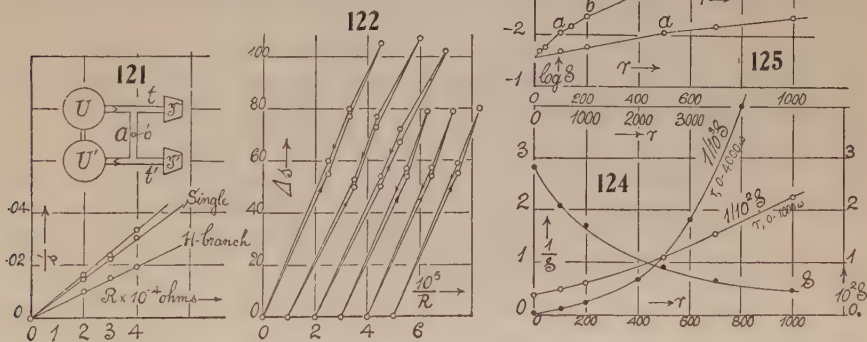
at times; but they reappear on reclamping the plate of the telephone, and the like. They are interesting as showing the wide limits to which sensitivity is subject. Finally, the different rates at which air would (incidentally) transpire out of the U-gage, through the pin-holes if not of identical diameter, further complicates the observed occurrences.

66. Telephonic response to varying current.—Using the favorable conditions of a U-gage filled in vacuo (§ 2), tests were made of the relation of the resistance r inserted into the telephone circuit and the corresponding dis-

placement, S, of the slide-micrometer needed to bring the fringes back to the fiducial point in the telescope. This was done throughout as wide a range as the acoustic pressures in the branch adjustment (fig. 56, § 47) admitted. As it is often of practical interest to know to what extent the simple equation $S(r+r_0)=$ constant applies when the external resistance r is diminished as far as zero (r_0 being the total resistance in the telephone for a fixed frequency), graphs are given to show the change of $1/S$ with r.

In the first survey a fixed resonance note was established in the telephone by aid of the electric siren at $r=1,000$ ohms. The siren was then left untouched, while r was successively diminished or successively increased. The graphs, for $1/S$ (example in fig. 123) were curved throughout, even with an apparent minimum at $r=100$ ohms. It seemed probable that a part of this result must be attributable to the gradual loss of resonance between the telephone-note and the branch-pipe, owing to incidental occurrences.

The work was therefore repeated in such a way as to reestablish the resonance at each of the successive r values. The new results found are summarized in the graphs (fig. 124). It thus appears that only for an external resistance between $r=500$ and $1,000$ ohms is the relation of r and $1/S$ practically linear. Below $r=500$ ohms, the graph departs from the line, a result which one would naturally expect. The data obtained are as follows:

$r=$	1000	700	500	200	100	0	ohms.
$10^4S=$	44	65	91	168	207	282	cm.
$1/10^3S=$	2.25	1.53	1.09	.595	.482	.354	
$10^3\Delta h=$	32	46	65	119	147	251	mm. Hg.

The corresponding acoustic pressure Δh in millimeters of mercury is also given, reaching a maximum of 0.25 mm. when all external resistance is excluded. For large resistances r, the data were (fig. 124):

$r=$	1000	2000	3000	4000	ohms.
$10^4S=$	44	15	5.5	23	cm.
$s=$	70	25	10	5	scale-parts.
$1/10^3S=$	2.27	6.67	18.2	40	

Here the graph is characteristically curved.

In the preceding report (Carnegie Inst. Wash. Pub. 310, Part II, 1923, § 38), the relation $S_0=Sc^{r/r_0}$ was proposed for these curves; but it was noticed that on plotting log s and r, the straight lines obtained always showed a break of continuity. The broken lines again appear in the present experiments, as shown in figure 125. In the range between $r=0$ and $1,000$ there is a break at a ($r=500$ ohms). In the range from $r=0$ to $4,000$ ohms there is a further break at b ($r=1,000$ ohms). The line ab as a whole might suggest a continuous curve; but this is improbable in view of the similar results given for smaller ranges in the last report. The inference seems reasonable that at points a, b the vibration of the telephone-plate changes form and with it the acoustic pressure. There are thus a series of values log $s_0=-1.55$ (observed), -1.75, -1.88, to which $r_0=448, 723, 923$ correspond.

MISCELLANEOUS PIPES AND EXCITATION.

67. Experiments with pin-hole resonators.—The most sensitive form of this apparatus consisted of a cylindrical pipe closed at one end by a doubly perforated adjustable cork, through which the paired salient and reëntrant conical pin-hole tubes were to be thrust. The latter were then connected with the corresponding shanks of the interferometer U-tube. This requires two connecting-pipes. Now, in a variety of experiments since made (*cf.* § 60), it was a matter of indifference whether both pin-holes are thus connected with the U-tube, or whether one of the pin-holes is merely open to the air, so that but a single connecting-tube is needed. It was of interest to find out to what degree a similar principle would apply to the pin-hole resonator.

These experiments were made at some length, but the evidence obtained was not clear cut, chiefly, I think, because the organ-pipe with which the resonator is in step (f'') changes its pitch, as usual, slightly with its intensity. If we denote by s and r the salient and reëntrant pin-holes, when joined to the U-tube, by s_0 and r_0, the same when disconnected from the U-tube and open to the air, and by p a plug inserted in place of the pin-hole tube, the results obtained may be most clearly expressed as follows: The combination $s+r$ always gives the maximum fringe displacement. The combination $s+s$ or $r+r$ gives no displacement; or if the pin-holes are not quite equally efficient, there may be a small residual displacement either positive or negative. On the other hand, as regards fringe displacement, $s+r_0$ or $s+p$ may come as near as 10 per cent of $s+r$. Rarely did it fall 30 or 40 per cent below it. The variable adjustment proved to be s_0+r or $p+r$. The latter often fell off 70 or 80 per cent, while the usual value of s_0+r was about 50 per cent of $s+r$, though it rose at times to 90 per cent. Supposing that in the last case there might be a small leak in the cork, I used different precautions without avail. The cause of the irregularity in the behavior of r was not detected. The r pin-hole differs from the s, inasmuch as the former lies at the bottom of a quill tube which necessarily becomes a part of the resonator.

As a result, perhaps, while $s+s$ or $r+r$ give a null effect (the pressures at the U-tube counterbalancing each other and the pin-holes therefore equally efficient), the $r+s$ effect in fringe displacement is often not summational. A certain maximum of acoustic pressure seems to be producible which can not be exceeded by apparently favorable adjustment of the pin-holes. A typical series of data may be added

|	$s+r$	$s+r_0$	s_0+r	$p+r$
Fringe displacement	100	70	50	30

If four identical pin-hole resonators be taken and the two salients joined to the U-shank, the two reëntrant to the U'-shank, the fringe deflection of a single pair is not increased. If the pin-holes for the same U are reversed the effect is zero.

68. Interference of resonators.—Results obtained for the interference of two identical single pin-hole resonators (inset, fig. 126), coaxially placed at a distance d apart with their mouths toward each other, were given in the last report (Carnegie Inst. Wash. Pub. 310, II, §§ 35, 36). Data of the same kind were incidentally found in connection with the present work and are recorded in figure 126. At least 10 cm. between mouths is needed before interference ceases (f'' resonators about 11 cm. deep responding to a closed f'' pipe). The pinholes are respectively salient and reëntrant. If they are similarly placed, reaction ceases for all relative positions. If the mouths are toward each other, but with slightly overlapping parallel contiguous tubes, there is no disturbance, as is also the case if the mouths point in the same direction.
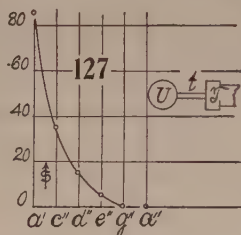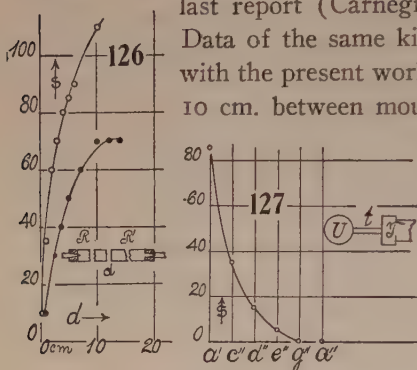
69. Immediate junction of U-gage and telephone.—In the earlier reports it was shown that in a rigorously closed tubular region no acoustic pressure could be registered. Thus in figure 127 (inset), where the telephone T is joined to one shank of the U-tube U by a short length of tubing t, no fringe displacement is observable, even when the telephone vibrates intensely with a loud burr, provided the plate, etc., are all sealed hermetically. But if there is a slight leak around the plate, even if tightly appressed by the cap, a very definite fringe displacement is observed, particularly at low pitch. It is again necessary that the telephone vibrate strongly.

The results obtained are given in fringe displacements s, for different pitches from a' to a''. Below a', s was found to decrease, so that there is probably a crest at a', as is usual with these short tubes. Above a', s falls off rapidly and nothing was observable beyond a''. Conformably with the small leak in question, these fringe motions are very gradual, so that the experiment takes some time. If the sound ceases, the zero is regained with the same slowness.

The experiment is interesting, as it might be supposed to admit of an interpretation on the energy of the sound excitation. If the pressure in the atmosphere is p, the same pressure occurs within the region UtT, if the telephone is not sounding. When the telephone is actuated, therefore, the energy per cubic centimeter within the region is $p+\rho v^2/2$, where v^2 is the average velocity squared of the vibrating air-particle. Thus the available energy would be in excess within; and p is therefore reduced to p', such that $p'+\rho v^2/2=p$. Thus $\Delta p=\rho v^2/2$.

Standardizing the fringes with the slide micrometer, $\Delta h=16\times10^{-6}$ cm. of mercury was found as the pressure equivalent to the displacement of 1 fringe; so that $\Delta h=0.213\Delta s$ dynes/cm.^{2} if Δs is the fringe displacement

observed. Hence the graph figure 127 corresponds to the following pressures
and kinetic energies per cubic centimeter:

| Pitch	a'	c''	d''	e''	a''	
$p \times 10^3$	1.36	0.56	0.24	0.18	0	cm. Hg.
$\Delta p = \rho v^2/2$ ...	18.1	7.5	3.2	1.1	0	ergs/cm³.

Rayleigh's value for the limit of audibility is $\Delta p/p = 6 \times 10^{-9}$. The strong
a' observed should thus be only $18/6 \times 10^{-3} = 3 \times 10^3$ more intense. This datum
thus seems to be not unreasonable for so highly energized a region.

70. The same. Different telephones.—It seemed necessary to endeavor to
compare these data with the corresponding behavior of other telephones. The
next one tried with a very tight cap gave no results whatever, the fringes
being subject to mere temperature fluctuation. After loosening the cap,
however, the data of figures 128 and 129 were worked out. Dilatations are
here laid off downward, as it was found that at very low pitch (e') slight
pressure was apt to occur. The scale also is reduced. These figures show
that there is actual resonance between g' to a' and the fringe displacement
for the loose plate reached about 80, so that the energy in question (caet. par.)
is about the same as before. On commutating the current through the tele-
phone, the whole action is much reduced in range and the pressures are
nearly equal to the dilatations. The tentative theory just advanced will there-
fore again have to be discarded, for the leak around the loose plate now
produces a pinhole-like effect, though of small intensity. Moreover, on tighten-
ing the cap moderately and fully, two graphs were obtained (fig. 130), in
which the character of figures 128 and 129 is quite obliterated.

Continuing the experiments with
an old bipolar telephone, the re-
sults, figure 131, were consistent
dilatations for both positions (I,
II) of the telephone switch. The
trough near e'' is peculiar. A
slightly loose cap is presupposed.

Similar experiments with two
radio telephones of high resistance
gave no fringe displacements for
any degree of looseness of the caps
of the telephone. Many modifica-
tions were tried, but all failed.

Finally, the results of figures 132, 133, and 134, obtained with a bipolar
telephone, threw critical light on the phenomenon. The cap must not be so
loose, of course, that sound escapes audibly, or there will be no fringe dis-
placement. Neither must it be air-tight. Between these limits the experiments
(fig. 132) now show a strong acoustic pressure, a result at variance, there-
fore, with all the preceding work. In figure 133, lower graph, the data obtained
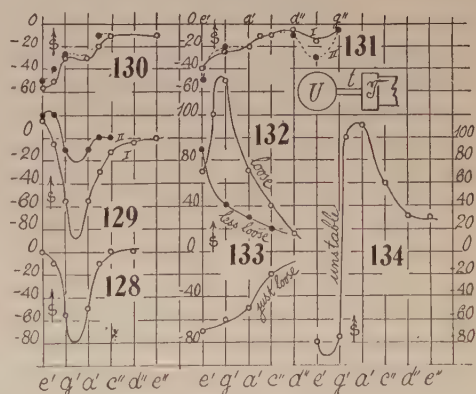
with the cap all but tight gave evidence of marked dilatations. Loosening the cap a little further (fig. 133, upper curve) the pressures of the upper curve again result. In figure 134, with a cap just loose, the adjustment incidentally obtained is such that marked dilatations followed by marked pressures occur in succession. At g' the conditions are unstable and the fringes sweep suddenly from negative to positive values.

Thus in the long run the suggestions of the preceding section are not sustained. While the dilatations are more frequent, marked pressures may also occur, provided the nearly closed region (U-tube, quill tube, telephone) is not air-tight. This implies that the shape of the crevice at the telephone-plate, where there is slow escape of air, is solely instrumental in producing the acoustic pressures observed. The very thin air-gap acts like a pin-hole, though much less effectively; and it may to this degree replace either the reëntrant or salient pin-hole, depending on the chance condition of loosening the plate to produce an adequately fine crevice.

71. Specially tuned H-pipe.—The advantage of the H-branch (fig. 135, inset) is the ease with which it may be tuned to any note by elongating the pipes b and c, which may be made of quarter or eighth inch pure-rubber tubing. These are attached to the rigid elbow of very thin brass ($\frac{1}{4}$-inch) tube, the cross-pipe a corresponding to the distance between the telephones T, T', which should be kept within 10 cm. A hole in a with a stopper allows of additional tuning; but as energy is lost here, the hole should be small. The behavior of open quill tubes attached to the hole O of the cross-branch a is peculiar and given in some detail in figure 136. Here l denotes the length of tube measured from O to the open end, and s is the corresponding fringe displacement. The relation is distinctly periodic, while the pitch changes from e'' to g'', the latter curiously enough corresponding to minimum fringe displacement. Lower harmonics are also present, though in small intensity, as shown at d'', b'. When the hole O is closed, the note is e''; when quite open $\sharp f''$ to g'', with a displacement of $s=95$ to 100 in each case. The pin-hole valves p, p' (fig. 135) should be at the end of very short tubes and placed as near the U-tubes as possible, as the sensitiveness depends very materially on this condition. Unfortunately, since an entrance tube to U and U' is necessary elsewhere, the length lost here in my apparatus was 3 to 5 cm.

The lower part of figure 135 gives a record of the length of b and c tube, between U and T, corresponding to different frequencies from a' to e''. The same figure shows the length of common wood diapason pipes. The mean rate at which pitch decreases with length is less in the latter case. At d'' the lengths would coincide, though it is probable that about 4 cm. (to pin-holes) should be deducted from the UT length, in which case coincidence would occur at a lower pitch. Since the UT pipes are less than 0.25 inch in diameter and form a doubly closed acoustic pipe, this coincidence is rather curious, as one would anticipate a much greater viscous effect in the quill pipe. The ease with which low values of pitch (even to c') may be produced here is equally

surprising; for one would expect the slender air column to break up. Just above the two curves in question are the corresponding semi-wave-lengths in free air.

At the top of figure 135 I have given the fringe displacements s in scale-parts (scale-part about a double fringe) for the different pitches. The response is unquestionably stronger for high-pitch values (e'') than for low values (a'); but the curve is not simple. It is difficult to discuss this result, as much depends on the action of the contact breaker, which interrupts the current of the primary of the small inductor energizing the telephones. Moreover, even the latter, whenever there is marked change of temperature, are liable to show very different degrees of sensitiveness, so that it is necessary to reset the plates by unscrewing and refastening the mouthpiece.

72. Experiments with horns.—With the **H**-branch (fig. 135) tuned to e'', it is interesting to test the response of a wireless loud-speaking horn (fig. 137) to a closed e'' pipe, blown in the vicinity of the flare. In this case the telephones TT' (fig. 135) receive the current from the moving coil attached to the diaphragm at the base of the horn. If x is the distance between the plane of the flare and the mouth of the closed e'' pipe, the graphs (fig. 137) show the fringe displacements in their variation with x. It is necessary here to tune the e'' pipe with great nicety if a strong response is desired (upper curve). Otherwise the fringe displacements, s, diminish very rapidly. An f'' pipe gives scarcely half the corresponding resonant deflection. Again, the maximum response is obtained when the e'' pipe is at a distance x of about 5 cm. from the plane of the flare. Within this distance the fringe displacements

fall off very rapidly, particularly so in the case of unison, less so (f'' pipe) when there is slight difference in pitch. In other words, there are interferences between the pipe, e'', and the horn and its appurtenances which are quite audible; for when the mouth of the pipe is too near the flare, or within it, the fundamental note of the pipe is quenched. This occurs in marked degree when the current through the electro-magnet at the base of the horn is on, and the pipe-note often breaks out again when it is off. There is an evident case here of "back feeding," the diaphragm reacting through the horn on the pipe. A distance of 50 cm. (which is the e'' wave-length) between mouth of pipe and diaphragm seems here to correspond with the maximum.

Beyond the maximum the graphs fall off regularly and there is little effect (for the present small size of fringes) beyond $x = 30$ cm. I had rather expected to find a second maximum in sequence, but it does not occur.

The endeavor to use the electro-magnetic diaphragm together with the closed e'' pipe (in the same way in which I combined the latter with a corresponding resonator in the preceding report), to map out the nodal planes of waves reflected upward from the table, did not succeed. With the horn removed, all fringe displacement vanishes when the organ-pipe (mouth downward) is but a few centimeters above the diaphragm. The details are shown in figure 138, curve 8, where the distances x are measured upward from the connecting neck or ring, just above (3 cm.) the diaphragm. When the mouth is but a half centimeter from the neck (as close as it may be put without quenching the note) the response is strong, but at 4 cm. above there is practically no fringe displacement appreciable.

As the intervention of some form of horn is thus necessary, it seemed interesting to test a number of forms in succession. These are sketched in figure 138 (inset), the lower part always being the conical horn, No. 2, 7, with its mouth, 6 cm. in diameter, about 20 cm. above the diaphragm. The flares given under 1, 5, 4, and 3, fit the mouth snugly and vary its shape and height. The closed organ-pipe indicated at p, with a tuning-plug at c, is energized by the pipe-blower, b, a, described in the preceding report. This must be rigidly attached to the pipe, as the pitch varies not only with the position of c, but with the angle θ of the lamella a and the plane of the mouth.

To get large fringe displacements, it is necessary that the H-branch (fig. 135, inset) and the pipe p be sharply in tune; i. e., the plug c must be placed within a millimeter. As would be expected, by far the largest displacements were obtained when the small horn 2, 7 was used alone, with the pipe just above it; for then the mouth subtends the largest conical or solid angle. Moreover, since the pipe and horn reciprocate acoustically, or make a single vibratory system, the tuning at c must be finally adjusted with relation to the horn. The graphs 2 and 7, figure 138, are examples of results in which this tuning was respectively good and moderate. Owing to the blowing mechanism of the pipe, the plane of the mouth of the horn can not be much nearer to the open end of the pipe than 1 cm. In fact, even here there is considerable interference, so that the pipe-note is only heard when the electro-magnet of the

loud speaker is energized. As soon as the current is broken, the shrill over-
tones of the pipe break forth. On closing it again, the pipe and diaphragm
vibrate in unison and the normal pitch is reached by accommodation. The dis-
turbances have not been actually eliminated, as is clearly apparent in the
hooked part at the top of the graphs, indicating a breakdown of normal
conditions of vibration. In general, it is not unusual to obtain small differ-
ences of pitch, according as the electro-magnetic current is on or off.

The graphs 1 and 5 were obtained by attaching the flare, 1, 5, which
was about 15 cm. high and 15 cm. in diameter, above. The response as a
whole is here less than in the preceding case; but it is much larger, of course,
than the small horn would have given 15 cm. above its mouth. Here the
pipe-mouth may be placed in the plane of the mouth of the wide flare. It is
not unusual, nevertheless (curve 5), to meet interferences in this case also.
Initially hooked graphs are common, showing that the normal increase of s
has been reduced by secondary disturbances.

The wider attachment, No. 4, 20 cm. in diameter and 9 cm. deep, makes it
possible to dip the pipe-mouth below the plane of the flare. Fringe displace-
ment is, however, inferior, as shown by the graph 4.

The cylindrical flare (3), 15 cm. in diameter outward, 18 cm. deep, gave
the worst response (graph 3) of the series; but in compensation, the small
displacements s vanish much more slowly than in the other cases and at
$x = 14$ cm. above the mouth of the flare, the present fringe displacements
actually exceed them. The hooked form of graph indicates the usual dis-
turbances at $x = 0$.

The most effective coupling is always obtained with the pipe p coaxial with
the horn. Moreover, the large fringe displacements are essentially a slow
growth, showing that the amplitude of the diaphragm is gradually increasing
to a maximum. No doubt the sensitiveness could in all cases be much increased
by selecting a depth of horn in unison with the pipe and performing the final
tuning at the **H**-branch of the interferometer **U**-tube. Using a well-tuned
system of this kind, I attached the flare 1, 5 again, the mouth being about
35 cm. above the diaphragm. Care was also taken to sustain each note (30 to
60 seconds) until the fringe displacement crept to its maximum value. The
results were (curve 9, fig. 138) surprising:

Pipe at $x =$	-2	$+0$	$+2$	4	6	11	16	cm. above mouth.
$s =$	105	93	70	47	26	10	5	scale-parts.

These data are as large as any obtained heretofore, showing the importance
of the secondary disturbances. It has also been possible to dip into the mouth
of the flare with some advantage.

With the same good adjustment at hand, it seemed worth while to prolong
the horn to a length of about 1 meter by the insertion of a cylindrical tube
about 60 cm. long, 5 cm. in diameter. Here the tube dominated the situation.
Shrill overtones and beats were frequent. Nevertheless, fringe displacements
of 50 scale-parts were at once obtained, and they could have been smoothed
out to much larger values by tuning, as above.

8

73. Electric-spark excitation of quill tubes.—The production of acoustic vibration in quill tubes by aid of a telephone vibrating at one end has the advantage of needing but small currents and potentials. It nevertheless seemed desirable to accomplish the same result by other methods. Thus a periodically heated wire has been used. In the thermophone (Bull. Nat. Res. Council, No. 23, VI, p. 16, 1922) a fine metal strip heated by an alternating current is in operation.

In the following experiments the millimeter electric spark of a little induction coil provided with the usual spring interrupter was employed. By tightening the spring, or weighting it more or less, something over an octave, naturally in the region of low frequency, was available. The acoustic part of the apparatus is shown in figure 139 (inset), tt being the quill tube, closed at one end by the plug carrying the platinum spark-gap g and the wires of the inductor ww'. The tube tt is closed at the other end of the salient (s) and reëntrant (r) pin-holes, the former leading to one shank of the interferometer U-gage.

As the spring platinum interrupter in the lapse of time changes its efficiency, the graphs obtained show considerable difference in detail. I will, therefore, give but two examples (fig. 139) of the many series tested, as all of them conform to the same type of variation. The quill tube tt in these cases was about 8 cm. long. The graph a was obtained with a heavy and, therefore, steadier vibrator of low pitch, the curve b with a lighter vibrator more liable to fail. Some of the curves were strongly concave upward.

The property apparently brought out by these graphs is the rapid increase of acoustic pressure (varying with s) with the increase of frequency n. Thus, for a two-fold increase of n, the increase of b is at least four-fold, i. e., as n^2. The other feature is the absence (probably to be inferred for these low frequencies and very short tubes) of any certain evidence of resonance, such as was obtained strikingly in all the preceding experiments with telephone-blown tubes and higher pitch. Tubes tt from $l=8$ cm. to $l=25$ cm. in length behave about alike, in so far as discrimination is possible.

Since the intensity i of the vibration is proportional to squared ratio of amplitude and wave-length, $a^2/\lambda^2 = a^2n^2/v$, where v is the velocity of the wave, the intensity $i \propto n^2$ if a^2 is constant. If the sparks at all frequencies be regarded as communicating the same energy to the sound-wave, a^2 may indeed be regarded as constant. Hence, if at low frequency conformably with the graph, the acoustic pressure $s \propto n^2$, we should obtain $i \propto s$. From this point of view these experiments have some interest and should therefore be pursued with more carefully designed apparatus, always remembering that s varies with the shape and size of the pin-holes and may be either positively or negatively increasing with i.

The preceding experiments (fig. 139) are remarkable for the very low frequencies (4-foot octave c, $n=131$) employed. The acoustic pressure is thus produced by pulses traveling in succession from the spark-gap to the

far end of the tube. They must therefore be supplemented by experiments at higher frequencies, in order that the approach to resonance conditions may be tested. Great difficulty was encountered in endeavoring to produce spark successions of this rapidity. The best results were obtained from a large induction coil (usual laboratory size), actuated by as weak a primary current as possible. In such a case the commutator interrupter (with small motor and resistance) could still be employed; but the break soon deteriorated and the fringe displacements (acoustic pressures, s) are steady and comparable for only a short time, after which the break must again be cleaned and reset.

Notwithstanding these irregularities, the resonance conditions were very clearly made out. The intensities at the nodes were often enormously beyond the ocular micrometer, showing acoustic pressures exceeding 0.1 mm. of mercury, so that the slide micrometer had to be used.
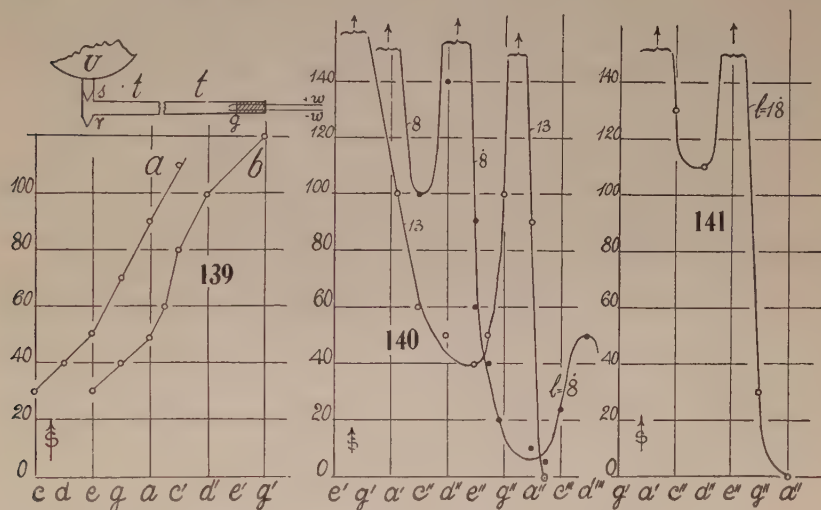

The survey for the tube-lengths 8.5 and 13.5 cm. is given in figure 140 and was made in some detail, so far as the method permitted. The resonance crests are far out of field. The low-pitch notes are continuously so, suggesting the relation to figure 139. For the longer tube-lengths (figure 141), $l=18.5$, 23.5, 29 cm., only the maxima were sought out, by using the displacement micrometer to bring the fringes in the field. These crests were often very sharp. In case of the tube, $l=23.5$ cm., the $♭d''$ crest corresponded to the acoustic pressure ($\Delta h = \Delta s \cos \theta$) of $\Delta h = 0.092$ mm. of mercury. In case of $l=29$ cm., the descent from the a' crest was measured as a', 0.084; c'', 0.047; d'', 0.016; e'', 0.012, etc., mm. Hg, the latter (e'') being of the order of the usual run of maximum acoustic pressures treated with telephones.

If we express the tube-length l in terms of the free semi-wave-length, $\lambda/2$, in air, the crests would lie as shown in figure 142. They are thus adequately reproduced by the equation $l+4.6=0.93\lambda/2$. Interpreting this as the first overtone, the confined wave-length $\lambda'+4.6=0.46\lambda$, agreeing in order of value

with the chief results obtained with telephones for the same tubes. Hence the strong d'' in figure 140, $l=8.5$ cm., belongs to the fundamental, as suggested in figure 142.

On further reducing the tube from 5.5 to 3.5 mm., the greater part of the length was made up of the T-branch and the spark-gap tube. This is equivalent to an appreciable increase of section, so that the crests no longer fit into figure 142. The acoustic pressures measured in millimeters of mercury are given in figure 143. At $l=5.5$ cm. a succession of three crests, a', $\sharp c''$, a'', is strongly apparent, but at $l=3.5$ cm. only a diffuse crest at g' remains.

74. Effect of spark-length, etc.—The energy of the spark is caught within the closed quill tube and expressed, as it were, in terms of acoustic pressure. Moreover, all sparks are produced in the secondary from the same primary mechanism. Thus it seemed that the acoustic pressure should be independent of the length of spark-gap in the quill tube. But this is by no means the case, as shown, for instance, in the two graphs of figure 144, for tube-length $l=5.5$
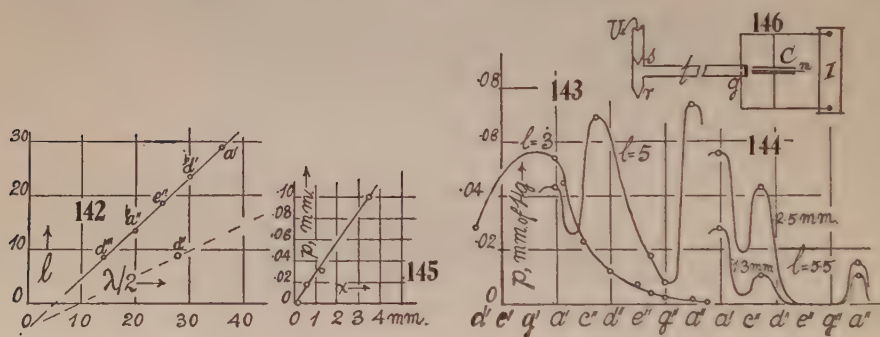
and spark-lengths 1.3 mm. and 2.5 mm., respectively. The crests have the same location as in figure 143, but the acoustic pressure for the longer gap is much in excess of that for the shorter. Similarly, for a tube-length of $l=24$ cm., while the 1.3-mm. gap gave a pressure of 0.051 mm. of mercury, the 3.5-mm. gap gave a pressure of 0.100 mm. Small spark-lengths of 0.1 to 0.2 mm. produced a deflection of only a few fringes, $i.\ e.$, less than 0.0005 mm. Hg, and were therefore inactive, while a spark-gap 0.6 mm. evoked a pressure of 0.0018 cm. Thus, in figure 145, the acoustic pressure (mm. Hg) at the nodes is roughly proportional to the spark-length, the values here obtained being something less than 0.03 mm. Hg per millimeter of gap. On the other hand, the long gap very much sooner misses fire as the pitch rises, owing to irregularities in the break circuit. The spark, moreover, is apt to be brighter at the resonance frequencies. This suggests that to start a vigorous acoustic wave, a sudden shock such as is conveyed by a single dense spark is necessary. A succession of small sparks of the same aggregate energy is relatively ineffective. (See § 76.) If N is the number of lines removed at each break of the primary, in a secondary circuit of resistance R and capacity C, we may

put $N = QR$, where Q is the constant charge available at each break. Hence if V is the potential corresponding to the spark-gap and if Q is discharged in n sparks, the total energy appears as $n(Q/n)V = nCV^2$ or $nC = N/RV$ is constant. If C is increased by the condenser, n is diminished.

The difficulties are increased when a capacity is inserted around the spark-gap, however; higher potentials being needed in the primary, the endeavor to eventually bring the electric oscillation of the spark into resonance with the quill-tube pitch is at the outset not very promising. A variety of subsidiary phenomena were observed. In figure 146, t is the quill tube, with its salient and reëntrant pin-holes at s, r, the U-gage at U, and the spark-gap is at g; I is the induction coil, and C the condenser. The latter is made variable by mounting the top plate on a micrometer screw (all properly insulated), so that it may be lifted up and down by a definite amount, as heretofore * described. A thin plate of mica or hard rubber, m, is inserted between the plates of C. The current in I is controlled by the electric siren in the primary, which may be set at any pitch from a' to c'''. When the plates of C are gradually approached, the spark at C is quenched at a definite distance, as is to be expected. If on further approach the metal plates of the condenser are moderately pressed against the thin mica insulator between, a loud note is heard in the condenser, of the same pitch as the electric siren. This occurs strikingly when the mica plate is less than 1 mm. thick. The note is louder for thinner plates (0.2 mm.) and softer for thicker plates (0.6 mm.). With a hard-rubber plate 1.6 mm. thick, the note was still audible, but now only at the resonance notes of the quill tube t, when sparks passed at the gap g.

In spite of the fact that quite thick brass disks (6 inches diameter and 0.25 inch thick) are active, the phenomenon is probably nothing more than electrostatic attraction and sudden release, the elasticity of the air-film between plates playing an important part. The insulation m now virtually conducts electrically. No Chladni figures were obtainable.

There is another phenomenon here much more difficult to interpret; for the condenser note modified the resonance pitch of the pipe t, according as the condenser plates are pressed snugly against the insulator and sounding, or as they are loose and not sounding. Thus, for the pipe length $l = 18$ cm., hard rubber (1.6 mm.) tight, sounding, crests at $c''g''$; hard rubber (1.6 mm.) loose, silent, crests at $e''b''$; mica (0.6 mm.) tight, sounding, crests at $c''g''$; mica (0.6 mm.) loose, silent, crests at $e''\flat b''$. Here mica and hard rubber behave alike and the pitch is raised to the normal value e'' (see fig. 142) when the insulator plate is loose (millimeter or more clearance). But in other cases pitch was depressed, so that one can hardly call in temperature phenomena at g in explanation. One may note that c'' and g'', e'' and b'', are not harmonics of the same series. These phenomena may be observed by the occurrence of sparking at the nodes, even without the measurement of fringe displacements at the U-gage.

When the spark-gap is sufficiently wide (1.5 to 2 mm.) the quill tube responds at all frequencies (a' and a'' tested), the nodal effects appearing as an accentuation of the uniform response. They may even be observed. It follows, therefore, that each individual spark impulse produces marked acoustic pressure, irrespective of the pitch of their succession on the pitch of the quill tube. In the case of the higher frequencies (a'' . . . c''') it ought therefore to be possible to obtain evidences of electric oscillation. How to recognize them among other crests is thus next to be considered.

75. Electric oscillation recognized. Inductance.—It is obviously necessary to have a very large inductance in the secondary in order that a small voltage (1 storage-cell) in the primary may produce sparks. Even then the high-frequency break-circuit in the primary is apt to behave capriciously. The break-circuit which gave me the best results is shown in figure 147, where w is a wheel of insulating material carrying equidistant metallic segments at its circumference. It is mounted on the axle A of a small motor of controllable speed. The two thin metallic strips a, a', through which the primary current circulates (clamp-screws cc') are made as short as possible, tightly stretched between the insulating holders C and b, the latter carrying a pin, the former a metallic plate p secured by a bolt. The holder b, being adjustable up and down, is so placed that the twin strips just touch the metallic commutator segments, to temporarily close the current. To deaden undesirable vibrations, pieces of soft rubber, r, may be wedged between the strips.

Though this break functions pretty well as far as c''' and above, it does not act equally well at all frequencies, owing to the incidental vibrations specified. Consequently, in the adjustment (fig. 146) the capacity only is to be changed to obtain different electro-magnetic frequencies, while the pitch at the break is kept constant. Furthermore, it is desirable to select a quill tube t of small length l, like the one for $l=3.5$ cm. in figure 143, in which resonances at high pitch are usually absent. Low-pitch response (g', a', etc.) is always present, as if these low notes broke up into higher harmonics. This is of little consequence, as they can not be reached electro-magnetically.

Under these circumstances the plan of attack is shown in figure 148, in which the acoustic pressure resulting from successive oscillations are given in the lapse of time. If a, the oscillation resulting from the first spark, is in phase with b, the oscillation of the second, and c, the oscillation of the third spark, etc., the acoustic pressure will reach a maximum.

Obviously, however, no distribution can be made between crests and troughs here, so that in relation to acoustic pressure all vibrations are rectified. Reenforcement occurs for acoustical half-period time differences between the impulses. A selection of an admissible period T is made by the experiment, among the available $T/2$, $2T/2$, $3T/2$, etc. The maximum interference occurs for phase differences of $T/4$. The compound rectified wave can not be annulled; but at it is far less oscillatory in character and with a period approaching $T/4$, it passes out of range as if it were annulled.

Examples of the results obtained in this way are given in figure 149, where the acoustic pressure is shown in terms of the distance apart d of the plates of the condenser. The break (fig. 148) was first set at c''', which it held pretty well. The curve c''' was thus worked out for varying capacity, by separating the plates of the condenser from $d=0$ to $d=9$ mm. There is a distinct optimum at $d=3$ mm. The break was then set at pitch a'' and the corresponding curve worked out. It reaches higher intensities (probably owing to increased length of contact) and is much sharper. The spark-gap was but 1 mm. The sparks must cease at $d=0$. This might have influenced the left side of the a'' curve, but not the c''' curve. A similar experiment with a condenser modified so as to secure greater precision in the separation of
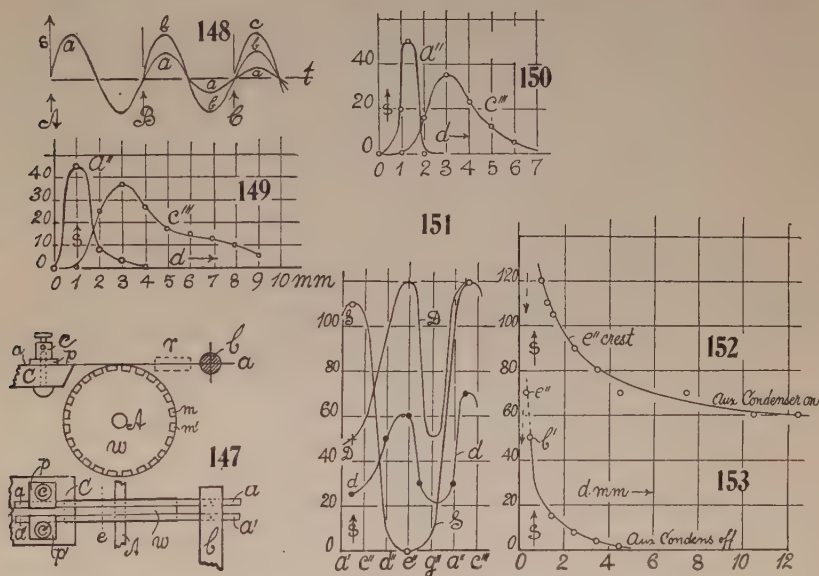
plates gave the results shown in figure 150. They are essentially like the preceding. The a'' crest, however, is sharper and has been somewhat displaced ($d=1.25$ mm.) in the d direction.

The interpretation of these data is not at once evident. The main oscillation must occur in the circuit IC (fig. 146) modified by the spark-gap g. The oscillation in Cg is clearly of much higher frequency and out of comparison with the pitches a'' and c'''. Leaving the spark-gap resistance out of consideration for lack of data, we may test the usual equation $T=2\pi\sqrt{LC}$ (where L is the inductance of the coil and C the total capacity of coil and condenser), tentatively, and since the only change appeared in relation to the a'' and c''' is the change of capacity, the coil capacity may be eliminated by writing

$$L=\Delta T^2/4\pi^2\Delta C$$

If, therefore, $C=A/4\pi d$, where d is the distance apart and A the area of the plates, C_0 the capacity in the coil

$$\Delta C=C_0+A/4\pi d-(C_0+A/4\pi d')=A\Delta(1/d)/4\pi, \text{ els. units}$$

whence

$$L = 9 \times 10^{11} \Delta T^2 / \pi A \Delta (1/d) \text{ henries}$$

Since for c''', $T^2 = 10^{-6} \times 0.92$ and for a'', $T^2 = 10^{-6} \times 1.29$, $\Delta T^2 = 10^{-6} \times 0.37$. $A = 78$ cm.², whence $\pi A = 245$. In figure 78, $d = 0.1$ and 0.3 cm., respectively, whence $\Delta (1/d) = 6.7$. This gives $L = 200$ henries. In figure 79, however, $d = 1.25$ and 0.3 cm., respectively, whence $\Delta (1/d) = 4.7$, so that $L = 290$ henries results. The order of these results would not seem to be unreasonable. If T for c''' and a'' are to be regarded as semiperiods, as explained, they would be too large; but, on the other hand, again, the conditions might be such that only when c''' and a'' represent a 3/2 period could response take place.

76. Further experiments.—In the summer I took up the work again, being in some doubt whether in the preceding experiments a state of resonance had actually been reached. The installation of apparatus was essentially the same, except that in addition to the variable condenser C (fig. 146), an auxiliary condenser was inserted in parallel. This consisted of two circular disks, each 14.9 cm. in diameter and spaced by one or two hard-rubber plates, 0.154 and 0.207 cm. thick. The difficulty with all these condensers is that with decreasing distance between plates and after some use, the insulator gradually conducts. Hence the descending branch on the left in figures 149 and 150 might be referred to this increasing conductivity, as it certainly is when d approaches zero and a loud condenser note is heard. In such a case the ascent of the curves in the right could be interpreted as a coalescence of a larger number of small sparks into a smaller number of larger ones and ultimately into a single spark, between successive breaks of the interrupter. If, then, the single spark is acoustically very active in exciting sound-waves, whereas the smaller sparks are relatively inactive, curves much like figures 149 and 150 would be obtained, implying a mere approach to electric resonance. With quill tubes no decisive results were reached, though one curious result may be mentioned: When the conical pin-holes were accidentally set pointing from each other (differentially) instead of in the same direction as in figure 146, pronounced negative deflections (*i. e.*, dilatations) were obtained from the spark excitation within the quill tube, the U pin-hole pointing away from the tube like the other.

In the following tests the interrupter (fig. 147) was also modified back again to the more conventional form. Stretched ribbons, aa'' as such, were discarded by severing them at say c. This cut is to be parallel to the insulation crevices between the plates mm' on the wheel w. The upper strips are then pressed down on the wheel and held in contact elastically. The free ends aa' should be made as short as possible. The advantage lies largely in the ease with which the contact edges of aa' are trimmed and reset if worn, in the very high frequency of their own vibration, and on the fact that the pitch to be observed is always clearly audible, coming from w. The plates mm', in spite of constant sparking, remain bright, or may be polished by light pressure from an old razor-blade. It is obvious that this break must function faultlessly.

Replacing the quill tube by a wide pipe 2.2 cm. in diameter and 13 cm. long, adjusted as at t (fig. 146), small single displacements only were obtained. The spark-gap was unable to produce a strong acoustic wave in this bulky tube and the harmonics were difficult to detect. An interesting and exceptional behavior was observed: On closing the spark succession, a violent throw of fringes toward larger pressures occurred, whereas in breaking the spark current, the throw was equally violent in the direction of dilatations. The appearance is thus very much like electric induction. A probable explanation is to be found in the fact that the air within the tube near the spark-gap is relatively warmer than sparkless air. Hence sudden thermal expansion of air or the reverse is put in evidence before the air escape at the pin-holes can reestablish equilibrium. The simultaneous occurrence of strong ionization is probably not appreciable in terms of pressure, though it would act similarly. The phenomenon is not observed with quill tubes, nor with the narrower tubes (diameter below 1 cm.) which follow. This, again, may be due to insufficient volume of air within the tube, so that the pin-holes are now large enough to maintain equilibrium at all times. Placing the spark-gap at the ends or at the middle made no difference in the unsatisfactory general performance of these wide tubes.*

The tube t (fig. 146) was now replaced by one length 10 cm. and diameter 0.7 cm., and this showed clear-cut crests at e'' and above b'', as indicated in curve d, figure 151; but the tube was never silent, provided the auxiliary condenser C was left in circuit. Without it, harmonics or crests could not be appreciably evoked in the tube. This is also indicated in figures 152 and 153, in which the abscissas denote the separation of plates (decreasing capacity) d of the variable condenser, in millimeters, while the auxiliary condenser is fixed in figure 152 and removed in figure 153. In the latter case the pipe shows no crests and the b' note was chosen at random. As the condenser space d decreases to the smallest value compatible with non-conduction, the fringe displacement rises very rapidly, and eventually with high capacity, even in figure 153, the e'' harmonic is brought out. Thus one might infer that only dense sparks excite these air-waves, while small sparks in succession, though conveying the same energy, per second, have almost no effect, a view in keeping with the remarks at the beginning of the paragraph. On the other hand, if the capacity falls, the period of the resonance note also falls, so that it may rapidly fall above (high frequency) the available pitch interval. The question is best treated by computation, which can here be made to rest on more substantial data than in case of figures 149 and 150, where the a'' and c'' pitches are rather too high for the apparatus.

77. Computation.—Admitting the reservations of the preceding paragraph, there remain nevertheless certain observations, as already indicated (§ 75), when the condenser capacity alone changes, which seem explicable

---

* A variety of other experiments with different lengths of wide tubes brought out only uncertain results. Sometimes a sharp tube crest appeared.

only in terms of electric resonance. The following results (fig. 151) are in some respects even more incisive. Using the glass pipe ($l=$ 10 cm., $2r=$ 0.7 cm.), leaving the variable condenser constant, but changing the hard-rubber plates of the auxiliary condenser in parallel from a thickness $d=$ 0.154 cm. to $d=$ 0.361 cm., the two curves D and S of figure 151 were obtained. Here the graph D, more intense but identical in character with the former graph d, corresponds to the smaller capacity or $d=$ 0.361 cm. Its salient feature is the crest at e'', very pronounced. Removing the extra hard-rubber plate ($d=$ 0.207 cm.) the curve S was obtained for $d=$ 0.154 cm. The feature here is the minimum at e'', whereas a crest appears at or below b. Both curves have crests near b''. The exchange may be repeated an indefinite number of times, always with the same results. The e'' crest is invariably transformed into an e'' trough, and (vice versa) similarly at b'. These crests are therefore of electric origin and do not belong to the tube, whereas the crest near b'' to which both cases of capacity contribute may belong to the tube.

The two crests observed in figure 151, viz, e'', period $T_1 = 1/658$ seconds and b', $T_2 = 1/494$ seconds, would seem to be too low to be compatible with electric oscillations, unless they are stimulated by their octaves here beyond range of the siren. Accepting them and putting K for the fixed capacity and L for the inductance of the circuit, the periods T are

$$T_1 = 2\pi\sqrt{L(K+C_1)} \qquad\qquad T_2 = 2\pi\sqrt{L(K+C_2)}$$

where C_1 and C_2 are the smaller and larger auxiliary capacities. Hence

$$T_1{}^2/T_2{}^2 = (K+C_1)/(K+C_2)$$

The capacities C_1 and C_2, computed as $\kappa A/4\pi d$ where $\kappa = 2.7$ is the specific inductive capacity of hard rubber, come out $C_1 = 104$ els. U., $C_2 = 234$ els. U. Hence the value of K computed from the periods is 75 els. U. If, therefore, we use the first equation and reduce to henries

$$L = \frac{9 \times 10^{11} T_1{}^2}{4\pi^2(K+C_1)} = 293 \text{ henries}$$

This agrees so well (considering the difficulty of the experiment) with the results of § 75, where virtually the same equation but a totally different treatment is in question, that the datum should be trustworthy. Thus the e'' and b' crests in figure 151 are to be regarded as placed by the electric oscillation and they have no bearing on the harmonics of the tube. It follows also that the construction of such relations as given in figure 142, if made with the spark exciters, must be interpreted with caution.

CHAPTER V.

MISCELLANEOUS EXPERIMENTS.

Exhibit of Telephonic Excitation of Acoustic Pressure.

78. Apparatus.—In Science (vol. 54, p. 155, 1921) I described a series of simple experiments bearing on the nature of the acoustic forces observed in connection with telephone-blown pipes. Having occasion to repeat this work in relation to the preceding chapter, I obtained a series of repulsions as well as the former attractions. This induced me to repeat the experiments with the bifilar suspension shown in figure 154. Here TT' are the telephones excited by a small inductor and break of variable frequency, each carrying the identical pipes PP', about 13 cm. long and 5 cm. in diameter, with a note ranging from below b' to $\sharp c''$, depending on the degree to which the mouth is open. RR' are two identical cylindrical resonators of heavily varnished paper, about 9 cm. long and 2.2 cm. in diameter, responding to a'' (in place), attached at right angles to a straw shaft ss' 26 cm. long. The deflections were observed with mirror and scale at a distance of 142 cm. To guard against air currents, the box BB' surrounds the whole, in such a way that the telephone pipes PP' may be more or less withdrawn, or that R may dip more or less into P. The period of the needle was about 30 seconds, and the total weight 4.5 grams. The addition of adjustable closed cylinders DD' improves the damping, etc.

79. Observations.—When the resonators R extend to about 3 cm. within P, the full telephonic current throws the light spot off scale. The current was therefore diminished by inserting 500 ohms resistance, which reduced the sound to the loudness of an ordinary organ-pipe. The survey in pitch (a to c''') then gave the deflections s reproduced in the graph (fig. 155), repulsion laid off positively. There are two marked attractions at b', the resonance pitch of P and at b, an octave lower, none at b'', an octave higher. Hence the overtones of the telephone note are probably responsible for b, though its intensity is surprisingly large. Similarly there are three repulsions, the strongest at a'', the resonance pitch of R, while a' and d' are probably again referable to the successive overtones of the telephone note.

When the pipes P are partially withdrawn, so that the mouths of R and P are coplanar, the deflections obtained are such as shown in figure 156. The repulsions (a'', a', d') have nearly vanished, but the attractions (now at the resonance pitch $\sharp c''$ of P) is still strong.
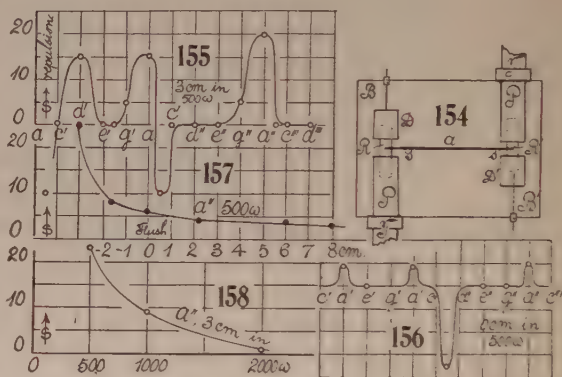
At a distance of 4 cm. between the mouths (organ-pipe loudness) the attractions at $\sharp c''$ also practically vanished; at a distance of 8 cm. quite so. One notes that P' attractions are more persistent.

Thus the acoustic pressures fall off very rapidly with the distance apart of the systems R and P. In figure 157 with 500 ohms in circuit and the steady note a'', this relation is indicated, the mouth of the resonator R being within P for negative abscissas, in centimeters. The note is a little louder than in figure 156. The effect increases as the mouth of R approaches the telephone plate, though it is still 9 cm. off.

In figure 158, the deflections at a'' pitch, with the mouth of R 3 cm. within P, are shown for increasing resistances (abscissas) in the telephone circuit.

Similar experiments made with a variety of resonators R of different lengths, widths, and shapes will presently be described, but the results were not essentially different from the above. The tuning at the crests must be precise—more so than the inductor was able to hold steadily. Hence the needle is usually in motion, and this with the long period makes it difficult to obtain sharp data. It is clear, however, that forces fall off very rapidly beyond the organ-pipe.

80. Estimates.—The pipes R having an area of about 4 cm.^{2}, the deflections s with the above constants of the bifilar may be reduced to pressures by the equation $10^4 p = 7s$ dyne/cm.^{2} Thus the maxima in the figures would not exceed an acoustic pressure of $0.0007 \times 20 = 0.014$ dyne/cm.^{2} If $p = 10^6$ is the atmospheric pressure, $\Delta p/p = 1.4 \times 10^{-8}$. This is only about twice as large as Rayleigh's minimum audible (6×10^{-9}), although the pipe P could certainly be heard at several hundred feet away. The high value $\Delta p = 0.25$ dyne/cm.^{2}, found for howling pipes, was similarly small, so that but a minute fraction of the acoustic energy per cubic centimeter is locked up in these acoustic pressures, the remainder being radiated.

81. Equation.—One may describe these phenomena * as a whole, by putting the locally available energy in the form $p + \rho v^2/2 = p_0 + \Delta p_0$, where p_0 is the atmospheric pressure and Δp_0 an increment contributed by the acoustic vibration, increasing with its intensity, but constant within the region bounded by the hollow resonators. When the pipe P is in resonance, the waves are merely reflected, without nodes, within R. When P sounds loud enough, pressure p at the mouth of P may with increasing v have fallen below that of the atmosphere, while at the same time it has increased above atmospheric pressure

---

* The rigorous treatment of pulsating sources is given by Bjerknes, Hydrodynam. Fernkräfte, Leipzig, 1902, J. A. Barth.

at the closed or nodal end of P.* Thus the reduced pressure at the mouth of R is harbored within it, and it is thus thrust inward by the full atmospheric pressure on the outside. Conversely, when R is in resonance, P merely reflects (without nodes) the waves emerging from R. If the vibration is of sufficient intensity, the pressure at the mouth of R falls below that of the atmosphere, while the pressure within R, at its closed ($v=0$, nodal) end rises above atmospheric pressure, so that R is now thrust outward from P.

82. Further experiments.—In the introductory work, single resonators counterpoised on the other side of the bifilar were tried, largely to test the pressures obtainable with very loud sounds. The bifilar corresponded to $p=1.37\ \theta$ dynes/cm.^{2} (θ radians, deflection). When a resonator 13 cm. long and 2.1 cm. diameter was used, the resonance notes were e', e'' for R and $\flat b'$ for P. The repulsions obtained reached 0.2 to 0.3 dynes/cm.^{2}, R being well within P. With a shorter cylinder R, 8.1 cm. long, the results were about the same. Beyond the mouth pressures fell off rapidly, as above.

Supposing that long tubes (length 17.7 cm., diameter 2.25 cm., period of bifilar 40 seconds) would show increased sensitiveness, as these could be thrust more nearly to the telephone plate within P, they were tested at some length. The contrary was the case, as shown in figure 159, the R resonance observed being at d''. Slight attraction (at $\sharp c''$) only was obtained when the mouths were flush and a few centimeters beyond this, there was no deflection appreciable. Going to the opposite extreme, R cylinders as short and wide as admissible (length 5.6 cm., diameter 3.8 cm., blowing $\flat e'''$) were examined in turn. Figure 160, where $p=10^{-4}\times 2.5s$, summarizes the s-effect of increasing resistance in the telephone circuit. The *attractions* of the P pipe (resonance notes now abnormally a' and a'') only were obtainable. There were no repulsions. Moreover, these attractions, though never very large, were sustained throughout lower intensities (up to 4,000 ohms in the telephone circuit). Later, on careful searching a weak repulsion at $\sharp c''$ was at times detected, which may be taken for an octave below the R pipe-note in place ($\sharp c'''$). The occurrence of the a'' resonance note for P is, however, quite puzzling; for P and R can not vibrate together as a double closed pipe without producing repulsion in R. Granting that the P frequency may be depressed from c'' to a' because of the stopped mouth, the origin of the strong a'' is left unexplained.

A careful survey in pitch with the mouths of P and R coplanar and with the full telephonic current ($\omega=0$) is given in figure 161a. Here there is multiple resonance from a' to e'' which naturally masks the possibility of repulsion at c''. Resonance at a'' is very strong, the light spot passing out of scale. With a distance of 2 cm. between the mouths of R and P, an accentuated attraction (fig. 161b) of the usual note of the P pipe (now at d'') shows itself with nothing else appreciable. The $a'a''$ resonances of figure 161a are gone. To make sure that these attractions are due to P only, R was reversed

---

* This may be tested by lowering a disk in P.

and its *closed* end just inserted into P (fig. 161, inset). The same graph, with its attractions at a', c'', and a'', appeared as before. Thus R as a resonator was throughout inactive.

The key to this dilemma is probably given in figure 114, where a pitch near a'' appears as the resonance note of the telephone-plate. Thus the a'' is to be regarded as a forced vibration impressed on P by the strongly resonant telephone, and the depression of a' is probably similarly influenced. Hence it makes no difference whether R presents its closed or open end to P, for the vibration of R does not appear. The frequent occurrence to a' and a'' crests is probably of like origin.

The preceding short R pipe was now provided with a conical front 4 cm. long and 1.3 cm. in diameter at the mouth. Figure 162 (inset) gives the results with the cone only submerged in P. The system was very insensitive
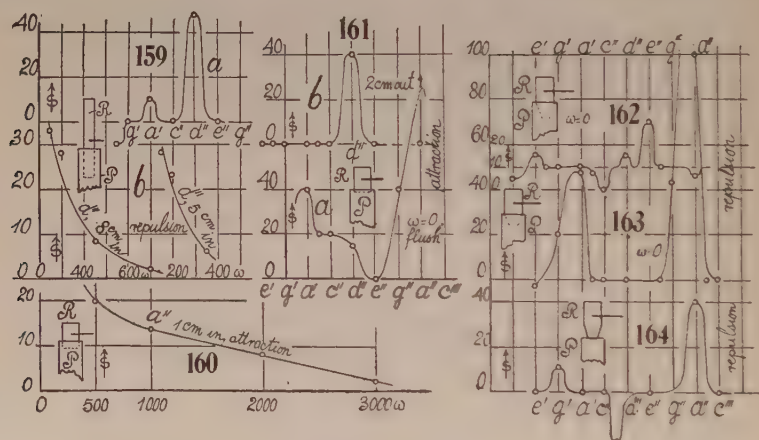
throughout, the full telephonic intensity ($\omega=0$) only just sufficing to bring out the graph characterized by cusplike repulsion at e'' and a minor one at e', the attraction near c'' being slight. Nothing further was obtained by thrusting R into P.

The front was now cut down to a length of 2.5 cm., with a mouth 2.2 cm. in diameter, the cone being as before just submerged in P (fig. 163, inset). An enormous increase of sensitiveness is at once obvious (fig. 163), with the repulsion crests at a'' and a'. No attraction (near c'') was detected. With 500 ohms in circuit, the sensitiveness was reduced to the usual order, so that there is no gain ascribable to shape.

The experiment was next modified by placing the neck of R (fig. 164) flush with the mouth of the pipe P. With the telephone at full power (no external resistance), only moderate repulsions appear at a' and a''; but the attraction of P at $\sharp c''$ is now normal and distinct. Thus the insertion of the cone into the mouth of P has been sufficient to quench its resonant vibration, while a narrow mouth quenches R also.

To obtain further evidence of the influence of telephonic resonance, the pipe P was cut down from 13.5 cm. to 8.5 cm. from the telephone-plate until its resonance note was e''. Using the resonator R of figure 154, the data were obtained as given in figure 165. Here a' and a'' are the R repulsions as before, while the e'' is the new attraction of the shortened P pipe. Figure 166 summarizes the results found on making the same test with the short wide resonator of figure 160, and inserting the closed end of R. The e'' appears correctly as the attraction of the resonant P pipe. Hence the two $a'a''$ attractions can only be referable to telephone-plate resonance.

A long, wide resonator, No. VI, 10.5 cm. long and 4 cm. in diameter gave no new results. There were strong repulsions at a'', smaller at a', and attraction at e'' of the usual value. With a somewhat improved mounting of R No. III, the full telephone-note was effective to a displacement of about 20 cm. between the mouth of R and the telephone-plate.

83. Disk explorer.—By far the most sensitive arrangement is the plate or disk, probably because its diameter (here 5 cm.) may be large. At about 8 cm. from the phone-plate and 1.5 from the mouth of P, the light index passed off scale even with 1,500 ohms in the telephone circuit. At 3.5 cm. from the mouth of P it did so when the resistance was removed. Two resonances a' and a'' were found; but the upper one extended from f'' to $\flat b''$, thus probably including the free pipe-note. The lower crest was also broad. With a long P pipe (14 cm. from telephone-plate) the arrangement becomes insensitive. The objection to the disk is that attractions only are possible, and that these increase very rapidly as the disk approaches the mouth of P, while at the same time the resonance note changes. The forces here are much like those of a magnet pole.

Pursuing the case further, the somewhat awkward arrangement, figure 167, was tried. Here two disks, d, d', 4 cm. in diameter, could be inserted into the P pipe, almost as far as the telephone-plate (T), the right-angled shaft s being supported by the bifilar at a. Although but small angles of rotation were possible, the nature of the forces was easily ascertained. From about 1 cm. inward within the mouth of P, these disks were strongly repelled when the a'' resonance note sounded, almost but not quite as far as the plate. From about 1 cm., as stated, outward the attraction increased, being at a maximum near the mouth. Thus there is a normal plane slightly within P, say at a, figure 168, at which the conditions are neutral, but at a short distance from which, in or out, either attraction or else repulsion, respectively, are experienced. It follows, as in Lord Rayleigh's experiments, that a disk oblique to the axis of P would have its near half attracted and its far half repelled, or would tend to rotate, a form of apparatus highly developed by Professors F. R. Watson,[*] G. W. Stewart, P. E. Sabine, and others.

Finally, on using the horizontal torsion-balance described in the last report $(l.\ c.)$, these data were confirmed and extended. The accurate measurement

---

[*] Bull. **127**, Eng. Exp. Station, Univ. of Ill., Urbana, 1922.

of the forces would well repay research. The experiment is a delicate one, as the conditions are usually unstable, and the registration decreases rapidly above or below the resonance note. With the horizontal torsion system used (figure 168), d being the exploring disk, a second neutral plane at b, about 1 cm. from the plate of the telephone, was detected. Below this the disk actually flopped down upon the mouthpiece of the telephone. The forces are thus essentially as shown by the arrows of the figure. There is a jerk at resonance. In case of a disk 3.5 cm. in diameter, figure 169 gives a record of the actual distribution of pressures (dynes/cm.²) for the pipe 8.5 cm. long and 5 cm. in diameter. Figure 170 supplies two records for a loud and a softer note, in case of a glass cylinder 18 cm. long and 5 cm. in diameter and
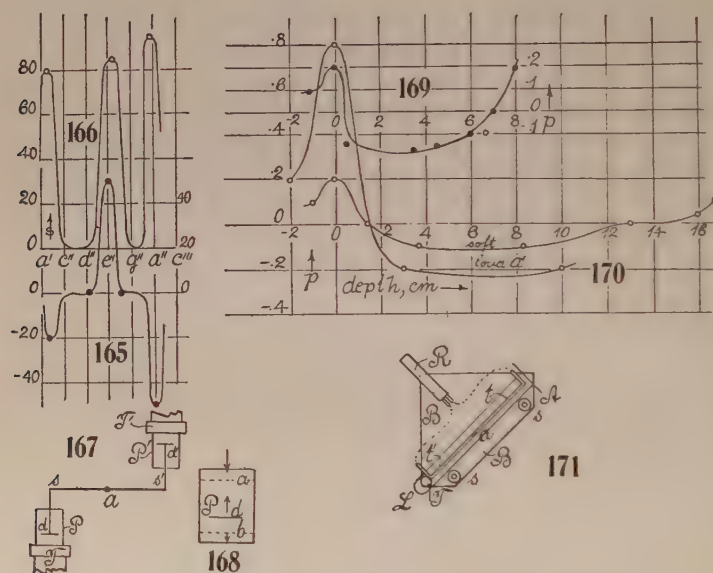
the same disk. At the outer neutral plane (1 to 2 cm. within mouth of pipe) a slightly sharp note produces repulsion. The nearly constant repulsion within the shaft of the pipes, together with the relatively marked repulsion at the mouth, are throughout noteworthy.

Pneumatic Gage for the Pin-Hole Resonator.

84. Apparatus. Observations.—Pressure measurement with the U-tube interferometer has the advantage of being absolute, sensitive, instantaneous, and with dead-beat fringe displacements. But the implicity of an inclined-plane arrangement consisting of a thread of liquid in a quill tube, so frequently used for measuring small pressures, commends itself, and I have often applied it. The apparatus is shown in figure 171, where BB is a triangular base-board on leveling screws ss'. The quill tube is seen at t with a thread of liquid at a. The ends of t are raised and communicate through short ends of rubber tubing

with the twin pin-hole resonator R, provided with salient and reëntrant pin-holes to the respective ends of t.

The quill tube t is fastened to a lath LA, hinged at A and carrying a tangent screw T at the other end, to give LA any desired small inclination.

The base-board is first leveled by the screws ss' until the liquid thread a is permanently stationary. An extra level on t may be used. In such a case it may be moved toward the pin-hole reëntrant in R, by blowing an organ-pipe in resonance with R, near it. Motion stops with the sound, but is always sluggish. At longer distances (1 or 2 meters) the thread creeps, but its speed increases as the pipe is moved closer.

With the pipe fixed, say at a foot, LA is raised at T, until the thread a is just stationary. It is then interesting to observe that when the pipe is moved slightly nearer, the thread rises, and falls with the pipe moved farther. In this way the pipe position for a given number of turns of T may be found.

As an example I give the following experiment chosen at random: The data were: length TA, $L=32.1$ cm.; inclination angle, $\theta=0.0024\,n$; pitch of screw, $T=0.077$ cm.; length thread a, $l=1.9$ cm.; number of turns, $n=7$; density (alcohol), $\rho=0.8$. Whence

$$p=l\rho g\theta=3.6n; \text{ or } p=3.6\times7=25 \text{ dynes/cm.}^2$$

The same resonator R tested by the U-tube interferometer gave about 60 fringe displacements for the same pipe and distance, so that

$$p=n(\lambda/2)\,13.6g=0.42n; \text{ or } p=25 \text{ dynes/cm.}^2$$

which happens to agree exactly with the preceding datum, though the correspondence would not in general be so close. The resonator was not specially sensitive as to pin-hole adjustment.

Experiments with Interferometers.

85. Modification of the Michelson interferometer.—The purpose is two-fold—to eliminate the need of compensator and to permanently protect the half-silver plates against sulphur corrosion. This may be accomplished very simply by cementing the half-silver film H, figure 172, with Canada balsam between two glass plates of the same material and thickness. If M (on a micrometer) and M' are the two opaque mirrors, it will be seen that each of the component beams passes identically through 4 thicknesses of glass at H, effectively through 3. One hurtfully reflecting glass face has been eliminated.

Using mirrors 3 inches square and an arc lamp at A, about 0.5 meter from H, the fringes of white light are easily projected on a white screen S, 10 or 20 feet from H. To make the image brilliant and the lines sharp, a weak lens (2 diopters) L must be used near H. With common plate glass the fringes are then somewhat irregular ovals, and covering a surface 6 inches to a foot square, look much like grained wood. They may be seen and used in subdued daylight. Placing the finger lightly on the $\frac{1}{2}$-inch base-plate in front of or

9

behind M, the fringes all pass toward or away from the center, respectively, indicating the flexure of the plate. The micrometer at M can scarcely be used with common plate, for the ellipses vanish when 10 or 12 fringes have passed (3×10^{-4} cm.). They are thus very easily lost and thereafter difficult to recover. It is easy to find them, however, by using a spectrotelescope in HS with a collimator in AH. The spectrum fringes are first found. These are made horizontal by aid of the micrometer at M and the white light fringes then almost always appear on removing the spectroscope. Compensators, if desired, may be introduced in pairs. Using the spectrum ellipses, however, a plate 0.5360 cm. thick required micrometer displacement of 0.2864 cm. to restore the yellow diameter of ellipses to its original position. Thus the index of refraction was 1.5344, correct to one or two units of the fourth place.

With the white-light fringes, only a soap film may be inserted. If such a film x cm. long and y cm. thick is stretched on a frame, we may write $\Delta x/x = -\Delta y/y = -\lambda/2(\mu-1)y$, so that $y = x\lambda/2(\mu-1)\Delta x$ if Δx is the stretch per fringe. Thus a film 2 cm. long stretched to 4 cm. for one fringe, must have been 7×10^{-5} cm. thick originally. The experiment does not work out as smoothly as I expected, because the film is eventually a wedge-shaped bag covering several fringes from top to bottom.

Although the micrometer is not available, the rings may be controlled by using a pair of identical compensator plates in the paths HM and HM'. On rotating one in a given direction, the central rings on the screen S move outward, leaving a blank field within, while the rings remain very sharp as they move to the limits of the field. The phenomenon is symmetrical for rotation in either direction. With the arc lamp the fringes are continually squirming. I at first supposed this to be due to air currents; but it results from the unsteadiness of the arc light, whereby the apex of the cone of light moves. With sunlight, condensed or not, the fringes are fixed. The fringes travel only if the condensing lens moves.

With the Michelson interferometer, the fundamental form is always oval, or was so in the many cases which I tested. If the two plates of the half-silver H in figure 172 are not equal, the spectrum fringes are small ovals and the white light fringes rapidly become too faint for projection. To obtain good achromatics, however, the fundamental form must be quasi-hyperbolic, as is always the case with the quadratic interferometer.   .

86. Achromatic fringes.—In the case of the Michelson interferometer, the fundamental fringe figure is elliptical, and the outer rings when the disk vanishes are progressively colored spectral rings. The achromatics are not producible. One may note (fig. 173) that even horizontally a ray of white light entering at L comes out at T as a ray of white light. There is no separation of colors if the half-silver is compensated, nor with additional compensators. There is dispersion in the absence of compensation, and in this case the displaceable and useful small spectrum ellipses occur.

In case of other interferometer adjustments, the displaceable achromatic fringes are producible with white light. The fundamental design may here be taken to consist of equilateral hyperbolas, with the horizontal black fringe as one of the asymptotes, though the figure is usually much more complicated, particularly with common plate glass, of course. This does not necessarily interfere with the occurrence of available small straight fringes (cf. Carnegie Inst. Wash. Pub. 249, Part IV, Chap. VII, §§ 54, 55). In these adjustments, one may note, an entering ray of white light issues with horizontal separation of colors. Thus, in the self-adjusting interferometer (fig. 174) with or without the compensator (the latter is here superfluous, except as a film protection), the incipient white ray L is replaced by the spectrum br. In the quadratic interferometer (fig. 175), in spite of the complete compensation in view of
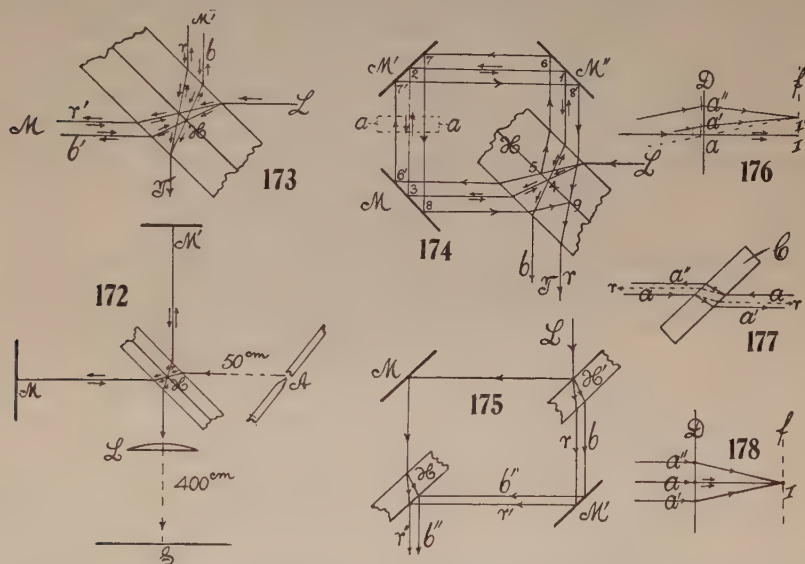
the identical half-silvers H and H', the entering white ray L is again changed to the horizontal spectrum r'', b''. There must, therefore, in these cases also be vertical spectra with inclined rays.

The achromatic fringes, as I have called them,* are in appearance like Young-Fresnel fringes, except that the central fringe is frequently not white but black. In other words, there is usually phase reversal corresponding to the black spot in thin plates. The black line flanked on either side by white lines is in fact the same thing. The slit-images in the telescope must be coincident throughout.

If, for convenience, we operate with the self-adjusting interferometer (fig. 174) and rotate the mirror M slightly about the horizontal axis, the fringes may be made to enlarge from horizontal hair-lines, through infinite size back again to hair-lines for the same sign of rotation. Here there is a change of

---

* They are really superchromatic, as will appear presently.

obliquity of rays; in other words, the coincident slit-images rise or fall in the telescope; at the same time the black fringe is changed in position correspondingly; *i. e.*, it does not remain glued to the cross-hairs of the telescope, but moves with the slit-images. The whole phenomenon as to color, etc., passes through infinity, symmetrically with respect to the black line, in spite of the marked change in angle of the rays.

Since the distances 34 and 3214 are unequal, it is obvious that the spots of light at 4 move vertically over each other when M is rotated on a horizontal axis, although the rays remain parallel. Hence let D, figure 176 (elevation), be the principal plane of the objective of the telescope at T, and let the coincident parallel rays a have an image at I on the focal plane f; then in case of rotation of M, the coincident rays a separate into the rays a', a'' with their focus at I', again coincident; but whereas the interference design from contiguous spots, a, is infinite in size, that of the separated spots is reduced proportionally to their distance apart. Thus we may regard $a'a''$ similarly to the two slits in Young's experiment, except that the position of the black line of symmetry will depend on the initially opposed phases of a' and a''. The experimental evidence shows that this line of symmetry, initially at I, as one would expect, moves with I toward I', though usually less than the slit-images.

If the mirror M' (fig. 175) is rotated on a horizontal axis, the slit-images move in the telescope as before, owing to the increasing obliquity of rays; but the fringes do not change in size because the distance $a'a''$ is relatively constant. M'' again operates like M. H rotated on a horizontal axis changes the size of fringes only, since but one component beam, 41234, is reflected. Being reflected in parallel, I remains in place, but a changes to $a'a''$ with a focus at I'.

There is another method of changing the size of fringes with a particular bearing on the present experiment, since the direction of rays is not changed. This consists in placing a compensator of good plate glass (aa, fig. 174), capable of rotating on a horizontal axis in the path of the beams. In the oblique position (fig. 177), this converts the originally coincident opposed rays a, a into the non-coincident but parallel rays $a'a''$. The result is, if D (fig. 178) is the principal plane of the objective of the telescope at T (fig. 174), that the coincident rays at a with an image at I, are converted into the symmetrically parallel rays $a'a''$, also with an image at I. The slit-images thus remain fixed, while the fringes decrease in size proportionally to the distance $a'a''$; and since a' and a'' are opposed in phase, the black line remains fixed at I throughout.

87. Iceland-spar compensator. Extraordinary ray.

—With a plate-glass compensator, no matter how thick (glass columns up to 7 cm. were tried), the fringes remain appreciably the same on the two sides of the position for infinite size; *i. e.*, they pass from hair fringes, through infinity, to hair fringes again, symmetrically when the compensator is rotated in a given direction. This is no longer the case when a calcite prism (C, fig. 179) with short diagonal vertical, is introduced, as in the figure, even if the prism is less than

a centimeter thick. To bring out the phenomenon vividly, however, a calcite block 3 cm. thick is desirable. With a Nicol 7 cm. long the results are correspondingly striking.

In dealing with polarized light it is well to observe at the outset that the ray at T having undergone successive reflections, is itself very nearly polarized, with a plane of polarization horizontal. It is therefore necessary to make adjustments for vertical vibration only, as the horizontal effects are extremely faint. Furthermore, if the long diagonal of C is vertical, the ordinary ray is in question and the crystal there behaves like common glass (max. index, $\mu = 1.65850$), as it should.

Next let the short diagonal of C be vertical (extraordinary ray, min. index, $\mu = 1.48635$) and the rotation of C on a horizontal axis be made from hair fringes on one side to hair fringes on the other. It will be found that on one side of the position for infinitely large fringes they are pronouncedly achromatic and very numerous (15 to 20 counted), whereas on the other side of the infinite fringes they are few and usually highly colored. In view of the thickness of C (3 cm.), a very small angle of rotation is in question and the position of the crystal to the rays is about as shown at C', figure 179, the edges sloping a little downward from the horizontal parallel to the ray. If an analyzer is used, it is possible to detect also the much fainter fringes corresponding to the horizontal vibration. Large-size fringes of one kind usually correspond to small-size fringes of the other kind of polarization, though of course the sizes pass in opposite directions through each other.

Using the Nicol 7 cm. long, with the short diagonal vertical, the number of achromatic fringes had further increased (contrasting therefore with the glass column 7 cm. long and its doubly symmetrical fringes). I counted 50, and they filled the field of the telescope from top to bottom. The colored fringes were much the same as with the calc-spar. In figure 180 I have given a record observed at successive stages of rotation, beginning on the colored side, b denoting black, w white, r red, g green, r' reddish, etc. The black fringe is stationary throughout the rotation. The ∞-fringes are of course too faint within the field of the telescope to be characterized. On the achromatic side (4, 5, 6) the fringes merely shut up, with loss of color, from large to small size. On the colored side (3, 2, 1) the few present are variegated, but also narrow down to hair-lines as the given rotation proceeds. The total rotation downward from the level edge, from small fringes to small fringes, will not exceed $5°$; but the fringes remain visible within an interval of about $15°$, symmetrically enlarged. One of the light spots on the mirror may then be seen passing from above to below the other. The design 2 is most interesting, consisting of a strong black line flanked by two vividly white lines on either side, the remaining colors soon fading off. If this pattern can be maintained, the black line b as an index in displacement interferometry should be very useful. With an analyzer at the telescope, the color contrast is often sharpened. The group 2 (fig. 180) appearing with analyzer in parallel may

be changed to appear like middle white flanked by two blacks, if analyzer and polarizer are crossed.

88. Theoretical remarks.—In the treatment of achromatic fringes and thin plates, it is customary to use as the equation of condition $\cos r/\lambda =$ const., where r is the angle of refraction of the ray within the thin plate (here air, $\mu = 1$) and λ the wave-length. There results (for instance for Talbot's fringes) an expression

$$\cos^2 r/\sin r = \sin \phi \cdot \sec R \cdot \lambda d\mu/d\lambda$$

where ϕ is the prism angle and R the angle of refraction at the initial incidence. In the Michelson interferometer the familiar method of rotating one of the rays on the trace of the half-silver reduces the treatment to the case of thin plates. The same may be done less directly with the self-adjusting interferometer; but as in all these instruments the angle ϕ is essentially zero, the equation vanishes. True, in my experiments the square half-silver plate was probably a wedge of very small angle ϕ; but by trying this plate on all four sides and by using an indefinite assortment of other plates, there was no essential difference in the phenomenon. Nevertheless, it is probable that the color factor (which may be transformed to $\lambda d\mu/\mu d\lambda$) will contribute to an explanation, quantitatively.

If we consider figure 180 as a whole, it is obvious that there must be two coefficients of vertical dispersion; one of these, resulting from the interference $a'a''$, changes its sign on the two sides of the black line of symmetry, while the other, resulting from the refractive dispersion of the compensators (compare fig. 177) also changes sign for the component rays a', a''. The dispersion instanced in figures 174, 175, being horizontal, is not available. Hence, in figure 180, groups 1, 3, 2, the coefficients cooperate; in groups 5, 6 particularly they annul each other and achromatism results. Thus it is also clear that the $d(\log \mu)/d(\log \lambda)$ must have a particular value to establish the balance. Various glasses tested (plates of flint glass and of crown glass, quartz plates, quartz columns 4 cm. long, ordinary ray of calcite, etc.) had no appreciable effect, while the extraordinary ray of calcite fulfilled the conditions strikingly. If the refraction does not change in distribution of color the fringes are the same on both sides of ∞. This is the case with the regular achromatics, which are thus always on the dispersion cooperating side. For instance, in figure 177, for all positions of the plate-glass compensator C, the red rays rr will be innermost and the blue outermost. Hence in figure 178 the red rays $a'a''$ will be closer together and will be additionally more dispersed than the blue rays in the interferences. The conditions will be symmetrical as C rotates through the vertical. There will be few fringes because of the large combined dispersion.

For the case of the calcite rhomb (C, fig. 181), the two spectra br above, $r'b'$, below, issuing from the corresponding white rays w, w', are opposite in direction. The red rays are nearer each other vertically than the blue rays.

Now, it is only an extraordinary ray that can pass through an oblique face collinearly. Hence when the rhomb is rotated on an axis A normal to the diagrams, so that $r'b'$ is above and rb below, the blue rays are nearer together than the red rays. In the latter case they would therefore counteract the dispersion due to interference, so that achromatic spectra would result. In the former case they are in the same sense as the interferences and accentuate the color effects. Thus if c is the vertical distance $a'a''$ in figure 178 (normal distance between r, r' or b, b' in figure 181), since a' and a'' are in opposed phases, the equation of a dark line is $n\lambda=cx/F$, where n is the ordinal number of the fringe at a distance x from the center I and F the focal length of the objective. Hence if, within a certain range approximately, $c=k\lambda$, where k
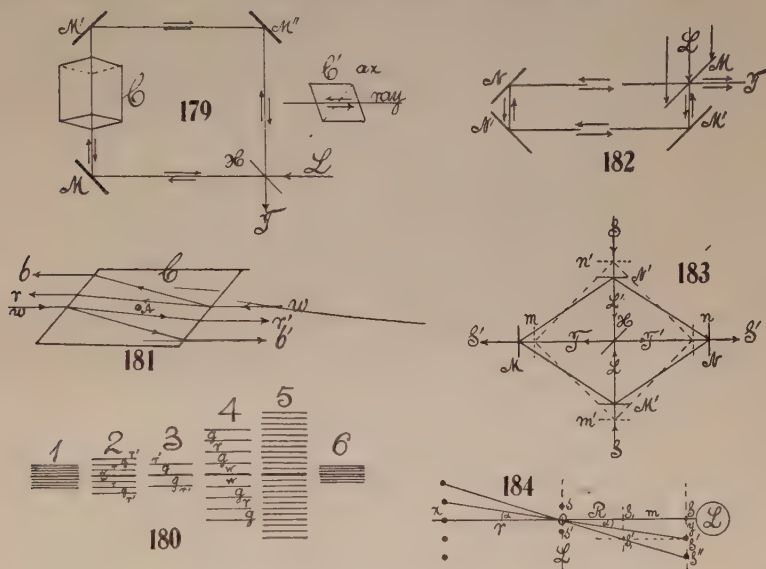
is a mean constant, $n=kx/F$ (blues closer together) and is free from color. In the other case we should have to write consistently $c=k/\lambda$ (reds closer together) and $n\lambda^2=kx/F$, accentuating color.

INTERFEROMETRY AT LONG DISTANCES.

89. Purpose.—Preparatory to certain experiments on the detection of shearing displacements of points on the earth's surface, the use of the interferometer suggested itself. Under such circumstances the source of light appears as a mere point, even if examined by as strong a telescope as would be useful. The interferences of two light points are not available even if they can be seen, for it is the measurable displacement of fringes in a fixed white field which is needed.

At short ranges, when an ordinary collimator is used, the rays are parallel in a plane (horizontal) normal to the slit, only. The vertical extent of the slit-image in the telescope is therefore practically indefinite. Particularly at

long distances, the interference fringes produced by the interferometer are as a rule present in the focal plane only. The endeavor to get fringes out of focus, with the light filling the field of the eyepiece, does not usually succeed, except with very good plate glass.

The case is different, however, when the collimator is discarded and a beam of sunlight L is used directly, as in figure 182. For convenience, the self-adjusting interferometer pattern was used, M being a half-silver and $NN'M'$ opaque mirrors with the distance NM very large. The telescope is at T and when focused for parallel rays shows a mere point of light, even when the mirrors (which must obviously be of optic plate) are a square decimeter in area. Nevertheless, the fringes must be present and are usually suggested by the irradiation. If, however, the telescope is put out of focus by thrusting the eyepiece either toward the front or rear, till the whole field is illuminated, the fringes will usually appear and may be enlarged by slight rotation of M' on a horizontal and vertical axis, supposing the other adjustments are nearly enough true. The beam MT is, as it were, lamellar throughout, even if the glass used is not exceptionally good. The conditions of good definition in the absence of the best optic glass may be further improved by narrowing the beam at L to small cross-section (5 mm. square), so that only a small part of the half-silver M is effective. In this case the fringes always come out strongly and there is, as a rule, still an abundance of light, if sunlight is the source. I have even used a condenser of 10 or 20 meters focal length in the beam L, without destroying the fringes and with a gain of illumination. Obviously the telescope itself is not needed and a good lens with a micrometer-plate in focus placed anywhere in the beam MT will suffice.

The available distances in the laboratory did not much exceed 11 meters; but this sufficed to make the tests, which succeeded at once in spite of rather poor glass plates. If the fringes are straight the spectrum fringes come out equally well, even with the grating, if the ruling is set at right angles to the fringes.

It will, of course, be very much more difficult to use the separated beams of Michelson's interferometer; but this either at 90° or 60° is essential for the purpose in view. If, as in figure 183, the rays were passed parallel to the directions of principal strain in a shear, the gradual increase of strain could hardly escape detection at an early date, particularly as the source of light L and receiving lens T could both be reversed 180° without any interference at the mirrors H, NN' and MM'. In the figure $mm'nn'$ suggest the original position of mirrors, and $MM'NN'$ their position under advanced strain, relative to each other.

90. Interferences resembling Michelson's diffractions for small angles.*—In figure 184, L is the objective of a telescope. No light is admitted except that passing two fine parallel slits s and s' close together at a distance

---

* Mr. Lloyd W. Taylor (Manual of Optics, p. 50 *et seq.*) describes somewhat similar experiments.

c apart. Consequently, even with white light, interference fringes at a distance x apart are seen in the ocular. They are practically equidistant, and if r is the focal length of the telescope

$$a=x/r=\lambda/c$$

λ being the mean wave-length of light and a the angle subtended by two fringes. With white light, three of these, flanked by two closed colored fringes, are usually obtained. A telescope of 20 cm. focal distance suffices. The plate ss' is best placed within the objective touching it, so that the distance r is definite. Two lines about 0.5 mm. apart, ruled with a needle in a black photographic gelatine-covered plate, if well chosen, do very well, though smoked plate glass is preferable.

91. Same. Outer plate for angular measurement.—This is shown at $S, S' \ldots$ and may be a similar but large black photographic plate with two parallel lines 1 or 2 mm. apart ruled across it with a needle. The incandescent lamp L is immediately behind SS', attached to the same standard and a screen of oiled paper (paraffine tissue) is placed between to equalize the illumination. If the distance R (1 or 2 meters) is as given in the diagram, the fringes from S are in step with the fringes from S' and reenforce each other. Hence

$$a=\lambda/c=y/R; \text{ or } y=R\lambda/c$$

and the value of y is thus given in centimeters. In the Michelson device, the adjustment is made by separating the slits ss' to the required amount. In the present experiment, however, it is more convenient to place the plate SS' on a slide R, so that the normal distance $R=Ss$ may be changed at pleasure. Thus for SS' the fringes are again in step and reenforced relative to the angle $2a$, while for a position of SS_1 at m, the fringes interfere. I have not, with white light, been able to make the fringes vanish; but the interference is marked. The distance R must be relatively very large. If R is too small, each of the slits S and S' produces its own group of interference fringes, more and more separated.

92. Data.—To give an example: The distance ss' being 0.06 cm., $a=\dfrac{\lambda}{c} = \dfrac{6\times 10^{-5}}{6\times 10^{-2}} = 10^{-3}$. The slits SS' were 0.15 cm. apart and produced clear fringes at about $R=70$ cm. and $R=130$ cm. Hence, $y=10^{-3}\times 130=0.13$ cm. instead of 0.15 cm. The criterion of clear fringes, is, of course, very coarse for white light. It would be interesting to repeat the experiment with homogeneous light and finer slits and fringes, when more alternations would appear. Instead of the telescope the eye itself might be used, the plate ss' being placed immediately in front of it; but though the fringes are obtained clearly, I had no success with the necessary alternations.

93. Diffraction substituted for interferences.—If in figure 184 the double slit ss' in front of the objective of the telescope is replaced by a single

micrometer slit of variable width $ss'=c$, the two slits at S being fixed in place, an experiment similar to the preceding may be made by successively widening ss'. When the slit at ss' is gradually opened, the broad white central patch gradually opens into two distinct and narrower patches corresponding to S and S'. On further widening, a sharp diffraction line appears between them for a slit, width c. We may then write, if x is the fixed distance apart of the images of SS' in the ocular:

$$\frac{x/2}{r} = \frac{y/2}{R} = 3\frac{\lambda/2}{c}, \qquad \text{whence} \qquad y=3R\lambda/c$$

In the experiment made, $R=110$ cm., $c=0.125$ cm., $\lambda=6\times10^{-5}$ cm., whence $y=0.16$ cm., the value measured.

On further widening the slit ss', two ($x/3$) and three ($x/4$) fringes appear between the images of SS'. But they are fainter and the adjustment much less sharp. The equation may now be put

$$x/2r:x/3r:x/4r:\ldots\ldots=y/2R:y/3R:y/4R:\ldots\ldots=$$
$$3\lambda/2c:3\lambda/2c':3\lambda/2c'':\ldots\ldots$$

whence c, c', c'' are the successive slit-widths when one, two, three, etc., fringes lie within the S images. The trial showed $c=0.125$; $c'=0.175$; $c''=0.225$ cm.; $y=0.16$; $y=0.17$; $y=0.176$ cm., the march of y being due in part to back-lash in the slit micrometer and in part to the lack of sharpness specified.

If the opaque strip between S and S' is removed, so that S is now a single broad slit, the light is too strong for the fringes to appear within the white image.
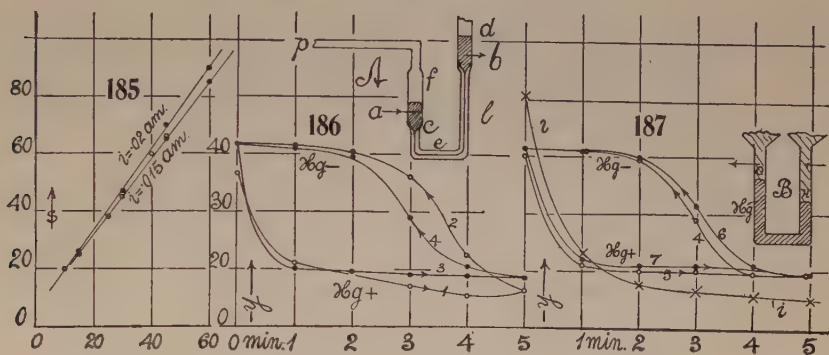
THE CAPILLARY ELECTROMETER.

94. Electrolysis.—Experiments were made in the endeavor to register the excursions of the mercury meniscus of the capillary electrometer, by the aid of interference fringes. To do this, the capillary tube carrying the moving meniscus (fig. 186, inset A, at l) was directly coupled with a small end of pure-rubber tubing to one shank of the interferometer U-gage. It was not, at first, possible to detect any displacement of fringes in this way. Naturally the large volume of air above the mercury in the U-gage, compared with the small volume displacement in the capillary tube, militates against this plan. It would be necessary to reconstruct the U-gage for the elimination of as much of the former volume as possible.

Later, however, on devising an apparatus of the type of the diagram (fig. 187, inset B), in which both menisci (capillary bore less than 1 mm.) are utilized, the closed shanks suitably connecting with the corresponding shanks of the interferometer U-gage, 5 to 10 fringe displacements were regularly obtainable. This is too small a number to be of practical value.

With the former apparatus set up, however, it seemed interesting to test it in a different way by determining the electro-chemical equivalent of water ($E=0.174$ c. c. of gas under normal conditions per ampere per second). For this purpose it was only necessary to increase the potential difference (1 to 2 storage cells) at the wet meniscus (dilute H_2SO_4) until evolution of gas

ensued, and to measure the current in the circuit with an ammeter. Naturally, the experiment, if so performed, is rough, both on account of the polarization incident to the use of filamentary non-blackened electrodes and to the heat produced during electric decomposition. The current, owing to the escape of bubbles of gas, was often fluctuating. The results, however, as seen in the examples (fig. 185; fringe displacement s in the lapse of seconds for currents 0.015 and 0.020 amperes, respectively), are better than was expected. The graphs are nearly linear, with a retardation at the beginning, owing to polariza-

tion. A curious feature of the results is the frequent increase of rates ds/dt with time, while the current i diminishes; for instance:

Time	0	15	30	45	60 seconds.
s	0	26	45	66	85 scale-parts.
$i \times 10^3$	19	17	16	16	15 amperes.

Between 15 seconds and 45 seconds $ds/dt = 1.14$; between 30 seconds and 60 seconds, $ds/dt = 1.33$. This, however, is not always the case, as, for instance,

t	0	15	30	45	60 seconds.
s	0	25	47	70	90 scale-parts.
$i \times 10^3$	21	..-	21	19	.. amperes.

the corresponding rates being $ds/dt = 1.5$ and 1.43.

To compute the electrical equivalent, s must be reduced to heads of the mercury column, the equation of reduction being $\Delta h = 10^{-6} \times 66 \Delta s$ in the first series and $= 10^{-6} \times 69 \Delta s$ in the second. Hence we obtain the mean normal rates $(dh/dt)/i = 10^{-3} \times 5.2$ and $10^{-3} \times 5.1$ per second per ampere for the two series. Owing to the infinitesimal increments of pressure p, volume v, and mass of gas m, at the absolute temperature τ, taken as constant, the intrinsic equation becomes

$$\frac{dp}{p} + \frac{dv}{v} = \frac{dm}{m} = \frac{dv'}{v}$$

where dv' is the fresh small increment of volume of electrolytic gas, practically at p, v, and τ. Thus, since $v = Ah$, A being the area and h the mean depth of the relatively large volume of air in the U-tube,

$$Ah \frac{dh}{B} + \tfrac{1}{2} Adh = dv'$$

where B is the height of the barometer corresponding to p. Now, $dv' = E$ per second per ampere, whence

$$E = A \frac{dh/dt}{2i} \left(1 + \frac{zh}{B} \right)$$

For the diameter of **U**-tube, 9.4 cm., $A = 70$ cm.²; $B = 77.5$ cm. at the temperature of dh; $h = 1$ cm. Thus $A(1 + 2h/B)/2 = 36.0$. Hence, in case of the two series,

$$E = 36 \times 10^{-3} \times 5.2 = 0.187 \qquad E = 36 \times 10^{-3} \times 5.1 = 0.184 \text{ cm.}^3/\text{sec.}$$

Reduced to 0° C. and 76 cm., these become $E = 0.178$ and 0.175, data as near the normal equivalent (0.174 c. c./sec.) as the present form of method warrants. In a modification of the apparatus, larger platinized (non-filamentary) electrodes would be the chief desideration.

95. Capillary electrometer.—To return to the capillary electrometer: Since the direct coupling is of no marked interest, the question occurs whether on compensating the depression at the wet meniscus by a pressure applied at the dry meniscus and measuring the latter with the **U**-gage interferometer, any advantage can be secured. A variety of instruments were tested, including one given to me by Professor W. Nernst; but they did not suffice as well as the improvised form shown in the inset of figure 186. Here *dec* is the capillary tube, about 1.4 mm. in diameter. The end *cf* is wide and contains the charge of Hg, above which is *pf*, a quill tube for applying pressure. A screw plunger with stuffing-box (not shown) was used for the purpose, and the platinum terminal is seen at *a*. The end *d* is also widened and contained a charge of acidulated water, meeting the wet meniscus *l*, *b* being the terminal. Acid water insures more rapid action, but it is liable to clog the meniscus. The great difficulty of this otherwise very interesting apparatus for the present purposes is its indecision. For example, figures 186 and 187 give 7 consecutive series of readings of the head of the meniscus on the scale of an ocular plate micrometer ($y = 24$ scale-parts per millimeter Hg in pressure) in the lapse of minutes. The first series are the more or less erratic; the last series are better, but one observes a wandering of the zero-point nevertheless. In view of the very weak electrolyte, it takes at least 2 minutes to obtain the full displacement y of the meniscus when it is positive, and at least 3 minutes when it is negative. One may therefore infer that the Hg meniscus itself contributes positive ions. The full displacement is here about $y = 40$ scale-parts or about 1.7 mm. of mercury for the standard Daniell cell used. Initially, as shown by the curve *i*, the electrometer had been much more sensitive, suggesting an incidentally greater strength of electrolyte. Later, with a constant voltage of about 0.110 volt, I carried the measurements through and obtained $y = 80$ scale-parts or 3.3 mm. of Hg depression, per Daniell. These microscope scale-parts were each found equivalent to $s = 50$ scale-parts of the interferometer **U**-gage. Thus, the Daniell is equivalent to 4,000 s, or an s scale-part (**U**-gage) would be a little over 0.0002 volt. Theoretically, the

mercury head is $\Delta h = 70 \times 10^{-6} \Delta s$ cm. and thus the Daniell at 3.3 mm. depression should be equivalent to $0.33/70 \times 10^{-6} = 5,000$ s, or 2×10^{-4} volts to the scale-part, as nearly corroborative as measurements of this character may be. It is thus rather a pity that these results can not be realized, the failure being inherent in the usual behavior of capillary phenomena. The sensitiveness is of course ultimately dependent on the accuracy with which the capillary meniscus may be set. For these reasons I abandoned the interferometer designs which I had prepared.

In wider tubes (3 mm. diameter), in which the meniscus just moves per volt ($y=3$ scale-parts, about; $h=0.1$ mm.), it is interesting to note the annular horizontal vortices, turning in opposite directions as the mercury is charged positively or negatively. They are shown by small crystals, etc., on the surface and apparently attributable to the sudden advance or retreat of the axis of the Hg column. Such vortices, nevertheless, also occur when the meniscus is quite stationary.

The addition of acid at the charged surface (always keeping the liquid very dilute, so that the meniscus remains clear) makes the displacements practically instantaneous, though there is residual adhesion and lag when the meniscus is positive. If the meniscus is previously raised and lowered by slight suction, the best results are obtained. I was unable, however, even after long trial, to render them sufficiently precise to be in keeping with the U-tube interferometer. As the phenomenon itself is of extreme interest, it has been discussed at great length, since the original discovery of Lippmann.*

The occurrences are well exhibited in Professor Nernst's apparatus, if both ends of a capillary U-thread of mercury are used symmetrically, as in the diagrammatic inset B, figure 187. This design, in fact, behaves with greater precision than any of the others which I have tried. Helmholtz and Lippmann adduce a beautiful theory, based on the second law of thermo-dynamics, from which $\partial T/\partial \phi = -\sigma$, T being the surface tension and ϕ the potential difference in the double layer at the mercury meniscus and σ its electrical surface density. The mercury surface is thus naturally positive, and passes through zero at maximum T into negative charges under the influence of the cation layer. Other theories have been advanced. It occurred to me that if one postulates an ion evaporation or ionic vapor-pressure at the mercury surface, the phenomenon has a close analogy to Kelvin's theory of increased vapor-pressure at a convex surface. The lower or negative meniscus (fig. 187, inset B) is more convex than the upper or $+$ meniscus, which may be coordinated with a more rapid evaporation, or a higher pressure of negative electrons from the negative mercury surface.

96. Dilution of electrolyte.—It may not be superfluous, therefore, to contribute the data which I obtained incidentally on the increasing slowness of

---

* *Cf.* Chwolson, Physik, vol. IV, I, p. 201 *et seq.* (Vierveg u. Sohn, 1908); Winkelmann, Physik, IV, I, p. 850 *et seq.* (Barth, 1905.)

adjustment as the electrolyte approaches more nearly to the case of pure water. Necessarily using the one electrolyte apparatus (fig. 188, inset) a drop of very dilute acid was added to the pure water at d and the capillary column preliminarily agitated by suction at the other end. The results of displacement y ($y = 24$ scale-parts, equivalent to 1 mm. of mercury) produced by 1 Daniell are shown in the lapse of seconds by the graph a. Successive cycles are given by different kinds of points. The main displacements are reached within 10 seconds. They would have been more rapid with a stronger electrolyte. As above, the displacement of the negative surface (reversed by the microscope in the graphs) is more rapid than that of the positive surface; a meniscus rises more quickly than it falls, or the negative ions escape or evaporate more copiously than the positive ion, even at the beginning.

188
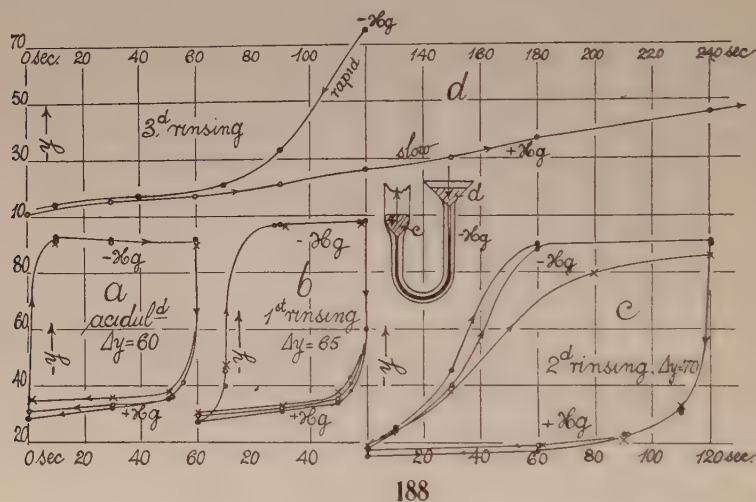
The liquid in the reservoir d (fig. 188, inset) was now removed by a capillary dropper and replaced by pure distilled water. After agitating by suction as usual, the graphs b, figure 188, were obtained. The response is, as a whole, slower than before, but not as much so as would be expected. Negative ions escape from the mercury meniscus much more rapidly than the positive ions, and the latter more slowly than before, in the first graph a. There is an enlargement of limits, Δy, of displacements, only partially reached, of course, in the single minute of observation.

The electrolyte was then cleansed in the same way with fresh distilled water at d, and the curves, figure 188, c, show that at least 2 minutes were needed to reach approximate constancy. The escape of positive ions is now relatively slow and not quite identical in the three cycles tested, as one would anticipate from the effect now producible by admixture of mere traces of impurity. The evaporation of negative ions, though still rapid by comparison, now shows a marked tendency to lag. The limits here are the largest obtained, being $\Delta y = 70$ at least, as compared with 65 and 60 before.

The results of the fourth rinsing are given by the curves (fig. 188*d*) in the lapse of seconds. Only the beginning of each graph can be shown, as the time unit is too small. We now have an extremely slow dissipation of positive ions compared with the cases heretofore, and even the negative ions escape slowly from the mercury meniscus.

The results after the third and fourth cleansing are given by the graphs (fig. 189), in a scale of minutes. It is interesting to note that the initial slow discharge of positive ions (graph *A*) is not present in the same degree in the
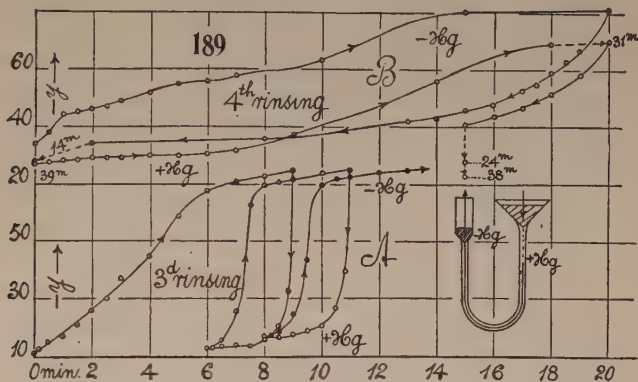
second cycle of this graph, possibly because some solute has been accidentally picked up. In no case has the limiting asymptote been reached even in 10 minutes.

The graphs *B* in figure 189 are the results of the fourth rinsing. Both positive and negative ions are now dissipated from the mercury surface with extreme slowness, and there is not on the whole much to choose between them, except at the beginning of each graph, where the negative ions escape more rapidly; but they do not reach an asymptote in 24 or even 38 minutes of observation. In pure water, therefore, a mercury meniscus is as liable to be positive as negative, though favoring the former, so far as here observed. The merest trace of electrolyte in the water makes the mercury dominantly positive.

CHAPTER VI.

GRAVITATIONAL EXPERIMENTS.

The Constant of Gravitation in Terms of the Viscosity of Air.

97. Introductory.—In the experiments heretofore, the occurrence of uniform motion in the case of a needle vibrating in air was not unusual, provided the quartz fiber used was not exceptionally thin, *i. e.*, provided the needle passed through the equilibrium position with sufficient velocity. Thus, in a preceding report (Carnegie Inst. Wash. No. 310, 1921, § 94, figs. 143, 150, and 151), the graphs of the excursions of the needle were often sharp zigzag lines. The straw shaft then used admitted of an estimate of the constant only. In the last report (Carnegie Inst. Wash. No. 310, Part II, 1923, § 62; also Proc. Nat. Ac. Sc. VIII, 1922, p. 66), the framework of the needle being filamentary, the equation for the motion of the balls at the end of the needle could be much more nearly given. In fact, when the needle passes through its equilibrium position, the torsion of the fiber is zero, and for a small angle, symmetrically on either side, the contribution of the fiber is respectively positive and negative. Hence the acceleration imparted is again removed. If, therefore, here the needle moves uniformly, the gravitational pull is exactly balanced by the frictional resistance, the latter rising asymptotically to a maximum, dependent on the speed imparted by the former. Only a very small excursion near the zero position is in question. In such a case Stokes' equation, as shown heretofore, leads to the value

$$\gamma = \frac{R^2}{Mm} \frac{3\pi\eta rl}{L} \frac{\Delta y}{\Delta t}$$

where M and m are the gravitating masses at a distance R apart, m of radius r being at the end of the needle of semilength l. L is the distance between the mirror on the needle and the scale along which, as seen telescopically, the small middle excursion Δy, is passed in Δt seconds. The viscosity of air is η, and is well known to be nearly independent of pressure, so that observation for the needle in moderate vacuo is permissible.

In this equation the resistance experienced by the filamentary design of the needle is neglected. It is supposed that the motion is slow enough that the viscosity of air (not any eddying resistance) is alone in question. This may be admitted in vacuo, I think.

To recognize the equilibrium position for the exhausted case of the needle, the attracting weights M are placed in the neutral position for a sufficient time. In work with a slow-moving needle, however, the observations are necessarily prolonged and the zero position of the needle changes in the lapse of time. Accordingly, different values of Δy will be found, according as the

needle moves toward or falls from the high numbers on the scale. If the difference is not large, the mean may be taken. Otherwise, if the swing of the needle has become steady in its repetitions, the mean of the extreme elongations of the swinging needle is probably a preferable value.

98. Apparatus and method.—As heretofore described, this consisted of a flat case (*cf.* fig. 191) capable of exhaustion. Each attracting weight M, near the corresponding end of the needle, could be moved expeditiously from one side to the other of the case, the reversible forces thus admitting of methods of multiplication. The quartz fiber was exceptionally delicate and the apparent period of the needle about 750 seconds, almost the whole of the effective weight being in the masses m at either end. The air-pump attached to the case was capable of exhaustion of about 10^{-4} mm. of mercury and a McLeod gage was continually in connection with the case, even after the air-pump attachment had been shut off. The vacuum in the case was thus determinable at any time. All observations were here made at night.

The values of the constants in equation (1) were as follows: $M=3,368$ g., $m=0.6295$ g., $R=5.67$ cm., $L=447.5$ cm., $l=11.0$ cm., $M'=2,947$ g., $m'=0.6295$ g., $R'=5.43$ cm., $r=0.23$ cm., $\eta=0.00019$. This makes $10^7\gamma=1.536\Delta y/\Delta t$ and $1.609\Delta y/\Delta t$, respectively, or conjointly * $\gamma=10^{-7}\times1.572\Delta y/\Delta t$.

To bring the needle into a steady state of vibration, the attracting weights are put on one side of it, and thereafter, when the needle has reached its maximum elongation, the weights M are quickly swung to the other side. The needle soon becomes steady. Two or three reversals usually suffice. When this is the case, observations are made for the time (Δt) consumed in passing between points 1 cm. on each side of the equilibrium position ($\Delta y=2$ cm.), a stop-watch or a chronometer being available for the time measurement.

In table 19, I have collected values of this kind. The question at issue is whether in case of a very delicate quartz fiber (the one in question gave a static double displacement of over $\Delta y=13.4$ cm.), the needle will acquire sufficient velocity from the swinging of the weights M, to meet the conditions of the equation. In the first series the telescopic arc of vibration was but $y-y'=20$ cm., the excursions being alternately positive and negative. The mean time taken was 20.5 seconds and 23 seconds, respectively, showing that the zero-point had wandered. The mean value of γ thus obtained is but 1.5×10^{-8}, with the implication of a gravitating force considerably in excess of the frictional resistances. Consequently, in series 2 of table 19, the excursions were gradually pushed to the limit ($y-y'=35$ cm.) by alternating the gravitational pull (reversal of M) in step with the swing of the needle. Here again the original position of equilibrium changed in the lapse of time, so that the values of Δt for positive and negative arcs are not the same. $\Delta y/\Delta t$ increases, though not quite regularly, with the size of the arc of vibration. Taking the last three data of the series, the value of $\Delta y/\Delta t=0.157$ cm./sec.

---

* In the original paper (*l. c.*), the sum instead of the mean constant was erroneously taken; *i. e.*, $10^{-7}\times3.145$ should be $10^{-7}\times1.572$.

10

on the scale, from which $\gamma = 10^{-8} \times 2.48$. This is but 37 per cent of the standard value of γ. In figure 190 I have given the mean observed values of 2γ, as depending on the arcs of vibration $y - y'$. If the curve is prolonged, an arc of $y - y' = 2 \times 49$ cm. would be needed to bring out the full value of γ, whereas 35 cm. could not be exceeded.

The third series, made after an unsatisfactory day of variable temperature, was inferior to the preceding. Although the exhaustion was higher (mean 0.015 mm.), the maximum arcs were not so large as before.

The behavior of the needle at its reversals, sometimes rapid, at other times deliberate, has a bearing on its period and logarithmic decrement. For if the radiant forces are repulsive on both sides of m, the period will be shortened to a minimum; if they are attractive on both sides the period will be long for an equivalent of these forces added to or subtracted from the modulus

TABLE 19.—*Values of Δt for $\Delta y = 2$ cm. $10^8\gamma = .314\Delta y/\Delta t$.*

Vacuum.	Arc.	Δt	$10^8 \times \Delta y/\Delta t$	$10^8 2\gamma$ (observed)	$T/2$	Vacuum.	Arc.	Δt	$10^8 \times \Delta y/\Delta t$	$10^8 2\gamma$ (observed)	$T/2$
mm.	cm.	sec.			sec.	mm.	cm.	sec.			sec.
About 0.1	—20	24	83	2.61	...	Plenum.	—23.2	25	80	2.5	489
	+20	20	100	3.14	...		23.1	22	91	2.9	...
	—20	23	87	2.74	...		—23.4	26	77	2.4	449
	+20	21	95	2.99	...		22.8	23	87	2.7	...
	—20	23	87	2.74	...		—23.0	26	77	2.4	426
	+20	20	100	3.14	...	Mean ..	......	....	.....	2.6	...
	—20	23	87	2.74	...						
	+20	20.5	98	3.08	...	0.03 ...	>60	10	20	6.3	365
Mean ...	......	....	.....	2.92	...	.17 ...	>60	12	17	5.3	...
0.046 ...	—35	12.2	164	5.17	...		>60	10	20	6.3	365
	+35	13.3	150	4.73	...		>60	10	20	6.3	...
	—35	12.2	164	5.17	...						
Mean ...	......	....	.....	4.95	...						

of the fiber. The periods will be intermediate if one side attracts and the other repels.

The data obtained in the third and subsequent series lay between 1 and 2 in figure 190 and were all in conformity, more or less closely, with the curve. They need not, therefore, be given. It is desirable, however, to determine the corresponding values for the case of the needle vibrating in a plenum of air. Data of this kind are also given in table 19; but they are far less trustworthy, chiefly, because the needle drifted at its high elongations gradually, from $y = 32$ to $y = 39$ cm., with a somewhat smaller drift, also towards high numbers, at the low elongations. The values of Δt for positive and for negative arcs of swing are thus unequal, though the mean position was aimed at in rating Δt. Although the needle moves very slowly, with an excessive period, it is questionable whether the frictional resistance is here purely viscous. The ("old") value of γ so found (necessarily small of course) even falls below the graph (fig. 190).

As a whole, the experiments show that the necessary arc of vibration under which the given equation would apply and for which there would be an equivalence of the gravitational and frictional forces, is not attainable with so fine a fiber by the mere passing of the weights M from one side of the needle to the other. As there was no other method for a safe use of the method of multiplication, the experiments were not carried further with this apparatus.

99. Excessive arcs.—During the course of the work in the succeeding paragraphs and in the presence of large radiant forces (July 30, 31), the needle fell through relatively very large arcs, probably exceeding 60 cm. A few measurements of the speed of the needle in passing through its equilibrium position (so far as determinable) were therefore also made. These are given at the end of table 19 and contain the closest approach (3.1×10^{-8})
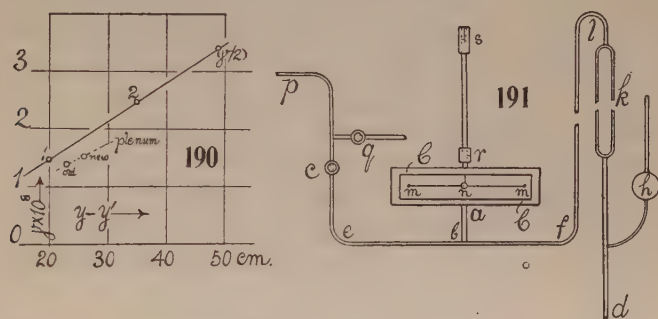
to the standard value of γ which could be obtained. They do not fit into the locus of figure 190, because the arcs have not the same meaning. Other measurements made at this time were similar to the first and second series of the table.

100. Recent summer tests.—About a year later, in the ensuing summer, I took the work up again, the conditions being favorable for vibrations in a plenum. A brief example of the results ($y_1 y_2$ telescopic elongations, Δt time of passing the middle collimeter):

$y_1 = 7.9$			8.4		8.5 cm.
$\Delta t =$	10.4	10.4	10.2	10.4	seconds.
$y_2 =$		34.3		34.6	cm.
$\Delta y / \Delta t =$	0.0961	0.0961	0.0980	0.0961	cm./sec.
$\gamma \times 10^8 =$	1.51	1.51	1.54	1.51	

The apparatus remaining the same, the above constants may be considered as nearly enough applicable, so that $10^7 \gamma = 1.573 \Delta y / \Delta t$. So computed, the values of γ in table 19 adhere to the excessively low orders heretofore obtained. The normal speed $\Delta y / \Delta t = 0.425$ second should have been found, equivalent to the time $\Delta t = 2.35$ seconds in passing the middle centimeter. In fact, the observed data for γ, etc., are only about 23 per cent of the normal data. The

remainder of the gravitational attraction must therefore have been exerted in changing the momentum of the needle and in overcoming such additional friction as the framework of the needle may have introduced. So large a discrepancy was not expected, seeing that the difference of elongations, $y_2 - y_1 =$ 26 cm., is fairly constant; but the lower locus in figure 190 shows that it fits last year's datum for the plenum.

<div align="center">PERIODS, LOGARITHMIC DECREMENT, AND STATIC DISPLACEMENTS.</div>

101. Apparatus newly installed.—The object of the present experiments is a completion of the work of the last report, by carrying the exhaustion of the case as far as practicable. Figure 191 is a sketch of the disposition of apparatus, where mm is the gravitation needle in its narrow case with plate-glass walls CC, n being the mirror. The attracting weights M are removed. The sides of the case are reëntrant, to receive the glass plates, and they and the quartz-fiber tube are sealed with resinous cement, poured into the crevices and the cups rs in the molten state. The exhaustion takes place through the pipe ab, communicating by a T-joint with the train of $\frac{1}{8}$-inch gas pipe $pcfl$. All joints are sealed with cement. The pipe p comes from a large oil air-pump, with fore pump, capable of exhausting to about 10^{-4} mm. of mercury. The MacLeod gage of the usual pattern is shown at khd. To shut off the case and gage there is a glass oil-sealed stop-cock at c, and a similar cock q allows of the admission of air. The pump is kept exhausted, no matter whether c is shut off or not. After the initial experiments, all parts of the apparatus worked very smoothly.

In spite of the care taken to seal all parts of the extended apparatus, it was not in the earlier work possible to hold the vacuum indefinitely. There remained a constant leak of 0.0038 mm. of mercury per hour, the seat of which I was unable to detect; but as experiments with gradually decreasing vacua were primarily contemplated, this leak was here no serious disadvantage, except that the highest exhaustions were not available. It is of course quite possible to keep the pump running and the stop-cock c open. When this is done, however, the needle (quite apart from tremor) is always in motion, so that gravitation measurements are out of the question. It is necessary to close the cock c and wait several hours until the case CC is in adequate thermal equilibrium. Thus the vacua below 5×10^{-3} mm. are lost.

102 Data. Logarithmic decrement, λ.—In the work of last year the logarithmic decrement, as obtained from observations largely made at night, seemed to remain fairly constant until the highest exhaustions were approached. This result needed the further qualification undertaken in the present paper. To compute $\lambda \log e$, the two arcs obtained from the first three elongations of the needle $y - y'$, $y' - y''$ were used. As there was a small leak in the apparatus of about 0.0038 mm./hour, the data for λ could be found with great accuracy in this way in the course of time, while the vacuum slowly

degenerated from about 0.0002 to 0.271. It was hoped that the viscosity of air in its relation to pressure could then be found; but this expectation was not realized, for reasons which will presently appear.

The data for λ, the time and the vacua to which they belong are given in table 20, observations being made in the morning (A), afternoon (P), and night (N). They are constructed relative to the lapse of time (minutes since exhaustion) in figure 192; and in relation to the vacua (mm. of mercury) in figure 193. F denotes that the attracting weight M, on the right, is in front, and R to the rear of the case and needle, the opposite conditions holding for the M near the left end of the needle. The first arc of swing was usually between $y = 20$ and $y = 30$ cm., depending on the time of day and the slow drift at either elongation, heretofore discussed.
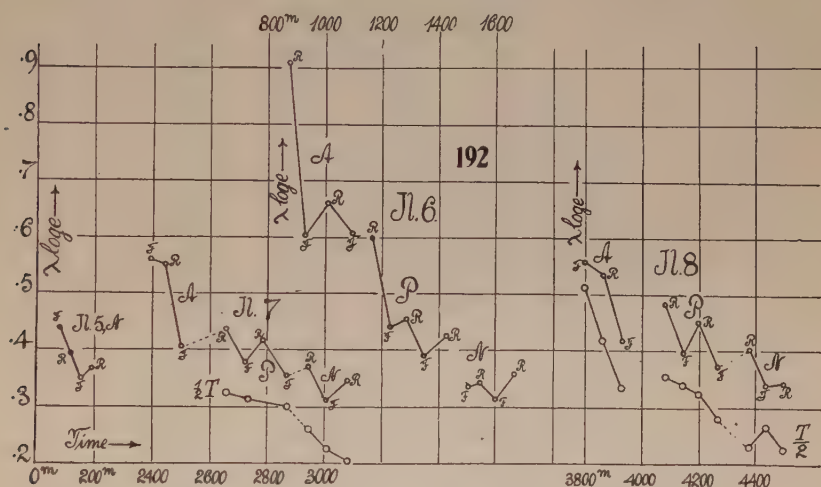
Inspection of figures 192 and 193 shows that changes of viscosity, due to changes of pressure, are not discernible in results of the present kind. In fact, the logarithmic decrement at the highest exhaustions (July 5) happens to be larger than at the lowest exhaustions (July 8, N). The logarithmic decrement is therefore also primarily and enormously under the influence of the radiant forces. It is largest in the morning and least at night. It therefore obviously oscillates once per day, though I did not make observations after 11 p. m. If $d\theta/dt$ be the change of atmospheric temperature per second in the environment of the apparatus, then this coefficient is the controlling factor in the marked variations of $\lambda \log e$.

Moreover, the values of $\lambda \log e$ are always larger for the rear positions R of M than for the front positions F, under otherwise like conditions. One or the other, or their mean, must therefore be taken in association with $d\theta/dt$. This may be due to a lack of symmetry of the position of the needle to the case; but it is more probably due to a lack of symmetry in the environment, as there is a wall immediately behind the case. The radiant forces from the

rear act as an attraction relatively to the radiant forces from the front, so
that the first swing of the right end of the needle to the rear is excessive as
compared with the swing from the rear. The conditions are reversed in the
first swing toward the front.

103. Periods. T.—The accurate method of finding $T/2$ from two succes-
sive passages of the needle through the position of equilibrium is very trouble-
some here; for T is long (over 12 minutes) and the position of equilibrium
varies. Moreover, as the variations of T are large, precise values of it are
here apparently of little use. Hence the measurement of $T/2$, from the first
to the second elongation, was accepted as adequate for the purpose. These
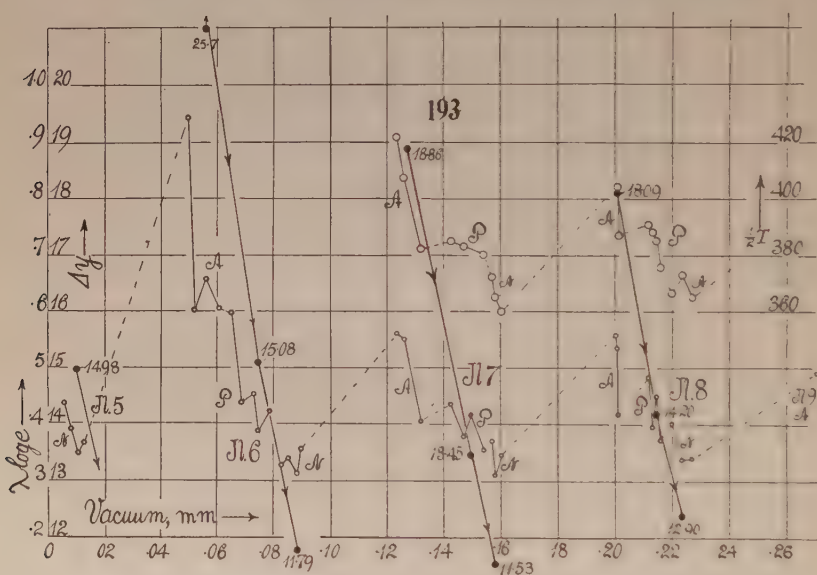
values of the first semiperiod, so far as taken, are also given in table 20 and
constructed in figure 193 (upper graph), in seconds. The variations may
run from 6 to 7 minutes, and the T values are largest in the morning and least
at night. They run about in parallel to the λ values, if either the R or the F
position alone is taken. T thus also varies harmonically in the lapse of time
with a period of 24 hours referable to $d\theta/dt$.

From these results it might be surmised that the true semiperiod $T/2$ can
be computed from the logarithm decrement observed at the same time, since,
ordinarily, $T = T_0 \sqrt{1 + \lambda^2/4\pi^2}$; but it is easily seen that the correction so
obtained is of an order entirely too small to account for the existing diver-
gencies. In fact, we are not at liberty to use the common theory of the damped
pendulum at all, and the expression $\lambda \log e$ is used merely as an analogy, for
convenience. It must also be observed that the first semiperiod of the highly
damped needle is alone in question.

104. Static displacements, Δy.—A continuous series of these data were given in the earlier report and obtained from night observations (7 to 11 p. m.), when they are liable to be most constant. Table 20 and figure 193 contrast these values for different parts of the same day. Δy is the static

TABLE 20.—*Logarithmic decrements (λ), vacua, first semiperiods $T/2$, and static deflections Δy.*

Date.	Time.	$10^4 \times$ vacuum.	$10^8 \times \lambda \log e$	$T/2$	Δy	Mean $10^8 \times \lambda \log e$	Mean $T/2$
	min.	*mm.*		*sec.*	*cm.*		
July 5, N.	0	2	...	...	...	...	...
	81	55	R438	...	...	...	...
	120	80	F393	...			
	155	102	R350	...	} 14.98	370	...
	193	125	F367	...			
July 6, A. M.	876	490	R942	...	...	...	...
	930	518	F602	...			
	1010	560	R658	...	} 25.73	622	...
	1098	606	F605	...			
P. M.	1169	650	R597	...	...	...	...
	1229	685	F438	...	...	...	...
	1290	730	R453	...			
	1350	745	F388	...	} 15.08	422	...
	1430	785	R424	...			
N.	1505	825	F334	365	...	...	...
	1549	850	R341	...			
	1600	880	F313	...	} 11.79	337	367
	1665	915	R357	369			
July 7, A. M.	2392	1234	F560	421			
	2447	1260	R550	407	} 18.86	505	403
	2503	1320	F405	382			
P. M.	2658	1425	R435	385	(13.74)	...	...
	2723	1470	F378	383			
	2785	1495	R416	...	} 13.45	383	382
	2869	1540	F354	380			
N.	2945	1570	R370	372	11.53	342	366
	3009	1580	F310	365	...	...	...
	3082	1600	R345	360	...	...	...
July 8, A. M.	3795	2006	F559	423			
	3861	2010	R536	404	} 18.09	504	405
	3930	2014	F418	387			
P. M.	4080	2120	R484	391	...	...	...
	4142	2133	F397	388			
	4197	2146	R451	385	} 14.20	407	383
	4265	2160	F373	376			
N.	4375	2200	R403	366			
	4435	2235	F340	373	} 12.40	362	368
	4499	2270	R342	365			
July 9, A. M.	5265	2710	F494	412	...	...	...

displacement finally obtained, when the attracting weights M are swung from one side of the needle to the other. As figure 193 shows, Δy is also markedly harmonic in the lapse of time or of the reduced exhaustion proportional to time, with a period of one day.

We thus come to the result that λ, T, and Δy are similar time functions; that as a first approximation they are independent of the change of viscosity of rarefied air, and that their relative variation is such as to admit of their expression in terms of each other. It does not necessarily follow that a correct

value computed for one (for instance for λ) would lead to correct values for T and Δy; but it is a project well worth testing and will presently be considered.

105. Comparison of λ, T, Δy.—It is next necessary, therefore, to more specifically compare all the quantities obtained in the present investigation. This has been done in figure 194, where the abscissas are $\lambda \log e$ and the ordinates $T/2$ and Δy respectively.
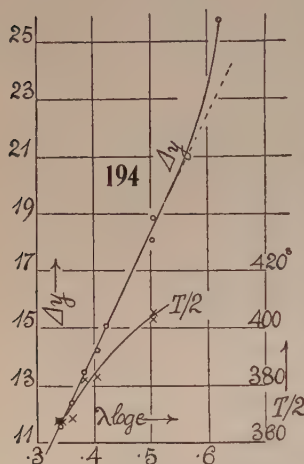
Turning to the latter, it is at first astonishing to find that λ and Δy, in spite of the marked amplitude of radiant forces, make up a rather definite graph. In fact, if we omit the exception $\Delta y = 25.7$ (inadmissibly large radiant forces), Δy and λ are nearly proportional. The values of λ in hand lie on both sides of $\lambda = 1$ to the extent of about 15 to 19 per cent. If this curve were known, Δy could be computed from λ; and vice versa.

The values of the first semiperiod of $T/2$, as already intimated, were not accurately taken, as I did not anticipate relations like the present. Nevertheless, figure 194 adequately shows that these also make out a definite graph, in which $T/2$ increases more slowly than the logarithmic decrement; in other words, so far as the observations go, λ and $T/2$ are not proportional. $T/2$ also increases more slowly than Δy. If, for instance, $\Delta y = 13.4$ cm., about the mean value in the preceding report, $T_1 = 758$ seconds should be its equivalent and $\lambda \log e = 0.385$ at the same time. If we take the vacuum period as $T = T_1 / \sqrt{1 + \lambda^2/4\pi^2}$, it would be $T = 750$ seconds.

106. Observations in plenum.—In contrast with the preceding oscillations under conditions of high exhaustion, the results of table 21, for the case of the needle vibrating in air under atmospheric pressure, are nearly aperiodic. The data for $T/2$, λ, Δy, are all enormously larger, and sometimes excessively so, as on July 10, $10^h 27^m$ a. m., when the drift was correspondingly large. These values of λ are not analogous to logarithmic decrements, but result from the continued drift of the position of equilibrium of the needle toward the direction in which it is deflected by the attracting weights M. In this respect the present results are quite different from the preceding under exhaustion; for the latter are like real vibrations under the conditions imposed and λ has a definite meaning. One may ask, moreover, whether in a plenum, in spite of the slowness of motion, the resistance encountered by the needle is purely viscous, i. e., whether a part of the resistance is not of the nature of dynamic pressure.

The motion of the needle in case of table 21 is peculiar. When the weights are exchanged, the needle falls from its high elongation to its low elongation

in the time given under $T/2$. It then turns toward a new high elongation for a time (usually about $T/4$ seconds in length), after which it again moves toward low numbers by slow, indefinite creeping, without again turning. Exactly the same phenomenon occurs when the needle rises from a low elongation toward a higher. In other words, the needle, which is practically dead beat, may be said to oscillate about a position of equilibrium continually advancing in the direction of the deflection; or the radiant attractions in either direction continually increase. The following is an example:

Plenum: 7h35m p. m.	$y=15.90$	Exhaustion: 7h20m p. m.	$y=19.65$
	37.35		1.07
	36.90		9.00
8h36m	40.15	8h24m	7.87
	17.05		26.55
	17.40		17.40
9h34m	16.62	9h37m	19.15
	39.17		1.08
	38.95		9.25
10h10m	41.40		....

In the exhausted case the next position of equilibrium lies between the preceding second and third elongations; in the presence of a plenum, it lies beyond the third of the preceding elongations.

Between these values of $T/2$, λ, and Δy (unlike the above data for the exhausted chamber), no relation can be detected. Nevertheless, if mean values are taken, they conform with the theoretical viscous resistance much better than the vacuum values, as will presently be shown.

TABLE 21.—*Plenum values of λ, $T/2$, Δy.*

Date.	Time.	$T/2$	Δy	$\lambda \log e$	Mean Δy	Mean $\lambda \log e$	Mean $T/2$
July 9, P. M.	2h36m	...	21.1	2.03	....	....	...
	3 00	520	20.7	1.54	....	....	...
	4 03	504	22.1	2.05	....	....	...
	5 00	543	21.5	1.53	....	....	...
	6 05	530	22.5	2.05	21.6	1.84	524
N.	7 35	533	21.2	1.67	....	....	...
	8 36	520	22.9	1.82	....	....	...
	9 34	561	22.4	2.01	22.2	1.83	505
July 10, A. M.	10 27	570	25.	(*)	....	....	...
P. M.	1 30	585	23.	2.02	....	....	...
	6 03	533	18.10	1.49	....	....	...
	7 17	516	19.50	1.52	20.2	1.68	545
N.	8 03	570	22.02	2.04	....	....	...
	9 05	585	23.43	1.45	....	....	...
	10 00	572	26.64	1.75	24.0	1.75	576

* Creeping.

107. Comparison with computed values of frictional resistance.—It is now desirable to endeavor to construe the values obtained for λ and T by the aid of the familiar theory of the damped pendulum. If the needle be regarded

as consisting of the two balls at its end, the frictional forces should be $6\pi\eta r v$, and therefore the frictional coefficient b is

$$b = 6\pi\eta r$$

If T_1 is the period of the damped needle and λ its logarithmic decrement

$$T_1 b = 2\lambda$$

and therefore

$$\lambda = 3\pi\eta r T_1$$

Hence λ should be proportional to T_1 and if $r = 0.23$ cm., $\eta = 0.00019$, the datum in the tables becomes

$$\lambda \log e = 0.00112 T_1$$

or $T_1 = 892\lambda \log e$ seconds. In figure 194, however, not only is proportionality of T and λ at long range excluded, but the factor would be for

$\lambda \log e =$	$T_1/\lambda \log e =$
0.35	2,103
.40	1,920
.50	1,720

i. e., about twice as large on the average. It would be necessary to suppose, therefore, that the viscosity η drops off in high vacua, which is untenable while in consequence of the resistance of the filamentary hanger of the needle η is effectively larger. The theoretical conditions of the equation do not, therefore, hold for the vibrations in vacua.

Curiously enough, however, if the mean be taken of the promiscuous experiments in a plenum (table 21), the results for two days are:

	P. M. $\lambda \log e =$	$T_1 =$	$T_1/\lambda \log e =$
	1.84	1,048	570
	1.68	1,090	649
Night	1.83	1,010	553
	1.75	1.152	658

In consequence of the peculiar motion of the needle, these values are necessarily crude; nevertheless, they come much closer to the theoretical result (coeff. 892) than the vacuum values.

FURTHER INVESTIGATIONS.

108. Change of apparatus.—After concluding the experiments of the preceding section, the apparatus was taken apart for more rigorous sealing. Moreover, the pipe p (fig. 191) was bent down and the cocks c, q placed in the down-going branch, so that all infiltrations from the oil-cups of the cock would pass into the pump. After putting the parts together again I found, to my astonishment, that the leak had increased to 0.042 mm./hour on the first day, which, however, on successive exhaustions fell off to 0.008 mm./hour at the end of the second. It was obvious, therefore, that the greater part of the leak was within the apparatus, and probably due to evaporation or sublimation from the resinous cements. The apparatus was then taken down again and put together with picein (rubber) cement, but with no great improvement.

Finally, I made use of tinned screws at the joints, so far as possible, and resolved to trust to continued exhaustion. The work began with a leak of 0.012 mm./hour on July 19, which had gradually decreased to 0.006 mm./hour on July 25, and fell continually thereafter. As a result of this labor (oil-cups and the connections separately were also tested), the apparatus showed a leak nearly twice as large as the original apparatus, in which the sealing happened to be nearly a year old. These annoyances seem to be inevitable in an apparatus necessarily to be sealed, and which can not be made wholly of glass.

Fortunately, as shown in the preceding paragraph, the amount of high exhaustion is of little consequence in its bearing on the present experiments, for about half a day must elapse after exhaustion before the needle is in a sufficiently steady state for observation. In the present case, where the apparatus had been frequently slightly warmed to facilitate the preliminary exhaustions, the needle persisted in sticking to the glass plates, before or behind, for over 3 days before it was released by the radiant forces and available for excursions. The result is that the vacua in the following series, figure 195, are moderate, beginning with 0.0633 mm. on July 24 and ending with 0.466 mm. on July 27, indicating a mean leak of 10^{-4} mm./minute.

Moreover, after the needle had swung free, a season of variable weather was at hand, with excessive and cold rains, etc., which seemed to make all normal observations useless. Nevertheless, as it proved, these very unsettled conditions afforded a means of exhibiting the interplay of gravitational and radiant forces more easily interpretable than any heretofore met with. The observations July 24 to 27 have therefore been very fully recorded in figure 196, where the ordinates denote the scale-reading y of the needle. The successive observations are inscribed at equal horizontal distances apart, with the nearest hour recorded, and not strictly chronologically, in which case the diagrams would be too diffuse. Little circles indicate the first of a set of three successive elongations (immediately after the reversal of the attracting weights, M), from which two arcs are obtained. By the aid of two stopwatches, the semiperiods of these arcs were also measured and are recorded (by numerals in minutes and seconds) in place in the diagram. The mean semiperiod (in minutes and seconds) is given at the peaks. A, P, N refer to morning, afternoon, and night (after 6 p. m.) observations. Front and rear positions of the weight M near the right end of the needle are indicated by F (open circles) and R (black circles).

If we connect the little circles of the same kind by a curve, we get the successive positions of the needle in equilibrium, remembering that though the abscissas are not quite chronological, about an hour elapses on a given day between successive circles, as a rule, and about 6 or 7 ($T/2$) minutes between the points of each triad. These equilibrium curves F and R, on July 24, 25, and 26, intersect at a time between 5 and 8 p. m., and they must intersect again late at night. When they do intersect, the equilibrium position

of the needle is the same, no matter whether the attracting weights M are on one side or the other of the needle. On July 27, the tendency of the F, R graphs to intersect (which has been gradually decreasing) is just missed. Similarly interesting graphs E, E' are obtained by drawing a line through the elongation of the first throw, after exchange of the weights M. These are, as a rule, convex towards each other, but they do not intersect. Their minimum distance apart in y is near the time of intersection of the equilibrium curves.

With regard to the successive semiperiods $T_1/2$ and $T_2/2$ obtained between elongations for the first two arcs of vibration, one may note that $T_1 > T_2$, as a rule, before the time of occurrence of the intersection of the equilibrium curves, and that $T_2 > T_1$ after passing this intersection. Moreover, the total
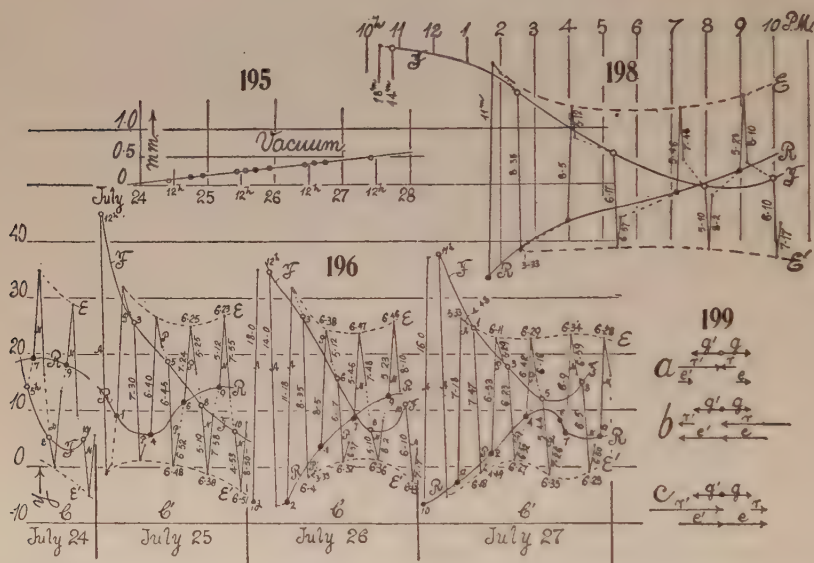

period $T_1/2 + T_2/2$, in spite of very large differences in the components, has more nearly the same value throughout. There is a determined attempt at compensation.

109. Remarks on the graphs.—What is extremely puzzling about these observations is the fact that the equilibrium curves F and R should intersect (*i. e.*, the needle occupy the same position of rest for either the front or rear positions of the attracting weights M), and that nevertheless marked throws of the needle should occur immediately after the weights M are exchanged in position. I have therefore, in figure 198, constructed the results of July 26 on a time scale, instead of by observations (incidentally correcting a wrong entry at 8 p. m. in fig. 196). The curves F, R and E, E' now appear in less abrupt outline and remain close together after intersection. One may notice the T_1 of the first arc becomes less than T_2 of the second some hours before the intersection of F and R; but the tendency remains. In figure 199 I have

represented the three force vectors, g for gravitation, r and r' for the radiant forces on the two sides and at one end of the needle (at m for instance), and e for the elastic force of the fiber. At the point of intersection we shall have (g taken positive) :

$$-g+r'=g+r=e \quad \text{or} \quad 2g=r'-r$$

In figure 199, case a, the r is negative and the sum $r'+r$ is twice g, both radiant forces being repulsive. In cases b and c, both radiant vectors have the same sign and g is half their difference, taken positively. At the point of intersection of F and R, r and r' may therefore, nevertheless, have any value, provided their difference is constant, $i.$ $e.$, the radiant forces on the two sides of the needle need not be equal.

July 28   July 29   July 30   July 31
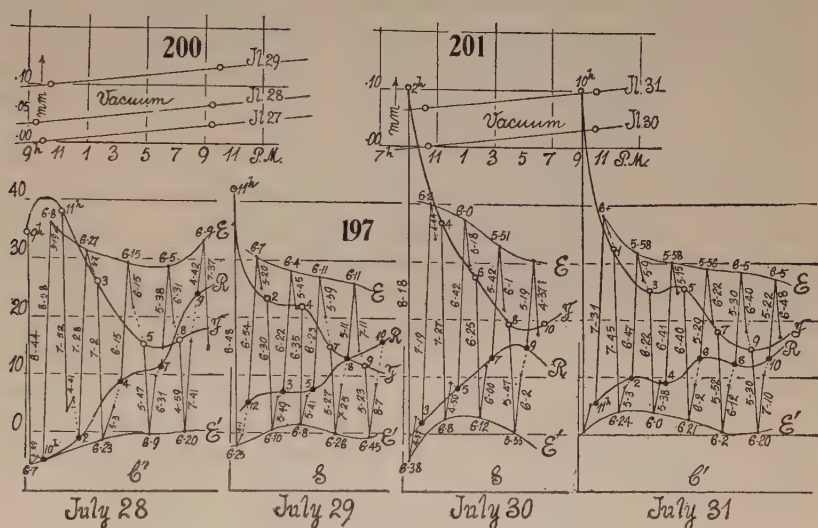
Moreover, in case b we should expect $T_2 > T_1$, since in the latter case the needle moves against a repulsion. In case c, $T_1 < T_2$, since the needle, in going toward the right in the diagram, moves away from an attraction. Thus T_1 and T_2 need not be equal at the intersection of F and R.

All this, however, affords no clue as to why there should be marked deflection in case of an exchange of weights M, when the positions of equilibrium F and R are the same. One possible suggestion is at hand. Whenever g' is changed to g there is a momentary removal of the gravitational force and hence a radiant impulse occurs. In case c this would act in the proper direction, but in case b it would act in the wrong direction; and since the deflection which follows an exchange of weights is, without exception, in the direction of gravitational attraction, the suggestion must be dismissed. Moreover, the impulse, lasting at best but a few seconds, would be altogether too small to account for the large throw of the needle observed. Again, the whole phenomenon is practically symmetrical; there is as marked a throw from curve R

to curve E, as occurs from curve F to curve E', on the average. The throw must therefore be essentially a gravitational phenomenon.

The next question is thus an inquiry into the seat of the radiant forces r and r'. If they arise in the glass-metal case they would be fixed; if in the weight M and fixed they would be indistinguishable from g. Hence the inference is suggested that the radiant forces are a relatively slow growth in the lapse of time and that their seat is effectively in the weights M. Immediately after the weights are exchanged, one may therefore assume that radiant forces are virtually absent. After the lapse of a fraction of an hour, however, they are again established in full equilibrium. The same mechanism acts in the next exchange. Hence, the view heretofore taken may be considered as corroborated, viz, that the weights M screen the case and needle from the radiation coming from without. The radiant forces grow in proportion as this radiation is absorbed by M and withheld from the case and needle. It may be conceded that the front and rear of the case make no difference here, since one of the two masses M is always in front and the other in the rear. The subject will be resumed in § 111.

110. New observations.—Owing to the enormous difference between these fluctuating results and the exceptionally constant data obtained last summer, it seemed desirable to study the present conditions somewhat more at length. One may notice, for instance, that on July 24 (fig. 196), the F, R intersection actually occurs before 5 p. m. The apparent gravitational deflection Δy is thus zero and negative throughout the night. On July 25 and 26, the intersection occurs between 7 and 8 p. m. and on July 27 it just fails between 5 and 6 p. m. In contrast with this, Δy at night in the older results was almost constantly 13.5 after 6 p. m. for months, so that the observations were often much like repetitions of each other. Unfortunately, $T/2$ was mostly observed for single arcs, as a rule; it should have been taken (as now appears) from two consecutive arcs of vibration.

The new results obtained on July 28 and 29 after fresh exhaustion, in the same way as the preceding, are given in figure 197, with insets (figs. 200 and 201) showing the vacuum). Successive observations are horizontally equidistant, and the nearest hour is attached to the initial circles. The graph also gives the $T/2$ for the ascending and descending branches and their mean $T/2$ in minutes and seconds. The F, R curves are somewhat different in form from the preceding, but they nevertheless intersect at about 8 p. m., after which Δy is negative, or the radiant forces overpower gravitation. EE' curves, though much the same as before, are somewhat farther apart, as a rule. On July 28 (9 p. m.) there is a negative decrement λ.

The apparatus had been exhausted on the night before July 28. The vacua are therefore moderate, 0.06 to 0.26 mm. On July 30 the exhaustion was made at 10 a. m.; as it was necessary to wait until the needle was free from the sides of the case, observations were not available before 2 p. m. The F, R curves trend rapidly towards an intersection after 8 p. m., but they nevertheless

just fail, and thereafter diverge again. The day was clear, and hence the large $d\theta/dt$ effect. On July 31 the F, R curves are more irregular; but they also fall short of intersection at 8 p. m., and recall the graphs of July 27. The vacuum has, meanwhile, been continually decreasing without producing any determinable impression on the graphs as a whole. On August 1 the equilibrium curves F, R have grown simpler, but they are as yet far removed from steady or normal Δy values, even at night.

After August 1, the extremely laborious procedure, involving much eye-strain, of determining T_1, T_2, and λ was dispensed with and measurements of Δy only, for time intervals about an hour apart, were taken. These, it was thought, would be adequate for comparison with similar data taken on the same day last summer. They will come up for consideration in § 111.

111. Values of λ and Δy.—It seemed at first useless to look for any relations here, in view of the confusion of data and the frequent occurrence of
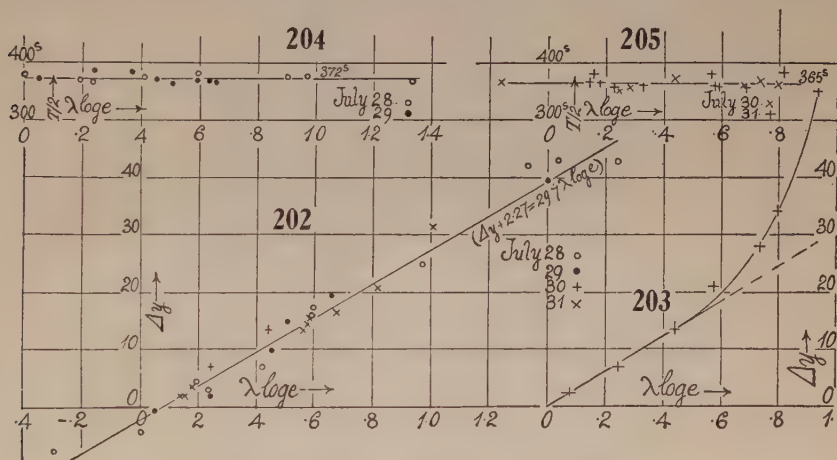
negative values of λ and Δy in the new results. Nevertheless, the indications of § 105 are sustained, though it has not been possible to adduce smooth graphs. The data so far as obtained are given in table 22. The quantity $\lambda \log e$ was computed whenever two successive arcs were available and is merely the common logarithm of their ratio, no other connection with the theory of λ under normal conditions being implied. In the early forenoon the needle passes beyond the limits of the scale or touches one of its glass plates. Considerable difficulty is encountered in the proper selection of Δy, the static displacement. Table 22 gives the observed values; but these are about an hour apart, and during this time there has been considerable change of the position of equilibrium, as indicated by the F, R curves. The value of λ, however, is taken from two consecutive arcs and the time consumed is only about 13 minutes. Hence λ and Δy (observed) do not belong together. In this dilemma it is perhaps more trustworthy to associate λ with a value of Δy to be interpolated from the F, R curves for the same time interval. The

TABLE 22.—*Values of $T_1/2$, $T_2/2$, λ, and Δy.*

Date.	Vacuum.		Hour.	$T/2$	$\dfrac{10^8 \times}{\lambda \log e}$	Δy	Mean $T/2$
		mm.		sec.		cm.	sec.
July 24	10h10m a.m.	0.0633	7h12m	...	− 92	} −13.88	...
	10 18 p.m.	.1560	8 3	...	−297		...
			9 0	...	−263	−12.88	...
			10 0	...	− 29	−13.20	...
July 25	10 43 a.m.	.2280	11 40	...	1,519	} 36	...
	10 0 p.m.	.2910	1 35	...	700		...
			2 53	...	972	16.75	...
			3 50	...	611	20.05	...
			4 46	408	514	12.95	...
			5 55	385	246	7.15	...
			7 40	398	62	− .53	...
			8 50	393	− 54	− 3.18	...
			9 42	410	− 63	− 7.78	399
July 26	10 42 a.m.	.357	2 56	364	1,453	} 23	...
	10 11 p.m.	.466	4 00	398	571		...
			5 35	397	496	12.00	...
			7 6	407	214	7.05	...
			8 4	396	87	1.10	...
			9 3	406	31	− 2.75	...
			9 55	403	377	− 1.45	396
July 27	...	...	11 20	...	...	} 40	...
			12 20	333	1,497		...
			1 23	378	1,180	27	...
			2 22	371	717	21.28	...
			3 14	387	630	14.40	...
			4 18	389	268	3.25	...
			5 13	395	289	3.85	...
			...	...	...	...	...
			7 15	394	388	} 8.95	...
			8 19	383	514		...
			9 19	388	418	9.65	386
July 27	10h 2m p.m.	.0005	...	...	...	...	...
July 28	9 27 a.m.	.0645	9 12	367	1,642	} 49	...
	9 27 p.m.	.1295	10 27	368	1,335		...
			11 32	376	901	42.92	...
			2 10	377	970	36.87	...
			3 22	383	597	24.80	...
			4 25	375	413	17.40	...
			5 22	369	194	6.67	...
			7 5	365	237	3.92	...
			8 10	380	50	4.60	...
			9 10	369	−291	− 7.80	373
July 29	10h25m a.m.	.197	10 37	385	1,370	} 36.65	...
	10 8 p.m.	.257	12 10	367	659		...
			2 16	370	591	17.80	...
			3 36	364	509	{ 16.05	...
						14.70	...
July 29	...	...	4 30	368	633	} 14.20	...
			5 34	371	453		...
			7 10	386	241	7.30	...
			8 00	371	522	2.00	...
			9 8	...	159	− 0.20	...
			10 6	...	...	− 2.95	373
July 30	10h30m a.m.	.0006	2 5	...	932	} 60	...
	9 54 p.m.	.0651	2 57	362	796		...
			4 00	368	735	34.65	...
			5 01	360	576	28.73	...
			6 08	372	440	19.38	...
			7 30	351	243	13.98	...
			8 35	355	280	5.98	...
			9 37	...	74	4.10	...
			10 10	...	...	4.30	361

TABLE 22.—*Values of $T_1/2$, $T_2/2$, λ, and Δy* —Continued.

Date.	Vacuum.		Hour.	$T/2$	$10^8 \times$ $\lambda \log e$	Δy	Mean $T/2$
		mm.		sec.		cm.	sec.
July 31	$10^h 10^m$ a. m.	0.1300	10 6	...	1,155	} 60	...
	9 57 p. m.	.1960	11 20	...	1,090		...
			12 34	384	818	26.98	...
			2 20	358	680	22.60	...
			3 10	360	574	15.20	...
			4 00	358	588	15.90	...
			5 00	381	561	16.30	...
			5 56	356	227	12.00	...
			7 25	362	327	4.60	...
			8 9	365	176	4.98	...
			9 0	380	153	1.98	...
			9 45	365	140	1.70	367
Aug. 1	$9^h 35^m$ a. m.	.254	12 0	374	1,042	} 25.68	...
	9 49 p. m.	.318	1 45	368	645		...
			3 5	372	687	17.05	...
			4 15	...	381	15.15	...
			5 15	384	634	10.93	...
			6 5	342	389	10.15	...
			7 25	385	305	5.60	...
			8 25	365	243	4.65	...
			9 35	386	308	4.75	...
			10 5	...	...	6.80	376

latter, however, are so irregular and vary so rapidly, particularly in the morning, that smooth curves can not be expected. I tested both cases of observed and interpolated Δy, finding that in afternoon and night values there was not much choice; but the forenoon data are unavailable in the former case. Hence in figure 206 (July 24–27) and figure 202 (July 28–31) the interpolated Δy is compared with λ. The high values are divergent for the reasons given; but both curves, as a whole, unquestionably point out a proportionality between these two quantities. The lines which I have drawn through both figures have the same slope, conformably with the equation

$$(\Delta y + \Delta y_0) = 29.7\lambda \log e = 12.9\lambda$$

The intercepts differ, being $4.5 = \Delta y_0$ in figure 206 and 2.2 in figure 202.

The observations of July 30 seemed to depart from these results and are specially given in figure 203. It is, however, only the high values (above the abscissa $0.5 = \lambda \log e$) which particularly diverge here, for some reason; the lower values conform to the same slope, but the intercept is zero. It is interesting to note that the negative values of Δy and λ, which I had supposed would rule out all possibility of comparison, conform pretty well with the locus as a whole, both in figures 202 and 206.

The values of $T/2$ of table 22 are the means of the semiperiods for the first and second arc of vibration. It has already been pointed out that the two components differ widely and exchange relative magnitudes somewhere near $\lambda \log e = 0.6$. Since both components must here be found between the elongations of a very slow moving needle, they can not be measured. More-

over, there is some uncertainty during the exchange of weights at the first elongation. If the first half period is taken too long the second will be too short, so that their sum or mean is liable to be much more trustworthy than either and is therefore given under $T/2$ in the table, as well as in figures 207, 204, and 205. The mean value on July 25 was $T/2=399$ seconds; on July 26, 396 seconds; on July 27, 386 seconds. The values for this exhaustion are thus larger than for the next, viz, July 28, $T/2=373$ seconds, July 29, $T/2=373$ seconds, and for the last, viz, July 30, $T/2=361$ seconds, July 31, 367 seconds. It is useless to speculate on the reason for the high values in the first exhaustion; but probably the later values, since the observer will gradually have gained skill in these difficult readings, are preferable. The final mean of this latter group will be $T/2=368$ seconds, while the mean of all would be 379 seconds.
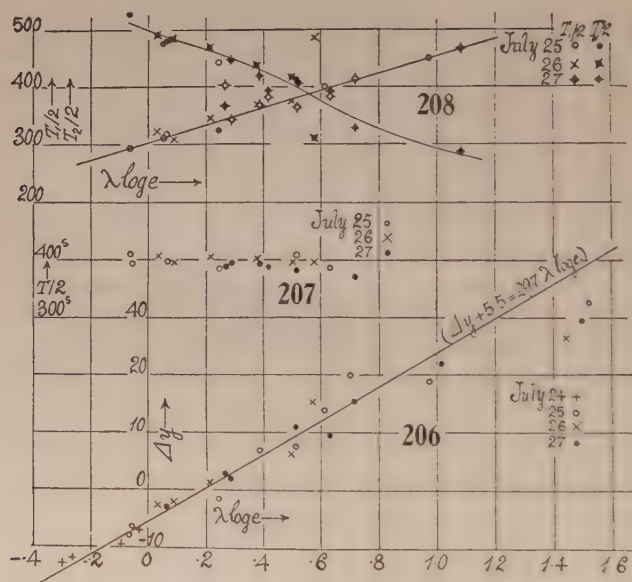
Although there is greater uncertainty attaching to the semiperiods (since if one is taken too long, the other will be too short, and vice versa), it is nevertheless worth while to give some examples of their relations, as in figure 208. Here the first half period $T_1/2$ is plotted in open characters and the second, $T_2/2$ in black characters of the same kind. There are a number of exceptions to the rule, no doubt; nevertheless, a glance at figure 208 indicates that first and second half periods lie on two lines which intersect somewhere before $\lambda \log c = 0.6$. Each of these quantities T_1 and T_2 is thus modified by the same agency as Δy and λ, which, however, is here nearly eliminated in their sum T_1+T_2.

In figures 209 and 210, finally, the first and second semiperiods are taken from the data of July 28–29 and 30–31. There are no exceptions, though the

graphs naturally lack definiteness for the reasons given. The intersection of graphs takes place sooner ($\lambda \log e = 0.4$) than in figure 208, so far as it can be located.

112. **Summary.**—It is now possible to bring these diverse data together in two groups: That of the morning, in which a gradual increase of the temperature of the environment ($d\theta/dt$, positive) supervenes, and that of the late afternoon and night, in which temperature gradually decreases ($d\theta/dt$, negative). Since the two sides of the case parallel to the needle are similarly circumstanced, it will suffice to consider the front face only. Hence when the weight M is on the right in front, that end of the needle is screened, while the left end receives radiation from without, if $d\theta/dt$ is positive. The result is an excess of molecular bombardment on the left in front, manifesting itself as a repulsion of the left end of the needle towards the rear, *i. e.*, a virtual increase of the attraction of M. Again, if M is near the left end of the needle and in front of it, the conditions are exactly reversed. There is excess of
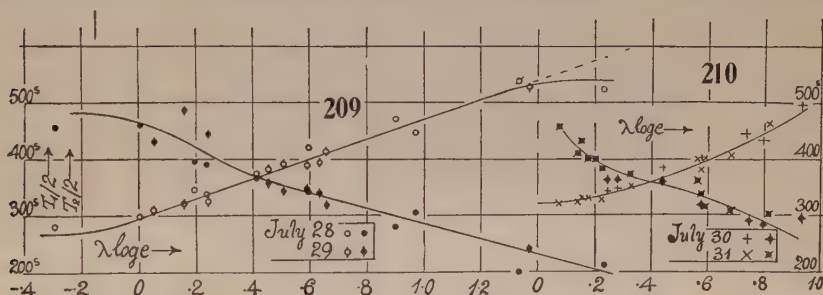
molecular bombardment or repulsion of the right end of the needle rearward, which is in turn equivalent to an increased attraction of M.

Finally, if $d\theta/dt$ is negative, the radiant forces are again reversed, in each of the two cases. For it is now the end of the needle screened by M which is continually the warmer, *i. e.*, subject to excess of bombardment toward the rear. Hence the gravitational pull of M is reduced by the radiant forces.

These preliminaries granted, we may proceed with the analysis of the interaction of the gravitational vector g, g' and the radiant vector r, r', assumed for convenience to be nearly equal (as they often are), in the way indicated in figures 211 and 212. It must be remembered that while g acts instantaneously with full strength, r requires time to reach its maximum value. Suppose, therefore, $d\theta/dt$ is positive (fig. 211) and that at a given instant g is acting alone (case 1). Soon thereafter case 2 will be established and the resulting static deflection of the needle may be called Δy_1. Now let the attracting weight M be suddenly passed from front to rear. In the neutral position, r will then alone act prolonging the attraction (case 3), but with M newly located, g reversed (g') acts in full against a reduced value of r (case 4). In case 5, r has vanished and eventually in case 6, r has its maximum

negative value, r' and the static deflection of the needle is now Δy_2. The total deflection of the needle is thus $\Delta y = \Delta y_1 + \Delta y_2$. Finally, let the attracting mass M be again passed to the front, its first position. For an instant the radiant vector r' acts alone and prolongs the former attraction (case 7). In case 8 the gravitational pull g is reestablished with a reduced radiant vector r'. The latter vanishes, restoring the original case 1.

In figure 212, $d\theta/dt$ is negative; but the consecutive cases are the same as before (*mut., mut.*), excepting that r is now negative. Here Δy_1 and Δy_2 and Δy may all be zero, an observation so common in the above results. The occurrence of large and small positive and negative values of Δy follows at once from the diagrams. In the latter case r must numerically exceed g.

In figure 211, λ must also be large; for the first deflection occurs in the direction of an increasingly favorable vector $r + g$, whereas the second deflection is resisted by the same vector, probably still continually increasing. In the second case, figure 212 with $d\theta/dt$ negative, the deflecting vector, algebraically $g' + r'$, passes through a maximum and may, if r' exceeds g, eventually become negative. Hence λ is smaller and may also be negative. Δy and λ are thus
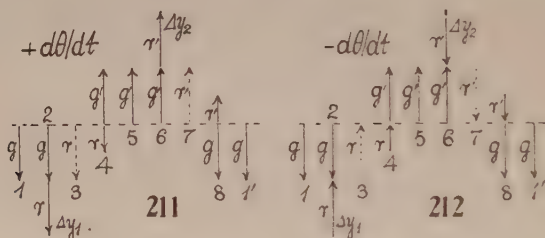
fundamentally subject to the same radiant conditions. These must also determine, though perhaps less uniformly, the first and second semiperiods, $T_1/2$ and $T_2/2$. For in case of figure 211, T is relatively long because the position of equilibrium is continually moving in the same direction as the pendulum, whereas in case of T_2, the pendulum moves in a direction opposite to the motion of the position of equilibrium. These relations may also be reversed in case of figure 212, so that $T_2 > T_1$. It is obvious also that $T = T_1 + T_2$ will be more nearly constant than either component, though it does not follow that T will be quite constant.

113. **Comparison of the equilibrium curves** F, R, **of 1921 and 1922.**— The apparatus used last year was identical with the present one, excepting only the minor appurtenances, added to secure greater convenience in exhaustion. These are without influence. Moreover, neither the location of the apparatus nor the mechanism of the weights M had been changed. The method of observation was substantially the same. It is thus very difficult to account for the erratic behavior of the gravitation needle during July and August of this year, as compared with the nearly constant deflections (Δy, y being the scale reading) obtained under like conditions last year. I have, therefore, in

figures 213 and 214, put the scale readings of the elongations, y, obtained on the same day in 1921 and 1922, together, successive observations of the position of equilibrium (about an hour apart) being inserted equidistant horizontally. Data for 1922 are distinguished by little circles, with the nearest hour number of the observation attached. Data for 1921 are given in points, in corresponding positions, for easy comparison. F denotes that the attracting weight M on the right end of the needle is in front of it; R, that M is to the rear of the needle. Complete sets of observations (*i. e.*, equilibrium curves F and R) are given between about 10 a. m. and 10 p. m. for each year from July 24 to August 11. The exhaustion (mm. of mercury) of the case in the morning and at night is shown on each day for 1922 only, as the data were not taken in 1921. In the same place C refers to cloudy, C' to partly cloudy
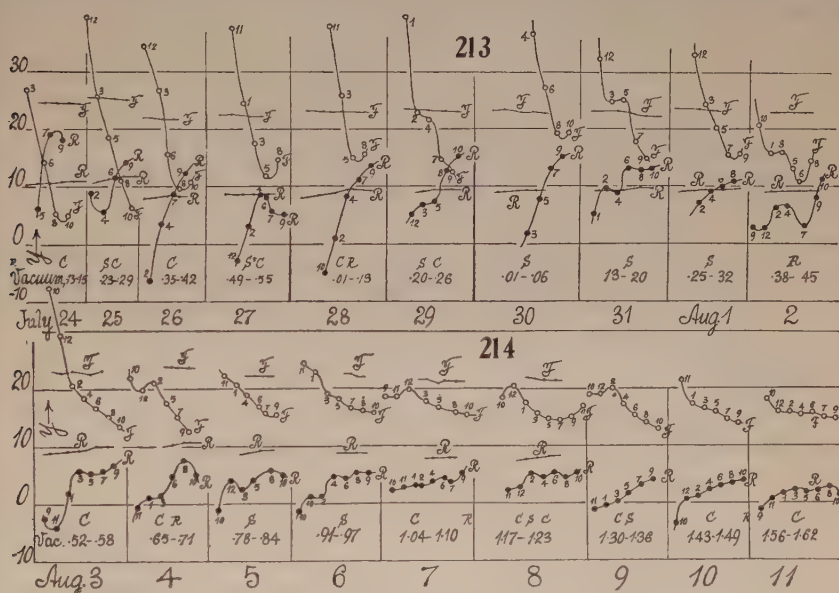
weather, S to sunshine or a clear day, and R to rain. It is seen at a glance that the variations of the position of equilibrium y in the lapse of time are of a different order in 1922 from their approximate constancy in the given scale in 1921. The contrast is startling, with nothing easily apparent to account for it. For the exhaustions, as a whole, were thought to be of about the same order of value in both years. In 1922 there was fresh exhaustion on July 24, 28, and 30. Thereafter I left the apparatus, with its slight leak, to itself. In 1921 there were no intermediate exhaustions, and unfortunately the McLeod gage was not attached to the case.

Figures 213 and 214 show, moreover, that all observations have a period of one day (24 hours). Consequently, the variations can not be contributed by anything within the laboratory, though enhancement is possible. They must, in other words, be originally meteorological, and due to solar radiation. Immediately after exhaustion (as on July 28 and 30) there are apt to be

large deflections, probably showing that the further exhaustion of the air within the case, though very rare, has nevertheless an appreciable cooling or other effect. The enhanced discrepancy persists half a day or longer. For this reason I ceased to make exhaustions after July 30, and the observations, possibly for this contributory reason among others, gradually grow smoother and more normal. Intersections of the curves F and R cease. Any slight cooling of the inside of the case would tend to exaggerate the daytime meteorological effect. If the cooling due to an exhaustion from 1 mm. to 0.001 mm. of pressure were instantaneous, one would estimate that about 0.01 calory would be abstracted from the air within the case. This is largely supplied, of course, by the massive case, and the exhaustion is very gradual. Nevertheless the effect on the needle is always very marked. One can not observe with the pump running. The needle in such a case clings to the glass plates.
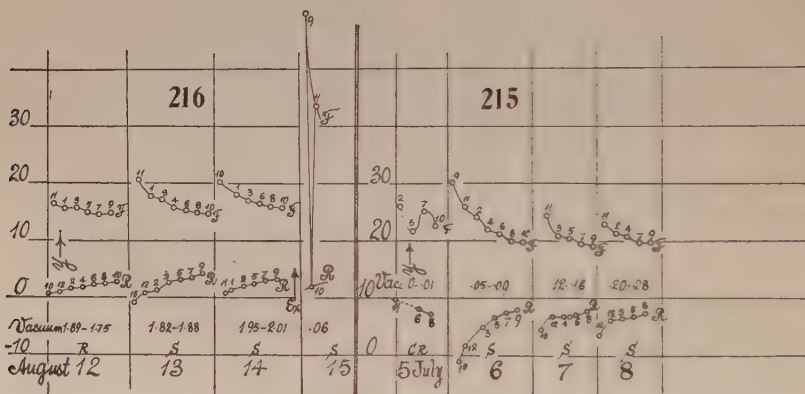

In figures 215 and 216 I have added a few supplementary observations obtained July 5–8 and August 12–15. The latter sustain the general run of figures 213 and 214 and the effect of the sun on August 13, after protracted cloudiness and rain, is marked but subdued when compared with the earlier graphs.

It was necessary to discontinue the observations on the morning of August 15. Consequently a final exhaustion was made to about 0.001 mm. 12 hours before that time, in order to test its effect on the now normal succession of results. Figure 217, like figure 216, shows (August 15) a relatively enormous enhancement of the radiation discrepancy, quite comparable with the earlier experiences. The conclusion is therefore trustworthy that the radiation forces are at a minimum in a partial vacuum of a few millimeters; that they are liable to be relatively very large in case of a plenum, or of a high vacuum, within a few tenths of a millimeter. The tendency of the needle to persistently cling to the walls of the case while the pump is running at high exhaustion is thus to be anticipated, in view of the excess of the radiant forces over gravitation, under conditions of high exhaustion. Moreover, since the slope of the F, R,

curves, always convergent, show a tendency to increase in proportion as the vacuum becomes more nearly perfect, the eventual intersection of these curves may be predicted and the enhancement be referred to causes within the apparatus accompanying the high exhaustions.

114. Static deflections (Δy) a year apart.—To obtain a final comparison, it will be necessary to measure the distances apart Δy of the F, R, graphs, at the same hour on successive days. As these graphs are often quite divergent, the interpolations will lose in accuracy; but the general relations of the results will nevertheless appear much more clearly. These static deflections, Δy, are given in table 23 and in figure 217. For 1922 the graphs are drawn for 1, 3, and 8 p. m. of the successive days, and are distinguished by circles or crosses. For 1921 the night observations (about 8 p. m. on the average) only are given, as the lines would lie too close to them at the other hours not to complicate
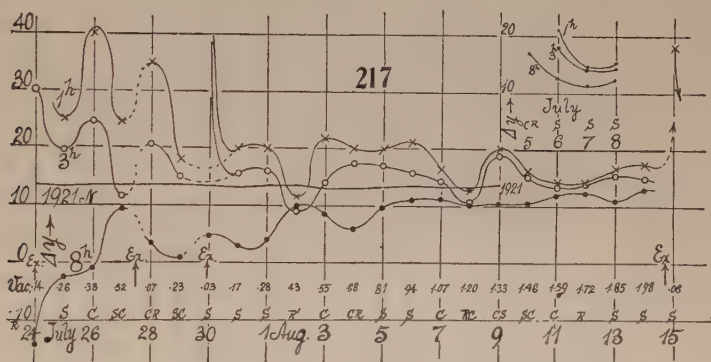
the diagram. In fact, the variations in 1921 are of a smaller order and must be given on a scale 10 times larger to be adequately shown.

The diagram brings out the striking difference of the results very well, and for 1921 the observations lie practically on a straight line, $\Delta y = 13.42$, for which the normal period of the needle in vacuo would be 752 seconds. In the results for 1922 the time of the successive exhaustions (ex) is indicated approximately. It will be seen that the cooling or other effect of such an exhaustion (though carried from 1 mm. to 0.001 mm. only) is still effective in exaggerating the radiant forces for at least 6 hours or more (cf. July 24 and 30) after the exhaustion has been completed. Consequently, the graphs for 1 and 3 should probably be joined by the dotted lines, as indicated.

In all cases the extraneous radiant disturbance, which is strong in July 1922, gradually recedes more and more, as the observations enter the days in August. On July 24, at 8 p. m., the combined gravitation and radiant effect of the attracting mass M was strongly repulsive (Δy negative), the radiant repulsion being about twice the gravitational pull. Positive values are not reached until after July 26. From July 28 on, the 8 p. m. increase is determined, though it has not quite reached the values of Δy of 1921 even at the end of

the diagram (August 13). In the afternoon observations (1922) the rain effect (or the absence of sun effect) is brought out very clearly by the synclinal inflections on August 2, 8, 11, and 12. At night this effect may be reversed; *i. e.,* if radiation is scantily received by the apparatus during the day, there is an equivalent absence of radiation during the night.

In case of the observations of 1922, the small fluctuations of the Δy curves throughout a month showed instances of resemblance to the run of atmospheric temperature; but in the large variations recorded in 1922 (as a consequence perhaps) I was unable to detect such resemblances in the night observations, which are here alone of interest. The same is true of the change of temperature per day, etc. Nevertheless, it is possible the relatively short atmospheric temperature changes from without, such as would not be otherwise recorded, may make an impression on the 8 p. m. graph. This, however, would not bear upon the 1922 graph as a whole, from July 24 to August 13.

TABLE 23.—*Values of Δy, 1922, interpolated.*

Date.	1ʰ p. m.	3ʰ p. m.	8ʰ p. m.	Date.	1ʰ p. m.	3ʰ p. m.	8ʰ p. m.
	cm.	cm.	cm.		cm.	cm.	cm.
July 24	....	>30.0	—14.0	Aug. 4	20	17.5	6.0
25	25	19.5	— 2.5	5	20	17.0	9.7
26	>40	24.5	— 1.0	6	21.2	15.7	11.0
27	24.5	11.5	+ 9.5	7	16.5	14.2	11.2
28	35	20.7	3.5	8	12.7	10.5	10.2
29	18	15.0	1.0	9	20.0	18.7	10.5
30	>40	43.0	4.7	10	16.0	15.0	10.5
31	20	15.5	3.0	11	14.0	13.2	11.8
Aug. 1	20	16.0	4.0	12	14.2	13.8	12.2
2	11.7	9.0	10.0	13	16.6	15.2	10.8
3	21.7	14.0	8.7	14	17.0	14.7	12.7

Supposing, moreover, that the medium within the apparatus is in some way modified by the high exhaustions (carried to within 0.001 mm.), it seems hardly probable that the apparatus would take so long to return to a normal condition, if radiation of some sort is alone in question.

What has gone down during this series of measurements is the vacuum. One would therefore conclude that states of high exhaustion (a few hundredths or tenths of a millimeter) are (like the plenum) more susceptible to the presence of radiant activity than the lower exhaustions of a few millimeters. The exhaustion made just prior to August 15 conspicuously bears this out. It not infrequently happens that night values are low when day values are high and, in general, there is a tendency of the graphs to converge toward rainy or densely cloudy weather. All this conforms with the view that the needle is screened from radiation by the large attracting mass M and that the radiant forces act with gravitation, if the temperature coefficient $d\theta/dt$ is positive, and act against gravitation when $d\theta/dt$ is negative, as elsewhere explained. I have been tempted to envisage a coefficient $d\theta/dt$ which is not

all temperature; for there may be some other radiation or agency behind the recent rains (for instance), as well as behind the difference in the character of the results of 1922 and 1921 as exhibited by figure 217. Unfortunately, accumulation of evidence of this nature is very slow and laborious. It is safe to conclude, however, that the radiant discrepancy is at a minimum in a partial vacuum of a few millimeters. It increases enormously as a plenum is approached. It similarly increases in high exhaustions, within 0.1 mm. In fact, the needle is then liable to stick to the case.

However puzzling it may be to account for the discrepancy which persistently clings to the observations in July and early August, and which in its long duration would seem to be incompatible with the practically immediate daily cycle, the suggestions of the last paragraph are still quite valid. If, in
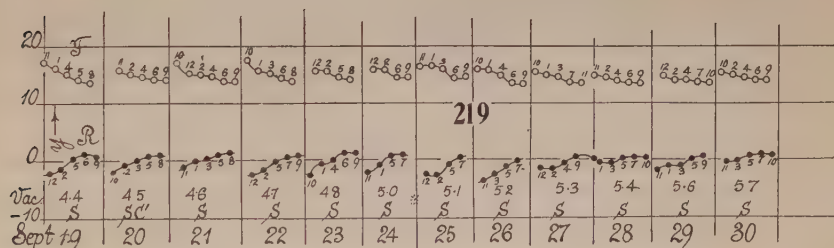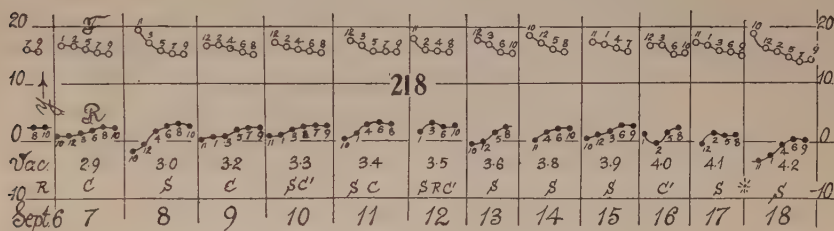

other words, the slope of the convergent F, R graphs is increased by causes evoked by high exhaustion within the apparatus, these graphs will ultimately intersect, with the result that negative values of Δy and repulsive forces make their appearance at night.

CONCLUDING OBSERVATIONS AND COMPARISONS.

115. Further observations.—The observations interrupted after the exhaustion of August 15 were resumed (figs. 218 and 219) on September 6. In the meantime the vacuum had slowly decreased to about 3 mm. and it was under these conditions that the new observations were to be made. They are given (F, R, equilibrium curves or elongations y) in the same manner as in figure 216, with the successive observations horizontally equidistant and the nearest hour marked at the points. It is at once evident that the F, R curves are very much more regular and more restricted in vertical extent than heretofore. This is the case until the arrival of the cold spell, September 15

to 19, which becomes effective on the night of September 17. After this there is a curious departure from the normal behavior, until the weather grows warmer again. At the time (marked * in fig. 218, September 18) the scale was slightly reset, so that both y's are somewhat smaller than before. On September 20 the results are again regular. It follows that the partial vacuum of a few millimeters of exhaustion, under which the work was done, is highly favorable to the appearance of more nearly trustworthy results, at least in the night observations. Toward the end of the month the observations become markedly regular even during the day, barring the cold spell on September 24 and 25. It was thought advisable to interrupt the work on September 30. The question occurs, however, whether on further reduction of the vacuum below 6 mm. of mercury in the same slow manner, conditions more favorable to measurement might not have been reached, though the previous experiences, with similar ends in view, make this improbable.

In figure 220 and table 23 I have given the corresponding deflections Δy, interpolated from the F, R curves of the month, for the mean time 3 p. m. and about 8 p. m. The figure also contains (dotted line) the mean atmospheric temperatures in degrees Fahrenheit. In contrast with figure 217, these curves
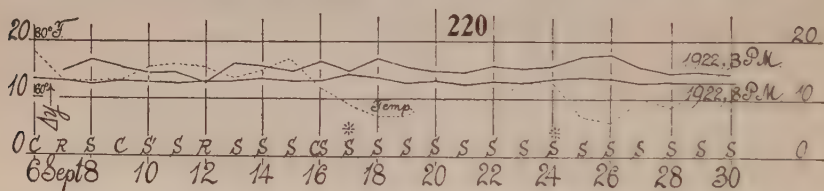
are very uniform and the new 8 p. m. observations compare quite favorably with the corresponding curve for 1921 in figure 217. The 3 p. m. curve is also much less discrepant, though it shows the degree of unavailability of after-noon observations. On a rainy day (September 12), the tendency to coinci-dence is marked, as usual. The effect of the cold spell beginning September 15 is here belatedly (September 17 at *) conspicuous, though the nature of the change is none the less puzzling. The 3 p. m. datum falls in value, but the 8 p. m. value rises. The former result is to be expected from deficient radiation and reduced $d\theta/dt$; consequently $d\theta/dt$ should be still further reduced and be definitely negative at night. In such a case, however, Δy should de-crease, whereas it increases. Thus it seems as if the needle, having received less radiation during the day, has less available energy to radiate at night. It is the same behavior which is often even more apparent on rainy days, on which afternoon observations of Δy may dip below night observations. It occurs again during the cold spell after September 24. It is difficult to account for it, for the markedly increased values of Δy during the morning, when $d\theta/dt$ is positive since the environmental temperature is rising, reciprocally demand low values of Δy for the cold spell. This is the case with the 3 p. m. data, but not with the 8 p. m. data, which are here of paramount interest.

The latter are given in full in table 22. If we throw out the observation on the cold day (September 17), which is evidently erroneous, the remaining 24 observations conform to the mean value (8 p. m.) $\Delta y = 13.07 \pm 0.05$ cm. This is somewhat smaller than the mean of last year ($\Delta y = 13.4$) owing to slight shifting of the weights M, from which the attraction proceeds, during the course of the year.

116. The same. Higher exhaustions repeated.—Having reproduced the conditions for the steady behavior of the needle as shown in figures 219 and 220, it seemed desirable to utilize the few remaining days of the season (steam heat was turned on October 13) to repeat the experiments with an intensified vacuum, in order to see whether anything could be made out of the chaotic behavior to be anticipated. The equilibrium curves are given in the same
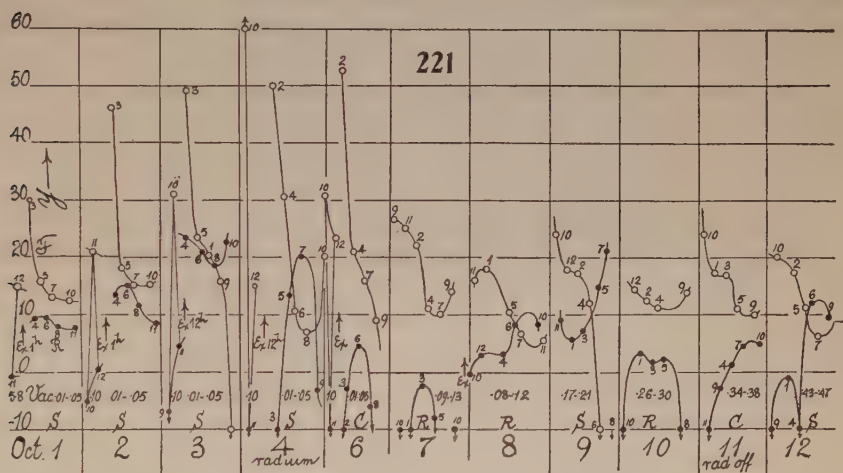
manner as heretofore in figure 221, open circles referring to the front and dark circles to the rear position of the attracting weight M on the right end of the needle. The nearest hour at which the observation was made is attached in each case. The figure, furthermore, shows the successive vacua (vac. in mm. of mercury) and the meteorological conditions (S sun, C cloudy, R rain). The time at which the exhaustions (ex. to 0.0003 mm.) were made is also given. Observations were begun 2 or 3 hours later, or as soon as the needle ceased to cling to the glass walls of the case. It was customary to complete one observation for Δy in the morning and thereafter to exhaust the case for observations at the higher vacua. On October 1, the first pair of equilibrium values of y has about the same separation, Δy as in September, the vacuum being low, 5.8 mm. After the exhaustion, however, and for the mean vacuum of 0.03 mm., these relations are totally changed, Δy becomes very small, and the two equilibrium curves tend to intersect. On October 2 the Δy for the residual vacuum 0.1 mm. in the morning is now very large, so that the effect

of the low pressure of the preceding day has not vanished. After the renewed exhaustion, the tendency of the F, R curves to intersect is accentuated and the drift of both into higher values of y is marked. The same effects are still further enhanced on October 3. The lower equilibrium curve has steadily risen in y; the upper equilibrium curve on October 3 actually intersects the other at about 8 p. m. and thereafter marked repulsion replaces gravitational attraction, until the needle actually clings to the glass plates on the wrong side. This condition is indicated at the lower ends of all curves by the arrows. On October 4 the observations made in the residual vacuum, 0.1 mm., begin with the needle adhering successively to the walls of the case on both sides.

An important result thus stands out; obviously, the effect of exhaustion is cumulative. It does not vanish in 24 hours nor in a number of days, the inference already suggested by figure 217. Meantime the daily cycles are practically immediate. Thus it does not seem that what accumulates can be temperature, particularly in view of the small range of exhaustion (0.1 to 0.001 mm.), *i. e.*, of the very rare air contained.

Electric excitation on the outside, in the damp atmosphere, would be out of the question. Neither is electric excitation within (for instance when the needle strikes the glass walls) under favorable conditions, since the exhausted air is now a conductor. Nevertheless, it seemed worth while to increase the ionization within by aid of the gamma rays of radium. Accordingly a thin aluminum tube was suspended on the outside of the glass walls near the middle of the needle on October 4. The effect of this in no manner changes the chaotic nature of the curves between October 4 and October 10, so that electrostatic discrepancies are not in question. There is, however, a change in the character of the progression of curves during this interval, for whereas the mean positions of the F, R curves were in general rising before, they are now gradually being depressed. The R curves, for instance, are deleted because the needle is usually at the walls. It does not follow, however, that this new condition is due to the presence of the γ rays (for on October 11, when the radium was removed, the same behavior continues), unless the effect of the rays on the air-content within the case is also cumulative. It is unfortunate that the observations after October 12 could not be continued in order to discern whether in the course of time the rise of y values of October 1–4 would have reappeared or whether the whole play of curves is merely an accentuated reproduction of meteorological conditions favored by high exhaustion.

It will be noticed that the exhaustions have the same range (average 0.03 mm.) between October 1 and 6. On October 3, the F, R curves actually intersect and the aggregated forces are repulsive. On October 5 the needle remained at the walls of the case all day, so that no measurements could be made until October 6 in the residual vacuum. On October 7, the morning exhaustion was omitted; but the needle still shows a marked tendency to adherence in the R positions. Barring the slight incidental exhaustion at the end of the day, the case was thereafter left without fresh exhaustion. The

irregularity of behavior, however, continues even when the vacuum pressure is as high as 0.5 mm.

As a whole, even if the circumstances are very complicated, and if the discrepancies from meteorological temperature changes are enormously magnified by exhaustion for a certain range below 0.5 mm. of mercury, it seems to me that the observations of October 1 to 6 indicate that something cumulative in the lapse of time under high exhaustion is added to the inner content of the gravitation chamber. What that something may be I do not venture to state, but without it, the progressive character of the data from day to day, both at a pressure of 0.1 mm. and at the lower mean pressure of 0.03 mm., would be difficult to explain. For on these days observations were made under the same mean pressure, throughout.

The question as to what will happen when the chamber is rigorously exhausted to a limit is still outstanding, and under present circumstances particularly interesting. Everything should ultimately vanish short of light pressure. The present apparatus did not admit of that extension, as the needle with the pump running merely adheres persistently to the walls, not to become free for hours thereafter. Pressures blow 10^{-4} mm. are thus essentially in question.

117. Conclusion. Observations of 1921.

—The above experiments carry the work with the thin quartz fiber, under the given conditions, as far as the form of apparatus used warrants. Seeing that the latter was tightened with sealing-wax and that the air-pump can not be kept running during observations, a steady vacuum much within 10^{-3} minutes could not be maintained; and it is just here that the radiant forces begin to be as formidable again, as they were for the plenum.

The work as a whole has yielded two series of systematic night observations (8 to 12 p. m.), one completed in the summer of 1921 and the other in the summer of 1922. Each is reasonably consistent, but different from the other, and it is therefore desirable to determine to what degree they have fallen short. Since the periods and logarithmic decrements are equally vitiated by the radiant forces, the only available procedure consisted in taking the apparatus apart and determining the torsion coefficient of this quartz fiber by a separate small mass of known moment of inertia. This was accomplished without accident to the fiber.

The damped period * of the needle in 1921 was provisionally taken as 728 seconds, giving a free period of 724 seconds. The corrected moment of inertia of the needle was $N = 159.4$ gcm.² If in the equations M is the attracting, m the attracted mass, R, their distance apart, $1 + s - t/\tau$ the correction for stem, etc., and κ the constant in $\gamma = \kappa \Delta y$ (where Δy is the (double) static

---

* Carnegie Inst. Wash. Pub. No. 310, § 55, 56, 57. By an error of entry, the datum $T = 746.14$ seconds is given in § 55 and 57. This does not occur in κ', κ'' and κ, where $T = 724.3$ seconds is used.

displacement seen in the telescope), the values inserted or deduced were as given in table 24.

TABLE 24.

M	R	$1+s-t/\tau$	$\kappa \times 10^8$
	cm.		
3,368 g	5.89	1.0206	0.9781
2,947 g	5.63	1.0212	1.0218
Together	....	......	.4997

Thus the deflection 13.3 cm. was to be expected. The night observations actually gave $\Delta y=13.416\pm0.033$ for the mean result between July 17 and September 15.

As the equation (apart from corrections) reads

$$\gamma = \frac{\pi^2 N}{LT^2 l}\frac{R^2}{Mm}\Delta y$$

or in a more useful form

$$\gamma = \frac{2\pi^2 lR^2(1+s-t/\tau)}{MLT^2}$$

it is merely necessary to put in place of the provisional period, the new value obtained by the aid of N'/T'^2 of the auxiliary body. This gives the corrected value of γ, since $T^2=T'^2(N/N')=T'^2(159.5/N')$.

Two smooth steel ball bearings of moments of inertia $N'=0.04166$ and 0.04158 and periods $T'=11.62$ seconds and 11.56 seconds on the given fiber, gave $T=719$ seconds and 716 seconds, respectively, the mean of the vibrations being taken. Although the arcs of vibration usually exceeded 360°, this disappointingly large difference suggested the possibility of an effect of the earth's magnetic field. The experiments were, therefore, checked by a pair of small brass cylinders which gave a mean value of $T=716.5$ seconds. The value $T=716$ seconds was accepted for the period of the needle, sufficing for the present critical purposes.

With $T=716$ seconds for the needle, the constants reduce to

$$10^8\kappa'=1.0011 \text{ and } 10^8\kappa''=1.0458$$

or for the two balls conjointly

$$10^8\kappa=0.5117$$

whence

$$10^8\gamma=\kappa\Delta y=0.5117\times13.416=6.865$$

Thus, in spite of the care taken with the observations in 1921 and the encouraging uniformity of static deflections Δy from day to day, the radiant discrepancies were still present and equivalent to an excess of about 3 per cent in the value of γ. The reduced performance of the thin fiber has thus fallen below the first result, obtained with a much thicker fiber.

118. Observations of 1922.—The constants of the apparatus were nearly the same as in the previous year and the same needle was used, so that $T=716$ seconds. The distances R measured are given in table 25.

TABLE 25.

M	R	$1 + s - t/\tau$	$\kappa \times 10^8$
	cm.		
3,368 g	5.89	1.0206	1.0011
2,947	5.67	1.0212	1.0606
Together	......	......	.5154

From this the values of κ in table 25 were computed. The mean value of Δy for the night observations from September 16 to 30, 1922, was found to be $\Delta y = 13.07 \pm 0.05$ cm., hence

$$\gamma = \kappa \Delta y = 10^{-8} \times 0.5154 \times 13.07 = 10^{-8} \times 6.736$$

Thus the 1922 datum for γ obtained later in the season than was the case in 1921 are nearer the normal value of γ. Nevertheless the discrepancy produced by the presence of radiant forces is equivalent to an excess about 1 per cent of the value of γ. By using the largest values of T' found with the auxiliary body, both γ values could be reduced about 1 per cent; but this is of no interest as the divergence remains.

Part 2

69831